CHEMISTRY OF THE LANTHANIDES WITH PYRAZOLYLMETHANE LIGANDS

Thesis submitted in partial fulfilment of

the requirements of UCL for the degree of

Doctor of Philosophy

Sarah Ellen Brown

Christopher Ingold Laboratories
Department of Chemistry

January 2010

I, Sarah Ellen Brown, confirm that the work described in this thesis was carried out in the Christopher Ingold Laboratories of University College London, UCL, from September 1999 to September 2002 under the supervision of Dr A. Sella. All the work described is my own unless stated to the contrary and it has not been submitted previously for a degree in this or any other university.

Abstract

The work presented in this thesis demonstrates the utility of the tris(3,5-dimethylpyrazolyl)methane ligand (TPm*) as an ancillary ligand for the lanthanides.

Compounds of the formula [Ln(TPm*)Cl_3] have been synthesised. These new complexes [YTPm*Cl_3] and [SmTPm*Cl_3] have been crystallographically characterised, showing an interesting variation of coordination geometry with differing metal centre. The triflate aducts have also been prepared. New compounds [YTPm*$(OTf)_3$] and [HoTPm*$(OTf)_3$] have been crystallographically characterised and are isomorphous, seven coordinate structures.

Substituting the chloride ligands for OPh^{Me2} groups afforded new complexes [Ln Tpm*$(OPh^{Me2})_3$]. They have been crystallographically characterised and are highly symmetrical six coordinate complexes with a trigonal, anti-prismatic structure. Further attempts at substituting the chloride groups with ligands X (X=Cp,BH_4,Tp*,$N(SiMe_3)_2$) have not led to any further definitive characterisation.

Further the fluoro-substituted alkoxide ligands (OPh^{Fn}) were prepared. This has afforded a new series of complexes of the type $MOPh^{Fn}$ (M=K,Na, n=1,2,5). They exhibit solvent dependent speciation, being essentially dimeric in THF and tetrameric in diethylether. The structural characterisation of a number of these complexes reveals interaction between the metal ions and the ortho fluorines. In $NaOPhF^5$,crystallised from ether, an extended cubic lattice structure was observed due to M-F interactions between metal centres and para-fluorines on neighbouring cubes.

Using these alkoxide ligands new lanthanide complexes of the type $Ln(OPh^{Fn})_3$ were produced. ^1H NMR studies show encouraging results, however no crystals could be obtained. The NMR reveals that complexes $Ln(OPh^{Fn})_3$ are dimeric in

solution with a combination of terminal and bridging OPh^{Fn} ligands. Synthesis of complexes of the type $LnTPm^{*}(OPh^{Fn})_3$ were attempted.

The reaction between the divalent lanthanide complex $YbTPm^{*}I_2$ and $NaNPH_2$ has given spectroscopic results suggestive of deprotonated TPm* ligands. Extreme air and moisture sensitivity of the product has precluded its full characterisation.

Table of Contents

List of figures

List of Tables

Abbreviations and symbols

acac	acetylacetonate
acacH	acetylacetone
Ar	Aryl group
br	broad
Bu^t or t-Bu	*tert*-Butyl
Cp	cyclopentadienyl (C_5H_5)
Cp*	pentamethylcyclopentadienyl (C_5Me_5)
δ	chemical shift (ppm)
d	doublet
ΔG	free energy of activation ($KJmol^{-1}$)
ΔH	enthalpy of activation ($KJmol^{-1}$)
Et.	ethyl
Et_2O	diethylether
I	nuclear spin
IR	infrared
J	Total angular momentum quantum number
J	electron spin & orbital angular momentum
Ln	lanthanide (La to Lu and Y)
M	metal
Me	methyl
MO	molecular orbital
ν_{XY}	infrared X-Y stretching frequency
OTf	trifluoromethanesulphonate (triflate O_3SCF_3)
Ph	phenyl
ppm	parts per million (chemical shift)
Pr^i or i-Pr	*iso*-propyl
py	pyridine
pz	pyrazolyl
pzH	pyrazole
θ	cone angle

t	triplet
q	quartet
R, R', R", R"'	alkyl or aryl groups
S	solvent
sh	shoulder
T	temperature (K)
THF	tetrahydrfuran
TMS	trimethylsilyl ($SiMe_3$)
Tp	*tris*(pyrazol-1-yl)borate
Tp*	*tris*(3,5-dimethylpyrazol-1-yl)borate
TPm	*tris*(pyrazol-1-yl)methane
TPm*	*tris*(3,5-dimethylpyrazol-1-yl)methane
triflate	trifluoromethanesulphonate (OTf, O_3SCF_3)
UV	ultraviolet
vis	visible

For

Faith & Elliot

Acknowledgements

I would firstly like to thank my supervisor, Dr Andrea Sella, for his continued support and expertise and his unfailing enthusiasm for chemistry. I would also like to thank Derek Tocher for his ideas and contributions to my work particularly the crystallography. I would also like to thank Clare Carmalt for the invaluable use of her glove box.

I am indebted to many of the technical staff of the chemistry department, in particular Alan Stones and Jill Maxwell for their expertise in obtaining elemental analysis on air sensitive samples. To Dave Knapp and Joe Nolan for ensuring that all the laboratory equipment works and to John Hughes for his unique glass blowing skills.

I would like to thank everyone I have worked with in the lab, Catherine Cross, Caroline Forth and Abdul Aliev for discussions and their company and to Maria Rossa Russo for her support and help with my work over the years.

Outside of UCL I owe thankyous to my parents and my sister for their support during my university years. I would like to thank my children, Faith and Elliot for their own unique contribution to my Phd! and for being very well behaved and quiet whilst I wrote this thesis.

Finally a special Thankyou is reserved for Andrew for his love, support, encouragement and belief and for his knowledge of things mathematical, physical and computational which, luckily for me, is far superior to mine. I owe this thesis to him.

This page is left intentionally blank

Chapter 1 Introduction [1],[2]

The lanthanides are the fourteen elements that follow lanthanum in the periodic table. The group three elements, yttrium and lanthanum are often included in discussions on the lanthanides on account of the very similar chemical properties that they share with these elements. As is usual the symbol Ln has been used throughout this thesis to denote some or all of the lanthanide elements and yttrium.

The history of the lanthanides began in 1794 when the Finnish chemist Gadolin isolated a new oxide 'yttria', discovered a few years previous as a black stone in the Swedish village of Ytterby. In 1803, Klaproth, Berzelius and Hisinger working independently, almost simultaneously discovered an oxide resembling yttria, for which the name 'ceria' was proposed. Both yttria and ceria were believed to be oxides of single new elements and it was not until 1839 that Mosander separated lanthanum from ceria and discovered yttrium, terbium and erbium from yttria. Over the next 60 years a further ten lanthanides were isolated. The periodic table as it appeared in 1869 gave little hint as to how many rare earths were to be expected. It was not clear that there were fourteen lanthanides plus yttrium and lanthanum until the electronic basis of the periodic table was elucidated early in the twentieth century, it then became apparent that there was still one lanthanide yet to be discovered. The fourteenth lanthanide was radioactive promethium, this was not conclusively identified until 1947 when Coryell and co-workers observed it as one of the products of ^{235}U disintegration.[3]

The problems encountered in early studies of the lanthanides were exacerbated by the difficulties involved in the separation of the elements. The almost identical chemistries of the lanthanides meant that laborious

repeated fractional recrystallisations were required in order to obtain pure compounds. Two events led to renewed interest and rapid advances in lanthanide chemistry. The first was the development in the late 19th century of the Thoria coal gas mantle by Auer Von Welsbach.[4] Welsbach found the combination of 99% Thorium and 1% Cerium gave a long lasting mantle with a brilliant white light. The principle source of thorium is the ore monazite, this also contains a considerable amount of lanthanum and other rare earths. The ensuing large scale mining of monazite to extract thorium produced large quantities of other lanthanide oxides as by products, this sparked an interest in the chemistry and the potential applications of these elements.

The second was the flurry of research into f element chemistry for the Manhattan project during the second world war. One of the main challenges of the Manhattan project was the identification of the fission products of uranium. This problem led to the development of ion exchange chromatography by the groups of Cohn[5]and Spedding[6] and solvent extraction techniques by Peppard *et al.*[7] These new techniques provided a way of separating the lanthanides and actinides on large scales, efficiently and economically.

It is now well established that the unique physiochemical properties of the lanthanides is a consequence of the fact that their valence electrons lie in 4f orbitals which are poorly shielding and have small radial extension.

The remainder of this chapter provides an overview of the properties and the chemistry of the lanthanides and of the poly(pyrazolyl)methane (TPm) ligand system.

Electronic Configuration of the lanthanides

The electronic configurations of the free lanthanide atoms are relatively difficult to determine due to the complexity of their electronic spectra. Table 1.1 presents the generally accepted ground electronic configurations of the lanthanides. It is shown that the principal change as the series is crossed is the gradual filling of the inner, well shielded 4f orbitals in preference to the 5d orbitals. The 4f orbitals are radially very contracted compared to the 5s and 5p orbitals, they are drawn into the inner core of electrons and do not protrude significantly beyond the filled $5s^2 5p^6$. This shell is thus filled to capacity before additional 5d electrons appear. In three instances however, the 5d orbitals are occupied more readily that the 4f orbitals. Gadolinium has an electronic configuration $[Xe]4f^7 5d^1 6s^2$, reflecting the spectroscopic stability of the half filled 4f shell. Lanthanum and cerium have configurations $[Xe]4d^1 5s^2$ and $[Xe]4f^1 5d^1 6s^2$ respectively due to the 5d orbitals lying below the 4f orbitals in energy.

Element	Symbol	Atomic N.o	Electronic Configuration
Yttrium	Y	39	$[Kr]4d^15s^2$
Lanthanum	La	57	$[Xe]5d^16s^2$
Cerium	Ce	58	$[Xe]4f^15d^16s^2$
Praseodynium	Pr	59	$[Xe]4f^36s^2$
Neodynium	Nd	60	$[Xe]4f^46s^2$
Promethium	Pm	61	$[Xe]4f^56s^2$
Samaruim	Sm	62	$[Xe]4f^66s^2$
Europium	Eu	63	$[Xe]4f^76s^2$
Gadolinium	Gd	64	$[Xe]4f^75d^16s^2$
Terbium	Tb	65	$[Xe]4f^96s^2$
Dysprosium	Dy	66	$[Xe]4f^{10}6s^2$
Holmium	Ho	67	$[Xe]4f^{11}6s^2$
Erbium	Er	68	$[Xe]4f^{12}6s^2$
Thulium	Tm	69	$[Xe]4f^{13}6s^2$
Ytterbium	Yb	70	$[Xe]4f^{14}6s^2$
Lutetium	Lu	71	$[Xe]4f^{14}5d^16s^2$

Table 1.1: Ground electronic configurations of the lanthanides[2]

Trends in metallic and ionic radii and the Lanthanide Contraction

The variations in the radii of the metallic lanthanides and the Ln^{3+} ions with increasing atomic number is shown below.

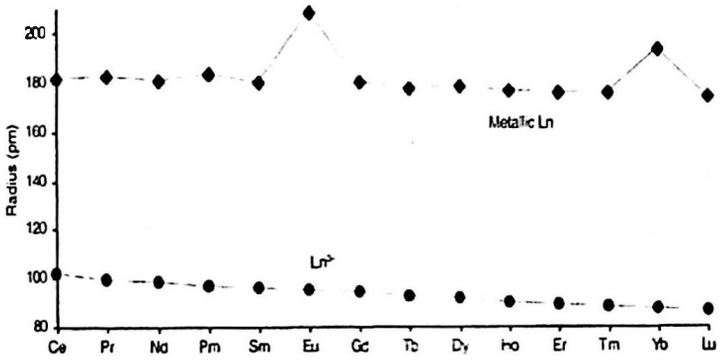

Figure 1.1: Variation of metal radius and +3 ionic radius for the Lanthanide elements

This contraction occurs because the 4f orbitals are drawn into the inner core of electrons and do not protrude significantly beyond the filled $5s^2 5p^6$ orbitals.[8] Their ability to screen other valence electrons from the nuclear charge is poor as result of their angular nodality and relativistic effects.[2] Consequently the 4f electrons imperfectly shield the increasing charge of the nucleus when traversing the series, thus the effective nuclear charge experienced by the 'closed shell' outer electrons increases across the series and the atom/ion contracts. This effect is responsible for the ionic radius of Y^{3+} (0.900 Å) being almost the same as that of Ho^{3+} (0.901 Å). The discrepancies in the metallic radii at europium and ytterbium reflect an inherent tendency for these two metals to exist in the +2 oxidation state. It should be noted that despite this contraction in ionic and metallic radii across the series, the lanthanides are comparatively large with respect to the d-block metals for example the smallest Lanthanide ion Lu^{3+} has an ionic radius of 0.85 Å, compared with 0.65 Å for Fe^{3+}.[9]

Oxidation states of the Lanthanides

The chemistry of the lanthanides is dominated by the +3 oxidation state with electronic configuration $4f^n 5d^0 6s^0$. The first two electrons are removed from the 6s orbital and the third from the 4f valence orbitals. In

all cases, removal of the first three electrons from the atom is relatively facile and is compensated for by the high lattice and solvation energies of the trivalent ions.[10] A stable divalent state might be expected for the lanthanides from the removal of only the 6s electrons. However in most cases the solvation or lattice enthalpy is sufficiently large to exceed the sum of the third ionisation energy and the solvation or lattice enthalpy of the divalent ions. For europium and ytterbium, removal of the third electron is from the stable half-filled ($4f^7$) and filled ($4f^{14}$) electronic configurations respectively, thus both elements have chemically accessible divalent states under reducing conditions.

Divalent ions have been detected for all the lanthanides by irradiation of Ln^{3+} ions doped into CaF_2.[11] Standard electrode potentials (E^o) between the divalent and trivalent oxidation states have been measured. [12]

Couple	Potential (V)
$E^0(Gd^{3+}/Gd^{2+})$	-2.85
$E^0(Tb^{3+}/Tb^{2+})$	-2.83
$E^0(Dy^{3+}/Dy^{2+})$	-2.56
$E^0(Ho^{3+}/Ho^{2+})$	-2.79
$E^0(Er^{3+}/Er^{2+})$	-2.87
$E^0(Tm^{3+}/Tm^{2+})$	-2.22
$E^0(Yb^{3+}/Yb^{2+})$	-1.18
$E^0(Lu^{3+}/Lu^{2+})$	-+2.72

Couple	Potential (V)
$E^0(Y^{3+}/Y^{2+})$	-
$E^0(La^{3+}/La^{2+})$	-2.94
$E^0(Ce^{3+}/Ce^{2+})$	-2.92
$E^0(Pr^{3+}/Pr^{2+})$	-2.84
$E^0(Nd^{3+}/Nd^{2+})$	-2.62
$E^0(Pm^{3+}/Pm^{2+})$	-2.44
$E^0(Sm^{3+}/Sm^{2+})$	-1.50
$E^0(Eu^{3+}/Eu^{2+})$	-0.34

Figure 1.2: Table of Standard electrode potentials (E^o) for the couple $Ln^{3+}/Ln2^{2+}$

The most stable divalent species are Sm^{2+}, Eu^{2+} and Yb^{2+}, Eu^{2+} being the most stable and Sm^{2+} being the most reactive in terms of reducing power. Thus for studies into the reactivity of divalent lanthanide complexes, Sm(II) is considered the best and is is widely used in reduction reactions in inorganic synthesis.[13]

The stability of the divalent oxidation state broadly mirrors the ease of removal of the third electron from Ln^{2+}, i.e the third ionisation potential. The magnitude of the third ionisation energy is determined by 1) the coulombic attraction between the nucleus and the electrons. 2) the inter electronic repulsion and 3) the change in exchange energy which accompanies the removal of the electron. Considering 1 and 2 vary smoothly with changes in ionic radius then any irregularities observed in the third ionisation energy across the series must originate in the exchange energy term. This value rises from zero upon removal of the single electron from an $[Xe]4f^1$ ion ($La^{2+} \rightarrow La^{3+} + e^-$) to a maximum value for a $[Xe]4f^7$ configuration ($Eu^{2+} \rightarrow Eu^{3+} + e^-$). Figure 1.3 compares the third ionisation energy of the lanthanides with the relative stability of the trivalent and divalent ions.[14], [12]

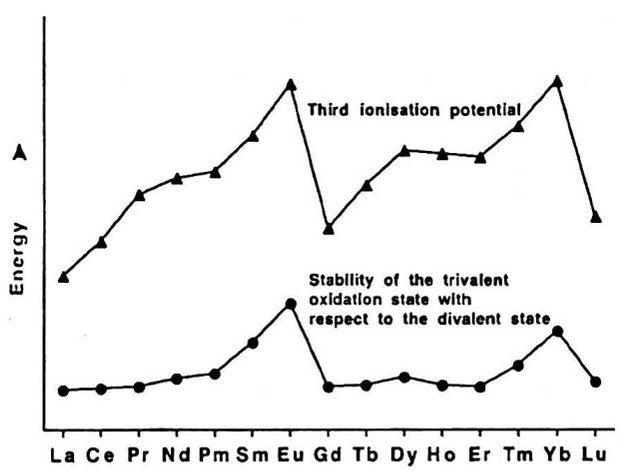

Figure 1.3: Comparison of the third ionisation energy of the lanthanides with the relative stability of the trivalent and divalent ions. [14], [12]

The low third ionisation energies of gadolinium and lutetium can be rationalised by looking at their electronic configurations. Lu^{2+} has an additional electron in the 5d orbitals ($[Xe]4f^{14}5d^1$), which are less stable than the 4f and therefore easier to ionise. If the electronic configuration of gd^{2+} is $[xe]4f^75d^1$ then the low ionisation energy may be explained in the same way, however there is some contention as to the correct electronic

configuration of gd^{2+}.[2] It may be $[Xe]4f^8$ in which case one f orbital must contain two paired electrons and the increased repulsion between this pair will destabilise the ion and make it easier to ionise. Furthermore there is no loss of exchange energy on ionization of the $[Xe]4f^8$ configuration as the electron that is removed has opposite spin to the other seven f electrons.

The relative stabilities of the divalent ions broadly follow the trend observed for the third ionisation energy of the lanthanides The divalent ions of La, Ce, Gd, and Tb are the exceptions to this general rule and are found to have greater stability than expected. This occurs because of promotion of a valence electron from a 4f orbital to a 5d orbital where it becomes stabilised by the ligand field. For the La^{2+} ion, the 5d orbitals lie below the f orbitals in energy and thus the valence electron 'naturally' occupies the 5d orbital ($[Xe]5d^1$). For the following element, Ce, the 4f orbital have contracted to an energy state below the 5d orbitals. However when the Ce^{2+} ion is subjected to the ligand field, it become energetically favourable to promote one electron to a 5d orbital where it becomes stabilised.

Practically however, most of the divalent Lanthanide ions are extremely unstable, with disproportionation or electron transfer to other substrates providing facile decomposition routes. Well defined divalent coordination chemistry is restricted to the compounds of Sm, Eu and Yb. Increased interest in this field had led to reports of complexes containing Ce, Nd, in their divalent state[15][16] $\{K(DME)\}2Ce(COT)_2$ and $\{K(THF)_n\}2Cp^*2NdCl_2$. The supporting characterising data in these reports is insufficient to say definitively that the species contain Ce^{2+} and Nd^{2+} respectively. The complex $TmI_2(DME)_3$ prepared by comproportionation of thulium metal with TmI_3, has however, been crystallographically characterised[17] and EPR spectroscopy on the reaction between $La(C_5H_3\{SiMe_3\}_2)_3$ with potassium in DME has identified an

La(II) compound.[18]

For all the lanthanides, the fourth ionisation energy is greater than the sum of the first three ionisation energies and is in general prohibitively large. The 4f orbitals become contracted into the core with increased positive charge at the nucleus, the remaining 4f electrons are so tightly held as to be chemically inaccessible. Cerium however, has a well defined tetravalent chemistry. The electronic ground state configuration or Ce is $[Xe]4f^{1}5d^{1}6s^{2}$ hence the Ce(IV) ion possess a f^{0} electronic configuration.

Finally, there are several reports of zero-valent Lanthanide compounds. These include the carbonyl species $Ln(CO)_n$ (n = 1- 6), which are only stable at very low temperatures and a series of compounds with unsaturated hydrocarbons such as hex-3-yne and butadiene. The latter complexes reportedly display very different properties from the typical trivalent compounds in as much as they display different colours, have low coordination numbers and different NMR behaviour. The condensation of Lanthanide metals with bulky arenes such as 1,3,5-tri(Bu^{t})benzene has afforded the first definitive examples of zero-valent Lanthanide complexes.[19],[20],[21] [Gd(1,3,5-tri-(Bu^{t})benzene)$_2$] has been characterised by X-ray crystallography as a monomeric sandwich structure with staggered Bu^{t} groups.

Thus many of the lanthanides can potentially exist in oxidation states other than the classical trivalent state. However although well characterised divalent ions of Sm, Eu, and Yb are known, the corresponding zero-valent species of these metals are among the most stable, in other words, two electron redox reactions at these metal centres are highly unlikely.

Bonding Considerations in Lanthanide Complexes

The metal-ligand nature of the bonding for lanthanides differs significantly to that of most transition metals. The valence d-orbitals of transition metals are radially extended and thus allow covalent metal-ligand bonding through the donation of electron density from a ligand into vacant metal d-orbitals, or through back donation of metal electron density from the d-orbitals into suitable ligand orbitals. This explains the strong, directional transition metal-ligand interactions.

For an incoming ligand, lanthanide ions have the appearance of a noble gas atom, except with a positive charge. The 4f orbitals are much more radially contracted than the transition metal d-orbitals and whilst the orbitals are of typical valence energy and may be capable of overlap with an incoming ligand orbital, their limited radial extension prevents this. The 5s and 5p core orbitals visible to the orbitals of a potential ligand are too high in energy to interact significantly with the ligand orbitals. The 5d orbitals differ slightly in energy and there is a possibility that they may be available for overlap with incoming ligand orbitals. As a consequence, the complexes formed are held together largely by electrostatic interactions and the coordination geometry of lanthanide complexes is determined not by ligand field effects as is the case with transition metal complexes but rather by the maximisation of electrostatic interactions between the metal and the ligand and the minimisation of inter ligand repulsions.[22] In order to maintain optimum metal-ligand interactions, the lanthanide contraction frequently causes changes in structure and coordination number to occur across the Lanthanide series. To illustrate this, in the anhydrous tri-bromides, the largest metals are nine coordinate (Ln = La, Ce, and Pr), they are eight coordinate for Nd, Pm, Sm and Eu and for the smallest lanthanides (ln = Gd, Tb, Dy, Ho, Er, Tm, Yb, Lu, and Y) they are six coordinate.

Interestingly, even without the directional influence of covalent interactions, there are a number of lanthanide compounds that adopt some

surprising geometries. For example, the divalent decamethyllanthanocenes, [Cp^*_2Ln] (Ln = Eu, Sm, Yb.) deviate from the expected sandwich structure to a bent geometry. Although several explanations for this phenomenon were offered, calculations based on molecular mechanics force fields show that the bent geometry in many metallocene complexes is likely to be due to the Van der Waals attractions between the Cp^* ligands.[23][24] All the postulated theories for this bent geometry agree that the potential surface for bending the metallocenes is very shallow, therefore the energy difference between the straight and bent geometries is very small. It should be noted that this unexpected structure is consistent with the bonding being predominantly ionic and does not arise from covalent interactions between the metal and the ligand.

Electronic Spectroscopy of the lanthanides

Ln^{3+} complexes are generally considered not to be as colourful as their D transition metal analogues. There are some exceptions to this; [$Ce\{\eta^5\text{-}C_5H_3(SiMe_3)_2\}_3$] has a strong absorption at 17650cm^{-1}.

For trivalent lanthanide complexes, electronic transitions generally involve only a redistribution of electrons within the 4f sub shell i.e. they occur between the ground and excited levels arising from the ground electronic configuration.[25] There are two factors which stop these transitions from being intense. They do not conform to the Laporte transition selection rules and the source and destination orbitals do not get involved in bonding to any great extent.

Laporte transition rules

In order to undergo an electronic transition, the dipole integral between (for example) ground and excited states must be non zero:

$$\langle \psi^{excited}_{l' m_{l'}} | \bar{x} | \psi^{ground}_{l m_l} \rangle \neq 0$$

Taking the nuclear centre as the origin of a Cartesian coordinate system, then the dipole operator, **x**, has inversion symmetry about the nuclear centre, i.e. **x** is an odd function. The effect of multiplying the ground state by x is to change its underlying *l* character by +1, which in turn means that

$$|x| \psi^{ground}_{l m_l} \rangle$$

now is effectively

$$|\psi^{ground}_{l+1 m_l} \rangle$$

which gives rise to the orthogonality relation

$$\langle \psi^{excited}_{l' m_{l'}} | \psi^{ground}_{l+1 m_l} \rangle = \delta_{l' l+1}$$

The above equation is a statement of the Laporte selection rule. The above treatment assumes that the electron wave function is either symmetric or anti-symmetric about the nuclear centre. Vibrational coupling can distort this symmetry (or anti-symmetry), so the orthogonality relation above is no longer strictly true

The Laporte selection rules forbid f-f transitions and the rules are not relaxed to any great extent by vibronic coupling as the 4f orbitals are radially contracted and thus remain largely unaffected by any transient lowering of the symmetry around the metal atom due to molecular vibrations. Consequently the intensities of these absorptions are low and as many of these electronic transitions lie within the visible region of the electromagnetic spectrum the colours of Ln^{3+} complexes are typically weak.

The lack of ligand - 4f orbital interaction means the f-f transition energies for a given Ln^{3+} do not vary significantly with a change in coordination environment hence the colours of Ln^{3+} are often characteristic. A further consequence of the small orbital/ligand interactions is that f-f transition energies are well defined leading to sharp bands in Ln^{3+} electronic absorption spectra.

The divalent lanthanide ions, with their smaller positive charge, have more destabilised f orbitals with respect to those in Ln^{3+} and hence they lie closer in energy to the 5d orbitals. Absorption of visible radiation generally corresponds to 4f-5d transitions. These bands are allowed by the Laporte selection rules and are thus far more intense than the Ln^{3+} absorptions, they are also much broader and the transition energy is more sensitive to the ligand environment of the metal since the 5d orbitals have a far greater radial extension than the 4f orbitals. It should be noted that in some trivalent complexes, the ligand field stabilisation of the 5d orbitals is sufficient to cause a much more intense orbitally allowed 4f → 5d transition in the visible region of the spectrum.

Magnetic properties of the lanthanides

Angular momentum

Magnetic physical observables are derivable from J, the total angular momentum. It leads to expressions for bulk magnetic properties of compounds containing the atoms or ions in the specified electronic state.

For Ln^{3+} the total angular momentum is calculated using the L-S, or Russell Saunders, angular momentum coupling scheme.[25]This scheme, as opposed to J-J coupling, supposes that the coupling effects are only really observable when the electron orbital angular momentums couple first. Thus in order to produce measurable effect they must couple mostly in parallel (the same applies to the electron spin angular momentum, which are coupled first). This then implies that less coherent coupling is easily swamped by other electronic effects such as inter-electronic repulsion and will not be observed. Or said another way that the spin-orbit coupling strength is small compared to other electronic effects.

For L-S couplings all orbital angular momenta are coupled together, and so are the electron spin angular momenta:

$$\vec{L} = \sum_i m_l^i$$

$$\vec{S}=\sum_i m_s^i$$

and then the results summed using the relevant Clebsch-Gordon coefficients to produce the total angular momentum vector $\vec{J}$.

$$\vec{J}=\vec{S}+\vec{L}$$

specifically

$$\vec{J}=\vec{L}+\vec{S}, \vec{L}+\vec{S}-1, ..., |\vec{L}-\vec{S}|$$

The ground state configurations of Ln^{3+} with the valence shell less than half full have

$$\vec{J}=\vec{L}-\vec{S}$$

With other higher energy states inaccessible at reasonable values of kT. The ground state configurations of Ln^{3+} with the valence shell more than half full (including the $4f^8$ configuration) have

$$\vec{J}=\vec{L}+\vec{S}$$

Magnetic susceptibility

Now J can be determined the bulk magnetic susceptibility, χ, given by the Curie law[26] is

$$\chi=\frac{N_A g_e^2 \mu_B^2}{4kT} J(J+1)$$

N_A is the Avogadro number

g_e is the free electron g-factor

μB is the Bohr magneton

k is the Boltzmann constant

T is the temperature

However this only applies to a magnetically dilute sample and predicts a reciprocal relation with temperature, with χ tending asymptotically to zero as T approaches infinity. The more general Curie-Weiss law is used to describe non-magnetically dilute samples above the Curie point T_c.

$$\chi = \frac{N_A g_e^2 \mu_B^2}{4k(T - T_c)} \; J(J+1)$$

Not withstanding, the paramagnetism of a complex is more normally quoted as its effective magnetic moment, μ_{eff}, (in Bohr magnetons), viz:

$$\mu_{eff} = \left(\frac{3}{2} \frac{S(S+1) - L(L+1)}{2J(J+1)} \right) \sqrt{J(J+1)}$$

As stated already excited states in Ln^{3+} are generally too far above the ground state to be accessible at room kT, so the above formula reflects the experimental data accurately. There are exceptions, however: Sm^{3+}, Sm^{2+} and Eu^{3+} are all known to be diamagnetic species.

Nuclear Magnetic Resonance Spectroscopy of Lanthanide Compounds

The NMR spectra of most lanthanide complexes can be observed, given due care and attention and favourable conditions. The resonances are however, often highly shifted and very broad. This complication is due to the intrinsic paramagnetism of the majority of the lanthanides. The only known diamagnetic species are Ce, Y^{3+}, La^{3+},, Lu^{3+} and Yd^{2+}. It has been observed that for ions with 4f shells that are less than half filled, the spin and orbital contributions to the magnetic moment to some extent cancel each other out. Those ions with 4f8 to 4f13 configurations, have additive spin and orbital contributions to their magnetic moment. Therefore compounds of the lighter lanthanides tend to be more suited to investigations by NMR spectroscopy than those of the heavier elements.

The NMR of compounds containing paramagnetic species, such as many of the lanthanide ions, are complicated by the coupling of their electronic angular momentum (J) with that of the NMR active nuclei. This coupling gives rise to a strong chemical shift and causes short lived nuclear excited

states to give rise to broadened NMR peaks in the spectrum.

The NMR of ligands within lanthanide complexes suffer from both of these effects if their state terms indicate a non zero J value (i.e. are not diamagnetic). To better prepare the NMR sample of a lanthanide complex for investigative work, and interpret the subsequent spectrum, the mechanisms of each effect must be known and understood.

Chemical Shift

The first effect, that of chemical shift, is due to the perturbation of the local field experienced by an NMR active nucleus. The angular momentum of the 4f electrons in the lanthanide valance shell produces a considerable local magnetic field which aligns itself with the applied field $\vec{B}_0$ (i.e. is paramagnetic) resulting in a greater energy level splitting of the ligand nucleus and hence a chemical shift of all NMR peaks associated with that active nucleus. As such it is usually only the ligand nuclei closest to the lanthanide centre that are affected.

The possible spin-spin splitting between nuclear and electron spins is never observed (even though in theory it is present) because any electrons caught in the dis-aligned spin state when the spectrometers field is applied will relax to re-equilibrate to a Boltzmann distribution very quickly, circa 10^{-13} – 10^{-7}s and once the field is applied, the first magnetically excited state of the 4f electrons is too far way to be easily accessible at normal values of kT. So in any case there will be negligible population in the dis-aligned state to give the expected spin-spin splitting.

The isotropic shift of a resonance (i.e the chemical shift difference between a resonance in a paramagnetic complex and the same resonance in an analogous diamagnetic system) depends on the temperature at which

the spectrum is recorded. If the species is monomeric (i.e the isotropic shift of each resonance is dependant upon just one paramagnetic nucleus) and there is no temperature dependent structural equilibrium, then a plot of reciprocal temperature against chemical shift will be linear. This is known as the Curie-Weiss relationship.[25]

Line broadening

Line broadening is due to the magnetic coupling of the 4f electrons allowing relaxation to occur, which reduces the lifetime of the nuclear spin state to such an extent that the quantum uncertainly principle makes it impossible to determine the energy of the nuclear state accurately. Clearly, then, if the energy of the transition is indeterminate, around some mean, then the NMR peak will be broadened around some average chemical shift, which is what is observed. The processes seems to be T1(spin-lattice) related as the electronic angular momentum cannot couple to an equivalent spin system to allow de-coherence to occur via T2 (spin-spin) processes. However if more than one chemically equivalent ligand nucleus is bonded to the lanthanide then the lanthanide can produce a greater T2 decay constant as well, which only compounds the problem.

Measurement of T1 and T2 relaxation are found in MRI imaging, where tissue image contrast is derived from the T1 and T2 time constants. Here lanthanides are helping to produce better clinical diagnosis; by introducing lanthanide species carried by specifically designed ligands healthy and diseased tissues produce markedly different T1 and T2 relaxation times and so produce clearer contrast on the constructed image.

Chemistry of the lanthanides

The study of lanthanide coordination and organometallic chemistry began in earnest in the 1950's after the development of ion exchange techniques

meant that large quantities of the pure elements were readily available.

The trivalent lanthanide ions are large ions with a high charge to radius ratio. A sterically unsaturated metal centre will be susceptible to attack by donor ligands, particularly those containing oxygen, thus acting as a hard Lewis acid. The lack of covalency in lanthanide complexes means that the metal-ligand bond is highly polarised, causing the ligands to be very basic and susceptible to attack from acids and thus bond formation from lewis acids harder than the Ln(III) ion. It Is for this reason that complexes of the lanthanides are often extremely air and moisture sensitive.

The two main factors that govern synthetic lanthanide chemistry are the high degree of ionicity in the bonding and the large size of the ions. Ancillary ligands should, therefore, be sterically demanding and not require covalent interaction or back bonding for stability. They should also be anionic to balance the metal charge and optimize electrostatic interaction. Bulky ligands can sterically block decomposition of the complex by blocking the coordination sphere of the metal. The first ligands used to stabilise organo-lanthanide complexes were the cyclopenatadienyl and cyclooctatetraenyl class of ligands. Commonly incorporated into the coordination sphere of the metal are chelating ligands, neutral bases and alkali metal halides, depending on the size of the lanthanide ion and the size of the ancillary ligand.

The lanthanides do possess a combination of physical properties such as size, ionisation potential, electron affinity and type of valence orbital which are not seen else where in the periodic table and thus they have been found to have a unique and interesting chemistry. Furthermore, the unique characteristics of f block complexes have required the development of new techniques for investigation into their chemistry and have subsequently led to a number of technological and scientific advances in, for example, medicine and catalysis.

Coordination Chemistry of the lanthanides

The highly charged lanthanide ions are particularly suited to polar environments and therefore the majority of the early lanthanide coordination chemistry was performed in water or other protic solvents. The aqueous coordination chemistry of the trivalent ions is the most readily studied. The divalent lanthanides have a tendency to reduce water to hydrogen whereas the tetravalent ions of neodymium, dysprosium, praseodymium, terbium and cerium, oxidise water to oxygen and only Ce^{4+} is sufficiently kinetically stable to form aqueous coordination compounds.

The lanthanides often have high coordination numbers as a consequence of the large size of the ions. Typical coordination numbers are 8 or 9 although numbers up to 12 have been found. Rapid ligand exchange is also common in lanthanide complexes due to the ionic character of the bonding and hence coordination numbers are not known with great certainty. X-ray crystallographic studies of hydrated lanthanide ions in the solid state generally show tricapped trigonal prismatic structures.

The kinetic instability of lanthanide coordination complexes in aqueous solutions can be overcome to some extent by increasing the thermodynamic stability of the complexes, this can be done by using strongly complexing, chelating and macrocyclic ligands. The chelate effect works on the basis that when one end of a bidentate ligand attaches itself to a metal centre the effective concentration of the other end of the ligand is artificially high thus moving the equilibrium position further to the right. Some O-donor chelating ligands that form complexes with the lanthanides include NO_3^-, which is notable for its high coordination

numbers, oxalate , citrate, tartrate , β-diketonates ($ACAC^-$) and ethylenediaminetetraacetic acid ($EDTA^{4-}$)

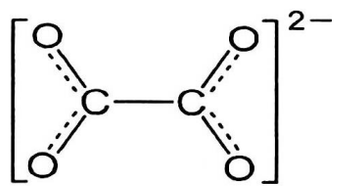

Oxalate

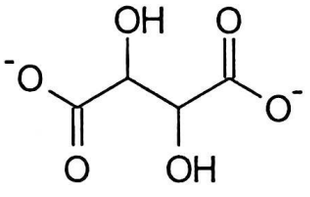

Citrate

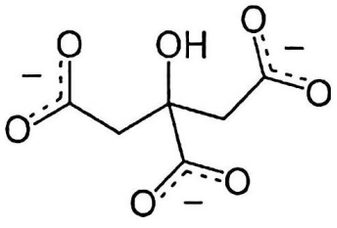

Tartrate

Diketonate

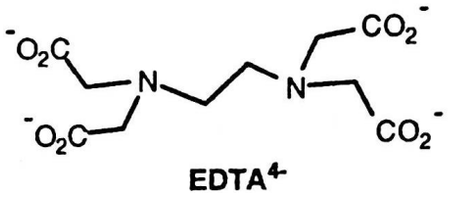

Ethylenediaminetetraacetic acid

Figure 1.4: O-donor Chelating ligands.

To illustrate the stabilizing effect of the chelating ligands, when the bidentate ligand acetylacetonate is used instead of the monodenate chloride ligand the formation constant (K) increases by five orders of magnitude and when moving to the $EDTA^{4-}$ ligand, K increases by 17 orders of magnitude, six water molecules are removed upon complexation leading to a large increase in entropy and a more thermodynamically stable complex.

$$[Nd(H_2O)_9]^{3+} + EDTA^{4-} \longrightarrow [Nd(H_2O)_3(EDTA)]^{-} + 6H_2O$$

The equilibrium constant K, is related to the standard Gibbs free energy ΔG.

$$\Delta G = -RT \ln K = \Delta H - T\Delta S.$$

Where R is the gas constant and T is the temperature in Kelvins, H is the standard enthalpy change of the reaction and S is the standard entropy change. The enthalpy term H is approximately the same for the bond formation in the $ACAC^-$ and $EDTA^{4-}$ complexes, thus the difference between the two equilibrium constants is due to the entropy term.

Macrocyclic ligands such as DOTA4- and 18-crown-6 also form complexes with lanthanide metals. The chelate effect is amplified with these large ligands as they are unlikely to be able to distort themselves so as to remove a ligating atom from the coordination sphere. **Figure 1.5**

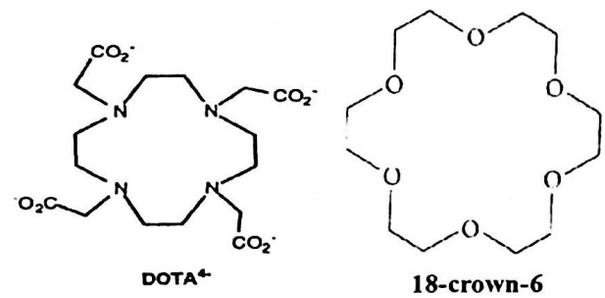

Figure 1.5: Macrocyclic chelating ligands

In more recent years the coordination chemistry of the lanthanides has been modified greatly by excluding water and concentrating on the use of ancillary ligands such as alkoxides and dialkylamines that are compatible with non-aqueous solvents. The resulting complexes have structures and properties more in common with organolanthanide compounds than they do the classical hydrated complexes.

Organometallic Chemistry of the lanthanides

Organolanthanide chemistry has witnessed a spectacular growth during the last two decades and some of the most important advances in understanding the f-elements have arisen from the study of their organometallic complexes. Like the early d-block compounds, f-element organometallics are particularly sensitive to oxygen and water, a problem exacerbated by the large atomic radii of the lanthanides Modern experimental techniques for the rigorous exclusion of air and water and the development of sterically demanding ligands have been responsible for the rapid expansion of this field and the important contributions that organolanthanide complexes can make as catalysts for polymerisation reactions are being realised.[27]

The low radial extension of the f orbitals and ionic character of the lanthanides implies that the chemical behaviour of complexes is determined mainly by electrostatic and steric factors rather than by interactions between the metals and the ligand orbitals. Thus in order to synthesise tractable organolanthanide complexes, ancillary ligands are required to be sterically demanding, form strong ionic bonds and have no dependency on any form of covalent interaction for stability.

The organometallic chemistry of the lanthanide metals has to date been overwhelmingly dominated by complexes containing cyclopentadiene groups. As examples of spectator ligands, cyclopentadienyl ligands rarely take part in chemical transformations, they solubilize and stabilise lanthanide complexes and their steric demand can be finely tuned by the introduction of alkyl group substituents on the ring.

Initial studies were based around the simple unsubstituted C_5H_5 ligand known as Cp. The trivalent complexes Cp_3Ln [28],[29],[30] were isolated soon after ferrocene and preparation of the heteroleptic species $[Cp_2Ln(\mu\text{-}Cl)]_2$ was found possible for the smaller lanthanides (Ln = Sm, Gd, Dy, Ho, Er, Yb and Lu). **Figure 1.6**

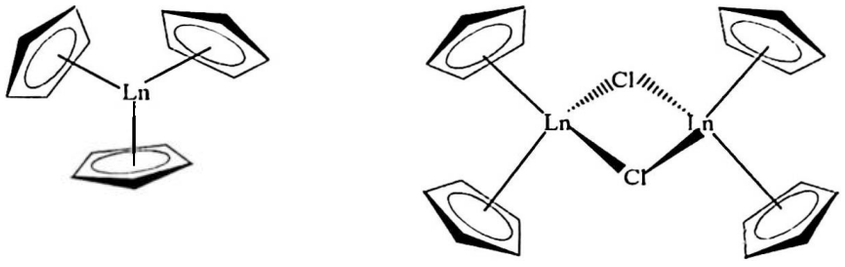

(a) (b)

Figure 1.6: Cp_3Ln (a) $[Cp_2Ln(\mu\text{-}Cl)]_2$ (b)

The combination of ligands shown in Figure 1.6 (b), is insufficiently bulky to sterically saturate the larger lanthanides and for La, Ce, Pr and Nd only the formation of Cp_3Ln was observed.[31][32] In addition to this, lanthanide metallocene complexes with unsubstituted cyclopentadienyl ligands are almost entirely insoluble in hydrocarbon solvents and generally show low activity, conversely the larger pentamethylcyclopentadienyl ligand (Cp*) usually provides excellent solubility and stability for a metal ion and is thus the most widely used ancillary ligand in organolanthanide chemistry.

A general method for the synthesis of a lanthanide metallocene complex is the metathetical reaction between an alkali-metal (M) salt (X) of the ligand and the Lanthanide halide. This route has been employed extensively in the preparation of homo and heteroleptic lanthanide compounds.

$$LnX_3 + n\,MCp \xrightarrow{THF} [\,LnCp_n X_{3-n}] + nMX$$

Ether solvents such as THF are most effective in these reactions, however they themselves are powerful ligands for lanthanide centres and it can often be problematic to remove them from the coordination sphere of the lanthanide compound.

Ligand redistribution can also be a problem in lanthanide systems

depending on the relative solubilities and stability constants of the compounds in a particular system. In salt metathesis, the preparation of the insoluble main group metal halide is usually the driving force, thus the relative solubility of the starting materials and the products is of key importance for this reaction. To illustrate: in equation above, the reagent MCp should be soluble in THF so as to drive the reaction forward and the corresponding alkali-metal salt (MX) should be comparably insoluble in THF, thus shifting the equilibrium to the right hand side. For these reasons lanthanide chlorides and sodium or potassium compounds are often the reagents of choice.

Another common problem with salt metathesis is one in which the isolated reaction products contain one, two or more equivalents of an alkali-metal salt bound within the coordination sphere of the lanthanide metal, resulting in the formation of salt or 'ate' complexes. Salt incorporation tends to accompany solvent coordination at the alkali metal and arises from the need to sterically saturate the lanthanide metal centre and thus tends to be a more important consideration when using larger lanthanides, less bulky ancillary ligands or lithium or sodium reagents. The formation of ate complexes may be prevented by the use of potassium reagents purportedly due to the greater insolubility of KCl in typical organic solvents.[33]-[34]-[35] This has by no means eliminated the problem of salt retention and the phenomenon has been widely observed during the synthesis of lanthanide cyclopentadienyl complexes as well as numerous other lanthanide organometallic compounds.[36]-[37]

Ligands that will stabilize the divalent state must meet similar criteria to those for the trivalent state in as much as they must be bulky and ionic, in addition to this they must be able to tolerate the relatively high reduction potentials of the Ln^{2+} ions, particularly the samarium ion which has a reduction potential of – 1.55 V and whose complexes are consequently the most difficult to stabilize.[38]

The favourable spectator ligand properties of the cyclopentadienyls make them of great use in the synthesis of complexes of the f elements in low oxidation states. Many synthetic routes to divalent organolanthanide complexes now use the Ln di-iodides as divalent precursors.

$$SmI_2(THF)_x + 2\mathrm{Na}(Cp) \xrightarrow{THF} Sm(Cp)_2(THF)_2 + 2\mathrm{NaI}$$

As shown above, the bis(cyclopentadienyl) complex incorporates at least two THF ligands into its coordination sphere which prove to be very difficult to remove. The bulky pentamethylcyclopentadienyl (Cp^*) ligand however, allows the removal of coordinated THF by heating and forms the complex $[(Cp^*)_2Sm]$.

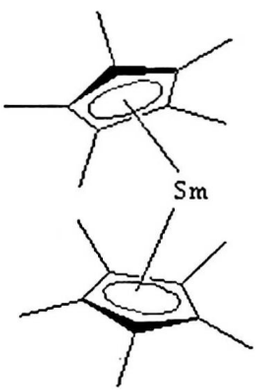

Figure 1.7: structure of [(Cp*)Sm]

Non-cyclopentadienyl organometallic compounds of the lanthanides have also attracted considerable attention, particularly the anionic Poly(pyrazolyl)borate class of supporting ligand.

Poly-(pyrazolyl)borate ligands

The Pyrazolylborate class of ligand was first reported by Trofimenko in

1966.[39] They are borohydride anions in which between two and four of the hydrides have been replaced with pyrazolyl (pz) groups or with a combination of pyrazolyl groups and other substituents. Figure 1.8

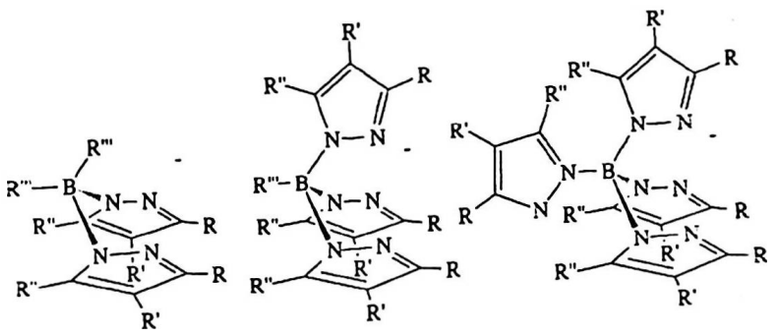

Figure 1.8: Bis(pyrazolyl)borate. Tris(pyrazolyl)borate. Tetrakis(pyrazolyl)borate

These ligands are abbreviated as such: Bp for dihydrido-*bis*-(pyrazol-1-yl)borate, Tp for hydrido-*tris*-(pyrazol-1-yl)borate, and pzTp for *tetrakis*-(pyrazol-1-yl)borate.[40] Substituents on the pyrazolyl ring are indicated by a superscript giving the nature of the group(s) and their position on the ring. The nitrogen directly bonded to the boron is in position 1, the second nitrogen is 2, etc. When two identical groups are indicted but no position is given (e.g. Tp^{Me2}), the pyrazolyl is substituted at the 3-(R) and 5-(R') positions.

The pyrazolylborates are synthesised by direct reaction between the pyrazolyl and alkali metal borohydride at elevated temperatures. Figure 1.9 The degree of substitution is controlled by the temperature and is also dependant on the size of the substituents on the pyrazolyl ring. The the B-N bond is generally formed adjacent to the carbon atom bearing the least sterically demanding substituent.

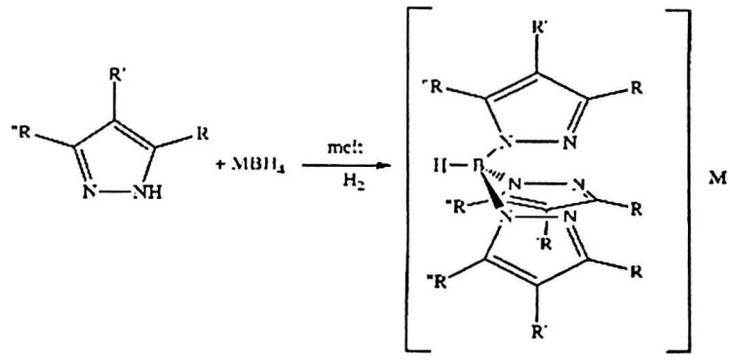

Figure 1.9: Preparation of poly(pyrazolyl)borate ligands

When coordinated in the tridentate binding mode, the tris(pyrazolyl)borates can be compared with the cyclopentadienyl class of ligand in as much as they are both six electron donors, share a uninegative charge, coordinate in a face capping manner and can form complexes with a wide range of metal centres. In fact there exist a large number pyrazolylborate analogues of cyclopentadienyl complexes.

An advantage of the pyrazolylborate ligand is the potential to tailor the ligand with specific properties by adjusting the substituents on the pyrazolyl ring. Using an alkyl group on position 5 of the pyrazolyl ring can provide steric protection for the B-H bond and tightens the bite angle of the ligand at the metal centre, 5-Me groups are often used for this reason. The substituents on position 3 of the ring maybe altered to allow for fine tuning of the steric environment at the metal centre in order to increase the steric bulk of the ligand. They also form a protective cradle around the metal centre which can add a degree of stability to the complex that is not possible with the planar cyclopentadienyl ligands. Its the combination of all the substituents on all positions of the pyazolyl ring that ultimately determines the solubility of the complexes as well as their electronic properties. Cyclopentadienyl ligands on the other hand do not enjoy this degree of flexibility, having only one type of substituent that may be altered.

One of the main objectives in lanthanide coordination chemistry is to sterically saturate the metal centre thus preventing ligand redistribution reactions. Therefore the sterically demanding *tris*-(pyrazolyl)borates are expected to be ideal ancillary ligands for the lanthanides. In addition, pyrazolylborates bind through the nitrogen donor atoms to the metal and thus satisfy the ionic bonding requirements of the lanthanide metals. Being chelating ligands they will be difficult to displace which is important when considering the significant lability of the lanthanide systems. They are also relatively resistant to reduction which will be important when synthesising divalent complexes. They are however less robust then the cyclopentadienyl ligands and have a greater tendency to undergo hydrolysis.

Lanthanide pyrazolylborate complexes

Pyrazolylborates have been used as ancillary ligands for the majority of metals across the periodic table. The first lanthanide pyrazolylborate complexes were reported by Bagnall *et al* in 1976.[41] Since then there have been a plethora of trivalent and divalent lanthanide complexes formed which have been the subject of a review by Santos and Marques[42], and more recently by Marques, Sella and Takats.[43]

Prior to 1993, all of the *tris*-(pyrazolyl)borate lanthanide chemistry reported in the literature was based on the use of the unsubstituted Tp ligand. Reaction of KTp in aqueous solution with the relevant lanthanide chloride afforded the compounds [Ln(Tp)$_3$] (where Ln = La, Ce, Pr, Sm, Gd, Er, Yb, and Y).[41]

$$3\mathrm{KTp} + LnCl_3 \longrightarrow [\mathrm{Ln}(Tp)_3] + 3\mathrm{KCl}$$

IR spectroscopy and solubility test have shown that the structures of the large early lanthanide (Ln=La-Tb) complexes and those of the heavier

metals (Ln=Dy-Lu), are different. For the larger lanthanide, 9-coordinate structures are obtained, whereas the smaller lanthanides are 8-coordinate such as the [$YbTp_3$] complex which displays a bicapped trigonal prismatic structure. Figure 1.10. This structure persists in solution on the NMR time scale. In general the ionic bonding in lanthanide compounds leads to highly fluxional species in solution.

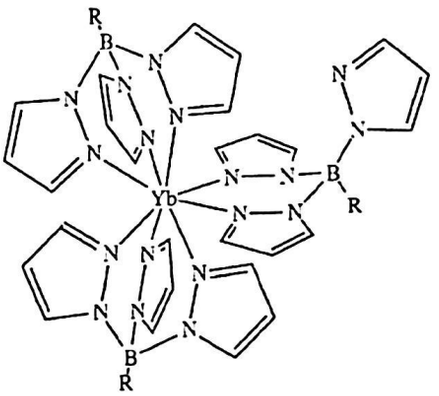

Figure 1.10: Bicapped trigonal prismatic [Ln(Tp*)$_3$] complex

Mixed ligand lanthanide pyrazolylborate complexes [$LnTp_2Cl(THF)$] are prepared by reacting Lanthanide trichlorides with Tp salts of sodium or potassium in a 1:2 molar ratio.[44] There are, however, no structure information available for these THF adducts. Structural characterisation is limited to the water and pyrazolyl adducts [$Y(Tp_2Cl\{L\}$] (L = H_2O, Hpz).[45],[46] These complexes are monomeric with an eight coordinate metal centre. More recently Sun and Wong have prepared the seven coordinate complex [$Nd(Tp)_2Cl$] by metathesis of anhydrous $NdCl_3$ with KTp. When moisture is present however, the eight coordinate aquo complex is formed. This complex has been shown to adopt a square antiprismatic structure by X-ray crystallography.[47]

$$NdCl_3 + 2KTp \longrightarrow [NdTp2Cl] + 2KCl$$

$$[NdTp2Cl] + H_2O \longrightarrow [NdTp2Cl(OH_2)]$$

In similar work, Onishi has synthesised complexes of the type $[Ln(Tp)_2 Cl(L)]$ for the metals Lu, Nd, Yb and Y[48] and have established the complexes of $[Nd(Tp)_2Cl(pzH)]$ and $[Sm(Tp)_2Cl(pzH)]$ by X-ray crystallography.[48]

Attempts to replaced the chloride ligand with other monodentate anions have been blighted by problems with ligand redistribution. The use of bidenate anions such as oxalates, carboxylates and β-diketonates has been more successful. Several eight coordinate complexes with the generic formula $[Ln(Tp)_2(L)]$, where L is a bidenate ligand, have been discovered and this work has been reviewed extensively by Santos and Marques.[42] Takats[49] and Reger[50] have described the synthesis of some related compounds. The samarium complexes $[Sm(Tp)_2(\beta\text{-dike})]$ and the mixed ligand $[Sm(Tp)_2Bp]$ (β-dike = $CH\text{-}(Co)_2R_2$, R = Me, CF_3), were prepared by metathesis from $[Sm(Tp)_2Cl(R)]$ complexes.

Recently there has been a lot of research carried out using the Tp^{me2} ligand, on account of the increased steric control offered by the methyl groups on the 3 position of the pyrazolyl rings. Complexes of the type $[Ln(Tp^{Me2})_2OTf]$ have been prepared by metathesis of $Ln(OTf)_3$ in THF. Some of the series of complexes are soluble in THF whilst others are completely insoluble. In the soluble complexes the triflate anion binds to the metal whereas a salt like structure exists for the insoluble compounds. Chloride complexes with the formula $[Ln(Tp^{Me2})_2Cl]$ are prepared by reacting $LnCl_3$ with Tp^{Me2}, the resulting complexes have been observed to have have a degree of stability in air, posses an intolerance to exposure to moisture and cannot be synthesised form aqueous solution, unlike their Tp analogues. These chloride complexes have been used as starting materials

for the synthesis of the corresponding alkoxides and β-diketonate complexes.[51] Such resulting complexes are eight coordinate, fluxional at room temperature and have C_2 symmetry.

The synthesis of mono Tp and Tp^{Me2} lanthanide complexes has proved to be problematic on account of ligand redistribution reactions. For the unsubstituted ligand there are only two known half-sandwich lanthanide complexes, $[YTpX_2(THF)_2]$ (X = Cl, Br) and $[NdTpI_2(THF)_2]$.[52] Substituents in the 3 position can suppress ligand redistribution thus the vast majority of chemistry has focused on the substituted ligand.

The half sandwich scandium complexes, $[Sc(Tp^{R,Me})Cl_2(THF)_n]$ (R = Me, n = 1; R = Bu^t, n = 0) were prepared by Piers *et al* by metathesis.[53] The corresponding alkyls were prepared by protonolysis in THF.

$$\begin{bmatrix} Sc(CH_2SiMe_3)_3 \\ (THF)_2 \end{bmatrix} + HTp^{R'Me} \xrightarrow[(R=Me,Bu^t)]{SiMe_4} \begin{bmatrix} Sc(Tp^{R,Me}) \\ (CH_2SiMe_3)_2 \\ (THF) \end{bmatrix} + SiMe4$$

Yttrium and Neodymium complexes of the type $[Ln(Tp^{Me2})X_2(THF)_n]$ have been reported in high yields by Bianconi and co-workers. The structure of $[Nd(Tp^{Me2})I_2(THF)]$ was determined and the complex was discovered to have only one coordinated THF. The analogous unsubstituted ligand complex, $[NdTpI_2(THF)_2]$ has two coordinated THF ligands, demonstrating the greater steric demand of the substituted ligand.[52],[54] The ytterbium complex $[Yb(Tp^{Me2})Cl_2(THF)]$ has been reported and structurally characterised.[55] Interestingly, crystallisations of this complex over a long time period produced two compounds, $[Yb(Tp^{Me2})Cl_2(Tpm^*)]$

and [(TPm*)[Yb(Tp^{Me2})Cl_3]. Similar observations have reported for the analogous complexes of Y and Lu.

Derivatising these half sandwich halide complexes with OR^-, Cp^-, Et_2N^- or R^- has eluded many research groups. Bianconi has however reported that addition of LiR in THF (R = Ph, CH_2SiMe_3) yields the corresponding hydrocarbyls for halide complexes with Y, La, and Nd.[48] These compounds are active ethylene polymerisation catalysts as are those using the unsubstituted Tp ligand and the Tp^{Ph} ligand.

$$[Ln(Tp^{Me_2})Cl_2(THF)]+2\text{LiR}\longrightarrow[Ln(Tp^{Me_2})R_2(THF)]+2\text{LiCl}$$

Divalent complexes

Jones and Evans prepared the complexes [Ln$(Tp)_2(THF)_x$] and [Ln(Tp^{Me2})$_2$] where Ln = Sm, Eu and Yb. These complexes were prepared by metathesis and were the first reported divalent complexes with poly-pyrazoyl ligands. The latter substituted Tp complexes were found to be insoluble whereas the unsubstituted Tp complexes demonstrate a suppressed reactivity when compared with the corresponding lanthanocenes. In more recent years Sella , Marques and Takats have reported further studies on these complexes. [43] The insolubility of the [Ln(Tp^{Me2})$_2$] complex made separation from the insoluble potassium halides and purification of the product extremely difficult. Pure Eu and Yb products were isolated by sublimation, however the samarium complex decomposes. A more convenient method involves the reaction between the sodium salt of the Tp^{Me2} ligand and the lanthanide iodide.[56]

$$LnI_2+2\text{NaTp}^{Me_2}\longrightarrow[Ln(Tp^{Me_2})_2]+2\text{NaI}$$

Crystal analysis of these complexes show they are trigonal antiprismatic and are unsolvated. A report by Sella, Takats and Marques discusses in detail the synthesis and structure of these complexes and of the related

complexes $[Ln(Tp^{Ph})_2]$ and $[Ln(Tp^{Tn})_2]$.[51]

Attempts at synthesising the half sandwich complexes containing the Tp^{Me2} ligand have been difficult, Takats *et al* have synthesised and characterised the complex $[Yb(Tp^{Me2})I(THF)_2]$, other groups have however reported an inability to reproduce the experiment. Using the more sterically encumbered ligand: $Tp^{tBu,Me}$, makes synthesis of half sandwich complexes more straight forward. $[Ln(Tp^{tBu,Me})I(THF)_n]$ (Ln = Sm, n = 2; Ln = Yb, n = 1) have been prepared by the reaction of LnI_2 with $Ktp^{tBu,Me}$ and their crystal structures have been determined.[57],[58] The complexes $[Yb(Tp^{tBu,Me})I(3,5\text{-}Me_2pyr)_2]$ and $[Yb(Tp^{tBu,Me})I(CN\text{-}Bu^t)]$ have been prepared by replacing the THF ligand with the pyridine and tert-butylisonitrile groups respectively.[59] Replacing the iodide for another anionic ligand has proved to be more difficult. Some success has been achieved using the potassium reagents $KHBEt_3$, $KCH(SiMe_3)_2$ and $KN(SiMe_3)_2$.[58],[60] The Samarium complex is less amenable to derivatization than the Ytterbium complex, in fact a number of attempts at replacing the iodide ligand has resulted in ligand redistribution and formation of $[Sm(Tp^{tBu,Me})_2]$, presumably as a consequence of the larger ionic radius of Samarium resulting in the coordination sphere being less effectively saturated by the pyrazolylborate ligand.

Preparation of the divalent lanthanide hydrides was attempted by treating $[Ln(Tp^{tBu,Me})I(THF)_n]$ with $KHBEt_3$. however the complex $[Ln(Tp^{tBu,Me})(\mu\text{-}H\text{-}BEt_3(THF)_n]$ was formed in preference to the hydride. Successful preparation of the elusive hydride was eventually achieved by hydrogenolysis of $[Yb(Tp^{tBu,Me})(CH_2SiMe_3)(THF)]$.[61]

$$[Yb(Tp^{tBu,Me})(CH_2SiMe_3)(THF)]+H_2 \longrightarrow [Yb(Tp^{tBu,Me})(\mu-H)]_2 + (2CH_3SiMe_3)$$

Well characterised lanthanide (II) tetrahydroborate complexes are rare[11]

and there are no reported examples of Ln(II) complexes with a single tetrahydroborate ligand accompanied by another anionic ligand. This is due to the large size of the Ln^{2+} ions and the lack of sufficiently bulky ancillary ligands to suppress ligand redistribution reactions.

The availability of the ytterbium hydride complex described above and of the ytterbium iodide complex [($Tp^{But,Me}$)YbI(THF)], has provided effective routes for the synthesis, isolation and characterisation of the mono-ligand Ln(II) tetrahydroborate complexes [($Tp^{But,Me}$)Yb(BH_4)] and [($TP^{But,Me}$)Yb(BH_4)(THF)] described by Takats and Sella [43] These sterically encumbered pyrazolylborate ligands have been shown to be effective ancillary ligands, capable of suppressing ligand redistribution for elements throughout the periodic table, including the lanthanides THF adduct [($TP^{But,Me}$)Yb(BH_4)(THF)] was prepared by salt metathesis using [($Tp^{But,Me}$)YbI(THF)] and the sodium or potassium borohydride. Its solid state structure was determined by single crystal x-ray diffraction. Analysis revealed a monomeric complex with the ytterbium centre bound to the tridenate pyrazolylborate ligand, the triply bridging tetrahydroborate ligand and a THF molecule. Figure 1.11.

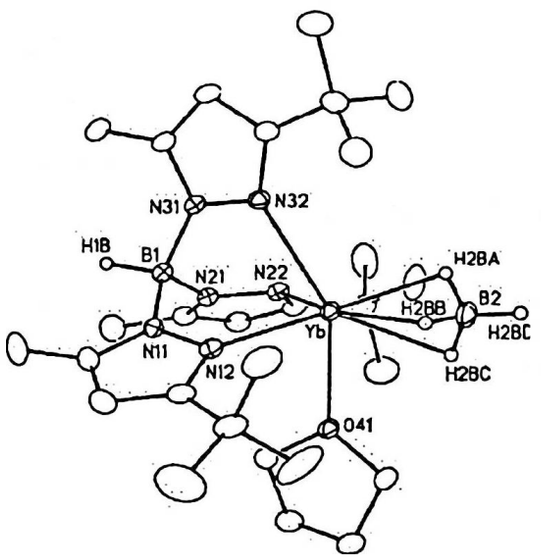

Figure 1.11: Molecular structure of [($Tp^{But,Me}$)Yb(BH4)(THF)]

The $Tp^{But,Me}$ ligand and the BH_4 ligand occupy sites opposite to each other, presumably to minimize electrostatic repulsions between the boron atoms. If one considers the triply bridging BH_4 ligand occupies one coordination site then the complex may be regarded as five coordinate. The geometry is best described as distorted trigonal bipyramidal with two of the pyrazolyl nitrogens (N12 and N22) and B2 forming the equatorial plane. The third nitrogen and the oxygen from the THF occupy the axial positions. Attempts to make the Samarium (II) analogue of this complex have been unsuccessful. This is considered to be because of the greater susceptibility of the larger samarium centre to ligand redistribution reactions.

For more than 90 years, the only divalent states considered accessible for the lanthanides were Eu^{2+}, Yb^{2+} and Sm^{2+}. Since 1997, the number of divalent lanthanides available has doubled to include the much more reducing Tm(II), Dy(II) and Nd(II). Transient observations of Tm(II), Dy(II) and Nd(II) ions in solutions were reported as far back as the 1960's. It was not until 1997 when the synthesis and structure of the first molecular $[TmI_2(DME)_3]$ complex was reported by Evans using the Bochkarev method.

Shortly after $[TmI_2(DME)_3]$ was characterised followed the preparations of $[DyI_2(DME)_3]$ and $[NdI_2(THF)_5]$ [62],[63]

The preparation of heteroleptic Tm(II) compounds, other than solvent adducts have remained elusive, as has the synthesis of Tm(II)-hydrocarbyl species. This is due to the fine balance required between the choice of ligand, solvent and inert atmosphere used. Recently, Takats has described the use of the bulky $Tp^{(But,Me)}$ in preparing heteroleptic Tm(II) species. Addition of $KTp^{(But,Me)}$ to a THF solution of TmI_2 at room temperature in a glove box, followed by a simple work up afforded $[Tp^{(But,Me)}TmI(THF)]$ in a reasonable yield.[61]

$$KTp^{(But,Me)} + TmI_2(THF)_x \xrightarrow[-KI]{THF} Tp^{(But,Me)}TmI(THF)$$

This complex was used as a starting material for a number of heteroleptic Tm(II) complexes. Including the hydrocarbonyl, [Tp(^{But,Me})Tm{CH(SiMe$_3$)$_2$}], [Tp(^{But,Me})Tm{N(SiMe$_3$)$_2$}] and the triethylborohydride complex [Tp(^{But,Me})Tm(μ-HBEt$_3$)(THF)]. Figure 1.12

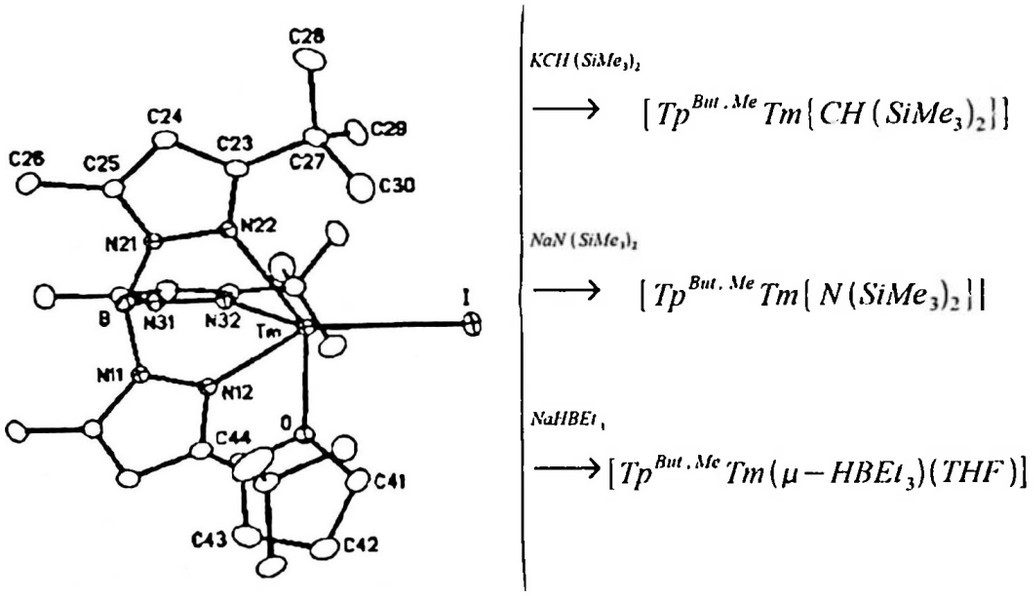

Figure 1.12: Preparation of Tm(II) complexes

The structures of these complexes have all been elucidated crystallographically. Figure 1.13.

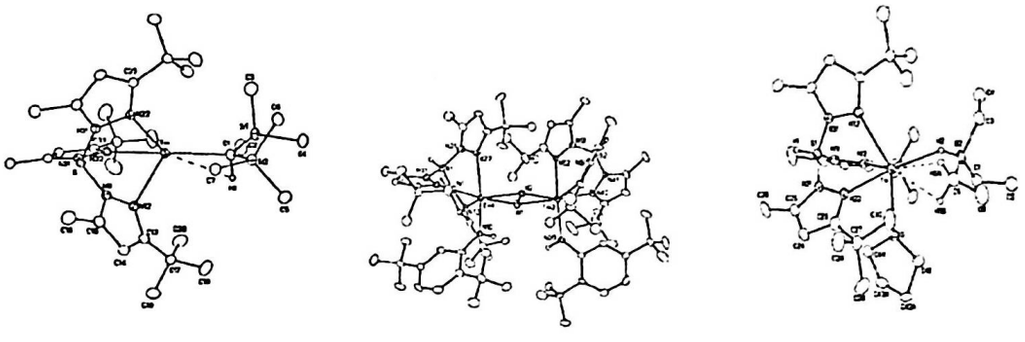

(1) (2) (3)

Figure 1.13: Crystal structures of Tp(But,Me))Tm{CH(SiMe3)2} (1), Tp(But,Me))Tm{N(SiMe3)2} (2) Tp(But,Me))Tm(μ-HBEt3)(THF) (3)

Complex 1 shows a classically bonding tridentate Tp ligand and a virtually planar $CH(SiMe_3)_2$ hydrocarbyl ligand. One $SiMe_3$ group (Si2) is wedged between two pyrazolyl ligands, (N12, N22) the other points towards the Bu^t group of the third pyrazolyl ring. The steric repulsion between the pyrazolyl group and the Bu^t would be expected to contribute to the distorted tetrahedral geometry of Tm. However electronic factors must also play a role. Complex 2 displays a similarly distorted tetrahedron. Complex 3 is one of the very few electropositive metal complexes that contains an intact alkyl borohydride ligand. [64]

Neutral Donor Ligands

In addition to the anionic ligands, a range of neutral donor ligands have been employed in group 3 and lanthanide chemistry. **Figure 1.14**

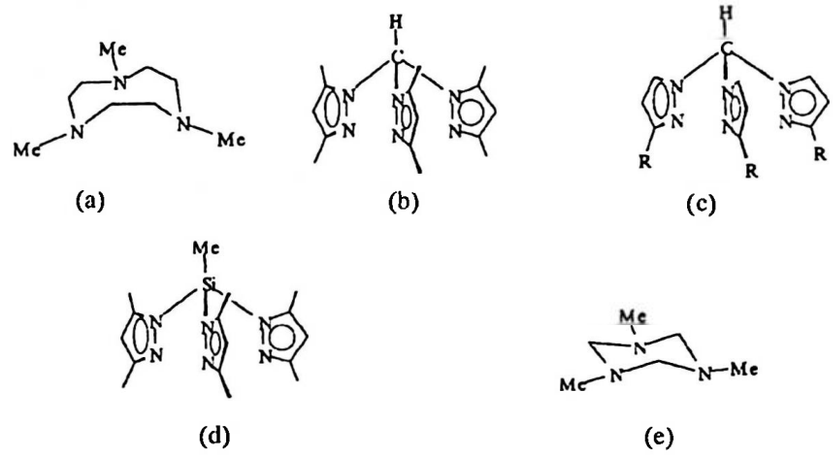

Figure 1.14: Some Neutral N3 Donor Ligands (a) Me3[9]aneN3 (1,4,7-trimethyltriazacyclonane) (b) HC(Me2pz)3(c) HC(Rpz)3 (R = iPr, Ph or But) (d) MeSi(Me2pz)3 (e) Me3[6]aneN3

The first group 3 complexes of 1,4,7-trimethyltriazacyclononane ($Me_3[9]aneN_3$), were reported by Bercaw *et al*[65]. These are the scandium and yttrium complexes: $M(Me_3[9]aneN_3)X_3$ (M = Sc, Y; X = Cl, Me.). Subsequently Hessen *et al* disclosed the triazacyclononane-amide group 3 complexes[66][67]. Figure 1.15. Activation of the yttrium complex with $[PhNMe_2H][BAr^F_4]$ forms a cationic alkyl complex which is active for the polymerisation of ethylene.

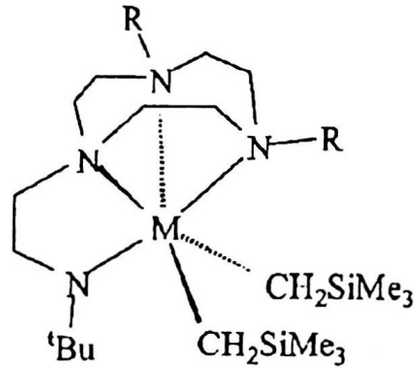

Figure 1.15: M = Y, La; R = Me, iPr

Mountford *et al* have reported that the Scandium complex, $Sc(Me_3[9]aneN_3)(CH_2SiMe_3)_3$ formed highly active ethylene

polymerisation catalysts.[68] recently Mountford *et al* have reported the synthesis and structural characterisation of new scandium and yttrium complexes of Me_3[9]aneN_3 and the preparation of the first group 3 organometallic and coordination complexes of 1,3,5-trimethyltriazacylohexane (Me_3[6]aneN_3) [62] **Figure 1.16**

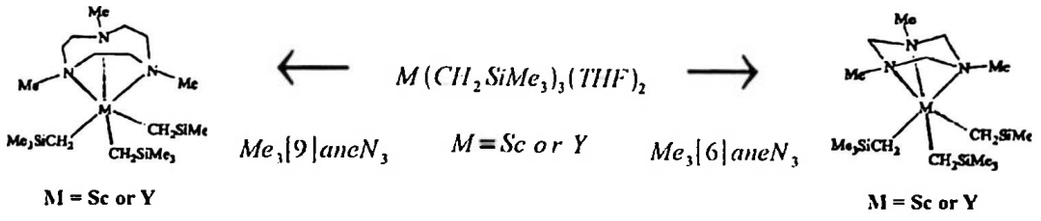

Figure 1.16: Synthesis of new Tris((trimethylsilyl)methyl) complexes of Me3[9]aneN3and Me3[6]aneN3

The complex $[Sc(Me_3[9]aneN_3)(CH_2SiMe_3)_3]$ has been structurally characterised. The crystals contain two independent molecules in the asymmetric unit with no significant differences between them. The geometry at the metal centre is approximately octahedral, there are relatively long distances between the metal centre and the CH_2SiMe_3 groups (average 2.279 Å). This is attributed to the cis-coordinate crowded environment in this compound. The smaller ring size of the 1,3,5-triazacyclohexane ($Me_3[6]aneN_3$) ligands has meant that their coordination chemistry is less extensively developed in comparison to the larger $Me_3[9]aneN_3$ ligands. The first reported rare earth complex supported by triazacyclohexane ligands was the praseodymium species $Pr(Me_3[6]aneN_3)_2(OTf)_3$ and $[Pr_2(Et_3[6]aneN_3)_2(OTf)_4(\mu\text{-}OTf)_3]^+$.[63] Mountford reports that although the structures of the $Me_3[6]aneN_3$ supported complexes of yttrium and scandium have not been formally characterised, they are believed to contain an octahedral metal centre and a face-coordinated Me3[6]aneN3 ligand.

The Tris(Pyrazolyl)methane ligands

Tris(pyrazolyl)methane ligands (Tpm) are the neutral analogues of the ubiquitous anionic tris(pyrazolyl)hydroborates. Figure 1.17

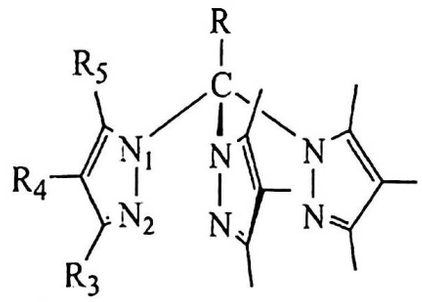

2

Figure 1.17: (Tpm) ligand (R = H)

These ligands are formally derived by replacing the central boron anion with a carbon atom. The unsubstituted ligand (Tpm) was first reported in 1937 by Huckel and Bretschneider, synthesised by the direct reaction of the potassium salt of pyrazole and chloroform.[69] Despite its early reports, the chemistry of the tris(pyrazolyl)methanes is relatively underdeveloped. This is possibly due to the low yields reported by synthetic methods and the multi-stage procedures required to isolate the product. In the mid eighties Elguero *et al* developed an improved method of synthesising tris(pyrazolyl)methane type ligands. This procedure involved the reaction of a pyrazole with chloroform under liquid-liquid phase transfer conditions using K_2CO_3 as a base. Yields of 60% were reported for the substituted ligand Tpm^{Me2}, however the unsubstituted parent ligand Tpm, was only reported in a 24% yield. Reger *et al* have recently reported a high-yielding route for the synthesis of several Tpm compounds[70]. Their method uses standard $CHCl_3$ - H_2O phase transfer conditions and a large excess of Na_2CO_3 as the base. Yields of over 60% were reported for for both the unsubstituted Tpm ligand and for the Tpm^{Me2} ligand. An additional advantage of this modified procedure is the purification stage involves simply washing the product through a plug of silica rather than a full chromatography.

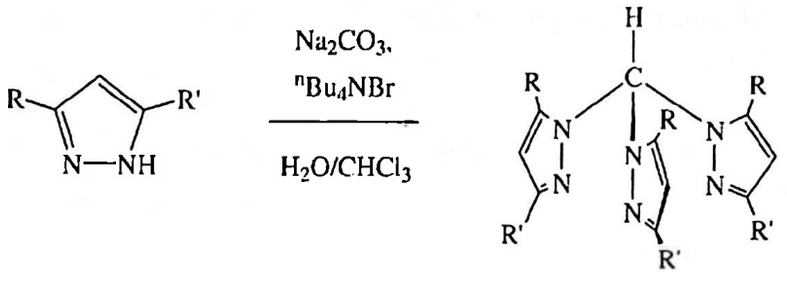

R = R' = H or Me; R = H, R' = Ph, ^{i}Pr or ^{t}Bu

Figure 1.18: Preparation of TPm ligands

Reger and Grattan have also reported a number of tris(pyrazolyl)methane ligands that have been functionalised at the apical carbon atom.[70] An alcohol functional group may be introduced using *para*-formaldehyde and water which serves to increase the hydrophilic nature of the system. Klaui *et al* have reported the tris(pyrazolyl)methanesulphonate ligand which is also hydrophilic and stable towards hydrolysis, these properties make them ideal for use in enzyme modelling.[71],[72]

The most common mode of coordination of the tris(pyrazolyl)methane ligand is that of a tridentate chelate of C_3 symmetry in which they are six electron donors and are isolobal with the Cp ligand.[73] They can however, also act as bidentate ligands.[74] Varying the pyrazolyl ring substituents can effect the geometry of the complexes of the tris(pyrazolyl)methanes, introducing very large substituents in the 3-position of the pyrazolyl rings can prevent the formation of sandwich complexes.[75]

Chemistry of Tris(pyrazolyl)methane ligands

There has been a steady increase in studies into the chemistry of the tris(pyrazolyl)methane complexes in recent years since the development of higher yielding multi-gram synthetic routes to the ligand. To date the coordination and organometallic chemistry of the tris(pyrazolyl)methane ligands has been predominantly centred around the mid to late transition

metals. There are however examples of Tpm complexes from other groups in the periodic table.

Reger *et al* have reported on the reaction of $LiBH_4$ and $NaBH_4$ respectively with Tpm. [76],[77]

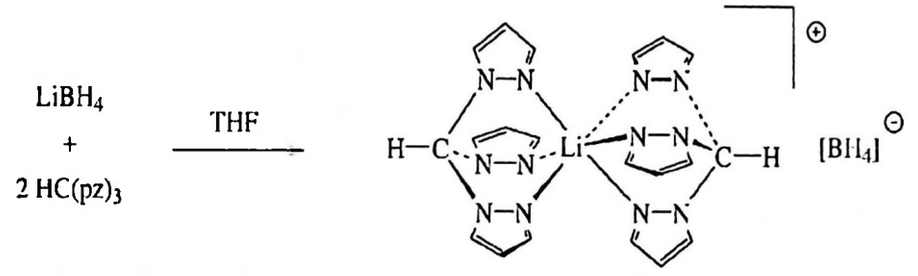

Figure 1.19: Reaction of $LiBH_4$ with TPm

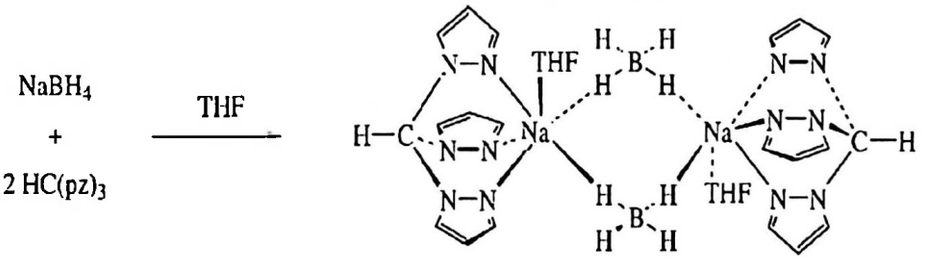

Figure 1.20: Reaction of $NaBH_4$ with TPm

The differenced in structures of the resulting complexes has been attributed to the size difference between Lithium and sodium cations. Reger has also reported the synthesis and solid state structures of several Tpm sandwich complexes of sodium, potassium, calcium and strontium.[78] Interestingly it was only possible to form sodium complexes with both the Tpm ligand and the Tpm* ligand. For calcium and strontium only the Tpm complexes could be formed, whereas potassium formed complexes only with Tpm*.

Group 3, 4 and 5 Tpm complexes are rare. Mountford and co-workers have a recently reported the reaction between scandium and yttrium trichloride and TPm in THF.[62] The C_3 symmetrical complexes $[MCl_3(TPm)]$ where M = Sc or Y, were formed. Reaction of the scandium

complex with ^{n}BuLi in THF forms the zwitterionic compound $[ScCl_2(THF)(TPm^*)]$. The disubstituted ligand, Tpm^{Me2} reacts with complexes of the type $[MR_3(THF)_2]$ (where R = CH_2SiMe_3 or Ph), to form the thermally sensitive species $[MR_3(TPm^*)]$ (where M = Sc and R = CH_2SiMe_3 or Ph, M = Y and R = CH_2SiMe_3).

Mountford *et al* have synthesised the complex $[Ti(N^tBu)(TPm^*)Cl_2]$ by the reaction of TPm* with $[Ti(N^tBu)Cl_2(py)_3]$ in dichloromethane.[79] Reaction of this complex with one equivalent of MeLi or $LiN(^iPr)_2$ in THF leads to the formation of a zwitterion: $[Ti(N^tBu)(TPm^*)Cl(THF)]$. Reaction of the imidotitanium compound $[Ti(N^tBu)Cl_2(py)_3]$ with $Me_3SiOCH_2C(pz)_3$ afforded the complex $[Ti(N^tBu)\{Me_3SiOCH_2C(pz)_3\}Cl_2]$.[80]

Vanadium(II) complexes are scarce due to the poor acceptor ability of the ion and the high sensitivity of the complexes to water and oxygen. Mani and co-workers have prepared the vanadium(II) sandwich complexes $[V(TPm)_2][X]_2$ (X = Br or PF_6) and $[V(TPm)_2]_2[V(NCS)_6]$. [81].

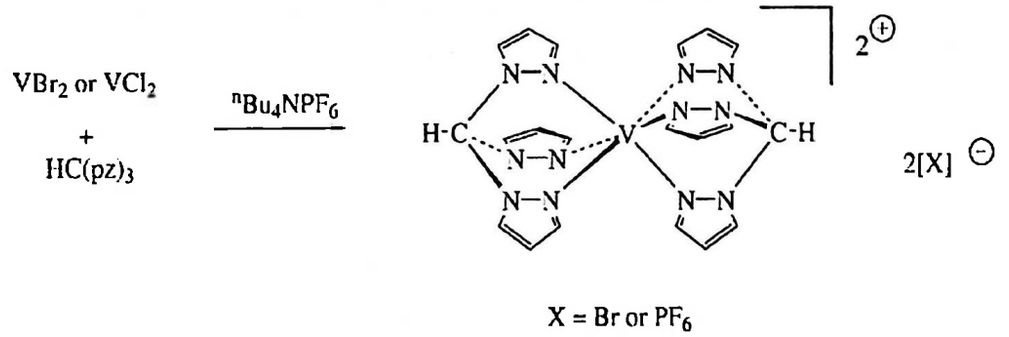

Figure 1.21: Preparation of $[V\{(TPm)_2][X]_2$ (X = Br or PF_6)

There have also recently been a series of VFe_3S_4 clusters with tris(pyrazolyl)methanesulphonate capping ligands.[82] In the mid nineties Otero *et al* synthesised the niobium complexes $[NbCl_2(L)\{HC(R_2pz)_3\}][BF_4]$ (where R = H and L = C_2Ph_2 or C_2Me_2 or R = Me and L = C_2Me_2).[83] In the complexes supported by the unsubstituted TPm ligand, NMR studies show that rotation of the alkyne moiety is fast on the NMR time-

scale whereas no such rotation of the alkyne is observed by NMR for the complex containing the disubstituted Tpm^{Mc2} ligand.

In 1970 Trofimenko reported on the reaction of group 6 hexacarbonyls with the unsubstituted Tpm ligand to form the insoluble compounds $[M(CO)_3(TPm)]$ where M = Cr, Mo or W. [84]

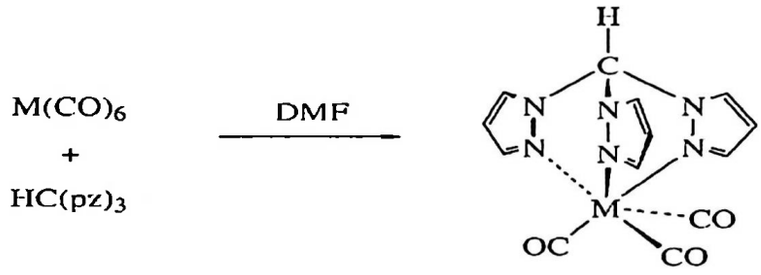

M = Cr, Mo or W

Figure 1.22: Preparation of $[M(CO)_3(TPm)]$ where M = Cr, Mo or W

Stone and co workers have used the molybdenum complex as the starting material in the synthesis of a number of Tpm* supported molybdenum and tungsten supported carbyne complexes.[85][86] Enemark *et al* have prepared the dimolybdenum complexes $[Mo(TPm^*)(O)(\mu\text{-}O)_2Mo(O)Cl_2]$. (a) . $[Mo\{(TPm^*)(O)(l\text{-}O)_2\ Mo(O)(1,2\text{-}O_2C_6H_4)\}]$ (b) Figure 1.23 Also the mononuclear $[MoI_3(TPm^*)]$ in (c) .[87] **Figure 1.23.**

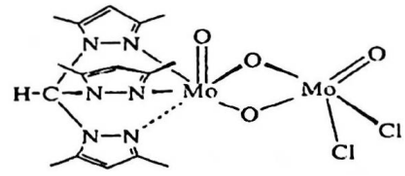

9

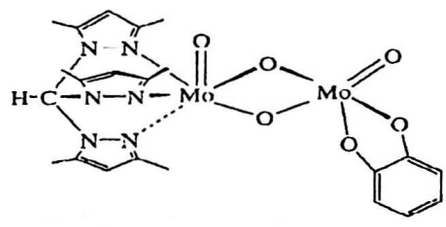

10

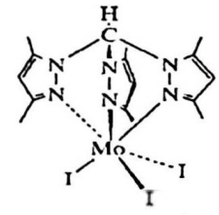

11

Figure 1.23: Mo TPm* complexes. As labeled 9=(a), 10=(b), 11=(c)

There are no reported technetium Tpm complexes, there are however a few complexes with manganese and rhenium. The manganese complex $[Mn(CO)_3(TPm)][PF_6]$ was one of the first complexes of Tpm reported by Trofimenko in 1970, Reger *et al* have prepared a series of manganese carbonyl complexes supported by Tpm ligands.[84] A similar series of rhenium carbonyl complexes have also been prepared, Gibson and co-workers have reported the structures of $[Re(CO)_3(TPm)][Br]$ and $[Re(CO)_3(TPm)][I]$.[88] Seymore and Brown have synthesised the rhenium (V) complex $[Re\{HC(pz)_3\}(O)Cl_2]^+$ and have demonstrated that oxygen transfer to triphenylphosphine using this complex is approximately 1000 times faster than for the isoelectronic, isoteric complex $[Re(Tp)(O)Cl_2]$. This effect had been attributed to the charge difference of the complexes. [89]

There are a several iron complexes supported by the tris(pyrazolyl)methane ligand. These were first reported in 1970 when Trofimenko reported the complex $[FeCl_3(TPm)]$.[84] More recently Field and Messerle have synthesised the iron(II) complexes $[Fe(TPm)_2][Cl]_2$ and $[Fe(TPm)(NCS)_2]$ and the ruthenium complexes $[RuCl(PPh_3)_2(TPm)[X]$ and $[Ru(CO)(H)(PPh)_3(TPm)][X]$ (where X = Cl or BF_4).[90],[91]

The triply bridged ruthenium complex $[(TPm)Ru(\mu\text{-}O)(\mu\text{-}L)_2Ru(TPm)]^{n+}$ was reported by Evans *et al.*[92] **Figure 1.24**. Later Tiekink and co-workers reported the crystal structure of the related tris(pyrazolyl)methane, oxo-bridged iron(II) complex $[(TPm)Fe(\mu\text{-}O)(\mu\text{-}O_2CH)_2Fe(TPm)]^{2+}$.[93]

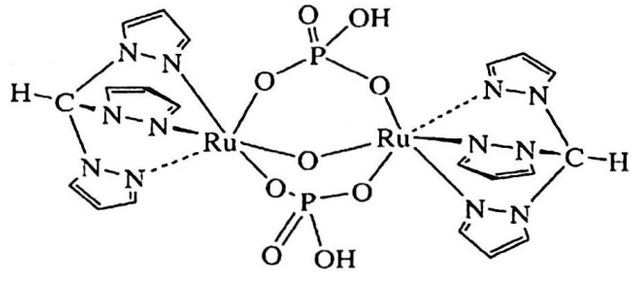

12

Figure 1.24: Molecular structure of [(TPm)Ru(μ-O)(μ-L)₂Ru(TPm)]ⁿ⁺

The above complex 1.24, reacts with an excess of pyridine to afford the

tris(pyridine) complex, $[Ru(TPm)(py)_3]^{2+}$, there are also reports of mixed tris(pyrazolyl)methane and pyridine supported ruthenium(II) complexes.[94] Reaction of [RuCl3(TPm)] with pyridine gives the complex $[RuCl_2(py)(TPm)]$. Tocher *et al* have synthesised several ruthenium(II) complexes supported by the Tpm* ligand and an η^6-arene group.[95] The reaction between TPm and NH_4PF_6 with $[Ru(\eta^6\text{-arene})Cl(\mu\text{-}Cl)]_2$ (where arene = C_6H_6, 1,2,4,5-$C_6H_2Me_4$ or *p*-cymene) in MeCN results in the formation of the dicationic complexes $[Ru(\eta^6\text{-arene})\{(TPm)][PF_6]_2$. In these complexes the Tpm ligand is μ^3- coordinated, if shorter reaction times are used however, the complex $[Ru(\eta^6\text{-arene})\{\mu^2\text{-}TPm)Cl]^+$ is formed, in which the TPm ligand is μ^2 coordinated and Cl^- anion displacement has not occurred fully.[96] It has also been discovered that nucleophillic addition of CN^- to the cation $[Ru(\eta^6\text{-}C_6H_6)(TPm)]^{2+}$ forms the cationic cyclohexadienyl complex $[Ru(\eta^5\text{-}C_6H_6CN)(TPm)]^+$.[97]

Macchioni *et al* have prepared the following cationic iron and ruthenium complexes containing bidentate Tpm ligands: $[M(PMe_3)_2(CO)(COMe)(\mu^2\text{-}TPm)][BPh_4]$, (M = Fe or Ru). This was done during investigations into insertion reactions involving the complexes *tran, cis*-$[M(PMe_3)_2(CO)_2(Me)I]$ (M = Fe or Ru). **(Figure 1.25)** The insertion of the methyl group following the ionic dissociation of iodide can only occur when the ligands can exert moderate steric hindrance.[74]

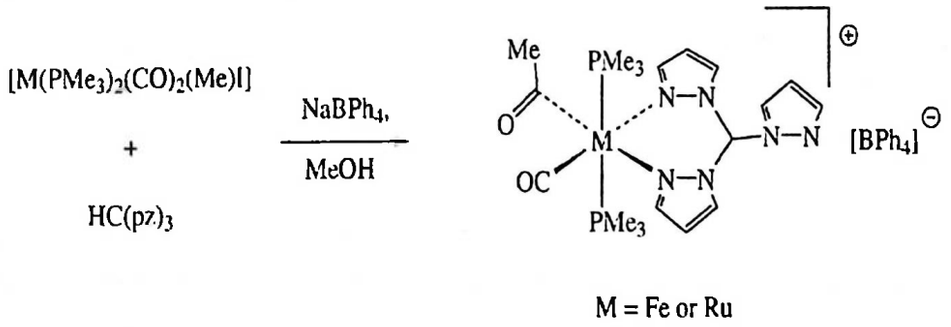

Figure 1.25: Preparation of $[M(PMe_3)_2(CO)(COMe)(\mu^2\text{-}TPm)][BPh_4]$

The first group nine sandwich complexes with the Tpm ligand was

reported by Trofimenko when he described the reaction between Tpm and aqueous solutions of Co^{2+}.[73] **Figure 1.26** The first 'mixed-sandwich' complexes were described by Lalor *et al* in which Co or Rh is bonded to a μ^3-Tpm ligand in addition to a η^5-Cp ligand.[98]**Figure 1.27**

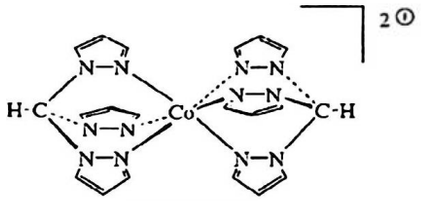

X = I, PF_6 or NO_3

13

Figure 1.26: First TPm group 9 sandwich complex

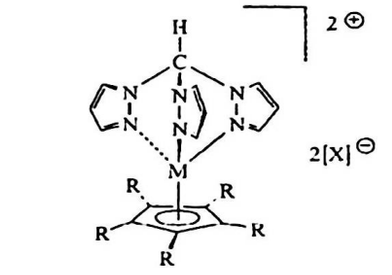

M = Co, R = H, X = I; R = Me, X = PF_6;
M = Rh, R = Me, X = PF_6

14

*Figure 1.27: Mixed ligand sandwich complex Cp*MTPm*

Iridium complexes supported by N-donor ligands have received a lot of attention in recent years due to their use in C-H bond activation reactions.[99] The complex $[Ir(PPh_3)(\eta\text{-}C_2H_4)(TPm)][BF_4]$ is formed by the reaction between $[Ir(\eta\text{-}C_2H_4)_2(TPm)[BF_4]$ and PPh_4 at -78°C. On warming this complex to -10°C, one of the pyrazolyl rings undergoes C-H activation to afford the product $[Ir(PPh_3)(\eta\text{-}C_2H_4)H\{HC(pz)_2(N_2C_3H_2)\}[BF_4]$.[100] There are also reports by Elguero and co-workers of Iridium and rhodium complexes of tris(pyrazolyl)methane incorporating cyclic olefins.[101]

Substitution reactions of the rhodium cationic complex $[Rh(CO)_2(TPM^*)]^+$ have been studied. In solution this dicarbonyl cation exists as a mixture of μ^2 and μ^3 coordinated isomers however when a carbonyl group is substituted with a sterically more demanding substituent ligand, the equilibrium is shifted, favouring μ^2 coordination of the Tpm* ligand.[102] In

2001, Klaui *et al* reported on the photochemical C-H activation of benzene with $[Rh(PMe_3)(CO)\{k^2\text{-}O_3SC(pz)_3\}]$ to afford the rhodium(II) complex, $[Rh(PMe_3)H(Ph)\{O_3SC(pz)_3\}]$.[103]. This complex is subsequently used as a catalyst for the formation of benzaldehyde from benzene and carbon monoxide. Figure 1.28

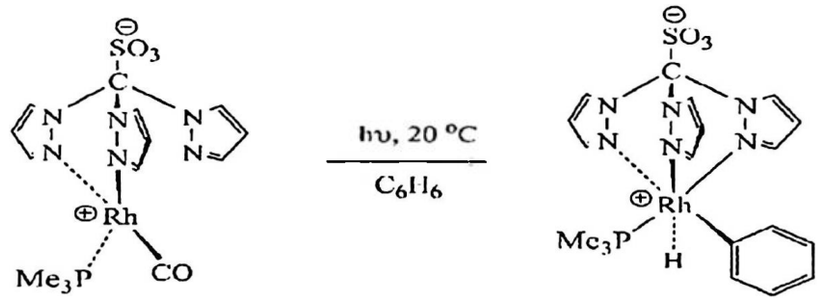

Figure 1.28: Preparation of $[Rh(PMe_3)H(Ph)\{O_3SC(pz)_3\}]$

The sandwich complexes $[Ni(TPm)_2][X]_2$, (where X = Pf_6, I or NO_3), were the first nickel derivatives of the tris(pyrazolyl)methane ligand.[73] Trofinmenko also showed that the tris(pyrazolyl)methane ligand can react with the η^3- allylpalladium chloride dimer, $[Pd(\eta^3C_3H_5)(\mu\text{-}Cl)]_2$ to give the complex $[Pd(\eta^3C_3H_5)\{\mu^2\text{-}HC(R_2pz)_3\}[PF_6]$ (where R = H or Me). Figure 1.29

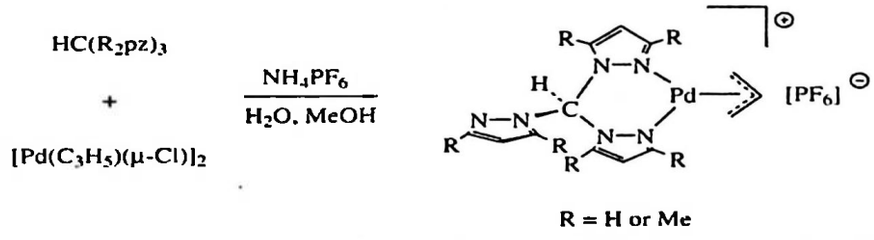

Figure 1.29: Preparation of $[Pd(\eta^3C_3H_5)\{\mu^2\text{-}HC(R_2pz)_3\}[PF_6]$ (where R = H or Me)

These resulting palladium cations are significantly more stable than their analogous neutral tris(pyrazolyl)borate complexes. Flores and co-workers have reported on the neutral square planar Pd(II) complex $[PdCl_2\{\mu^2\text{-}Me_3SiOCH_2C(pz)_3\}]$ and the bis(tris(pyrazolyl)methane complexes $[Pd(TPm)_2][X]_2$ (X = NO_3, BF_4 or ClO_4) were prepared by Canty *et al.*[104] In all of the complexes the tris(pyrazolyl)methane ligand coordinates in a bidentate manner to give square planar geometry. The complex $[Pt(TPm)_2]$

$[PF_6]$ was examined more recently by Connick and co-workers and was found to have a square planar geometry around the Pt atom with the tris(pyrazolyl)methane ligand coordinating in a bidentate fashion, forming a boat conformation.[105] Figure 1.30

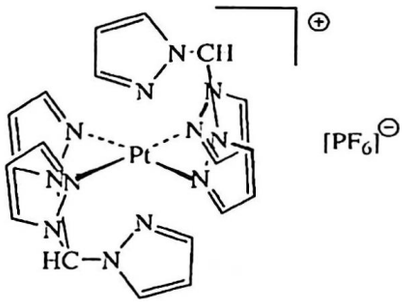

17

Figure 1.30: structure of $[Pt\{HC(pz)_3\}_2][PF_6]$

Canty *et al* have reported on the formation of Pd(IV) and Pt(IV) cations $[M'Me_3\{HC(pz)_3][I]$.[106] When the Platinum complex $[PtMe_2(TPm)]$ is heated in pyridine, metallation occurs on the C(5) position of a pyrazolyl ring to give the complex $[PtMe(py)\{HC(pz)_2(N_2C_3H_2)\}]$.[107] Figure 1.31

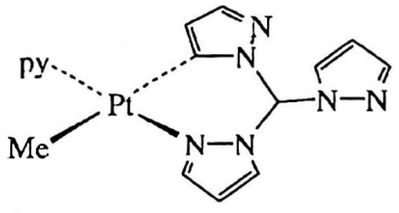

18

Figure 1.31: $[PtMe(py)\{HC(pz)_2(N_2C_3H_2)\}]$

Five coordinate cationic complexes of Pt and Pd olefin complexes have been prepared recently. $[M(\eta^1\eta^2\ C_8H_{12}OMe)(TPm)][PF_6]$. In these compounds the PF_6 counter ion has strong intercations solely with the protons of the pyrazolyl ligands.[108]

Reger and co-workers[109] have reported the first examples of Cu(I) derivatives of tris(pyrazolyl)methane ligands. These were formed by the reaction of $[Cu(NCMe)_4][PF_6]$ with an equivalent of tris(substituted

-pyrazolyl)methane ligand.

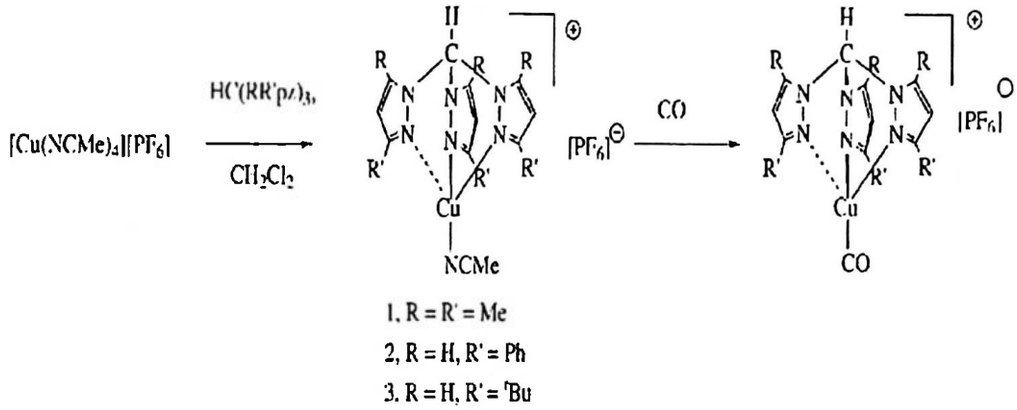

Figure 1.32: Cu(I) derivatives of tris(pyrazolyl)methane ligands

A shown in Figure 1.32, the complexes react with Carbon monoxide to afford the stable $[Cu(CO)\{HC(RR'pz)_3\}][PF_6]$ adducts.[109] Subsequently Murray has demonstrated that $[Cu(TPm^*)(MeCN)][PF_6]$ undergoes reversible oxygenation in dichloromethane to form $[(TPm^*)Cu(\mu\text{-}O_2)Cu(TPm^*)][PF_6]_2$[110] **Figure 1.33**

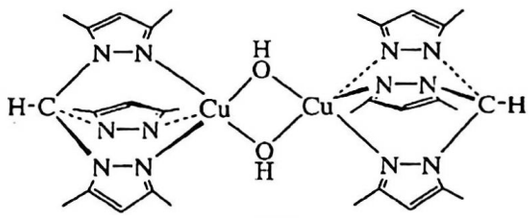

19

Figure 1.33: $[(TPm^*)Cu(\mu\text{-}O_2)Cu(TPm^*)][PF_6]_2$

The first tris(pyrazolyl)methane copper(II) complexes, $[CuX_2(TPm)]$ (X = Cl or Br) were reported by Mesubi and Anumba in 1985.[111] Reactions with oxylate salts formed the complex $[Cu(C_2O_4)(TPm)]$. The tris(pyrazolyl)methane ligand can be displaced by reactions with acetylacetonate, dialkyldithiocarbamate and poly(pyrazolyl) hydroborate salts in aqueous solution.

A number of copper(II) and silver(I) Tpm complexes incorporating oxyanions, for example, ClO_4^- and NO_3^- have been described.[112]The stoichiometry of these complexes is largely determined by the nature of

the counter ion as well as the substituents on the pyrazolyl ring.

Reger *et al,* have reported the cationic tris(pyrazolyl)methane Silver(I) complex from reacting $Ag[O_3SCF_3]$ with the ligand in THF. Reaction with the dimethyl substituted ligand: TPm* ligand forms the six coordinate sandwich complex $[Ag(TPm^*)_2][O_3SCF_3]$. Figure 1.34 The more sterically demanding ligand: $HC(3\text{-}^tBupz)_3$ ligand formed only the mono ligand product $[Ag\{HC(3\text{-}^tBupz)_3\}][O_3SCF_3]$.[113]

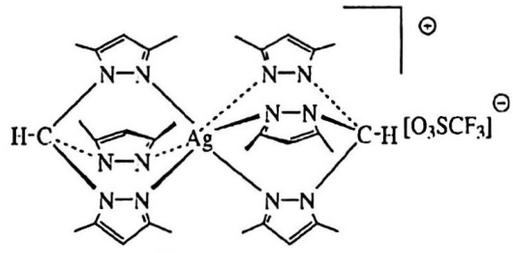

20

Figure 1.34: $[Ag\{HC(3\text{-}^tBupz)_3\}][O_3SCF_3]$

The sole example of a gold complex with a tris(pyrazolyl)methane ligand was reported by Canty *et al.*

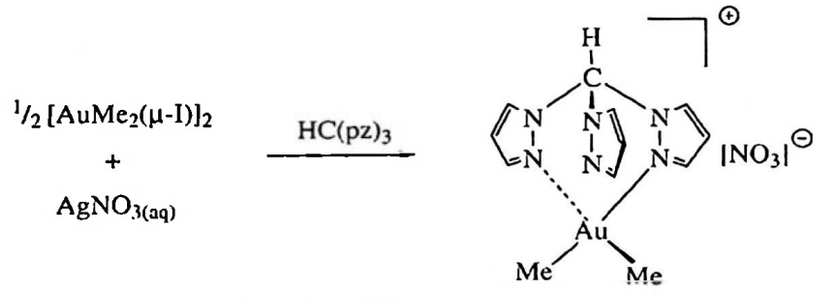

Figure 1.35: TPm complex with Au

The d^8 Au(III) has a square planar geometry and the tris(pyrazolyl)methane ligand is bidenate.[114]

There are a few reports of post-transition metal complexes of tris(pyrazolyl)methane complexes driven by their potential use in bio-organic and medicinal chemistry. There has been only one report of an aluminium derivative $[(AlMe_3)_3(TPm)]$, by Looney and Parkin.[115] Figure 1.36

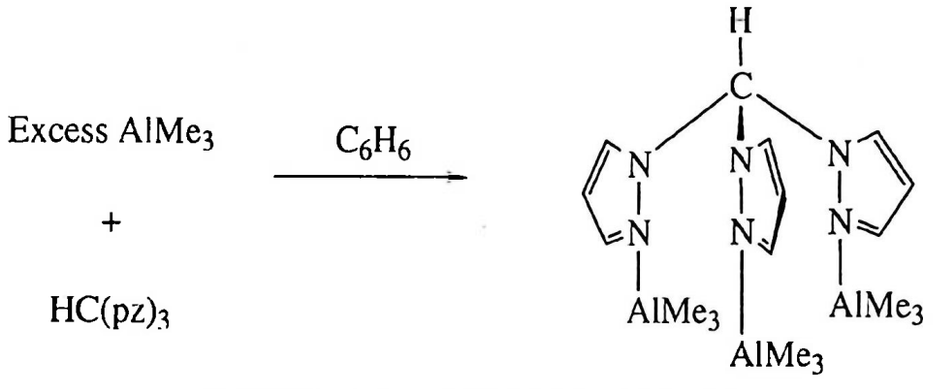

Figure 1.36: Preparation of [(AlMe$_3$)$_3${HC(pz)$_3$}]

Reger and co-workers have reported the sandwich and half sandwich thallium complexes [Tl(TPm*)$_2$][PF$_6$] and [Tl(TPm*)][PF$_6$]. Isolation of a pair of complexes containing one and two tris(pyrazolyl)ligands per metal centre is unusual, NMR studies of a mixture of these complexes in acetone-d$_6$ clearly show individual spectra for each of these complexes suggesting that there is no rapid exchange of ligands on the NMR time scale.[116]

After the discovery that organotin derivatives containing N-donor ligands exhibited anti tumour activity, Pettinari *et al* conducted an research into the coordination chemistry of tris(pyrazolyl)methane ligands with tin(IV) and organotin(IV). The following ligands: HC(pz)$_3$, HC(4-Mepz)$_3$, HC3,5-Me$_2$pz)$_3$, HC(3,4,5-Me$_3$pz)$_3$ and HC(3-Mepz)$_2$(5-Mepz) react with tin reagents to form ion pairs.[117].

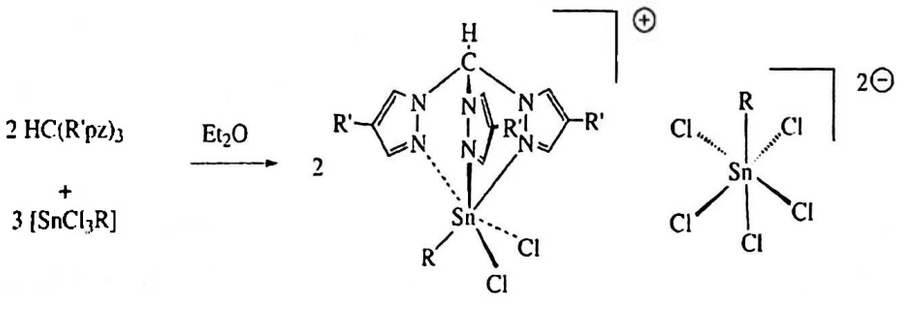

R' = H or Me; R = Me, ^{n}Bu or Ph

Figure 1.37: Sm ion pair

New Chemistry

A number of rules regarding the lanthanides were established from the early studies into these metals. Limited f valence orbital radial extension results in minimal orbital effects. Reactivity is not strongly dependant on f electron configuration and ligand geometries simply need to optimize electrostatic interactions. Whilst one might argue that the characteristics of the lanthanides would not generate any interesting chemistry, an alternative view was that, because these metals are different to the d-block metals they could potentially display unique chemistry, not seen with the transition metals. The special combination of the physical properties of lanthanides as large highly electropositive metals with gradually changing size and limited orbital extension has been the basis for unique chemistry for these elements.

The reactivity of the lanthanides is largely controlled by the choice of ancillary ligand. Ligands of choice are required to be sterically demanding and capable of forming strong ionic bonds. The success of the sterically demanding pentamethylcyclopentadienyl ligand (Cp*) as a suitable ligand for lanthanide centres has long been established. Previous studies in our laboratory have focused on the anionic tris(pyrazoly)borate class of ligand (Tp). Reactions with the unsubstituted Tp were however, plagued by problems with ligand redistribution and the formation of $[Tp_3Ln]$. Increasing the steric bulk of this ligand by adding substituents in the 2 and 6 positions of the pyrazolyl rings have successfully suppressed these reactions and have produced new classes of sandwich and half sandwich lanthanide complexes.

There has been little research into the analogous tris(pyrazolyl)methane class of ligand with regard to anthanide chemistry. Mountford *et al* has carried out research concurrently with ours into the reactions of this ligand with lanthanides[118]. We anticipated that the bulky hydrido-tris(-3,5-dimethylpyrazolyl)methane ligand (TPm*) would be a viable ancillary ligand for the lanthanides

The work presented in this thesis is divided into four chapters. Chapter 2 describes the synthesis of the trivalent anthanide complexes of the hydrido-tris(-3,5-dimethylpyrazolyl)methane ligand (TPm*) and their derivitisation. Chapter 3 largely mirrors the work described in chapter 2, however in this chapter we focus on the divalent lanthanides In chapter 4 we initially describe the preparation of some new fluorinated phenoxide complexes of the alkali metals K and Na and the interesting M-F interactions that these complexes display. The TPm* ligand is then introduced in reactions with the phenoxide complexes. We describe the substitution of the alkali metals for lanthanide ions by metathesis reactions with the appropriate lanthanide chloride in order to tie this chapter in with the previous ones. The experimental details of this work are covered in chapter 5. This study has resulted in a number of X-ray crystal structure determinations. Collection data, fractional coordinates and bond lengths and angles are present in appendix 1.

Chapter 2 Synthesis of Trivalent Lanthanide Complexes of Hydrido-tris-(3,5dimethylpyrazol1yl)methane

Introduction

The disubstituted (TPm^*) was chosen as an ancillary ligand for the lanthanide ions. We anticipated that the steric control afforded to the ligand by the methyl groups would saturate the large lanthanide centres and prevent ligand exchange reactions. In addition to this, the methyl groups provide characteristic proton NMR peaks which helps to identify a complex containing this ligand. This work is complementary to the work carried out previously in our laboratory by Maunder and Hillier. They used the anionic and well established ligand [Tp^*] to form complexes with lanthanides. Direct comparison of the results will allow us to observe similarities and differences between the nature of the binding of the respective ligands to the lanthanide metal centres.

Preliminary studies with the TPm^* ligand focused on its coordination to tri-valent lanthanide ions, prompted largely by the redox stability of this oxidation state. The lanthanide precursors initially chosen were those of the halides. The triflates , $(OTf)^-$ were then employed for their solubility and poor ligating properties. This is particularly important in lanthanide chemistry, to prevent the coordination of unwanted reaction bi-products to the metal centre.

The above compounds are useful starting materials for simple aryloxides. Reaction of $[Ln(TPm^*)Cl_3]$ with $NaOAr^{Mc2}$ produces the expected $[Ln(TPm^*)(OAr^{Mc2})_3]$ in reasonable yields. We attempted these reactions with other substituent groups on the aryloxide ring.

We then proceeded to attempt to prepare some mixed ligand complexes using ligands such as Cp, Tp and BH_4. These reactions had mixed success and gave some fairly uninterpretable NMR spectra.

Preparation of the starting ligand, Tpm*

The first preparation of the tris(pyrazolyl)methane ($HC(pz)_3$ or TPm) was reported by Huckel and Bretcscneider in 1937,[119] by the direct reaction of the potassium salt of pyrazole with chloroform. The isolated yields of the product were low (34%). It has been suggested that carbene associated side reactions may be responsible for such a low yield, since under strongly basic conditions the chloroform is unstable and can lose HCl to form the reactive diradical dichlorocarbene.][120] This radical in turn attacks the unsubstituted pyrazolyl ring positions, resulting in ring expansion reactions.[121][122] More recently Elguero modified this reaction, carrying it out under liquid-liquid phase transfer conditions using K_2CO_3 as a base.[123] The procedure was still hampered by the formation of dichlorocarbene and whilst yields of up to 60% were reported for the preparation of the methyl substituted $HC(3\text{-}Mepz)_3$, the yield for the unsubstituted ligand was only 24 %. Reger *et al* have modified this procedure further. Standard $CHCl_3$-H_2O phase transfer conditions were used, coupled with replacing the K_2CO_3 base with a large excess of Na_2CO_3[1]. For the reaction to go to completion it was carried out over three days in refluxing conditions using tetra-*n*-butylammonium bromide as the phase transfer catalyst. **Figure 2.1**. Under these conditions, yields in excess of 60 % for both the unsubstituted ligand (TPm) and the dimethylsubstituted ligand (TPm*) were consistently observed. The purification procedures were also greatly simplified, rather than a full chromatography, it was found to be sufficient to wash the product through a plug of silica.

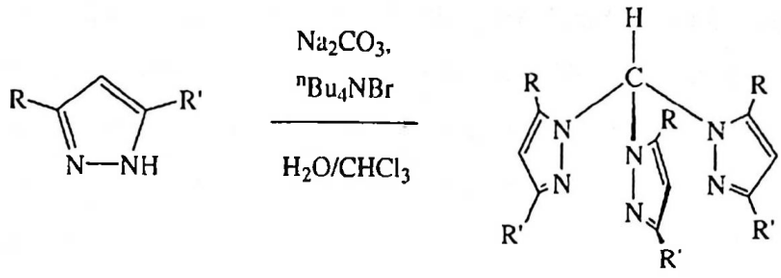

R = R' = H or Me; R = H, R' = Ph, ^{i}Pr or ^{t}Bu

Figure 2.1: Preparation of Tris(pyrazolyl)methane ligand

We carried out large scale preparations of tris(3,5-dimethyl-1-pyrazolyl)methane (Tpm*) following the literature procedure reported by Reger *et al*[124] The product yield was 35 % which is considerably lower than the 65 % reported in the literature. Despite the low yield, the compound was found to be pure by its NMR spectra and its elemental analysis and was thus used in subsequent reactions.

Further attempts at this preparation were less successful. Rather than obtaining a brown solid on removal of the chloroform, red oils were formed. The oils was titrated with 40/60 petrol to remove impurities and form red oily solids. Sublimation of these crude products revealed a large amount of unreacted pyrazole. Dissolving the solid in DCM and passing through a plug of silica afforded a deep red oil on removal of the solvent. Titration of the oil with 40/60 petrol afforded a pure sample of the ligand in less than 10 % yield.

After several attempts at synthesising the ligand it is apparent that the literature procedure is not straight forward to reproduce. During the reflux stage the literature reports an orange/red emulsion, whereas we report a deep red emulsion. Greater discolouration suggests increased impurity and thus in future reactions the 'work-up' may require a full chromatography to increase product yield rather than simply passing through a plug of silica.

Preparation of Ln(TPm*)Cl_3 complexes and their characterisation

Having successfully prepared the analytically pure TPm* ligand. The next stage was to synthesise complexes with lanthanide ions. The lanthanide trichlorides were chosen as the 'starting materials' for reactions. The chlorides make ideal ligands for binding to 'hard' acidic lanthanide metal ions, on account of being small, hard and basic.

The reaction between molar equivalents of anhydrous metal trichloride and the tris(pyrazolyl)methane ligand (TPm*) in polar, dry solvents such as THF or acetonitrile affords the corresponding complexes of the type [Ln(TPm*)Cl_3] (Ln = Y, (**2.1**), Sm (**2.2**), Nd (**2.3**), Yb (**2.4**), and Ce (**2.5**).) in reasonable yields. (Figure 2.2) Initially the ligand and metal chloride were used the ratio 2:1 in an attempt to prepare a sandwich complex. Elemental analysis studies showed that the 1:1 adduct was formed, regardless of the molar ratio of ligand used.

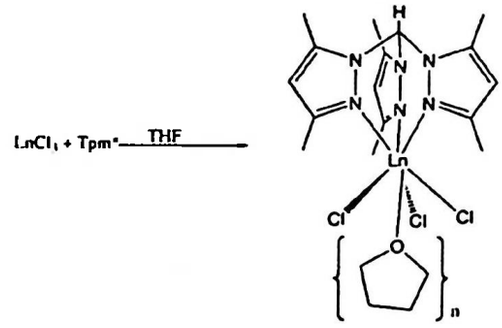

Figure 2.2: The preparation of Trivalent Lanthanide complexes of TPm*

There are several reports of sandwich complexes containing the TPm* ligand and transition metals and metals of the s and p blocks[125]. There have been no previous reports of sandwich complexes containing the TPm* ligand and rare earth metals. The first ever TPm compound of the rare earth was disclosed in a crystallographic report in 2002. This was the monomer: Ce{$HC(pz)_3$}$(NO_3)_4$.[126] Whilst we were carrying out our research into the LnTPm* complexes, we discovered that Mountford and his group were concurrently investigating similar complexes which complimented our work. The recent reports by Mountford *et al* describe the complexes, [Sc(Tpm*)Cl_3], [Y(TPm*)Cl_3], [Sc(TPm*)$(CH_2SiMe_3)_3$] and

$[Y(TPm^*)(CH_2SiMe_3)_3]$ as monomers.[118]

We observed a distinct differences between the solubilities of the complexes in THF, Complex **2.2** demonstrates good solubility in THF and the starting metal halide, $SmCl_3$, dissolved immediately upon addition of the solvent to produce a clear solution. The metal trichlorides of Nd and Ce form
turbid suspensions when stirred in THF, the solids partially dissolved on addition of the TPm* ligand to afford a pale blue suspension and a beige, turbid solution respectively. Complexes of the smaller metal ions **2.1** and **2.4** are virtually insoluble in THF, the preparation of **2.1** was carried out in acetonitrile on account of the complete insolubility of YCl_3 in THF.

Mountford *et al* [118] have reported similar insolubility for the complexes $[M(TPm^*)Cl_3]$ (M = Sc, Y).
In a similar trend, Graham Maunder has observed some interesting solubility patterns for the pyrazolylborate lanthanide complexes $(Tp^*)_2LnOTf$. When Ln = Y, Dy and Yb, the complexes were found to be very insoluble, whereas the complexes with the larger ions lanthanides, Ln = La, Nd and Sm were found to be sparingly soluble.[127] Solid state infra-red studies carried out by Maunder showed that for the complexes containing the lanthanide metals, Y, Sm, Dy and Yb, stretches for the discrete, uncoordinated $[OTf]^-$ anions were observed, suggesting that $Ln(Tp^*)_2$ and the OTf groups exist as ions pairs. Conversely, studies on the complexes with La, Nd, Ce and Pr lanthanide metals show a splitting of the stretching modes in the SO_3 group. This is consistent with a reduction in symmetry from C_3v to C_s which occurs when a triflate group coordinates to a metal, suggesting that these species are molecular. There are contradictions between the experimental observations for the samarium complex. Whilst the solid state IR suggests an ionic structure, the solubility of the complex in non-polar solvents indicates a molecular species. Solution IR spectra recorded in $CDCl_3$ were taken for all the complexes. The complexes of the lighter lanthanides, La, Ce, Pr, and Nd displayed strong absorptions in the region 1203 to 1208 cm^{-1}, this is consistent with the solid state spectra and indicate a η^1- coordinated triflate group. The smaller metals display bands that suggest ion pair structures, again consistent with

the solid state spectra. The solution spectra of the Sm and Eu compounds indicate that both molecular and ion pair species were present in $CDCl_3$ solution. A summary of results is shown in the table below. Table 2.1 . The coexistence of ionic and molecular structures in solution demonstrates the fine balance between steric and electrostatic interactions in lanthanide complexes.

Lanthanide	Kbr Disc ν_{S-O} cm^{-1}	$CDCL_3$ ν_{S-O} cm^{-1}	Implied Structure
La(2.2), Ce†, Pr†, and Nd (2.3)	*ca* 1203	ca1208	Always molecular
Sm (2.4)	1273	1208 1263,1277	Solid: ionic Solution: 70% molecular, 30% ionic
Eu†	1274	1207 1263, 1274	Solid: ionic Solution: 45% molecular, 55% ionic
Gd†, Dy (2.5), Ho†, Yb (2.6) and Y (2.1)	1276	*ca* 1264	Always ionic

Table 2.1: A summary of the IR data for the complexes (TP*)2LnOTf 3

The difference in solubility for our neutral, and thus molecular (Tpm*)$LnCl_3$ complexes appears also to be related to their structures and atomic radii of the metals.[Y(TPm*)Cl_3] (**2.1**) and [Yb(TPm*)Cl3] (**2.4**) are the only complexes that do not appear to coordinate solvent. The greater than expected percentages of carbon and hydrogen in the elemental analysis of the larger complexes suggests that THF is coordinated. The THF does however, appear to fairly weakly bound, recording of elemental analysis on samples heated to *ca* 50° under dynamic vacuum demonstrate a reduction in the percentage of carbon and nitrogen, presumably due to desolvation. The coordination of THF possibly disrupts the crystal packing to an extent that makes the complex soluble. The smaller

lanthanides Y and Yb, are presumably too small to accommodate an additional solvent ligand within their coordination spheres.

^{1}H NMR's of the complexes recorded in acetonitrile clearly display the peaks associated with the TPm* ligand. The tertiary C-H, the three protons in the 4 positions of the pyrazolyl rings and two peaks integrating to 9 protons each for the 3 and 5 methyl groups on the pyrazolyl rings. The spectrum of the samarium complex (**2.2**) show the presence of one molecule of THF. All of the compounds displayed only one set of pyrazolyl resonances and thus are likely to be highly symmetrical. The fact that chemical shifts of the pyrazolyl protons differ to those recorded for the free ligand indicate that the ligand is indeed coordinated to the metal centres. The insolubility of (**2.4**) precluded the recording of an ^{1}H NMR spectra. Infra-red spectra recorded for the complexes as Kbr discs, are very similar, suggesting that the compounds have largely similar solid state structures.

The colours of the lanthanide products were typical of trivalent complexes of these metals: all were white except that of the neodymium complex, [Nd(TPm*)Cl_3] which was pale blue. Crystals of [Y(TPm*)Cl_3] (**2.1**) suitable for X-ray analysis were grown by slow diffusion of a solution of TPm* in acetonitrile into a solution of $LnCl_3$. Crystals of [Sm(TPm*)Cl_3] (**2.2**) were grown by diffusion of solutions of $SmCl_3$ and TPm* in THF sandwiched around a layer of THF.

The molecular structure of 2.1

The complex [Y(TPm*)Cl_3]. (**2.1**), crystallized as six-coordinate molecules in the monoclinic space group P21/n. There are two molecules of acetonitrile contained within the lattice. The molecular structure is shown in Figure 2.3. The Yttrium centre has C_3 symmetry with a geometry that is best described as trigonal antiprismatic.

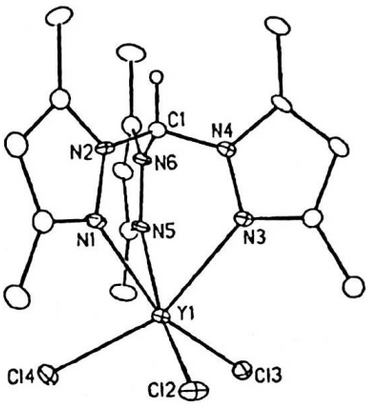

Figure 2.3: The molecular structure of 2.1; hydrogens omitted for clarity.

The structure shows distinct similarities with the related trispyrazolylsilane yttrium complex reported by Mountford *et al*; [Y(MeSi(TPm*)Cl_3][118]. The average metal-chloride distance Y-Cl_{Av} 2.555(2) Å is comparable to those in Mountford's complex (2.568(5) Å) and to that of the tris(pyrazolyl)hydroborate supported anion [Y{HB(TPm*)Cl_3]$^-$ (2.554(4) Å).[128] The Y-N distance, 2.459(2) Å, is also comparable to that of Mountfords pyrazolylsilane (2.464 Å)[118]. Indeed a more detailed comparison with literature data is limited by the scarcity of reported relevant systems. The 'upper' triangle of this trigonal antiprismatic structure is defined by the nitrogens of the TPm* ligand. The average N-Y-N angle in this triangle is 73.8°(2), which is considerably less than the 'lower' triangle as defined by the chloride groups, this is more open with the average Cl-Y-Cl angle, being 100.35°(5). The average yttrium-nitrogen bond length (2.459(5) Å) is generally longer than the corresponding bond distance in the anionic TP^{Me2} analogues, for example in [(Tp^{Me2})YCl_2(3,5-dimethylpyrazole)] is 2.402 (5) Å.[6] Figure 2.4. This is unsurprising as one would expect a weaker interaction between the metal and nitrogen in the neutral ligand in comparison with the anionic TP*. Similar bond distances are noted by Cheng and Takats in their unpublished [($TP^{Me2,Me2}$)Y(CH_2SiMe_3)$_2$(THF)] (bond distance 2.429-2.491 Å).[129]

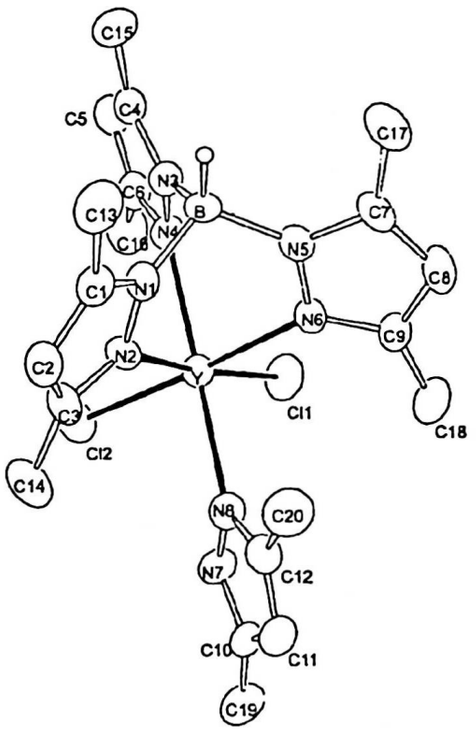

Figure 2.4: Crystal structure of [(TP)YCl2(3,5-dimethylpyrazole)*

The molecular structure of 2.2. (THF)

Unlike the 6-coordinate unsolvated **2.1**, the structure of **2.2**(THF) is seven coordinate, containing a coordinated THF ligand. Figure 2.5. The larger coordination number is likely to be due to the greater atomic radius of Sm in comparison with Y, giving samarium the ability to accommodate an additional ligand within its coordination sphere.

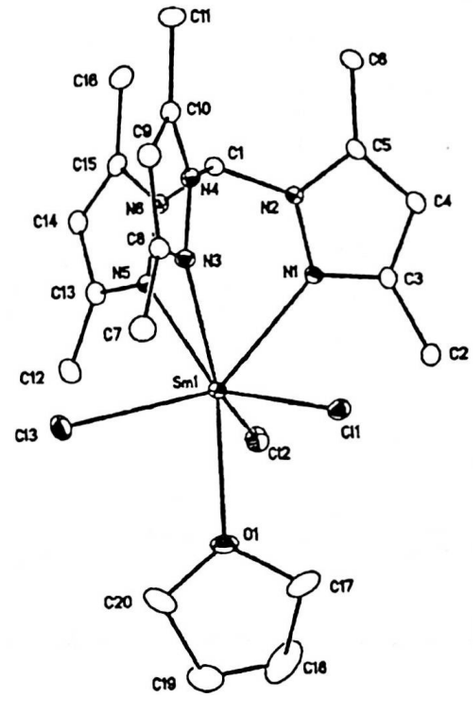

Figure 2.5: The molecular structure of 2.2(THF); hydrogens omitted for clarity.

The average Sm-Cl bond distance is 2.621(2) Å. This is similar to the corresponding bond length reported in the sandwich complex containing the anionic TP*, $[(TP^*)_2SmCl]$ (2.637(3) Å). [130] The complex $[SmCl_3(THF)_4]$ reported by Chen *et al* has a similar Sm-Cl bond length, (2.683(5) Å). [131]

One could describe the coordination sphere of the samarium to be that of a capped trigonal antiprism. In this case the TPm* nitrogens and the chloride groups define the structure. The THF ligand sits along the C_3 axis as described by the TPm* ligand and caps the triangular face of the chloride groups. Figure 2.6. An alternative description of the geometry would be that of a tricapped trigonal pyramid. In this case a pyramid is defined by the THF ligand as the point of the pyramid and the three nitrogens of the TPm* ligand as the base. The chloride groups each cap one of the faces of the pyramid, creating Cl – Sm – O angles of approximately 77°. Figure 2.7.

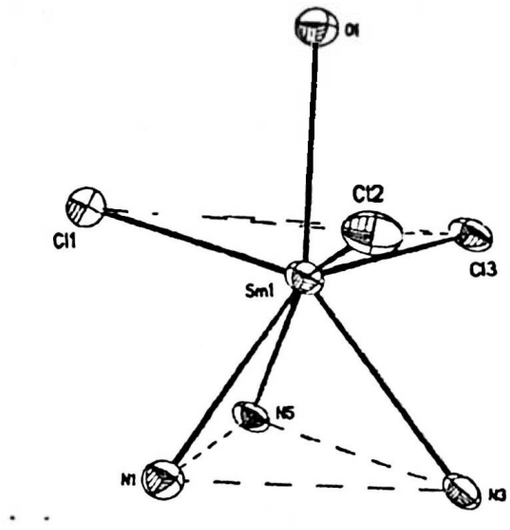

Figure 2.6: [Sm(TPm)Cl3.THF] as a capped trigonal antiprism*

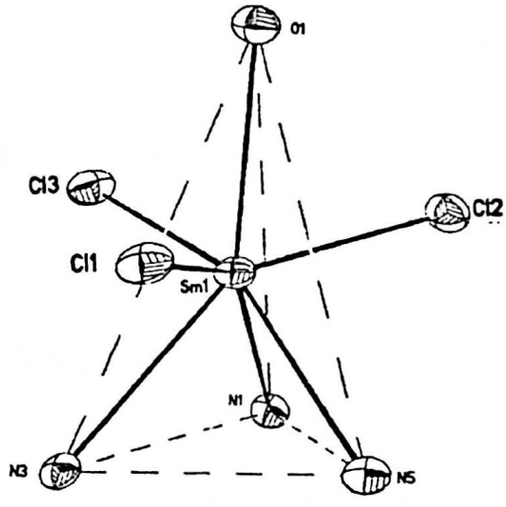

Figure 2.7: [Sm(TPm)Cl3.THF] as a tricapped trigonal pyramid*

Crystallographic studies of some lanthanide complexes of the pyrazolyborate ligands, synthesised in our laboratory have shown similar coordination geometries. The samarium atom in the isocarbonyl complex $[\{Sm(TP^{tBu,Me})(THF)Mo(\eta\text{-}C_5H_4Me)(CO)_3\}_2]$, has a bicapped trigonal pyramidal geometry. Two oxygens of the bridging carbonyl groups form the apex of the pyramid and caps one of the faces while the other face is capped by the THF ligand. In this case the capping

groups are virtually perpendicular to the axial carbonyl. (87.46(6)° and 83.91(9)°).[132] The divalent ytterbium in the complex [$Tp^{3-t\text{-}Bu\text{-}5\text{-}Me}$YbI($Me_2py)_2$] also possesses a bicapped trigonal prismatic geometry, with the Tp ligand forming the base and the iodide being the apex of the pyramid. The nitrogens of the pyridine molecules each cap one face of the pyramid.[127]

As is the case with the six coordinate (**2.1**), the 'lower' triangle in (**2.2**) defined by the TPm* nitrogens is much tighter than the 'upper' triangle defined by the chloride ligands. The average N-Sm-N angle is 70.4(2)° compared with 115.29(6)° for the average Cl-Sm-Cl angle. The average Sm-N bond length in complex **2.2** (2.572(5) Å) is longer than in the six coordinate complex **2.1** (2.469(5) Å). The difference is consistent with an increase in coordination number at the metal centre. The introduction of a THF molecule situated between the three chloride groups widens the angle, Cl-Ln-Cl, from 100.35(5)° in **2.1** to 115.29(6)° in **2.2**.

Attempts to grow crystals of **2.3** ([Nd(TPm*)Cl3]), **2.4** ([Yb(TPm*)Cl3]) and **2.5** ([Ce(TPm*)Cl3]) suitable for of X-ray crystal analysis were unsuccessful. At best semi-crystalline solids were obtained (**2.3** and **2.5**). The ytterbium complex **2.4** afforded only a highly insoluble cream coloured powder.

Preparation of LnTPm* triflate complexes. (Ln(TPm*)$(OTf)_3$

In light of the insolubility of the lanthanide chloride complexes, we opted to prepare a number of lanthanide Tpm* complexes of the trifluoromethanesulphonates (OTf = triflate = O_3SCF_3). The lanthanide precursors ($Ln(OTf)_3$) to these complexes are easy and inexpensive to prepare, involving the reaction of lanthanide oxides with aqueous trifluoromethanesulphonic (triflic) acid followed by dehydration under dynamic vacuum at 200°C.[133] This is in stark contrast to the difficulties associated with preparing the anhydrous trichlorides where strict procedures have to be followed in order to prevent hydrolysis and thus the formation of LnOCl. A number of lanthanide triflate complexes were prepared

by another member of our group and stored in the glove box. The triflate anion is regarded as a 'good leaving group' on account of the stability of the free anion and its poor ligating properties.[134] This reduces the risk of any unwanted by-products remaining coordinated to the metal centre and also makes them potentially good precursors to other complexes such as aryloxides or cyclopentadienyls.[135],[136] Finally the characteristic IR spectrum of the triflate group provides a handle on detecting its presence in complexes and allows one to postulate as to whether the group is coordinated to a metal centre or exists as one half of an ion pair.[137]

Combining lanthanide triflates ($ln(OTf)_3$, ln = Y, Ho, Dy,) with a molar equivalent of TPm* in THF afforded clear solutions in all cases. After stirring overnight and filtering, the volume of the solvent was reduced until the product just started to precipitate from solution. At this point the the flask was placed inside a water bath and warmed until the precipitate redissolved, it was then placed inside a dewar in the freezer for slow cooling. In all cases clear flat colourless crystals formed after approximately 12 hours.

$$Ln(OTf)_3 + TPm^* \longrightarrow Ln(TPm^*)(OTf)_3(THF)$$

$$(Ln = Y\,(\mathbf{2.6}),\ Ho\,(\mathbf{2.7}),\ Dy\,(\mathbf{2.8}))$$

Elemental analysis of all three triflate complexes are consistent for complexes with the formula: [ln(TPm*)$(OTf)_3$(THF)]. The large magnetic moments of Ho and Dy give rise to ^{1}HNMR spectra that are too broad to be interpreted. The ^{1}HNMR spectrum of the yttrium complex (**2.6**) displays the expected pyrazolylmethane peaks. There are two sets of multiplets at δ 1.84 and 3.67 ppm respectively that integrate to four protons each and have been assigned to the presence of THF in the complex.

The solid state IR spectra for all three of the triflate complexes as KBr discs, afforded us additional information regarding the structure of these compounds. All three compounds have strong absorption bands at 1207 cm^{-1} . When the triflate

exists as a free ion ,$[O_3SCF_3]^-$, the SO_3 stretching frequencies appear at *ca* 1032 and 1273 cm^{-1} and are the symmetric and antisymmetric modes respectively.[17] However when coordinated in a unidentate arrangement, the antisymmetric band is characteristically shifted to approximately 1210 cm^{-1}. Thus the observation of bands at 1207.4 cm^{-1} is a very strong indication of η^1 coordination of this ligand and thus as expected, a molecular species.[137] This is in contrast to the ion pair arrangement observed by Maunder for the complexation of lanthanide triflates (ln = Yb, Dy, and Ho) with the anionic trispyrazolylborate ligands. **Table 2.1**.

In addition to the triflate bands, the IR spectra also contain many absorptions due to vibrations within the pyrazolylmethane ligand, some of these bands appear to be masked by bands associated with the triflate ligand when the spectra is compared to that of the free TPm* ligand. The spectra of all three of the triflate complexes are virtually super-imposable suggesting that the metal has little affect on the vibrations within the TPm* ligand. **(Figure 2.8)**

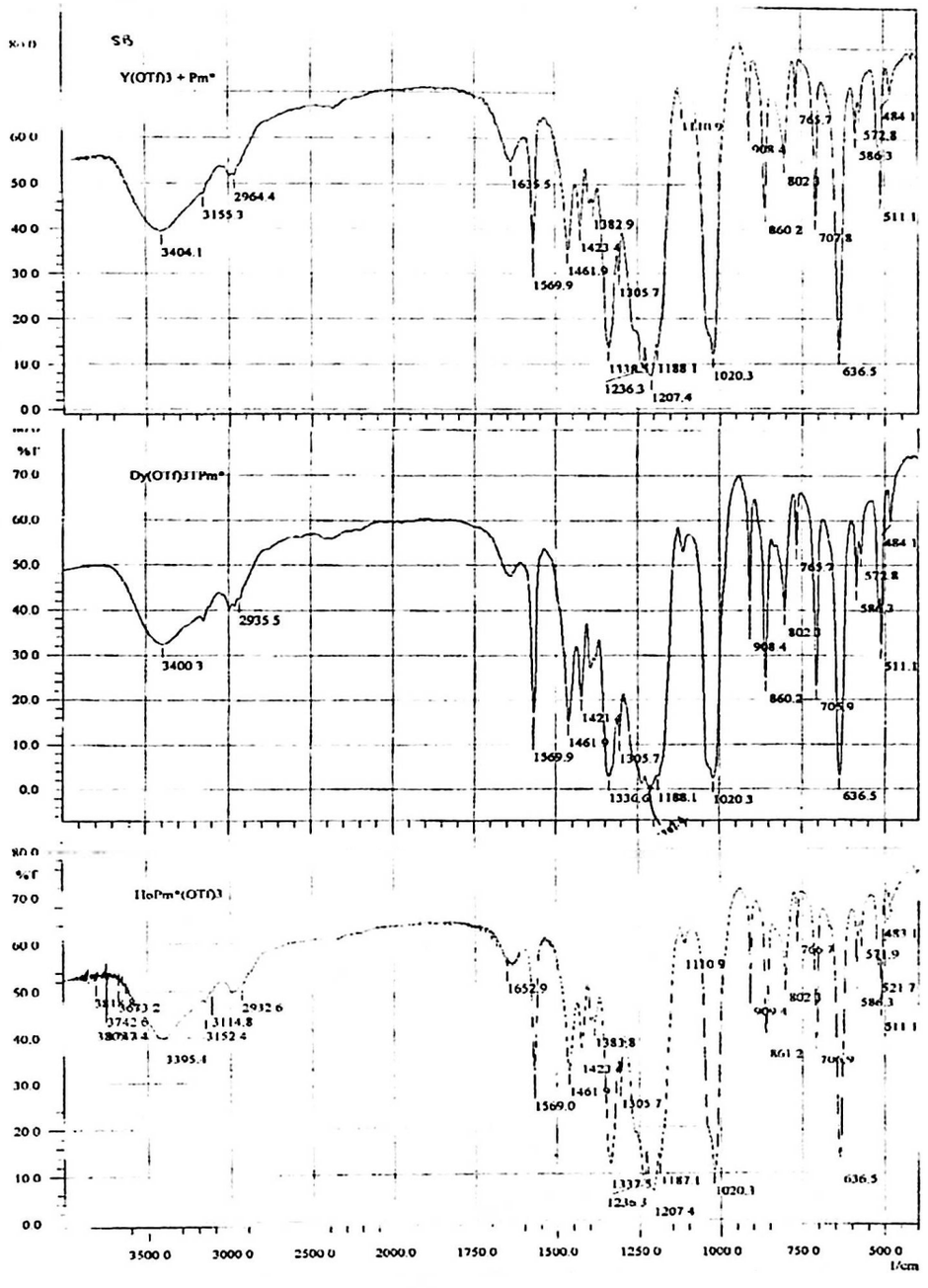

Figure 2.8 A comparison of the IR spectra of LnTPm*(OTf)3 (Ln = Ho, Y, Dy)

Molecular structures of [Y(TPm*)(OTf)3(THF)] (2.6) and [Ho(TPm*)(OTf)(THF)] (2.7)

The crystals were too small and flat for successful X-ray crystal analysis. Larger crystals of [Y(TPm*)$(OTf)_3$(THF)] (**2.6**) and [Ho(TPm*)(OTf)(THF)] (**2.7**) were prepared by slow diffusion of a solution of $In(OTf)_3$ in THF into a solution TPm* in THF. Attempts at growing crystals of [Dy(TPm*)$(OTf)_3$] suitable for X-ray analysis using this method were unsuccessful.

The complexes crystallized as seven coordinate molecules in the monoclinic space group *C*2/*c*, with two molecules of THF in the lattice. The three triflate groups bind to the metal centre through their oxygens. Considering the virtually identical atomic radii of Y and Ho, the crystals are as expected, isomorphous. Figure 2.9 and Figure 2.10.

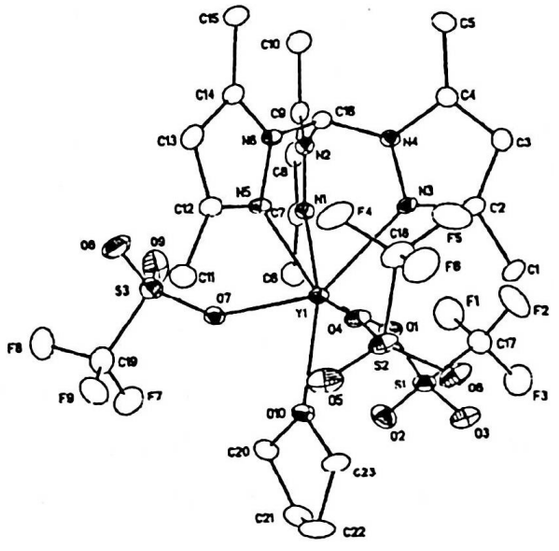

Figure 2.9: Molecular structure of [Y(TPm*)(OTf)3 (THF)] (2.6); hydrogens omitted for clarity

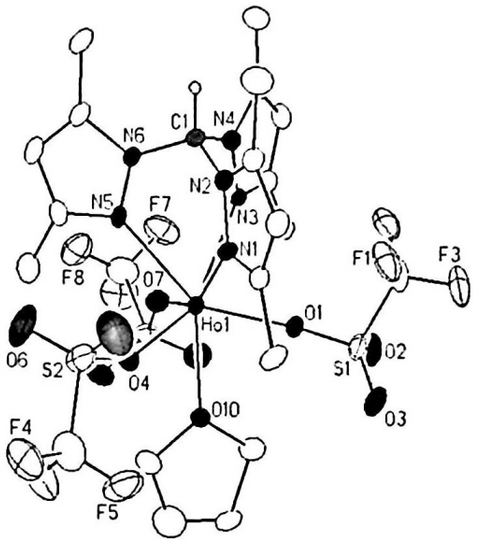

Figure 2.10: Molecular structure of [Ho(TPm*)(OTf)3(THF)] (2.7); hydrogens omitted for clarity.

The coordination geometries of the metals are much the same as for the seven coordinate complex **2.2** and can either be described as capped trigonal antiprismatic or as a tricapped trigonal pyramid as discussed previously. **(Figure 2.6 and Figure 2.7)**. In the first case, the Tpm* nitrogens and the oxygens of the triflate ligands form the lower and upper triangles of the prism respectively, with the THF group lying directly along the C_3 axis. In the latter case, the THF molecule forms the apex of the pyramid and the nitrogens of the TPm* group form the base. The oxygens of the triflate groups caps one of the faces of the pyramid each. The average Ln – N bond distances for **2.6** and **2.7** are 2.449(8) Å and 2.461(6) Å respectively, these lengths are little different to the corresponding bond distance in the six coordinate complex (**2.1**), suggesting perhaps a degree of flexibility in the coordination sphere. The average Ln – OTf distances are 2.243(7) Å and 2.258(12) Å. These bond lengths are somewhat shorter than in the trichloride samarium complex (**2.2**) and are slightly shorter than those observed in the triazacyclononane derivative $[Y(TCMT)(OTf)_2(H_2O)]OTf$, (2.40(1) Å).[138] There are, to date, no other sufficiently ordered yttrium triflate complex in the Cambridge Crystallographic database with which to compare bond lengths.

In the yttrium complex (**2.6**), the average OTf-Y-OTf bond angle is 114.9(3)°, the corresponding angle in complex **2.7** is 114.8(5)°. These are broadly similar to those

in **2.2** (115.29(6)°) as expected with a similar seven coordinate complex. The angle between the metal centre and the TPm* nitrogens (N-Ln-N) are 73.4(3)° for **2.6** and 73.1(3)° for **2.7,** slightly larger than in the samarium chloride complex, **(2.2),** however similar to that of the six coordinated yttrium complex **(2.1)** (73.8(2)°).

Preparation of Phenoxide complexes

The substitution chemistry of the lanthanide Tpm* chloride complexes was investigated using the more sterically demanding aryloxide ligands. The chloride complexes Ln(TPm*)Cl_3 were metathesized with sodium aryloxide to produce the corresponding tris aryloxides. We discovered that the reaction could either be carried out by first preparing and isolating the lanthanide trispyrazolylmethane chloride complexes and then combining them with the sodium aryloxide in THF. Alternatively, the synthesis can be carried out as a 'one pot' reaction whereby a solution of TPm* is added to a solution of lanthanide chloride in THF. This reaction mixture is stirred at room temperature for approximately 2 hours after which a solution of sodium aryloxide in THF is added drop-wise and stirring is continued for a further 2-3 hours. The NaCl formed is allowed to settle from the solution overnight and is then removed by filtration. The volume of the solution is reduced and the flask is placed in the freezer for crystallisation.

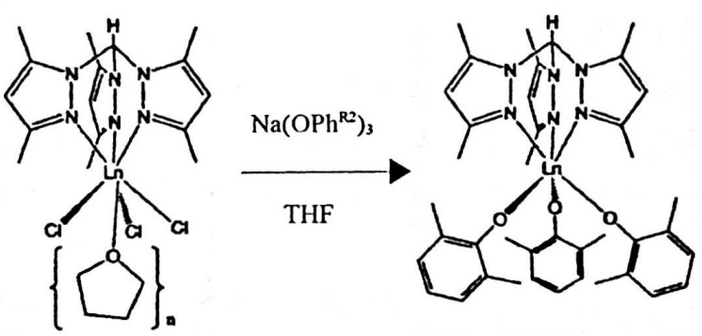

Figure 2.11: The preparation of Ln(Tpm*)(OPh^{R2})$_3$. Ln = Y, Nd, Sm, Yb),

The reaction between solutions of Y(TPm*)Cl_3 and Sm(TPm*)Cl_3 in THF with

three equivalents of the unsubstituted sodium phenoxide (NaOPh) afforded [Y(TPm*)$(OPh)_3$] (**2.9**) and [Sm(TPm*)$(OPh)_3$] **2.10**) respectively. Sodium chloride precipitated from the solution as a white solid which could be removed by filtration. These products were discovered to be insoluble in aromatic solvents but dissolved easily in acetonitrile and THF. Several attempts at crystallisation of the products by slow cooling in the freezer in a minimum of solvent were unsuccessful and thus the solvent was removed to leave the products as free flowing white powders. The elemental analysis of these complexes on a number of different reaction 'batches' were inconsistent and generally were found to contain lower percentages of carbon and hydrogen than expected, on further investigation it would appear that the samples may contain between a half and a molar equivalent of NaCl.

Salt incorporation is a known problem when synthesising lanthanide organometallic complexes, especially those of the smaller cyclopentadienyl ligands, using the salt metathesis route (chapter 1) and arises because of the need to sterically saturate the metal centre. One might expect the complexes of the more sterically encumbered TPm* ligand not to 'suffer' from the problem of salt incorporation particularly when complexed with large ligands such as the phenoxides. Anna Hillier has observed a similar problem when preparing complexes of the mono(pyrazolylborate)lanthanide halides, [Ln($Tp^{Me,Me}$)X_2] (Ln = Y, X = Cl, I; Ln = Yb, X = Cl).[139] Without obtaining a sample of the product that has crystallised from solution, it is not possible to ascertain whether the salt is present in the coordination sphere of the product or indeed whether it is simply residual salt that has not precipitated from solution. Increasing the reaction times and redissolving and filtering the products several times did not make a significant difference to the purity of the products according to their elemental analysis.

An ^{1}HNMR of the yttrium complex (**2.9**) was recorded in acetonitrile. The methyl protons on positions 3 or 5 of the pyrazolyl rings of the TPm* ligand are assigned at 2.01 and 2.09 ppm. The C-H proton of the ligand is present at 8.03 ppm and the three protons on position 4 of the pyrazolyl rings are present at 5.92 ppm. The phenoxide group protons display two very broad peaks in the aromatic region at

6.59 and 7.03 ppm. This may indicate an equilibrium process occurring in solution and restricted rotation around the Y-OAr bonds . There are a number of extra peaks at approximately 1.7 and 2.2 ppm, we think these may be due to impurities in the acetonitrile.

The ^{1}HNMR spectra of the samarium complex (**2.10**) clearly displays peaks corresponding to the single TPm* C-H proton in addition to the three protons of the pyrazolyl rings. There is a broad peak on the base line at 7.18 ppm, similar to that observed in the yttrium analogue which likewise we are attributing to the aromatic phenoxide protons. It is difficult to assign the pyrazolyl dimethyl peaks reliably as the large acetonitrile group masks their expected position. An infra-red spectra of **2.10** displays the expected bands associated with the TPm* ligand.

At this point our attention turned to dimethyl substituted phenoxide ligand ($NaOPh^{2,6Me2}$) in substitution reactions with lanthanide TPm* chlorides. We anticipated that the greater steric demand of this ligand above the unsubstituted phenoxide may preclude the incorporation of salt in the complexes and allow for a more tractable crystalline product. The methyl groups will also provide us with more detailed ^{1}H NMR spectra.

Solutions of $LnCl_3$ (Ln = Y, Yb and Sm) were stirred with solutions of TPm* in THF to afford the $LnTPm^*Cl_3$ complex in-situ. Stirring was continued for approximately 2 hours after which three equivalents of $NaOPh^{Me2}$ in THF was added drop-wise. NaCl precipitated from solution and was removed by filtration leaving pale yellow solutions of $[Y(TPm^*)(OPh^{Me2})_3]$ (**2.11**) and $[Yb(TPm^*)(OPh^{Me2})_3]$ (**2.14**) and a dark orange solution of $[Sm(TPm^*)(OPh^{Me2})_3]$ (**2.12**). The neodymium complex was prepared by dissolving a pre-prepared sample of $Nd(TPm^*)Cl_3$ in THF and adding a solution of $NaOPh^{Me2}$ in THF to afford a green/brown solution. This method was chosen simply because a lack of sufficient sample of $NdCl_3$ precluded the formation of NdCl3(TPm*) in-situ. The compounds were crystallised from the reaction mixture after the removal of salt, by reducing the volume of THF and placing the flasks in the freezer for slow cooling. In all cases a crystalline product formed. The pale blue crystals of $Nd(TPm^*)(OPh^{Me2})_3$

(**2.13**) and the clear crystals of Yb(TPm*)(OPh^{Me2})$_3$ (**2.14**) desolvated upon removal of the solvent. Y(TPm*)(OPh^{Me2})$_3$ (**2.11**) formed as large colourless crystals and Sm(TPm*)(OPh^{Me2})$_3$ (**2.12**), as large pale orange crystals.

All of the samples were analytically pure with no evidence of salt incorporation suggesting that the metal centres are sufficiently sterically saturated without the addition of NaCl in their coordination spheres. On samples of the products obtained directly from solution by removal of solvent and drying under reduced pressure, as opposed to slow crystallisation from solution, the elemental analysis suggests the presents of some residual NaCl.

Interestingly, whilst complexes of the unsubstituted phenoxides (**2.9, 2.10**) dissolve readily in acetonitrile and THF, the complexes of the 2,6 dimethyl substituted phenoxides are somewhat insoluble. Dissolving only partially in THF and acetonitrile, even after stirring and gentle warming. This may suggest that introducing the larger methyl groups onto the phenoxide ring prevents binding of THF to the metal centre which disrupts the crystal packing of the complex, hence decreasing the solubility.

^{1}HNMR Spectra

The ^{1}HNMR of complexes **2.11, 2.12,** and **2.13,** in DCM are relatively straight forward and display the seven peaks expected (CH Pz, 3CH Pz, 3,5 Me (Pz), 3.5 Me (Pz), OPh^{Me2}, OPh *meta* H, OPh *para* H) **Figure 2.12**. This is indicative of a coordination sphere that is highly symmetrical and therefore fluxional with free rotation around the metal-phenoxide axis.

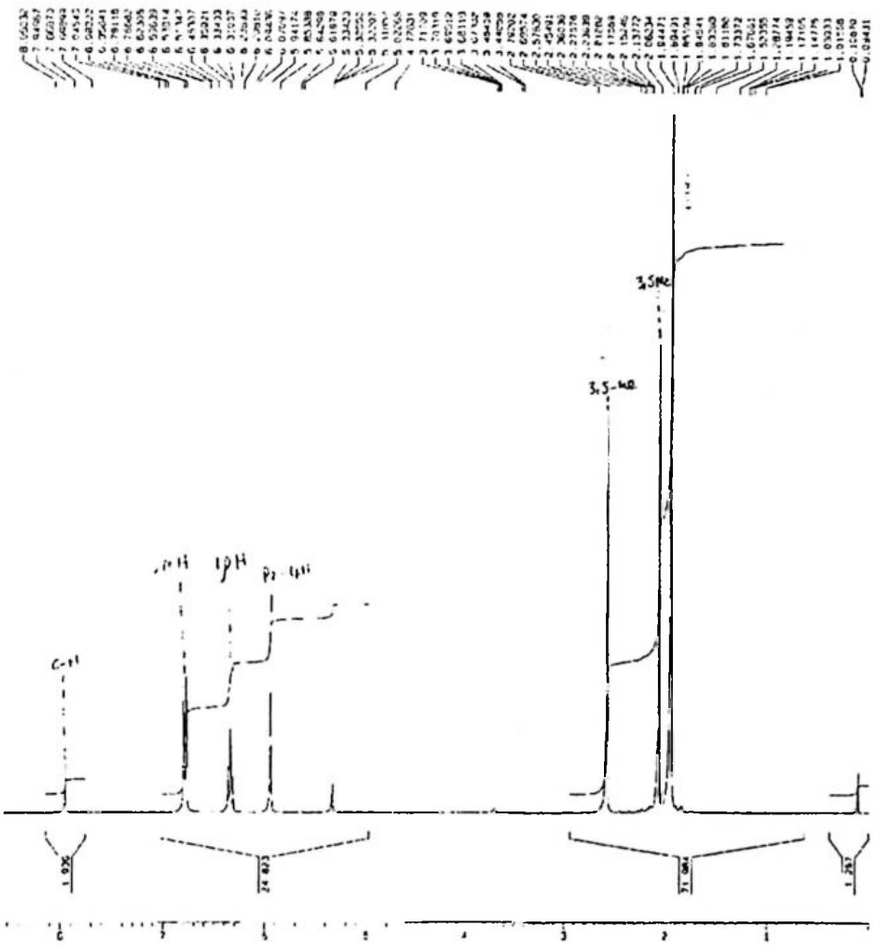

Figure 2.12: 1 H NMR spectra of YTpm(OPhme2)$_3$*

The 1HNMR of the related scandium complex Sc(TPm*)(OPh^{Me2})$_3$, synthesised by Mountford *et al,*[118] shows broad resonances for the ortho and meta protons on the 2.6 dimethlyphenyl substituent. This suggests there is restricted rotation of the phenoxide groups around the phenoxide metal axis due to the crowded coordination sphere of the much smaller scandium metal centre. At -20°C, the fluxionality of the complex was 'frozen out' and two distinct ortho methyl group environments for the phenoxide ligand became apparent, the 'up' environment, towards the TPm* ligand and the 'down' protons, away from the TPm* ligand. The shielding ring current effects of the pyrazolyly TPm* groups is postulated as the reason for the relatively high field shift of the 'up' *o*-Me resonance.

The ytterbium complex (**2.14**), has an ^{1}HNMR spectra with very large paramagnetic shifts. Only the peaks of the TPm* ligand and the *para* hydrogens of the OPh^{Me2} substituents can be observed at room temperature. When the sample is cooled to 204 K, two sets of broad singlets in the ratio 9:3 rose from the base line. Considering this is a molecule of high symmetry, according to its ^{1}H NMR spectra, it is reasonable to assume that protons lying along the C_3 axis will be strongly desheilded. Indeed the central C-H proton of the TPm* ligand appears at +74 ppm. Conversely, hydrogens lying perpendicular to this axis will experience a strong up-field shift, as is the case with the nine 3Me protons of the TPm* ligand which appear at -52.1 ppm, the orientation of the 5Me protons means they are more desheilded and hence appear at +22.1 ppm. Using this assumption, the 'down' methyl protons of the phenoxide ligand lie virtually along the principle axis have been assigned at +78.9 ppm and the meta protons of these substituents are placed at +10.4 and -6.3 ppm, each peak integrating for three protons.

VT NMR

Dynamic NMR spectroscopy is a useful tool with which to study intermolecular and intramolecular exchange reactions in solution. It is now possible to study reactions that are too slow for optical spectroscopic methods but too fast for investigations by classical chemical methods. Whilst the NMR spectra themselves provide qualitative evidence for the dynamic processes, the results can also be analysed quantitatively. From the temperature dependence of the resonance lines one can obtain rate constants and activation parameters. There are two methods commonly used to determine these rate constants and activation parameters, namely complete line shape analysis and the use of the coalescence temperature T_c and the corresponding rate constant K_c.

Line shape analysis involves recording a number of spectra at different temperatures. For example several spectra at temperatures for which the dynamic process is very slow, several more in the region of the coalescence spectra and then finally a number of spectra taken at temperatures where exchange is rapid. For the

spectra taken at temperatures approaching that at which coalescence occurs, the rate constant is given by the equation

$$K_A = \frac{4\pi\rho_A\rho_B^2\Delta\nu^2}{\Delta_e}$$

Where p_A and p_B are the populations of the two exchange sites. $\Delta\nu$ is the frequency separation in Hz between the two signals in the absence of exchange and Δ_e is the broadening of the peak due to exchange. Once values of the rate constant have been obtained at different temperatures, these may then be used to determine the activation enthalpy $(\Delta H^{\ddagger})$ and entropy $(\Delta S^{\ddagger})$ by plotting $\ln(K_A/T)$ against reciprocal temperature.

When interpreting an exchange process it is often sufficient to know only the order of magnitude of the rate constant at room temperature. When the populations (p_A and p_B) are equal of two exchanging sites (A and B) are equal, an approximation to the rate constant (k_C) for the exchange process at the coalescence temperature (T_C) is calculated by:

$$Kc = \frac{\pi\Delta\mu}{\sqrt{2}}$$

This equation is only valid if the dynamic process occurring is first order kinetically, the two singlets have equal intensities and the exchange nuclei are not coupled to each other.[140] k_C can then be substituted into the Eyring equation to obtain a value for the free energy of activation ($\Delta G^{\ddagger}$) for the transition state.

$$\Delta G^{\neq} = \ln\left(\frac{k_c h}{k_B T_C}\right) RT_c$$

K_B = Boltzmann constant = 1.3805×10^{-23} J K^{-1}

h = Plank constant = 6.6256×10^{-34} J s

R = Universal gas constant = 8.3144 J K^{-1} mol^{-1}

T_C = Coalescence temperature in K.

In attempts to 'freeze out' the fluxionality in the highly symmetrical Y(TPm*)

$(OPh^{Me2})_3$ **(2.11)** complex. **(2.11)** we recorded a variable temperature ^{1} H NMR. **Figure 2.13**

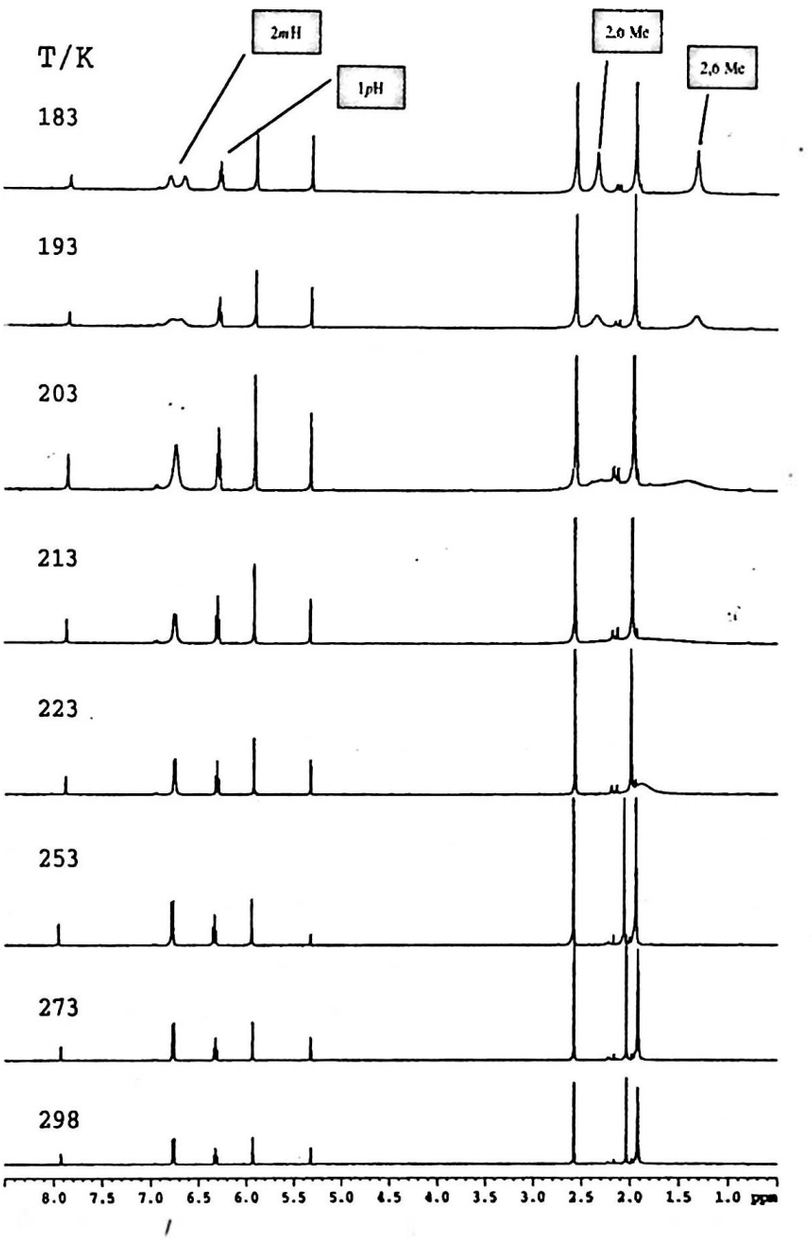

Figure 2.13: Variable temperature ^{1}H NMR of YTPm(OPh^{Me2})$_3$*

The spectra show that on cooling of the product, the rotation of the phenoxide groups around the yttrium-phenoxide bonds slows until the 2,6 methyl groups on the phenoxide rings become inequivalent and two resonances integrating for nine

protons each are apparent. The coalescence temperature of the peaks is recorded at 213 K. from the spectra the difference in chemical shifts ($\Delta\nu$) of the two peaks (is 1.01642 ppm (thus in Hz: (1.01642/0.25)x 100.03379 = 406)

Following the analysis above the rate constant k_A is calculated as 903 s^{-}
Therefore:

$$\Delta G^{\neq} = \ln\left(\frac{903\,x\,6.626\text{x}10-34}{1.3805\text{x}10-23\,x\,213}\right)(8.814\,x\,213)$$

$$\Delta G^{\neq} = 39.5\ KJ\ mol-1$$

Using the same analysis the free energy of activation for the protons in the meta positions of the phenoxide ring can be calculated. The peaks coalesce at 203 K and have a difference in frequency of 57.2 Hz. Using this, the rate constant is calculated to be 127 s^{-1}. From this, $\Delta G^{\ddagger}$ is calculated as 40.9 KJ mol^{-1} .

There are several sources of error in these calculations, the main one being that absolute values of temperature can seldom be measured with an accuracy better that +/- 2K. One can also assume an additional error range in T_C of at least +/- 2K due to the complexity of the spectrum. A generic value for the order of magnitude of the error in $\Delta G^{\ddagger}$ has been estimated to be +/- 0.8 KJ mol^{-1}.
Taking this into account, the values for free energy of activation of the 2.6 methyl phenoxide protons and the meta protons are extremely similar.

Crystal analysis – Molecular structures of 2.12 and 2.13

As discussed, analytically pure crystals of all of these compounds can be grown directly from solution after salt has been removed. Recrystallisation to obtain crystals for x-ray analysis is more difficult. Once isolated as solids, these disubstituted complexes are less soluble in THF than the unsubstituted complexes. Heating the solutions of THF to aid dissolution appears to result in the loss of coordination of the TPm* ligand form the metals centre. When [Nd(TPm*)$(OPh^{Me2})_3$] (**2.13**) was recrystallised from hot THF, large pale blue block crystals

were formed, analysis and ^{1}HNMR studies of these revealed them to be the trisaryloxide $[Nd(OPh^{Me2})_3(THF)_3]$.

Zang *et al*, have reported the related complex, $[Nd(OPh^{Me2})_3]$ however its structure has not been fully elucidated.[141][142] The analogous yttrium complex $[Y(OPh^{Me2})_3(THF)_3]$ has been reported and structurally characterised by Evans *et al.*[143] The crystal structure of this complex shows a distorted *fac*-octahedral arrangement of the six ligands around yttrium. We presume that our neodymium complex $[Nd(OPh^{Me2})_3(THF)_3]$ is structurally analogous the yttrium complex. Figure 2.14

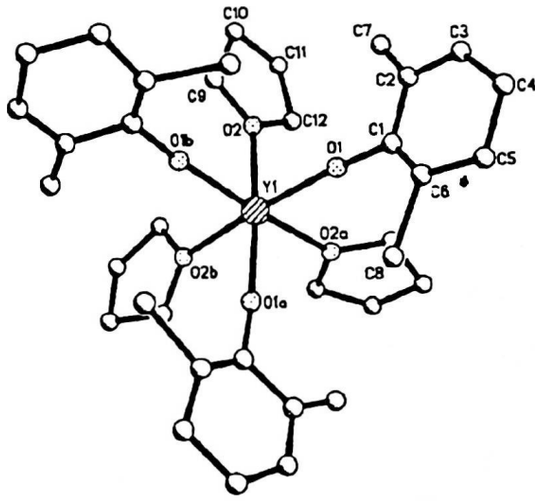

Figure 2.14: The molecular structure of $Y(OPh^{2,6\text{-}Me2})_3(THF)_3$; hydrogens omitted for clarity. [143]

Clark *et al* has reported the synthesis and structural analysis of a number of similar lanthanide complexes with 2.6 diisopropyl substituted phenoxide ligands, $[Ln(OPh^{iPr2})_3(THF)_2$ (Ln = Sm, Nd, Er, Pr, Gd and Lu)[144],[145] The complexes of Sm, Er, Pr, Gd and Lu have all been structurally characterised and are isostructural. The structure consists of the lanthanide metal centre coordinated in a pseudo-trigonal bipyramidal arrangement by three equatorial and two axial THF ligands.

Bearing in mind the potential to lose the coordinated TPm* ligand from the

complex, recrystallisation of complexes **2.11-2.14,** had be to be carried out with due care. Crystals of the samarium complex **(2.12)** and the Neodymium complex **(2.13)** suitable for X-ray crystal analysis, were grown by gently warming a sample of the product [Ln(TPm*)(OPh^{Mc2})$_3$] (Ln= Sm, Nd.) in THF. The solutions were then filtered and the solutions were concentrated. Flasks cooled inside a dewar in the freezer at *ca* -30°C to afford large pale orange crystals of **2.12** and pale blue crystals of **2.13.**

The complexes crystallized as six coordinate structures in the triclinic space group P1 and each contain three molecules of THF in their lattice. Figure 2.15 and Figure 2.16

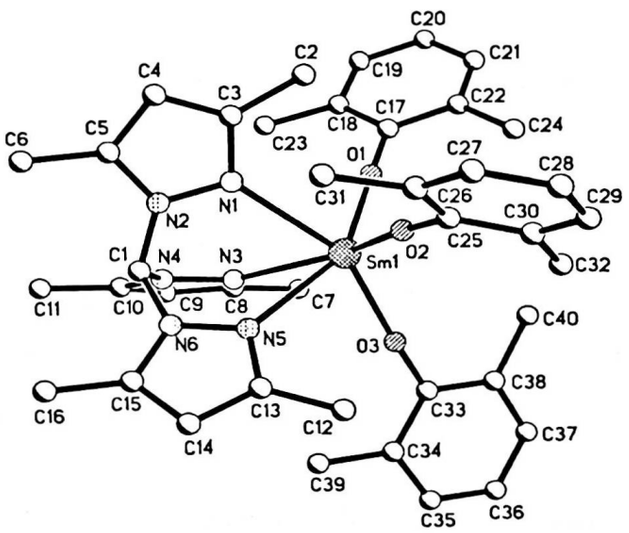

Figure 2.15: Molecular structure of [Sm(TPm*)(OPh^{Mc2})$_3$] (2.12) ; hydrogens omitted for clarity.

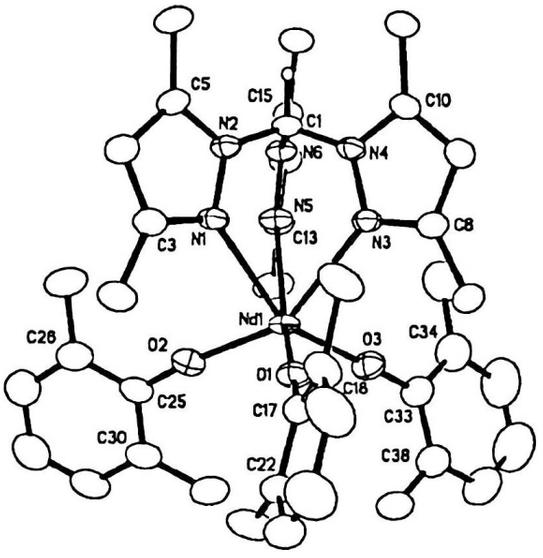

Figure 2.16: Molecular structure of [Nd(TPm)(OPh^{Me2})$_3$] (2.13); hydrogens omitted for clarity.*

The structures are analogous to that of the six coordinate yttrium chloride complex (**2.1**) and thus can be regarded as a trigonal antiprism with the aryloxides being terminally bound to the metal centre through the oxygen atoms. The complexes are highly symmetric as indicated by their ^{1}HNMR spectra and the aryloxide ligands lie virtually parallel to the C_3 axis of the TPm* ligand. The 'up' methyl groups of the three aryloxide ligands, pointing towards the TPm* ligands, are contained within the grooves between the pyrazolyl groups.

Comparing the chloride and aryloxide substituents, one can observe the bond length between the metal centre and the TPm* nitrogens are considerably longer in the aryloxide complexes (*cf* Ln-$N_{av.}$ 2.565(5) Å (**2.12**), 2.599(5) Å (**2.13**) and 2.459(5) Å(**2.1**). This cannot be accounted for solely by the difference in ionic radius between the metal centres and suggests that the binding of the TPm* ligand to the metal centre is sensitive to changes in the steric demand of the other ligands within the coordination sphere of the metal. The affects of the larger steric demand of the alkoxides are also demonstrated when considering the angles between the C_3 axis of the TPm* ligand and the aryloxide/chloride ligand. The chloride groups are able to bend away from the TPm* ligand to an average angle of 117.5°(2) whereas the increased steric presence of the alkoxides and the interactions between

the three ligands prevent further tightening of the groups and limit this angle to 111.7(2)° The angles between the alkoxides are similarly larger than those in the corresponding chloride complex, again reflecting the greater steric bulk of the alkoxides.

The average distances between the aryloxide oxygens and the lanthanide metal centres are 2.180(3) Å (**2.12**) and 2.207(5) Å (**2.13**). These are broadly comparable to those observed in the novel complex $[Ln_2(OAr)_6$ (Ln = Nd, Sm and OAr = 2,6-iPr$_2$C$_6$H$_6$) synthesised by Clark *et al,*[144] which consists of a dimer bridged by intermolecular η^6-π-arene interactions of unique aryloxide ligands. These complexes display average Nd-O bonds of 2.122(9) Å for the terminal aryloxide ligands and 2.211(9) Å for the bridging aryloxide ligands within the complex. The values for the samarium complex are 2.101 (6) Å and 2,198(5) Å for terminal and bridging ligand respectively. A number of other related aryloxide complexes show similar Ln-O (aryloxide) bond lengths. For example the tris(2.6-diphenylphenolato)Neodymium(III) ($Nd(Odpp)_3$ complex reported by Shen *et al,* [146] has an average Ln-O (aryloxide) bond length of 2.169(2) Å. The samarium tris(pyrazolyl)borate complex: [Sm(Tp*)$_2$OPh-4-Bu^t], has an Sm-O bond length of 2.159 Å[147] and the related metallocene complexes , [Cp*$_2$Sm(O-2,3,5,6-Me$_4$C$_6$H) and [Cp*$_2$Sm]$_2$($O_2C_{16}H_{10}$) have Sm-O bond distances of 2.13(1) Å and 2.08(2) Å respectively.

Overall, when comparing these six coordinate TPm* complexes with those containing the isoteric but anionic tris(3,5Me$_2$Pyrazolyl)borate (Tp*) ligands, it is apparent that the average M-N(pyrazolyl) distance is longer in the TPm* complexes, suggesting that the Tp* forms the stronger bonds as expected.

Attempted preparation of the para substituted LnTPm*(OPh^{4tBu})$_3$ complexes

In view of the limited solubility of the LnTPm* complexes with 2,6 dimethyl substituted phenoxides, substitution reactions were attempted with the para substituted phenoxide, (Oph^{4But}). Substituents in the para position of the phenyl ring can enhance solubility of metal derivatives but have little steric influence within the coordination sphere. (chapter 1).

Evans *et al* reported that mono-metallic lanthanide complexes with the larger 2,6-di-tert-butylphenoxide ligands with formula $Ln(OR)_3$ have been crystallographically identified. The smaller para substituted phenoxide ligands, can form polymetallic species, which have also been identified. These often contain solvent molecules, ligands other than alkoxides and metal atoms other than yttrium and the lanthanides. Evans and co workers[148] reacted $LaCl_3$ with a large excess of sodium 4-methylphenoxide ($NaOPh^{4Me}$), resulting in the formation of the cluster molecule: $La_2Na_3(\mu_4\text{-}OPh^{4\text{-}Me})_3(\mu\text{-}OPh^{4\text{-}Me})_6(THF)_5$. Figure 2.17

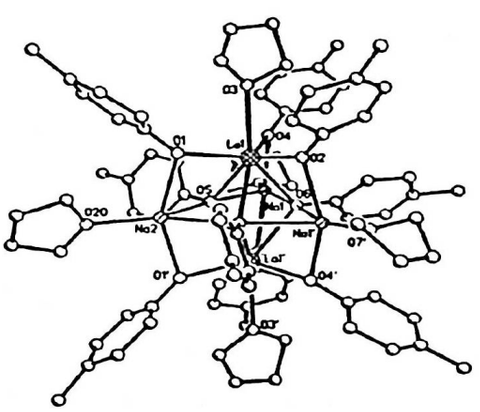

Figure 2.17: Molecular structure of $La_2Na_3(\mu_4\text{-}OPh^{4\text{-}Me})_3(\mu\text{-}OPh^{4\text{-}Me})_6(THF)_5$.

The structure in Figure 2.17 consists of a trigonal bi-pyramid of metal atoms with the lanthanum atoms in the apical positions and the sodium atoms in the equatorial sites. The phenoxide ligands are present as both quadruply and doubly bridging ligands. Crystallographically characterised quadruply bridging alkoxide ligands are rare.[149] Each sodium is 5 coordinate and each lanthanum is 7 coordinate which

is unusually high for a lanthanum alkoxide complex.

Synthesis of the related Tp* complex ($Sm(Tp^*)_2OPh\text{-}4\text{-}Bu^t$) has been achieved successfully by the metathesis reaction between $Na(OPh\text{-}4\text{-}Bu^t)$ and $[Sm(Tp^*)_2Cl]$.[147] This complex has been structurally characterised and contains two tridentate pyrazolylborate ligands and the phenoxide in a distorted pentagonal bipyramidal arrangement around the samarium centre.

In order to synthesise a half sandwich complex using the TPm* ligand we attempted the metathesis reaction between a turbid solution of $YTPm^*Cl_3$ in THF and $NaOPh^{But}$ in THF. A white precipitate of NaCl formed after approximately two hours and was removed by filtration. Attempts at growing crystals from THF and toluene respectively were unsuccessful therefore analysis was carried out on the white powder acquired from removal of the solvent under reduced pressure. Attempts at preparing the analogous samarium complex were carried out in the same way.

Elemental analysis of both yttrium and samarium complexes show much lower carbon values than expected based on the formulation $[LnTPm^*(OPh\text{-}4\text{-}Bu^t)_3]$ with an NaCl in the coordination sphere. The hydrogen and nitrogen values for the yttrium complex (**2.15**) are both slightly high, whereas in the samarium complex (**2.16**) they are both a little low. Considering Evans *et al* observed cluster complexes of the para-methyl phenoxide which contained both the sodium and lanthanum metals,[149] it is possible that we have also synthesised clusters containing both sodium ions and solvent molecules which, in absence of a crystal structure, would make it very difficult to calculate an expected elemental analysis.

The ^1H NMR of the complex (**2.16**) was largely uninterpretable , with only the solvent peak and two very broad ortho and meta phenoxide proton resonances visible. The less paramagnetic yttrium complex, on first observation, gave a much clearer spectrum. With broad peaks for the ortho and meta protons. The expected doublet for the ortho and meta protons is alluded to with the presence of a slight split in the ortho resonance. The rotation around the phenoxide bonds at room

temperature is evidently somewhat restricted, this is possibly due to steric crowding in the complex. The situation is similar with the 4-Bu^t protons which have a broad resonance at *ca* 2.687 ppm. The CH from the TPm* and the three Pz Protons are all present in the correct ratios. There are two resonances at 3.330 and 3.098 ppm that appear to be from the 3,5 dimethyl groups on the pyrazolyl rings. These however, integrate to between 4 and 5 protons each, as opposed to the expected 9. It is unclear why this value should be so low when all the other integrations are correct.

The solid state infra-red spectra of both complexes are super-imposable suggesting a very similar structure in the solid state. It is not surprising that the spectra of the free TPm* ligand and those of the complexes **(2.15 and 2.16)** are similar as the vast majority of the absorptions are in the aromatic region. There are however two absorptions in the complexes at 1602 and 1566 cm which are not present in the free ligand. These are attributed to the C=C bends in the phenoxide rings.

Mixed ligand complexes

Reaction with the Borohydride complex: $Nd(BH_4)_3(THF)$ (2.21)

There are many reported lanthanide borohydrides prompting a review of this chemistry by Ephritikhine.[150] Interest in the lanthanide borohydride complexes has been driven largely by their potential as hydroboration catalysts and as precursors to metal hydrides. A number of different binding modes are observed for the borohydride ligand depending on the method of synthesis of the complex and the steric considerations at the metal centre. Figure 2.18

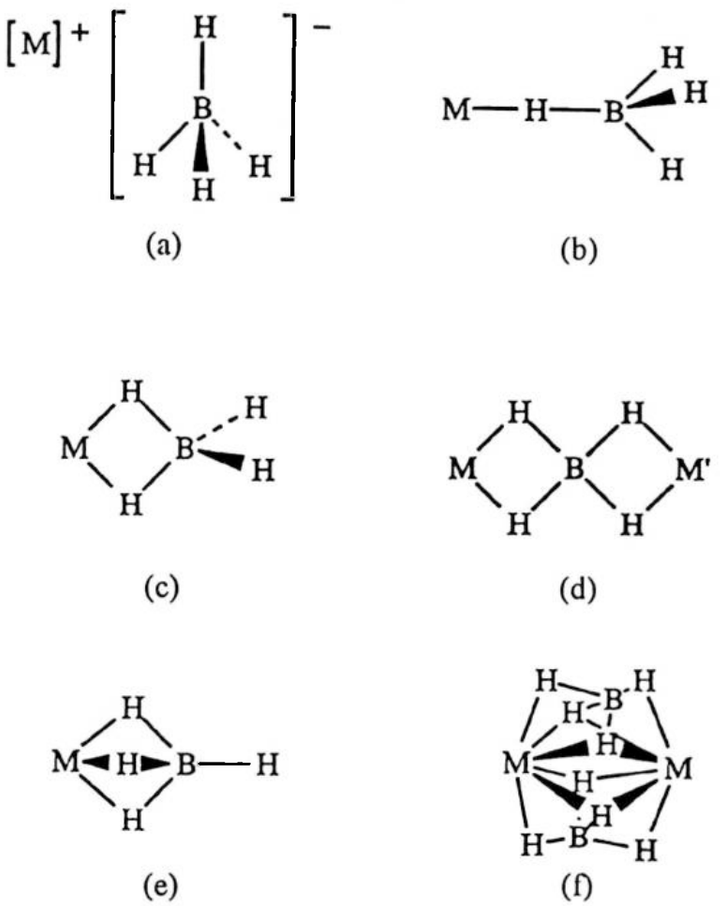

Figure 2.18: Binding modes of the tetrahydroborate group with metal atoms.

A valuable insight into the the denticity of the borohydride groups within complexes can be gained by recording their IR spectra as different binding modes give rise to variations in stretching frequencies. Table 2.2

Structure	Approx freq., cm^{-1}	Type of internal coordinate change	Symmetry type
(a) ionic	2200-2300	$B\text{-}H_t$ stretch	T_2
	1050-1150	BH_2 deformation	T_2
(b) monodentate	2300-24500	$B\text{-}H_t$ stretch	A_1,E
	2000	$B\text{-}H_b$ stretch	A_1
	2000-1700	$M\text{-}H_b$ stretch	A_1
	1000-1150	BH_3 deformation	A_1,E
(c.i) bidentate (monomer)	2400-2600	$B\text{-}H_t$ stretch	A_1,B_1
	1650-2150	$B\text{-}H_b$ stretch	A_1,B_1
	1300-1500	Bridge stretch	A_1
	1000-1200	BH_2 deformation	B_2
(c.ii) bidentate (dimer,polymer)	ca. 2290	$B\text{-}H_b$ stretch	A_1
	ca. 1200	BH_2 deformation	B_2
(d) tridentate	2450-2600	$B\text{-}H_t$stretch	A_1
	2100-2200	$B\text{-}H_b$ stretch	A_1
	1150-1250	BH_3 deformation	A_1
(e) tetradentate	2400-2420	$B\text{-}H_b$ stretch (η^3)	
	2250-2280	$B\text{-}H_b$ stretch (η^2)	

Table 2.2: Infra-red vibrational transitions observed for MBH_4 species.[150][151]

The organic chemistry of the lanthanide borohydrides largely involves the cyclopentadienyl ligand.

Synthesis is by the reaction of of a halide precursor with $LiBH_4$ or $NaBH_4$.

$$Ln(Cp)_2Cl.THF + M(BH_4) \longrightarrow Ln(Cp)_2(BH_4)(THF) + MCl$$

The predominant determining factor of the ligation mode of the borohydride group is the ionic radius of the metal centre. Thus, in the above complex, the smaller complexes Lu and Yb will contain borohydride ligands that are bidentate whereas the larger Sm metal contains tridentate borohydride ligands. The IR of the europium complex, $ErCp_2(BH_4)(THF)$, shows that the BH_4 ligand adopts a coordination intermediate between bi- and tridenate. Tetradentate ligation has been observed in the complexes of the larger metals, Ce and Sm, $[(1,3\text{-}Bu^t_2\text{-}C_5H_3)_2Ln(BH_4)]_2$.[152][153] The bonding mode of the BH_4 is also effected by

coordination of a solvent. Removal of THF from the complex $LnCp_2(BH_4)(THF)$, where Ln = Lu, Yb or Er, results in the formation of the unsolvated complexes $LnCp_2(BH_4)$. Infra-red spectra show that these complexes are polymeric with (μ-η2-H2)2B units bridging between lanthanide centres.[154]

Ephritikhine *et al* developed an alternative synthetic route to a number of organometallic borohydride derivatives starting from the solvated complex $Nd(BH_4)_3(THF)$, which was first reported by Mirsaidov *et al.*[155] The first cyclooctatetraenyl lanthanide borohydride complex was reported, $(COT)Nd(BH_4)(THF)_2$ (COT = η-C_8H_8). The Infra-red spectrum of this complex indicated that the BH4 ligand is tridentate and and non-bridging, thus the complex would adopt a monomeric structure. Dissociation of a THF ligand from this complex occurred in benzene to afford the dimeric complex $[(COT)Nd(BH_4)(THF)]_2$ as green crystals. The IR spectrum of this complex displays a strong absorption at 2255 cm^{-1}, which is characteristic of bridging borohydride ligands. The crystal structure demonstrates the $(\mu_3\text{-}H)_2B(\mu_2\text{-}H)_2$ coordination mode of the BH_4 ligand which is unusual having only been encountered and crystallographically once previously in the cerium compound, $[(C_5H_3{}^tBu_2)_2Ce(BH_4)]_2$.[152] Figure 2.19.

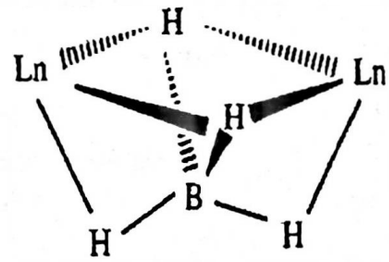

***Figure 2.19: A representation of the $(\mu_3\text{-}H)_2B(\mu_2\text{-}H)_2$ binding mode*[153]**

The more familiar $(\mu_2\text{-}H)_2B(\mu_2\text{-}H)_2$ bridging mode of the BH_4 group is also very rare in *f*-element chemistry and has only been found in the polymeric uranium compounds $U(BH_4)_4$ and $U(BH_4)_4(OR_2)$ (R = Me, Et).

The reaction of $(COT)Nd(BH_4)(THF)_2$ with NEt_3HBPh_4 in THF affords the

complex, $[(COT)Nd(THF)_4][BPh_4]$. These two complexes have been used in the development of the chemistry of mono(cyclooctatetraenyl) neodymium compounds. A number of (COT)NdX derivatives were prepared where X = Cp*, C_4Me_4P, OEt and S^{t}Bu.

The preparation of (pyrazolylborate)lanthanide borohydrides was explored by Anna Hillier.[139] The reaction between $[Ce(Tp^*)_2(OTf)]$ with $NaBH_4$ afforded a yellow micro-crystalline product with an elemental analysis consistent with the formulation $[Ce(Tp^*)_2(BH_4).THF]$. A weak IR band was observed in the borohydride B-H terminal region along with two intense bands at 2391 cm^{-1} and 2304 cm^{-1} which could be due to a dimeric structure containing two η^4-BH_4 groups although one would not expect the sterically demanding Tp* ligands to accommodate a polymeric structure containing BH_4 bridging ligands. The insolubility of the product precluded the recording of a ^{1}HNMR or the growing of crystals.

The half sandwich Yttrium complex $[Y(Tp^*)(BH_4)_2]$was also prepared as a colourless micro-crystalline solid. The infra-red spectrum showed two intense bands at 2286 cm^{-1} and 2228 cm^{-1} along with a number of weaker bands in both the terminal and bridging B-H regions. The splitting of *ca* 50 cm^{-1} between the bridging bands in the spectrum suggests that the BH_4 groups are bound in a tridentate fashion. The weaker bands may indicate the presence of some minor species or possibly that the two borohydrides exhibit different ligation modes, one being bidentate and the other tridentate.

In an attempt to synthesise a borohydride complex of the TPm* ligand, we combined a solution of TPm* in THF directly with the neodymium complex, $[Nd(BH_4)_3(THF)_3]$. After cooling in the freezer overnight a light blue solid formed which was dried under reduced pressure. This powder is extremely moisture sensitive and insoluble in hydrocarbon solvents, it does however, dissolve easily in THF. The elemental analysis of the product was consistent with the formula $[Nd(TPm^*)(BH_4)_3(THF)]$. The IR spectra displays a strong terminal B-H stretching band at 2425 cm^{-1} and two broader bands at 2215 cm^{-1} and 2150 cm^{-1} which are

highly indicative of the BH_4 ligands having tridentate ligation.

Attempts at growing crystals of the product suitable for analysis by slow cooling from THF were unsuccessful however a combination of the data obtained strongly suggests that we have synthesised $Nd(TPm^*)(BH_4)_3THF$ which contains the BH_4 ligands in a tridenate ligation mode.

Attempts to prepare Mixed Ligand complexes

Having made a number of successful attempts at substituting all three chloride groups of the 'parent' complex: $[Ln(TPm^*)Cl_3]$, we subsequently made attempts at substituting just one of the chlorides for other ligands in order to create tractable mixed ligand species. The ubiquitous cyclopentadienyl (Cp) class of ligand has already proved its worth in lanthanide chemistry with the early isolation of Cp_3Ln for the larger lanthanides, La, Ce, Pr, and Nd and the formation of the heteroleptic species $[Cp_2Ln(\mu\text{-}Cl)]_2$ for the smaller lanthanides, Sm, Gd, Dy, Ho, Er, Yb and Lu. (Chapter 1). We anticipated that a metathesis reaction between $[Ln(TPm)^*Cl_3]$ (Ln = Y, Sm) and an equivalent of sodium cyclopentadiene in THF would result in the substitution of one chloride ion for a Cp group.

The preparations of both the ytterbium and samarium complexes proceeded in an identical manner. On combination of the reactants in THF and continuous stirring for *ca* 20 hours, a pale yellow solution and white precipitate formed. The mixture was filtered and crystallisation was attempted by reducing the volume of THF and placing the flask in the freezer for slow cooling. When crystallisation was unsuccessful the solvent was removed under reduced pressure to leave a pale yellow powder. The elemental analysis for $[Sm(TPm^*)CpCl_2]$ (**2.18**) has very high values for all three elements. The ^1H NMR of the product taken in acetonitrile displays the resonances expected for the TPm* protons, there is also half a molecule of THF present and two multiplets at 1.310 and 2.392 ppm which are possibly impurities in the acetonitrile. Notably there is no resonances present for a

Cp groups, and we have not formed the mixed ligand complex expected. The NMR suggests that the TPm* ligand is bound to the metal centre and we may have formed [SmTPm*$Cl_3(THF)_{0.5}$], however the elemental analysis is inconsistent with this formulation also.

The elemental analysis for the yttrium complex [YTPm*Cl_2Cp] is consistent with a product of this formulation. The values for carbon and hydrogen are slightly high whereas nitrogen is a little low, suggesting that there some solvent in the product. The ^{1}H NMR is difficult to interpret. It confirms that there is a small amount of THF present in the product. There is a a peak present in the Cp region, however none of the integrals are correct for the product [YTPm*$CpCl_2$]. There is a possibility that the TPm* ligand has been displaced for the anionic Cp ligand and we have synthesised [$YCpCl_2$.(THF)] leaving the free ligand in solution. A review by Schumann [156] describes several mono(cyclopentadienyl)rare earth halides. These complexes were first reported in 1963 by Manastyrskyj *et al.*[31] Their preparation was by metathesis between sodium cylopentadiene and the lanthanide trichloride. The crystal structure of [$YCpCl_2(THF)_3$] was reported by Jamerson *et al.*[75] The complex is monomeric with the yttrium atom coordinated by one Cp ring centroid, three oxygen atoms from the three THF molecules and two chloride atoms to give rise to a distorted octahedral coordination. The spectrum of our product shows only one THF molecule per yttrium atom. There are several peaks that appear to be from the TPm* ligand, however the inconsistencies in the integrals suggest that the metal is not bound to both the TPm* and the Cp ligand. In the absence of any crystal data on the product it is hard to predict the structure. It would however, be surprising if the yttrium can bind both TPm* and Cp ligands, whereas the larger samarium complex can only bind the TPm*, in its coordination sphere.

Introducing the tris(3,5-dimethlylpyrazolyl)borate ligand, (Tp*)

Numerous studies using the anionic hydrido-tris-(3,5-dimethylpyrazol-1-yl)borate (Tp*) ligand have demonstrated that it is a successful ancillary ligand for the

lanthanide metals in the trivalent and the divalent states. Having demonstrated that the neutral hydrido-tris-(3.5-dimethylpyrazol-1-yl)methane (TPm*) ligand is also an effective ligand for use in lanthanide chemistry the next stage was to attempt to produce a mixed ligand complex in which a lanthanide metal is sandwiched between Tp* and TPm* ligands.

Reger *et al* have observed such systems for cadmium and lead.[157] Mixed mono-cationic tris(pyrazolyl)borate/tris(pyrazolyl)methane complexes of cadmium (II) were prepared by a conproportionation reaction between dicationic tris(pyrazolyl)methane complexes with neutral tris(pyrazolyl)borate complexes in refluxing CH_2Cl_2.

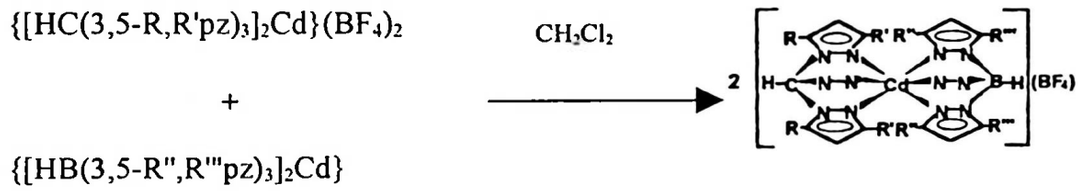

R = R' = R" = R'" = Me

R = R' = Me, R" = Ph, R" = H

R = H, R' = Ph, R" = R'" = Me

R = H, R' = Ph, R" = Ph, R'" = H

These complexes demonstrate a slow exchange of Tpm* ligands on the NMR time-scale and suggest preferential bonding of the TPm* ligand, over other substituted TPm ligands. For example, mixing $\{[HC(3\text{-}Phpz)_3](Tp^*)_3Cd\}^+$ with TPm^*_3 results in the exchange of the $HC(3\text{-}Phpz)_3$ ligand and the formation of $[(TPm^*)(Tp^*)Cd]^+$. When the latter complex is mixed with $HC(3\text{-}Phpz)_3$ however, no such exchange is observed in the NMR spectrum. A mixture of [(TPm*)(Tp*)Cd]+ with TPm^* shows ^{1}HNMR signals for both the free and coordinated ligand.

The structure of [(Tpm*)(Tp*) Cd](BF4) was determined by X-ray crystallography, however the TPm* and Tp* ligands were disordered. There was no such disorder in the structure of [(TPm*) (Tp*)Cd]{B[3,5-$(CF_3)_2C_6H_3]_4$}. Reger *et al* made direct comparisons between the metrical parameters of this complex and those of the homoleptic complexes: $\{[(TPm^*)]_2Cd\}^{2+}$ and $[(Tp^*)]_2Cd$. Table 2.3

Distances **(Å)**	A	B[a]	C
Cd-N (methane)	2.321	2.38	
Cd-N (borate)		2.29	2.348
C (methyne)-N	1.439	1.44	
B-N		1.54	1.553
Angles **(°)**			
N-Cd-N (methane intra-ligand)	80.000	80	
N-Cd-N (borate intra-ligand)		84	82.700
N-Cd-N (*trans*-inter-ligand)	180.000	173	180.000
N-Cd-N (*cis*-inter-ligand)	100.000	99	97.300
N-C(methyne)-N	109.600	112	
N-B-N		110	110.640

[a] ***Average values***

Table 2.3: A table of selected bond distances and angles for $\{[HC(3,5\text{-}Me_2pz)_3]_2Cd\}^{2+}$ *(A),* $\{[HC(3,5\text{-}Me_2pz)_3][HB(3,5\text{-}Me_2pz)_3]Cd\}^{+}$ *(B) and* $[HB(3,5\text{-}Me_2pz)_3]_2Cd$*, (c)*[157]

All three structures are similar. The average Cd-N bond in the mixed ligand complex is only 0.09 Å shorter for the borate ligand than for the methane ligand. The bond angles are similar in all of the structures as are the average C-N bond distances, thus one can conclude that the tris(pyrazolyl)borate and tris(pyrazolyl)methane ligands bond to Cadmium(II) in a very similar fashion.

The mixed Tpm*/Tp* lead complexes observed by Reger *et al* were synthesised by the reactions of $\{[(TPm^*)]Pb\}(BF_4)_2$ with an equivalent of K[Tp*] or K[Tp].

$$\{[(TPm^*)]Pb\}(BF_4)_2 + K[HB(3,5-R_2pz)_3] \xrightarrow{CH_2Cl_2} \underset{R=Me\ or\ H}{\{[(TPm^*)]Pb[HB(3,5-R_2pz)_3]\}(BF_4)}$$

The lability of the neutral TPm* ligand caused difficulties in purifying theses two complexes. Washing with hexanes resulted in the displacement of TPm* and the formation of {(Tp*)Pb}(BF_4) or {(Tp)Pb}(BF_4) respectively. Likewise addition of hexanes to a CH_2Cl_2 solution of {(TPm*)Pb(Tp*)}(BF_4) results in the precipitation of {(Tp*)Pb}(BF_4). Addition of five equivalents of TPm* to a saturated CH_2Cl_2 solution of {[HC(3,5-Me_2pz)$_3$]Pb[HB(3,5-Me_2pz)$_3$]}(BF_4) followed by slow diffusion of hexanes into the homogeneous mixture results in formation of crystals of {(TPm*)Pb(Tp*)}(BF_4) suitable for X-ray structural analysis. Figure 2.11

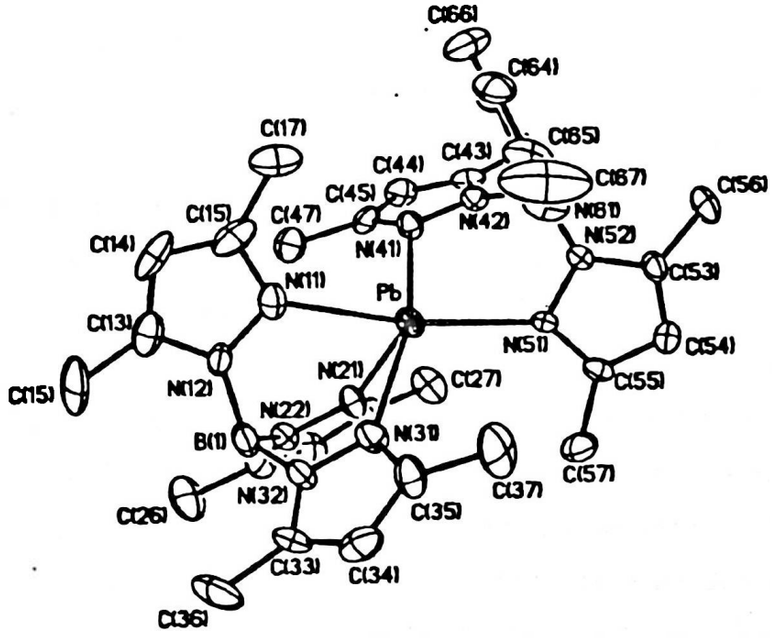

Figure 2.20: ORTEP diagram of {[TPm]Pb[Tp*]}$^+$ (hydrogens omitted for clarity)* [157]

The structure of this complex is very asymmetric The lead(II) ion is five coordinate bonded to a tridentate [Tp*]$^-$ ion and a bidentate TPm* ligand. The geometry of the complex is square based pyramidal with two nitrogen donor atoms from each ligand occupying the basal positions (N(11), N(41), N(51) and N(31))

and the donor atom from the tridentate $[(Tp^*)]^-$ ligand, (N (21)), occupying the apex position. Both Pb-N bond distances from the TPm^* are long (2.745 and 2.827 Å) when compared to the three Pd-N bonding distances of $[Tp^*]^-$ which have an average length of 2.43 Å. One presumes that the open face of the square based pyramid is occupied by the lone pair of electrons on the lead (II) ion.

The analogous mixed ligand cadmium(II) complex, $\{[TPm^*][Tp^*]Cd\}\{B[3,5\text{-}(CF_3)_2C_6H_3]_4\}$, is six coordinate with both the Tp* and TPm* ligands binding in a tridentate fashion. The reasons for the structural differences between the lead and cadmium complexes in bonding is not fully understood although its possible that the lone pair on the lead may be influential.

Attempts were made to prepare sandwich complexes of yttrium and samarium containing both the TPm* and TP* ligands bound to the metal centres. Obtaining structural data for these complexes should allow an insight into the differences in bonding between the two ligands to the lanthanide metal centres. Comparisons can also be made between the bonding and coordination numbers of yttrium and samarium complexes in light of the differences in their atomic radii. Studies have shown that pyrazolylborate ligands can accommodate a large range of metal centres of differing atomic radius by altering the ligand bite angle. An increase or decrease of this bite angle in the sterically encumbered 3,5-disubstituted ligand can cause changes in the inter and intra-ligand steric repulsions between the ring substituents which may cause the rings to twist about their B-N bond, altering the local symmetry of the metal. For example, twisting of the pyrazolyl rings in the Indium complex $[In(Tp^{tBu2})]$ due to repulsions between the substituents in the 5 position results in the reduction of the local symmetry of Tp^{tBu2} from C_3v to C_3.[158]. [159]

We anticipated that a metathesis reaction between $MTPm^*Cl_3$ (M = Y, Sm) and NaTp*.THF would result in the formation of a mixed ligand sandwich complex, $MTPm^*Tp^*Cl_2$ and NaCl.

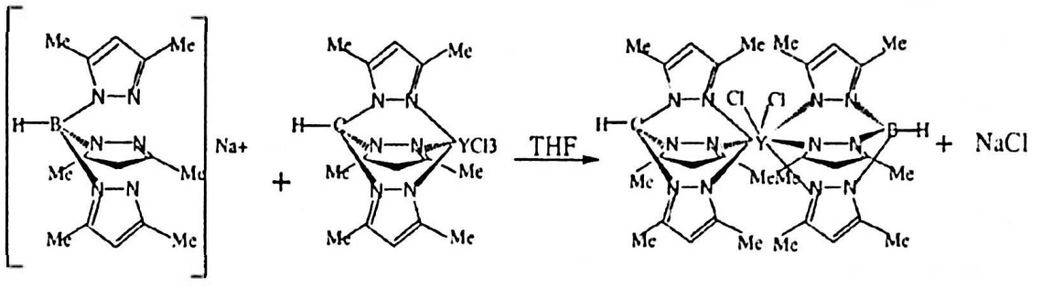

*Figure 2.21: Preparation of YTPm*Tp*Cl₂*

$YTPm^*Cl_3$ and $SmTPm^*Cl_3$ were prepared in-situ and a THF solution of NaTp*.THF was added drop-wise. For both reactions, stirring overnight resulted in the formation of a pale yellow supernatant and a white precipitate. The long reaction time was chosen in light of the problems encountered by Hillier in the preparation of $[Sm(Tp^*)_2Br]$ and the bis(Tp*)halide complexes of yttrium and ytterbium. The cleanliness and extent of the reaction appears to depend on the length of time for which the reactants are stirred. ^{1}HNMR data suggests a stepwise reaction for the formation of $[Sm(Tp^*)_2Br]$ with the initial coordination of one Tp* ligand to form the half sandwich complex followed by the coordination of the second ligand and the loss of salt. To militate against obtaining half sandwich complexes or mixed products, we opted for a relatively protracted reaction times. Attempts at crystallisation from concentrated solutions of the products in THF and toluene were unsuccessful.

The elemental analysis for the yttrium complex **(2.19)** is consistent with a complex of formula $[Y(TPm^{\bullet})(Tp^{\bullet})Cl_2]$. An IR spectrum of the product taken as a KBr pellet clearly shows the presence of the B-H stretch at 2551.6 cm^{-1}. This is very similar to the B-H observed by Hillier for the yttrium sandwich complex $[Y(Tp^*)_2Cl.1/2THF]$, thus indicating the Tp* ligand is within the coordination sphere of the metal. The elemental analysis for the samarium complex **(2.20)** is also consistent with the formula $[Sm(TPm^*)(Tp^*)Cl_2]$. The values for carbon and hydrogen are a little high, suggesting there is some solvent in the product. The IR spectra is also consistent with a Tp* ligand that is bound to a metal centre.

^{1}H NMR spectra are complicated. The NMR for complex **(2.19)** displays the CH

resonance for the TPm* ligand and the BH resonance for the Tp* ligand. Two peaks for the 4-H pyrazolyl ring protons of the respective ligands are also evident as is a small amount of THF. There are two peaks for the methyl proton groups, integrating for 18 and 10 protons respectively, there are also two broad peaks of 6 protons each at 2.46 and 1.54 ppm respectively. The fact that the two methyl peaks integrate for unequal protons suggests that the complex is not symmetrical and the two broad peaks indicate a fluxionality in solution. We tentatively suggest that the anionic Tp* ligand may bind to the metal centre preferentially and the TPm* might alter its chelation mode causing the broad resonances. Without a X-ray analysis on the product we cannot be certain of how the ligands are bound to the metal centre. It was not possible to interpret the ^{1}H NMR for the samarium complex.

Attempted preparation of Y[N(SiMe$_3$)$_2$]$_3$TPm* (2.22)

Finally, we combined a solution of Y[N(SiMe$_3$)$_2$]$_3$ in THF to TPm* in an attempt to synthesise a half sandwich yttrium TPm* complex containing trimethyl silyl amide ligands (N(SiMe$_3$)$_2$. Anna Hillier reports the preparation of the half sandwich complex of Y(Tp*)(N{SiMe$_3$}$_2$)$_2$, whilst the complex has not been characterised fully, its ^{1}H NMR spectrum is consistent with this complex being the major product.

The elemental analysis of **(2.21)** shows carbon and hydrogen values lower than calculated. The nitrogen value is slightly high which might point to some excess amide. The ^{1}H NMR displays resonances which integrate correctly for Y[N(SiMe$_3$)$_2$]$_3$TPm*. There are also some minor products in the spectrum which cannot be assigned although one of them appears to be a small amount of free TPm* ligand.

Summary

In this chapter we have demonstrated the utility of the dimethyl substituted tris(pyrazolyl)methane (TPm*) as an ancillary ligand for the trivalent lanthanide

ions.

The trichloride complexes [Ln(TPm*)Cl_3] (Ln = Y (2.1), Sm (2.2), Nd (2.3), Yb (2.4) and Ce (2.5)) have been prepared and complexes 2.1 and 2.2 have been characterised crystallographically. [Y(TPm*)Cl_3] (2.1) is six coordinate with a trigonal antiprismatic structure. The larger samarium ion can accommodate an additional ligand in its coordination sphere, thus complex 2.2 [Sm(TPm*)Cl_3] displays a seven coordinate metal centre with a coordinated THF group. The structure of 2.2 can be described as a capped trigonal antiprism or alternatively a tricapped trigonal pyramid.

The combination of lanthanide triflates, (Ln$(OTf)_3$, Ln = Y, Ho, Dy) with TPm* resulted in the structural characterisation of new complexes [Y(TPm*)$(OTf)_3$] (2.6) and [Ho(TPm*)$(OTf)_3$] (2.7). The crystals are isomorphous seven coordinate structures with one bound THF group. Similarly to complex 2.2, the geometry around the metal centre can either be described as capped trigonal antiprismatic or as a tricapped trigonal pyramid.

Substituting the chloride ions by metathesis with unsubstituted sodium phenoxide (NaOPh) did not produce fully characterisable products. It would seem that these ligands are not sufficiently large enough to sterically saturate the metal centre and thus we observe the incorporation of salt (NaCl) within the products.

Substitution reactions using the larger dimethyl substituted sodium phenoxide ($NaOPh^{Me2}$) , afforded the complexes [Nd(TPm*)$(OPh^{Me2})_3$] (2.12) and [Sm(TPm*) $(OPh^{Me2})_3$] (2.13). crystallographic analysis of these complexes reveals them to be highly symmetrical and thus fluxional, six coordinate trigonal anti-prisms with the alkoxide ligands terminally bound to the metal centre.

When comparing these new LnTPm* complexes with those of the established tris(pyrazoly)borate ligand (Tp*), it is apparent average M-Ln bond lengths are significantly longer in the former. This suggests that Tp* forms the stronger bonds with the metal centre as one would expect from the anionic ligand.

The preparation of the half sandwich borohydride complex [Nd(TPm*)$(BH_4)_3$(THF)] was carried out by the direct reaction of TPm* with [Nd$(BH_4)_3$$(THF)_3$]. The elemental analysis of the complex is consistent with the formulation [Nd(TPm*)$(BH_4)_3$(THF)]. The Solid state IR spectrum of the product displayed terminal B-H stretching bands, indicative of tridentate BH_4 ligands. We were unable to obtain crystals of the product suitable for X-ray analysis. Attempts at preparing complexes of LnTPm* with Cp, TP* and $N(SiMe_3)_2$ groups have produced a number of promising results, however at this stage it has not been possible to obtain crystalline products fro these reactions in order to obtain a full structural analysis.

Chapter 3 Synthesis of Divalent Lanthanide Complexes of Hydrido-*tris*-(3,5dimethylpyrazol1yl)methane (TPm*)

Introduction

The criteria for ligands to stabilise lanthanides in the divalent state is much the same as those required for stabilisation of the trivalent state in that they must be bulky and anionic. In addition they must also be able to tolerate the high reduction potentials of the Ln(II) ions

The first divalent organo-lanthanides were prepared by the reaction of cyclooctatetraene or cyclopentadiene with lanthanide metal in liquid ammonia[160]

The introduction of di-iodide precursors, $LnI_2(L)_x$ (Ln = Sm, L= THF; Ln = Yb, L = THF; NH_3; Ln = Eu, L = NH_3) from the reaction between the metal and 1,2-di-iodoethane, marked the increase in activity in divalent organolanthanide chemistry. Many synthetic routes to divalent organolanthanide complexes now use these di-iodides as divalent precursors rather than reducing a trivalent precursor such as $Ln(C_5H_5)_2Cl$. An advantage of using the iodide ion is it ability to impede coordination of the alkali metal salt formed in the metathesis reaction on account of its considerably larger size.

$$SmI_2(THF)_x + 2Na(C_5H_5) \longrightarrow Sm(C_5H_5)_2(THF)_X + 2NaI$$

One would expect the structures of the complexes $[Ln(C_5Me_5)_2]$ (Ln = Sm, Eu, Yb) to be parallel ring structures, with the substituted ligands as far apart as possible. considering they are ionic complexes, predominantly governed by electrostatic factors. The crystal structures however, show that both the solvated and unsolvated

complexes have a bent metallocene geometry.[161]-[162] Small intra molecular non-bonded Van der Waals interactions between the ligand have been suggested to account for this discrepancy between the calculated optimum geometry and actual bent geometry. (chapter 1)

Divalent lanthanide complexes containing alkynyl ligands have also been prepared. One synthetic route is by transmetallation with mercury reagents.[163],[164]

Divalent alkynides can be formed from terminal alkynes from metal vapour synthesis.[165] Several synthetic routes to divalent alkyl and aryl lanthanide complexes have been reported in the literature, such as the reaction between the alkyl or aryl iodides with Sm, Eu or Yb metals.[166]

The chemistry of the decamethyllanthanocenes has been well developed, particularly that of $[Sm(C_5Me_5)_2]$ and $[Sm(C_5Me_5)_2(THF)_2]$.[167] Bis(cyclopentadienyl) Yb and Sm complexes react with several alkyl-halides to produce the trivalent halide complexes, Ln(C5R5)2X(solvent).[168] Similarly the reaction of $(C_5H_5)_2Yb$ in THF or DME with metal halides and pseudo halides: HgX_2, TIX, AgX_2, CuX, (where X = O_2CMe, $O_2CC_6F_5$, $O_2CC_5H_4N$, Cl, Br, I, C_6F_5, CPh Cph, $CH(OCMe)_2$) gives the oxidation products.[169]

$$[Yb(C_5H_5)_2(L)]+MX \longrightarrow [Yb(C_5H_5)_2X(L)]+M$$

$$M = Ti, Cu \quad L = solvent$$

$$2[Yb(C_5H_5)_2(L)]+MX_2 \longrightarrow 2[Yb(C_5H_5)_2X(L)]+M$$

$$M = Hg, Ag \quad L = solvent$$

A variety of bridged species can also be formed using these divalent cyclopentadiene complexes. $[Sm(C_5Me_5)_2(THF)_2]$ abstracts oxygen from a number of substrates , including NO, N_2O and C_5H_5NO, to form the trivalent oxo-bridged complex $[[Sm(C_5Me_5)_2]_2(\mu\text{-}O)]$.[170] Treating $[Yb(C_5Me_5)_2(OEt_2)]$ with a chalcogenide containing species such as R_3PE (R = Ph, n-C_4H_9; E = S, Se, Te)

affords the corresponding chalcogen-bridged species $[[Yb(C_5Me_5)_2]_2(\mu\text{-}E)]$.[171]

$[Sm(C_5Me_5)_2(THF)_2$ reacts with unsaturated molecules in reductive coupling reactions. An example is the reaction between the samarium complex and pyridazine or PhCH=NN=CHPh, a one electron process where coupling occurs via C-C bond formation.[167] **Figure 3.1**

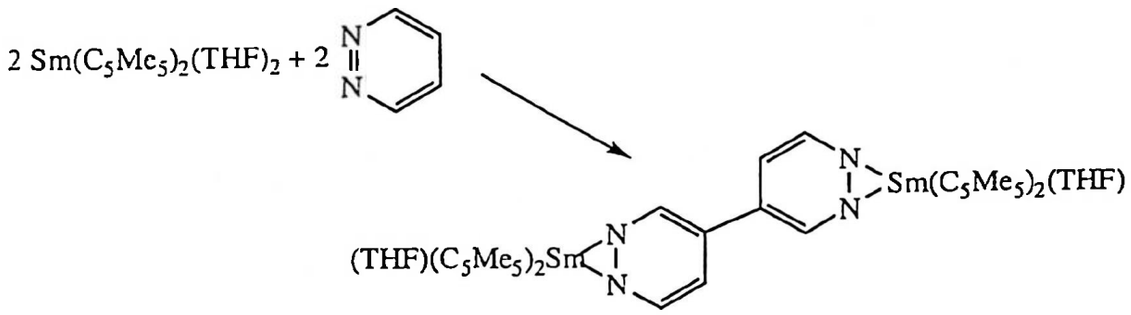

Figure 3.1: $Sm(C_5Me_5)_2(THF)_2$ reaction with unsaturated molecule

Graham Maunder, a student in our laboratory, studied the preparation and reactivity of divalent lanthanide complexes of the pyrazolylborates in order to develop a similarly rich chemistry to that of the cyclopentadienyl analogues. The reduction of solutions/suspensions of $[(Tp^{Me2})_2Sm]^+[OTf]^-$ and $[(Tp^{Me2})_2Yb]^+[OTf]^-$ in THF with an excess of sodium amalgam afforded the partially soluble sandwich complexes $[(Tp^{Me2})_2Ln]$ (Ln = Sm, Yb). The corresponding Eu complex was prepared by mixing two equivalents of KTp* with $Eu(OT)_3$ in THF and then reducing with sodium amalgam in-*situ*. The complexes $[(Tp^{Me2})_2Ln]$, (Ln = Sm and Yb) were also synthesised by the metathesis reaction between SmI_2 or YbI_2 with two equivalents of KTp^*, KI was also present in the isolated products. Crystals of $(Tp^*)_2Yb$ and $(Tp^*)_2Eu$, suitable for X-ray crystallographic studies were grown by slow sublimation under vacuum and a temperature gradient in a sealed tube. The structures of these complexes show each metal lying in a six coordinate environment which is best described as trigonally distorted octahedral. The complexes are isomorphous, crystallising in the space group R3. The molecules have S_6 symmetry, consistent with a single pyrazolyl environment. The two pyrazolyl ligands in the complex are crystallographically parallel, this is in

contrast to decamethyllanocenes, $[CP^{Me2})_2Ln]$, which display bent geometries. This is presumably due to the much larger size of the Tp^* ligand over Cp^{Me2}. **Figure 3.2**

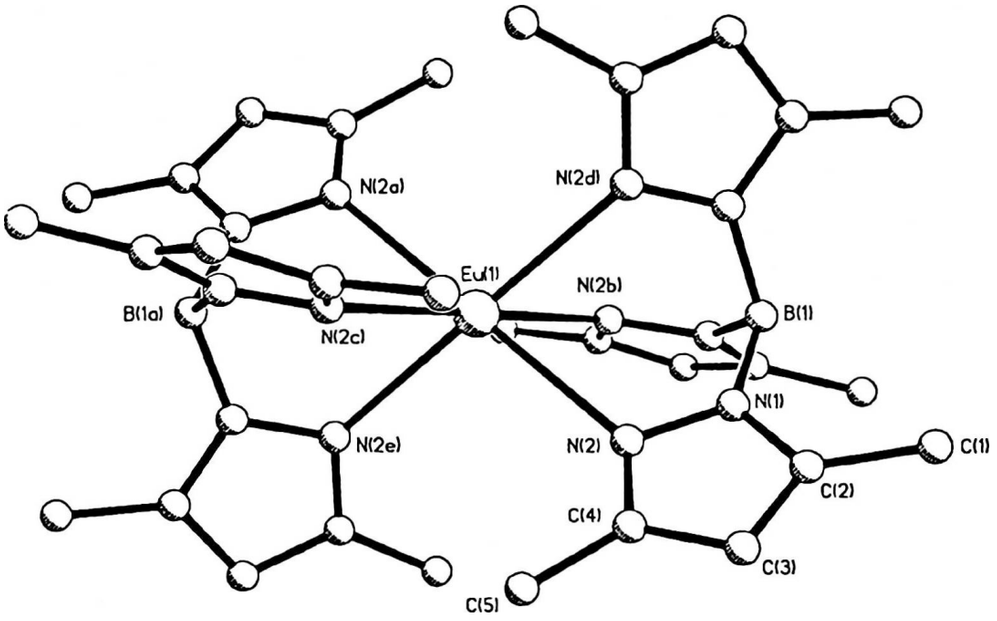

Figure 3.2: molecular structure of [(Tp*)$_2$Eu], hydrogens omitted for clarity.

In an attempt to enhance the solubility of the products, Maunder introduced an ethyl group in the 4 position of the pyrazolyl ring. Reaction of two equivalents of $KTp^{Me2-4-Et}$ with the Sm and Yb di-iodides produced purple complexes that were soluble in THF, ether and aromatic solvents. Attempts at growing crystals suitable for analysis were not successful, however spectroscopic data pointed strongly to a six coordinate structure, analogous to that of the Tp^* derivatives.

The presence of two ancillary ligands in theses complexes somewhat limits their chemistry by the availability of only neutral binding sites at the metal centre. Therefore forming the half sandwich complexes, where steric control is adequately provided by a single ancillary ligand is important. Studies by Maunder using the $Tp^{Me2-4Et}$ ligand did not produce the desired half sandwich complexes, due to the inability of the ligand to sterically saturate the large Ln^{2+} ions. Thus the more

sterically demanding tris-(3-tert-butyl-5-methylpyrazol-1yl)borate ligand was utilised. Consequently Maunder has described the preparation and crystallographic characterisation of the first stable half sandwich derivatives of the lanthanide di-iodides, $[Tp^{3\text{-}t\text{-}Bu\text{-}5\text{-}Me}SmI(THF)_2].(Et_2O)_{0.5}$ and $[Tp^{3\text{-}t\text{-}Bu\text{-}5\text{-}Me}YbI(THF)]$.[172] Slow cooling of the Sm and Yb complexes in diethyl ether, resulted in crystals suitable for analysis by X-ray diffraction studies. The samarium complex crystallised in the space group C2/*m* and the geometry around the metal can be describes as distorted 'bicapped trigonal pyramidal'. In contrast to this, the Yb complex crystallised in the space group $P2_1/n$ and contains only one THF molecule within its coordination sphere. The metal centre is five coordinate which is consistent with smaller ionic radius of Yb^{2+} relative to Sm^{2+}. The best description of the coordination geometry around the metal centre is that of distorted trigonal bipyramidal.**Figure 3.3**

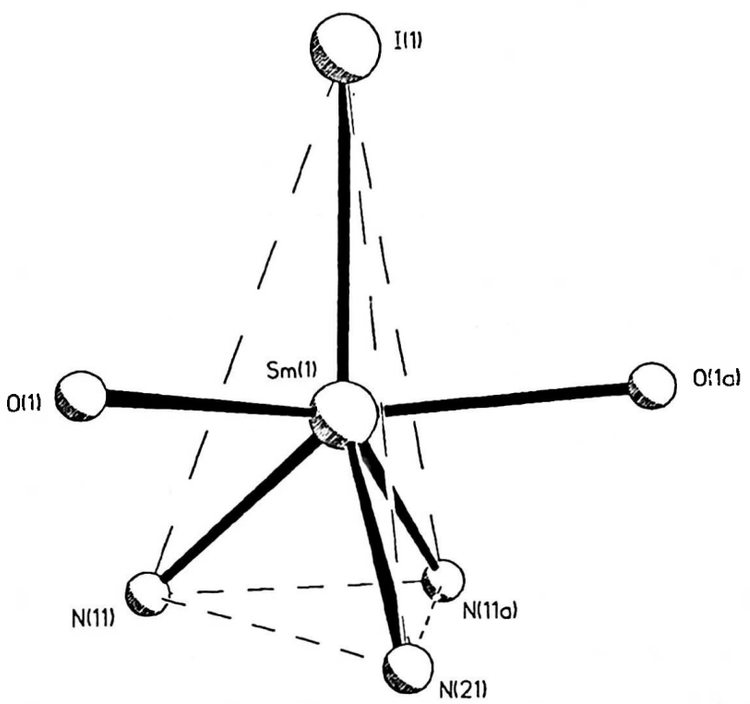

Figure 3.3: The inner coordination sphere of $[Tp^{3\text{-}t\text{-}Bu\text{-}5\text{-}Me}SmI(THF)_2].(Et_2O)_{0.5}$[172]

This chapter describes the preparation of the divalent ytterbium tris(3,5-dimethylpyrazolyl)methane complex and its subsequent reactions with unsubstituted and disubstituted sodium phenoxide. This work can be compared with the substitution reactions carried out on trivalent lanthanide tris(3,5-

dimethylpyrazolyl)methane complexes. (Chapter 2). Attempts at synthesising a mixed ligand complex with both the TPm* and Tp* ligands were made, this is also in line with the trivalent lanthanide chemistry described in chapter 2. Efforts to deprotonate the ytterbium complex using sodium diphenylamine are also discussed. Ytterbium was chosen on account of the ytterbium diiodide readily available in our laboratory.

Preparation of YbTPm*I_2 (3.1)

Solutions of ytterbium diiodide and two equivalents of TPm* in THF were combined slowly resulting in a deep red solution and the formation of an orange precipitate. The precipitate was isolated by filtration and was found to only partially redissolve in THF, thus crystallisation from slow cooling in THF was not successful. The product was found to be extremely unstable in air, decomposing immediately. We attempted to form crystals of the product by layering a concentrated solution of YbI_2 in THF with a layer of THF topped with a concentrated solution of TPm* in THF in a sealed Youngs tube. A red solution gradually appeared, however no crystals had formed after several days. Similar reactions carried out by Maunder with ytterbium diiodide and Tp* afforded the sandwich complex [Yb(Tp*)$_2$]. It was anticipated that combining two equivalents of TPm* in THF with an equivalent of YbI_2 may produce the analogous sandwich complex [Yb(TPm*)$_2$$I_2$]. The elemental analysis indicates that we have formed the half sandwich complex [Yb(TPm*)I_2], with a THF present in the coordination sphere. [Yb(TPm*)I_2].(THF). Indeed the yellow/orange colour of our final product is in contrast with the pink sandwich complex [Yb(Tp*)$_2$] synthesised by Maunder. A half sandwich ytterbium complex, using the much more sterically demanding tris-(3-tert-butyl-5-methylpyrazol-1-yl)borate ligand ($Tp^{3\text{-}t\text{-}Bu\text{-}5\text{-}Me}$) was also prepared and structurally characterised by Maunder. When prepared in THF, this complex displayed a similar yellow colour in solution, this is another strong indication that we have prepared the half sandwich complex. Several repeat reactions show that the half sandwich complex is is formed, regardless of the reaction stoichiometry used, highlighting the weaker interaction between the

neutral TPm* ligands and the metal centre compared with the anionic Tp* ligands. **Figure 3.4**

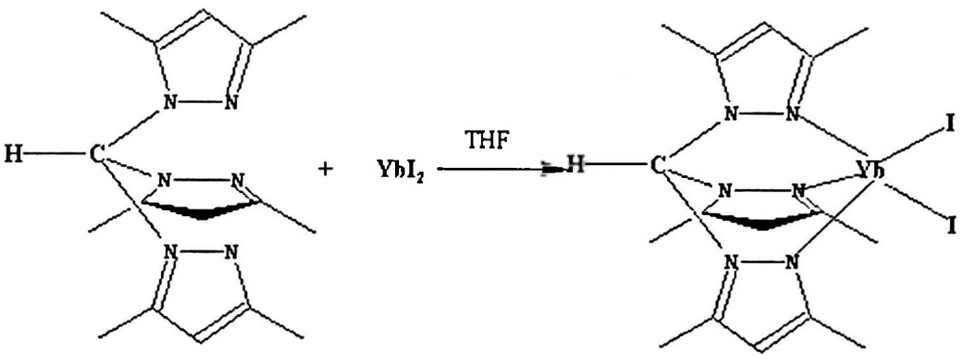

*Figure 3.4: Synthesis of YbTPm*I₂*

The IR spectra of the complex recorded as as KBr pellet displayed the usual peaks associated with the TPm* ligand. The precise structure of the complex remains undetermined as its relative insolubility precludes the recording of an ^{1}HNMR spectra and molecular weight measurements. Attempts at growing crystals suitable for X-ray analysis were unfruitful.

The reaction between YbTPm*I_2 and $NaNPh_2$

In order to see if a reaction with a base such as $NaNPh_2$ would result in the addition of the amide into the coordination sphere of the metal or a deprotonation of the TPm* ligand, the YbTPm*I_2 was combined with $NaNPh_2$

The reaction was carried out in-situ, with TPm* and YbI_2 present in a 2:1 stoichiometry. Two equivalents of the $NaNPh_2$ were added drop-wise to a suspension of the ytterbium complex (3.1). The immediate formation of a burgundy solution and precipitate suggest that a reaction has occurred. The red oily solid isolated from the reaction mixture gives an intense purple solution with a grey solid when extracted into toluene. The product is extremely air sensitive and stirring of the purple solution for more than 20 minutes results in decomposition

of the product as indicted by a dull grey solution. Thus the toluene is removed immediately and the purple solid dried under vacuum and stored in the glove box.

The colour changes occurring during the reaction can be compared to those observed by Graham Maunder for the preparation of the sandwich complex $[(Tp^*)_2Yb]$. The synthesis of this complex by reduction of $[(Tp^*)_2Yb]^+[OTf]^-$ with an excess of sodium amalgam and by the metathesis reaction of YbI_2 with KTp* resulted in pink/purple THF solutions.

For direct comparison with Maunders work we recorded the UV-Vis spectra of our product in toluene. Maxima in toluene were recorded at 350.2 nm and 523 nm. These are very similar to the maxima recorded for the $[Yb(Tp^*)_2]$ (340 nm and 530 nm). This may suggest we have made a homoleptic complex of the deprotonated ligand analogous to the complex $[Yb(Tp^*)_2]$. Figure 3.5

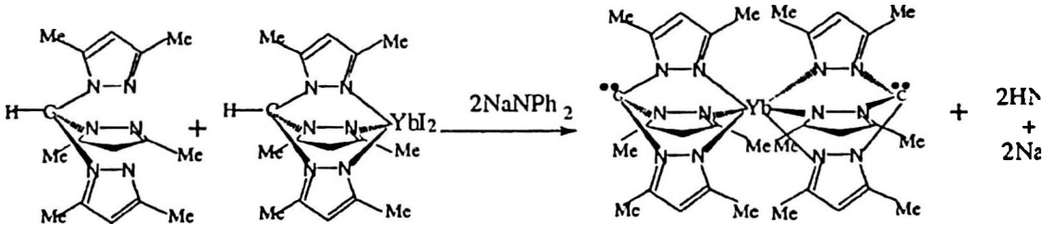

Figure 3.5: Reaction between $NaNPh_2$ and $YbTPm^*I_2$

An NMR of the product in benzene displays shows a large excess of diphenyl amine in relation to the amount of product present in solution. The NH resonance of the diphenyl amine is present at δ 4.97 and the aromatic resonances associated with the diphenyl amine are present in the δ 7 region. There is also a notable absence of any peak corresponding to the C-H proton. One would expect the C-H proton to occur in the same region as the aromatic diphenyl amine protons, thus whilst it is possible that the complex is deprotonated, it is also possible that the large diphenyl amine resonances are simply masking the C-H peak. The resonances for the protons on the pyrazolyl rings and the methyl groups in the 3 and 5 positions of the pyrazolyl rings have been tentatively assigned at δ 4.97 and δ 2.08 and δ 1.90. It is not possible to integrate the spectra due to the large excess of diphenyl amine present.

The infra-red of the product taken as a KBR disc is different to the spectrum of [YbTPm*I_2.THF]. The peaks corresponding to the pyrazolyl groups are present, in addition to these there are strong stretches at 2358 and 2341 cm^{-1} corresponding to carbon dioxide

An elemental analysis of the product is not consistent with the results expected for the deprotonated sandwich product. Whilst the percentage of carbon is reasonable, the hydrogen and the nitrogen are low. It is probable that the extreme air and moisture sensitivity of this complex makes the analysis particularly challenging.

The analysis of this intriguing purple product has given mixed results, purple colour change and UV-Vis spectra point to a positive result for a deprotonation reaction whereas the elemental analysis does not concur and the ^1H NMR is inconclusive with a very large excess of diphenyl amine present. Clearly more effort is required in extracting crystals of the product suitable for crystallographic analysis, the extreme air and moisture sensitivity of the product makes this very difficult.

When the solution is left to stand in a sealed tube for two days a colour change from purple to red is observed. An ^1H NMR taken in $CDCl_3$ does not provide any information on the reason for the colour change. The spectra is similar to that obtained for the reaction between YbTPm*I_2 and $NaNPh_2$. There is a large excess of diphenlyl amine with the aromatic peaks masking any peak present due to the C-H resonances.

Further attempts at the deprotonation reaction using alternative bases did not give the same colour change observed with $NaNPh_2$. Addition of a yellow solution of [YbTPm*I_2] to a suspension of $LiNH_2$ in THF did not form the burgundy solution as anticipated, rather the solution remained pale yellow even after heating. On leaving to settle a white precipitate settled out. The yellow colour of the product suggests that is not a sandwich complex, in fact the elemental analysis of the resulting yellow powder is correct for [YbTPm*I_2.THF]. The IR of the product

recorded as a KBr disc is almost identical to that taken for [YbTPm*I_2]. The lithium amide is apparently not able to deprotonate the complex and no reaction occurs. The elemental analysis shows that there is no amine present in the final product.

Substituting the iodide ions

In order to compare the reactivity of the divalent ytterbium complex with that of the trivalent yttrium and samarium complexes we carried out substitution reactions using unsubstituted sodium phenoxide and the 2,6 dimethyl substituted sodium phenoxide. We anticipated that by combining THF solutions of [Yb(TPm*)I_2] and $NaOPh^{R2}$ (R = H, Me), the iodide ions will be substituted for phenoxide groups in a metathesis reaction. **Figure 3.6**

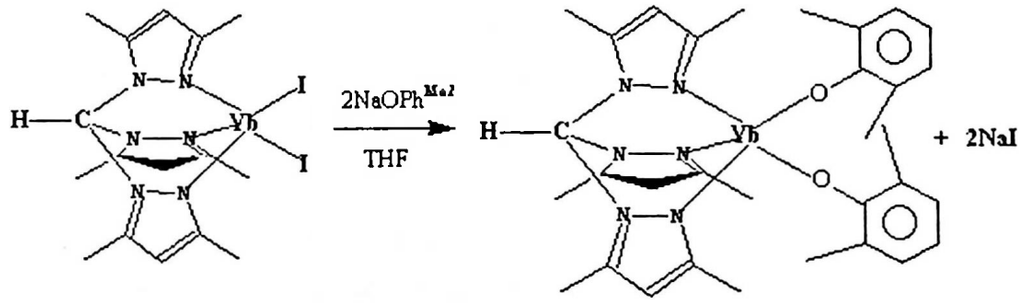

Figure 3.6: Preparation of Phenoxide complexes.

The reaction between [Yb(TPm*)I_2] and two equivalents of NaOPh resulted in an orange/brown emulsion after stirring for approximately 24 hours. An orange solution was isolated by filtration and orange crystals were grown by slow cooling of a concentrated solution of the product in THF. The ^{1}H NMR of the crystals recorded in acetonitrile only displays resonances of acetonitrile and THF, no ligand is present in the crystals. The elemental analysis confirms this with percentage values for carbon, hydrogen and nitrogen being extremely low. Closer analysis of these numbers along with the ^{1}H NMR spectra suggests that we have may crystallised a THF adduct of a sodium iodide salt. [YbI_2.THF]

Subsequent reactions with phenoxide ligands were carried out using the bulkier sodium 2-6-dimethyl phenoxide. This ligand should be more able to satisfy the

coordination sphere of the lanthanide and produce tractable products.

Adding two equivalents of $NaOPh^{Me2}$ in THF to solution of $[YbT(Pm^*)I_2]$ in THF, resulted in a dark orange/red solution which became pale yellow after stirring for 5 minutes. The colour change from dark orange to yellow indicates that the reaction has progressed differently to the reaction between the unsubstituted phenoxide and the ytterbium complex. Attempts at crystallising the product from THF were not successful therefore the solvent was removed under dynamic vacuum. The elemental analysis of the product was not consistent with that expected for a complex of the type $[YbTPm^*(OPh^{Me2})_2]$ with all values being much lower than calculated. To account for these values there would have to be considerable amount of sodium iodide in the product, indeed very little salt precipitated during the reaction. . Salt incorporation is an issue in lanthanide chemistry (chapter 2) however we have previously isolated trivalent complexes of the type $LnTPm^*(OPh^{Me2})_3$ where Ln is Y, Yb and Sm, which are shown to be free of salt by elemental analysis and crystal data. Its possible that the disubstituted phenoxide is not able to sterically saturate the divalent metal centre alone.

The ^1H NMR of the product taken in acetonitrile displays the resonances corresponding to those expected in the 3,5-dimethylpyrzolyl ligand. The two resonances corresponding to the methyl groups on the 3 and 5 positions of the pyrazolyl rings are however shifted slightly down-field relative to those displayed in the ^1H NMR of the free ligand recorded in acetonitrile, indicating that the ligand is bound to the metal centre. The 3. 5 *meta* protons of the two phenoxide rings and the *para* protons are clearly present as a doublet and a triplet respectively, consistent with the expected splitting pattern for protons in these positions of a six membered ring. The resonances occur at δ 6.90 and 6.66 ppm and integrate to four and two protons respectively. The methyl groups at positions 2 and 6 on the phenoxide rings give a broad resonance at δ 2.103 ppm, Suggesting some restriction in rotation around the M-O bond.

Attempting to prepare a mixed ligand sandwich complex [Yb(TPm*)I(Tp*)]

To align the divalent chemistry further with that carried out for the trivalent lanthanide complexes discussed in chapter 2, we attempted to prepare a mixed ligand ytterbium sandwich complex containing both the neutral TPm* ligand and the anionic Tp* ligand. **Figure 3.7**

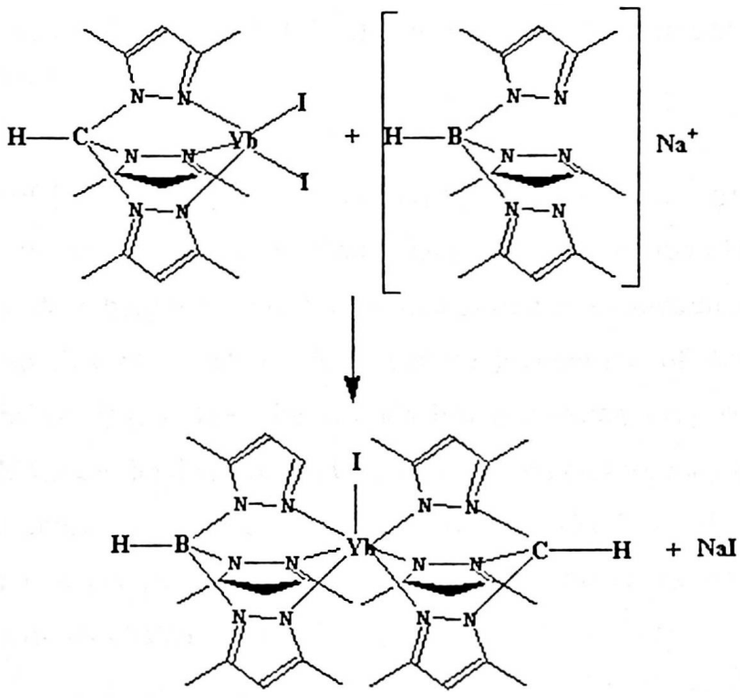

Figure 3.7: Preparation of [YbT(Pm)I(Tp)*]*

The addition of a solution of NaTp* ligand in THF to one equivalent of [YbTPm*I_2] in THF resulted in an immediate colour change from orange to bright yellow and the formation of a white precipitate.

The precipitate tested positive for iodide ions and is thus expected to be the sodium iodide by-product of the reaction. Attempts to crystallise the product from a concentrated solution of THF were not successful , thus the solvent was removed and the remaining yellow powder was taken into the glove box for analysis.

The elemental analysis for this complex is high in both carbon and hydrogen and

low in nitrogen which points to the presence of solvent. Unfortunately the ^{1}HNMR recorded for this complex was largely uninterpretable.

Summary

In this chapter we have described the preparation of [YbTPm*I_2] **(3.1)** and have noted the propensity of the TPm* ligand to form half sandwich complexes with lanthanide ions regardless of the reaction stoichiometry. Similar studies using the anionic Tp* ligand have resulted in the formation of a number of sandwich complexes.[173],[174]

The reaction of [YbTPm*I_2]with sodium diphenyl amine **(3.2)** produced some potentially very exciting results. A colour change on combination of the reactants, from yellow to deep burgundy and then vibrant purple on extraction into toluene is very similar to that observed my Maunder on preparation of the related Tp* complex, [Yb(Tpm*)$_2$], indeed the UV/vis has a maxima very similar to that observed by Maunder, lending weight to the suggestion that we may have formed a deprotonated sandwich complex analogous to [Yb(TPm*)$_2$]. The extreme air sensitivity of this complex to air and moisture has made the analysis of this complex particularly challenging.

The attempted preparation [Yb(TPm*)(OPh)$_2$] (3.3) was unsuccessful, affording only the THF adduct of a sodium iodide salt. Results from the reaction of YbTPm*I_2 with the larger dimethyl substituted phenoxide (NaOPh^{Me2}) are more promising with an NMR spectrum consistent with [Yb(TPm*)(OPh^{Me2})$_2$]. The 2,6 methyl groups of the phenoxide ring display broad resonances, suggesting some restriction in the rotation about the M-O bond.

Chapter 4 Flurophenoxide Chemistry

Introduction Alkoxide ligands

Research into metal alkoxide complexes has gained considerable momentum in recent years, driven, primarily, by their extensive use in industry. The more volatile metal alkoxides are renowned for readily undergoing hydrolysis to form pure metal oxides. and thus make excellent precursors for depositing thin metal oxide films by chemical vapour deposition.

$$M(OR)_4 + 2H_2O \longrightarrow MO_2 + 4ROH$$

These thin metal oxide films have found applications as insulators, piezoelectric materials, fast ion conductors and high Tc superconductors.[175]

The less volatile metal alkoxides can be used in the sol-gel technique for producing oxide glasses and ceramics. Essentially the metal alkoxide is dissolved in a suitable organic solvent to form a homogeneous solution. Controlled hydrolysis of the metal alkoxide affords a gel which can then be dried and fired to produce a ceramic or glassy material.[176]

In synthetic chemistry, metal alkoxide complexes are used as strong lewis bases and there have been recent developments in the use of metal alkoxides as catalysts in a wide range of homogeneous reactions. The metal alkoxides of Ti and magnesium are used as active components of multicomponent Ziegler-Natta type catalysts for the catalytic polymerisation of alkenes.[175] In 1980, Katsuki and Sharpless discovered that a mixture of titanium tetra-isopropoxide and (+)-diethyl tartrate was an extremely efficient enantio-selective reagent for the epoxidation of allylic alcohols using tert-butyl hydroperoxide as the oxygenating reagent.

Recently Schrock *et al* have developed a wide range of transition metal alkylidyne and alkylidene complexes in which the catalytic performance of the metal is optimised significantly by alkoxy groups, for the metathesis and polymerisation of alkenes and alkynes.

Synthesis

The methods for synthesising metal alkoxide complexes have long been established.[175] The extreme moisture sensitivity of the complexes require synthesis to be carried out in a dry environment. The precise synthetic method employed depends on the electronegativity of the metal. The electropositive alkali, alkaline earth and lanthanide metals react directly with the alcohol to afford the corresponding metal alkoxide with the production of hydrogen.

$$M + xROH \longrightarrow M(OR)_x + \frac{x}{2} H_2$$

For divalent and trivalent metals it becomes necessary to use a catalyst such as iodine or mercury chloride which clean the surface of the metal and thus initiate the reaction. For metals with even greater valencies, synthesis involves a metathesis reaction between the metal chloride with an alkali metal alkoxide, usually in a hydrocarbon solvent such a benzene or an ether solvent.

$$MCl_x + xM'OR \longrightarrow M(OR)_x + xM'Cl$$

This reaction is unsuitable for metals such as Zr, Hf, Nb and Ta as the reaction does not go to completion, rather, stable hetero-metal alkoxides are formed ($M_xM'(OR)_x$. In such cases it is necessary to use ammonia for dechlorination of the metal.

$$MCl_x + xNH_3 + xROH \longrightarrow M(OR)_x + xNH_4Cl$$

Structural Chemistry

Since the 1950s there have been systematic studies into the structural chemistry of alkoxide complexes with metals across the periodic table.[177] Until the 1980s spectroscopic investigations into these species were limited to the infra-red, electronic and NMR. Since then the advances in X-ray crystallographic analysis and improvement in the techniques for growing and mounting single crystals of the air sensitive alkoxides have allowed for the elucidation of the structures of many more of these complexes.

The majority of metal alkoxides form aggregates both in their solid states and in solution. This is driven by the bridging propensity of the alkoxo group which can bond through its oxygen to two (μ2) or three (μ3) metals. The degree of aggregation depends on the valency and size of the metal ion. For the monovalent alkali metal oxides with one alkoxide group per metal atom, alkoxo bridging is very apparent. The larger the metal, the greater its tendency to expand its coordination number above its covalency number by forming alkoxo bridges. The nature of the solvent also has an affect, with coordinating solvents binding to the metal and reducing alkoxo bridging. It is however accepted that it is the steric effect of the alkyl group that ultimately determines the extent of aggregation with the larger groups inhibiting alkoxide bridge formation.[175]

Some examples to exemplify the above are the unsolvated group 1 methoxides (MOMe) and isopropanolates (MO^{i}pr), where M = Li-Cs, and the methoxides of Ca, Sr and Ba. These complexes have layered polymer arrangements.[178]-[179] When the steric demand of the alkoxo group is increased the formation of these layered chains is no longer possible, rather spherical or cyclic structures are built. This is demonstrated by the complex [K(OBu^t)$_4$] which displays a cubic structure where the metal and oxygen atoms sit on alternate corners of a distorted cube. Figure 4.1.

Molecular mass measurements show that the cubic structure is maintained in solution and the mas spectrum of $[K(OBu^t)_4]$ indicates a similar state of aggregation in the gas phase. Many of the alko and aryloxo structures have since been discovered to be based on the cube.

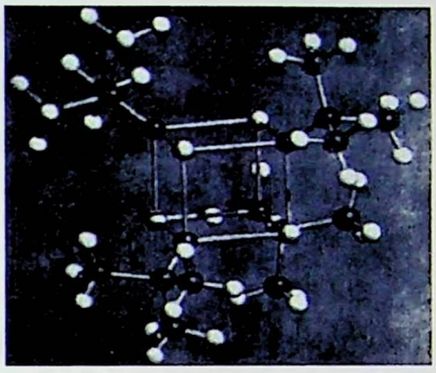

Figure 4.1: Cubic structure of $[K(OBu^t)_4]$[180]

For the smaller metal, sodium, a more complicated structure is observed. Hexamers $(NaO^tBu)_6$ and nonomers $(NaO^tBu)_9$ coexist in the unit cell in the solid state.[181]-[182] **Figure 4.2**

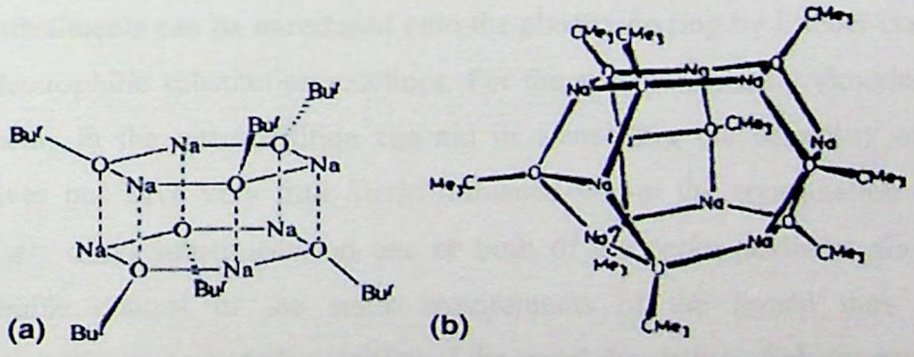

Figure 4.2:Structure of hexameric $(NaO^tBu)_6$ (a) and nonomeric $(NaO^tBu)_9$ (b)
[181]

Solubility and Volatility

The extent to which metal alkoxides can be used in organometallic synthesis and in industry depends on their solubility and volatility, properties derived from their

structures.[183] The methoxides of the group 1 metals are shown to be neither volatile nor soluble owing to their polymeric layered arrangements and high lattice energies.

The cubic structure of $[K(OBu^t)_4]$, however, explains why many alkoxides are surprisingly soluble in non-polar solvents considering the high electronegativity of oxygen and thus predominantly ionic character of the metal-oxygen bond. The alkyl groups surround the metal-oxo cluster and form a hydrophobic shell around it, thus shielding it from the solvent.

The Aryloxide Ligand

Recently there has been growing interest in the organometallic chemistry associated with metal aryloxides. The use of non-protic solvents has greatly increased the variety of derivatives that can be isolated. Synthesis of metal aryloxide derivatives depends largely on the metal precursor and the nature of the ligand. The synthetic routes to simple aryloxide derivatives are however much the same as for the corresponding metal alkoxides.[175]

Alkyl substituents can be introduced onto the phenoxide ring by Friedel-crafts and other electrophilic substitution reactions. For the simplest mono aryloxides, alkyl substituents in the *para* position can aid in controlling the solubility of metal derivatives but have very little steric influence within the coordination sphere. Conversely alkyl substituents on one or both of the *ortho* positions allows for considerable control of the steric requirements of the ligand thus greatly influencing the structure and reactivity of the metal derivatives. Substituents in the *meta* positions of the phenol ring affect the steric properties of the ligand by limiting the conformational flexibility of the substituents in the adjacent *ortho* positions.[184]

The aryloxide ligand can adopt a number of bonding modes. The group 1 complexes, for example $[Li_6(\mu_3\text{-}OPH)_6(THF)_6]$ and $[Na_4(\mu_3\text{-}OAr)(DME)_4]$ (OAr=

OC_4H_4-4Me) demonstrate hexagonal and cubic clusters respectively with triply bridging aryloxide ligands. Tri and hexanuclear clusters of Ca, Ba and Sr also contain triply bridged phenoxides. Quadruply bridging ligands are rare, however a few mixed metal clusters of the lanthanides have been shown to contain them, e.g.: $[Me_4N][La_2Na_2(\mu_4\text{-}OAr)(\mu_3\text{-}OAr)_2(\mu_2\text{-}OAr)_4(OAr)_2(THF)_5]$ where OAr = 4-methylphenoxide.[185] **Figure 4.3**

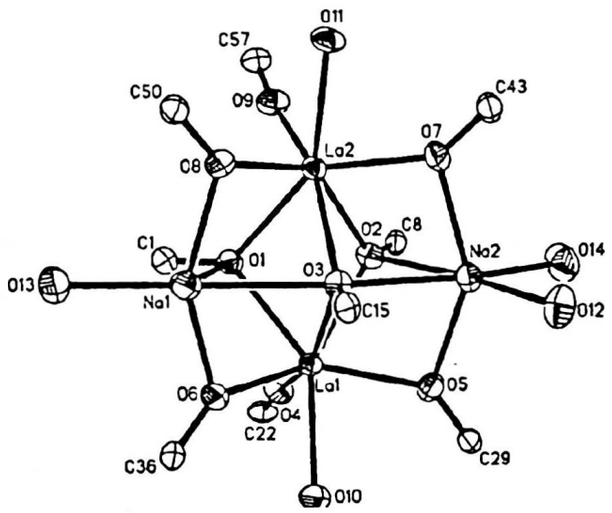

Figure 4.3: ORTEP diagram of the anion in $[La_2Na_2(\mu_4\text{-}OAr)(\mu_3\text{-}OAr)_2(\mu_2\text{-}OAr)_4(OAr)_2(THF)_5]$ [185]

There are considerably more complexes containing doubly bridged aryloxide ligands, in many cases these complexes contain two different metals where one is a group 1 element. Another important bonding mode for aryloxides involves interaction of the metal with the phenoxide ring. The aryloxide ligand binds to a metal centre via the oxygen atom whilst a second metal centre in π-bound to the phenoxide ligand. This bonding arrangement often arises for aryloxide derivatives of electropositive metals where there is also a deficiency in lewis bases to provide electron density to the metal centres.

The most prolific bonding mode for the aryloxide ligand is the terminal one where the phenoxide is bound to one metal atom. The presence and extent of oxygen-P to metal π-bonding has been the focus of many a discussion. Changes in the oxygen

atom hybridisation from sp^3 to sp^2 and sp allows the the oxygen to interact with one, two or three orbitals on the metal centre. If these orbitals are filled with 2,4 or 6 electrons, this would lead to the formation of M-O single (σ^2), double ($\sigma^2\ \pi^2$) and triple ($\sigma^2\ \pi^4$) bonds respectively. The extent of aryloxide oxygen to metal π-bonding depends on the formal oxidation state of the metal, the molecular symmetry of the complex, the coordination number as well as the nature of the ancillary ligands. The combination of these factors determines how electron deficient the metal centre is and thus the availability of of suitable π-acceptor orbitals. It follows that the extent of oxygen to metal π-bonding will also effect terminal M-OR bond distance, as the extent of metal to oxygen π-donation increases so the M-O bond distance decreases.

Fluorinated Alkoxide and Aryloxide Complexes.

Fluorine has traditionally been considered as a common constituent in large and weakly coordinating anions. However, like oxygen, an important hard donor centre, fluorine is also highly electronegative, small and hard and therefore a promising donor for hard metal ions.

The first detailed investigation into the coordination chemistry of the CF unit was not published until 1983, when very short contacts were observed between the CF unit and the metal ion in the crystal structures of several group 1 and 2 metal salts.[186] Subsequently many complexes of the alkali and alkaline-earth metal ions with fluorinated ligands have been observed containing a variety of structural types. This suggests that the coordination of such hard metal ions by the CF unit is preferred over softer metal ions. CF-metal interactions have also been observed for a number of other metal ions, a subject which has been comprehensively reviewed by Plenio *et al.*[187]

The chemistry of fluoroalkoxo and aryloxo groups as ligands has not been exhaustive. Initially a number of sodium salts of fluorinated alcohols were synthesised for use as precursors for chemical vapour deposition on account of

their greater volatility with respect to their hydrocarbon analogues. This increased volatility is postulated to be due to greater intramolecular repulsions between the fluorine lone pairs or perhaps the reduction of van der Waals attractive forces due to the low polarisability of the fluorine atoms.[187] When used as precursors for CVD it was quickly discovered, that metal fluorides were deposited rather than the desired pure metal oxide. This suggests that the close contact between the CF unit and the metal in the gas phase opens up an kinetic route to the formation of metal fluorides.[188] Bradley *et al* have reported on the reactions of $M\{N(SiMe_3)_2\}_3$ (where M = Lanthanum, Praseodymium and Europium) with stoichiometric proportions of hexaflurotertiary butanol. The tris-hexafluoro-tert-butoxides of La, Pr and Eu where prepared as oligomeric compounds $[M(hftb)_3]_n$ which could be sublimed *in vacuo* with decomposition. An excess of fluoroalcohol affords the production of ammonia in a side reaction which also coordinates to the metal centre.[189] Hubert-Pfalzgraf *et al* have reported on the reactions between YCl_3 and sodium fluro-isopropoxide and the formation of a mixed metal YNa_3 species.[190] They also report the formation of volatile Cerium (IV) hexafluoroisopropoxide and tetrafluoroisopropoxide complexes.[191],[192] Whitmire *et al,* have studied the reactions of sodium pentafluorophenoxide with bismuth chloride and aryloxide complexes. The compounds formed are high oxide containing aryloxide complexes, in some cases the retention of sodium is apparent with ions being tightly bound by interaction with the O and F atoms of the pentafluorophenoxide groups. The highly lewis acidic bismuth atoms in the compounds readily form clusters and oligomeric structures in the solid state, enhanced by the bridging propensity of the pentafluorophenoxide group. The most common bismuth atom coordination geometries observed are the distorted square pyramid and the pentagonal bipryamid with solvent molecules often found bound to the metal centre.There have been a number of studies on the use of metal fluoroalkoxide complexes as weakly coordinating anions. Transition metal based perfluroaryloxide anions have been studied by Marks and co-workers as co-catalyst/counter ions for single site Ziegler-Natta olefin polymerisation.[193]

Shriver *et al* has reported the synthesis and characterisation of Li^+ and CPh_3^+ salts of the related fluoroalkoxide anion, $[Nb(OCH(CF_3)_2)_6]^-$. The lithium salts were

found to demonstrate excellent catalytic activity in lithium catalysed Diels-Alder reactions and 1,4-conjugate addition reactions. Royo and co-workers were also interested in the $(OC_6F_5)_2^-$ group and have obtained an X-ray structure of $[ZrCp_2(OC_6F_5)_2]$, the structure was found to consist of a typical bent sandwich geometry with coordination around the Zr atom being pseudo-octahedral. The short Zr-O bond length suggests significant multiple bond character by Pπ-dπ interaction with the vacant d orbitals of the metal.[185]

There has been little research carried out into simple complexes of sodium with fluoroalkoxo or aryloxo ligands. Caulton *et al* have synthesised and characterised the tetrameric $[NaOCH(CF_3)_2]_n$ with a slightly distorted cubane structure. Studies of this complex were carried out in order to demonstrate the interactions between metal and fluorine and the preference of C-F over C-O cleavage to form the metal fluoride.[194]

In this report we discuss the synthesis and characterisation of five new sodium and potassium fluoro aryloxide complexes and their structural variations. Complexation of these compounds with tris(3,5-dimethylpyrazolyl)methane (TPm*) has been investigated. The ultimate goal of this work is to replace the alkali metal atoms with lanthanides and synthesise complexes of the type: [Ln(TPm*)(OPhFn)3].

Having successfully prepared and characterised 2,6 dimethylphenoxide complexes with LnTPm*, our attentions turned to the fluorinated aryloxides. There have been many crystallographic studies into the interaction of CF units with metal centres. Much of this work has been reviewed by Plenio.[187] One might expect dative interactions from the fluorine atoms to the metal centre to have an effect on the overall structure of the complex, perhaps departing from the six and seven coordinate structures that we observed for the halide, triflate and aryloxide complexes. (chapter 2).

The work in this chapter is divided into four main sections. First we investigate the deprotonation reactions between fluorinated phenols and sodium and potassium

hydride respectively. We then introduce the (TPm*) ligand by addition of THF solutions of the potassium and sodium fluorinated phenoxides to molar equivalent solutions of the ligand. We then look at metathesis reactions between the sodium and potassium fluorophenoxides and the trichlorides of some lanthanides with a view to synthesising lanthanide complexes of the type $[Ln(OPh^{Fn})_3](n = 1, 2, 4, 5)$. The final section discusses the coordination of the TPm* ligand with the lanthanide phenoxide complexes to achieve complexes of the type $[LnTPm^*(OPh^{Fn})_3]$.

Preparation of Sodium and Potassium Fluorophenoxide Complexes

Fluorine-metal interactions in complexes containing fluorinated ligands are relatively common place for sodium and potassium metals. Caulton *et al* and Purdy *et al* have synthesised a number of sodium salts of the following fluorinated alcohols, $(CF_3)(CH_3)_2COH$, $(CF_3)_2HCOH$, $(CF_3)_2(CH_3)COH$ and $(CF_3)_3COH$, resulting in the determination of several x-ray crystal structures. The example below shows the cubic structure of the $[NaOCH(CF_3)_2]_4$ tetramer.[24] **Figure 4.4**

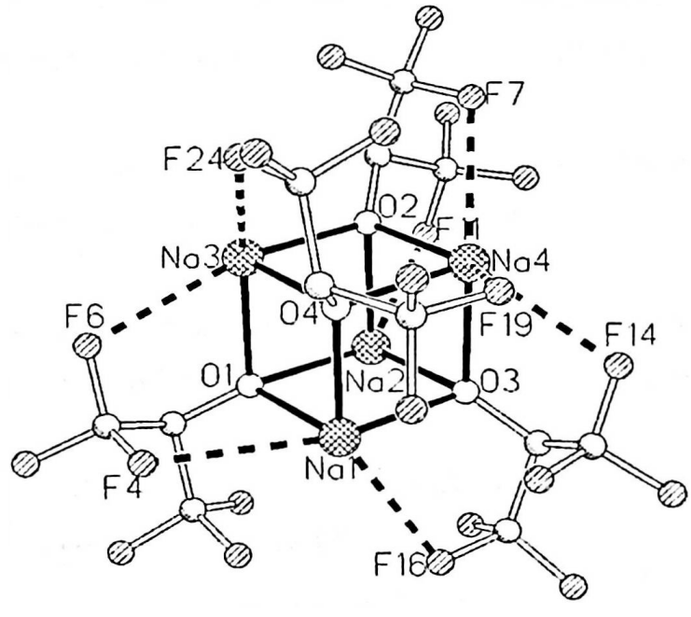

Figure 4.4: Crystal structure of $[NaOCH(CF_3)_2]_4$, Displaying the intramolecular CF...Na⁺ contacts.[138]

EdelMann *et al* have observed short CF...Na⁺ contacts in two structures with bridging fluorinated Phenoxy and benzenethiolate ligands.[195] The O-bridged salt:

$[\mu_2\text{-}\{2,4,6\text{-}(CF_3)_3C_6H_2O\}Na(THF)_2]_2$, is a dimer with four short CF...Na^+ contacts. **Figure 4.5**

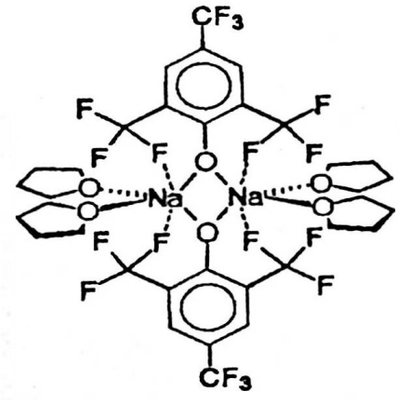

Figure 4.5: The dimeric $[\mu_2\text{-}\{2,4,6\text{-}(CF_3)_3C_6H_2O\}Na(THF)_2]_x$[195]

The related S-bridged $[\mu_2\text{-}\{2,4,6\text{-}(CF_3)_3C_6H_2S\}Na(THF)_2]_x$ complex also has two short CF...Na^+ contacts per metal ion, however the crystal structure demonstrates a zigzag chain polymer structure. The two related potassium complexes ($[\mu_2\text{-}\{2,4,6\text{-}(CF_3)_3C_6H_2O\}K(\mu_2\text{-THF})\text{-}(THF)_2]_2$ and $[\mu_3\text{-}\{2,4,6\text{-}(CF)_3C_6H_2S\}K\text{-}(THF)]_x$) are very similar other than the fact the O-bridged dimer contains two additional μ_2-THF and the S-bridged complex prefers a ladder type chain polymer structure.

Some of the many other examples of sodium and potassium complexes containing short M^+...CF contacts are discussed further in Plenios review. [187]

There are few examples of sodium and potassium complexes with simple fluoroalkoxo or aryloxo ligands . One example is $[NaOCH(CF_3)_2]_n$, which was synthesised by the deprotonation of hexafluoroisopropylalcohol with sodium hydride in ether. The extended structure of which is shown below. [188] **Figure 4.6**

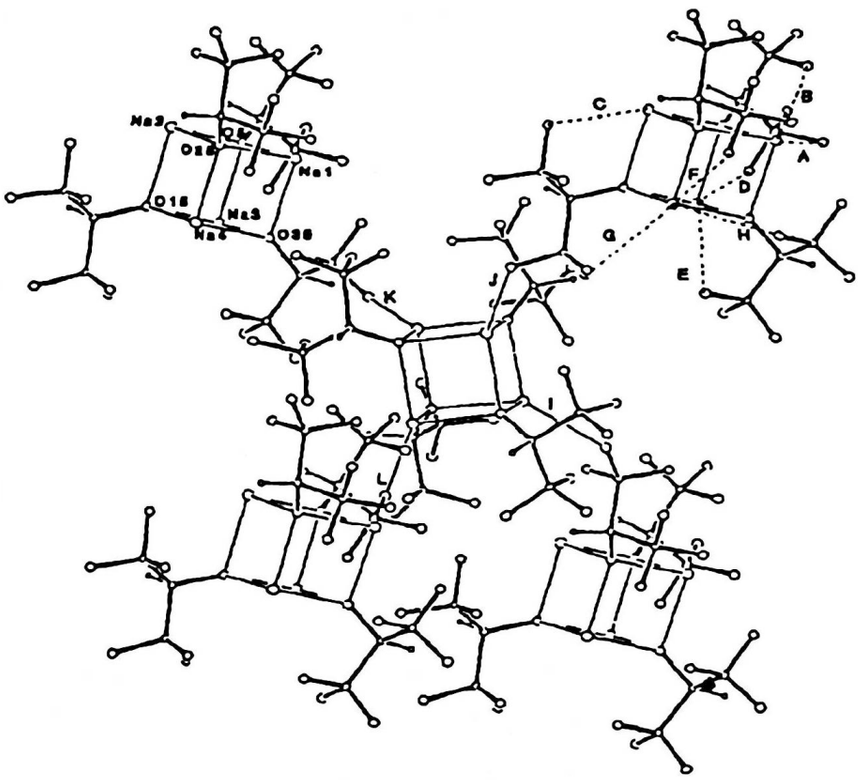

Figure 4.6: Ball and stick drawing of five molecular units of $[NaOCH(CF_3)_2]^2$ [188]

Preparation of sodium and Potassium Fluorophenols

The first stage of our work was the preparation of fluorophenoxide complexes of potassium and sodium.

The pentafluorophenoxide complexes of sodium and potassium were prepared by the drop-wise addition of a solution of the fluorinated phenol to a suspension of sodium or potassium hydride in THF or ether. As expected vigorous effervescence with the production of hydrogen gas occurred immediately on addition. In order to study the effects, if any, of the solvents on the structures of the compounds, the sodium and potassium pentafluorophenoxide were prepared from THF and ether respectively. The parent alcohol and the resulting complexes all dissolved smoothly in both solvents and there were no observable differences in any of the

reactions. Crystalline products of all of the products were obtained by reduction of the solvent under reduced pressure to a point where the product was just starting to precipitate. Any precipitated material was redissolved by warming the flask gently in a water bath. Ether solutions were then layered with toluene. The flasks were placed inside dewars for slow cooling. Crystals suitable for x-ray crystallographic studies were obtained for $NaOPh^{F5}$ **(4.2)** in ether and $NaOPh^{F5}$ **(4.1)** and $KOPh^{F5}$ **(4.3)** in THF. Whilst $KOPh^{F5}$ prepared in Et_2O was clearly crystalline, we were not successful in growing crystals suitable for x-ray analysis. On removal of the solvent, the products obtained from diethyl ether crumbled immediately, presumably as a result of desolvation, whereas the products obtained form THF appeared to have greater structural integrity when dry.

The reaction between sodium hydride and *p-f*luorophenol in Et_2O and THF afforded complexes $NaOPh^{F1}$ **(4.5)** and $NaOPh^{F1}$ **(4.6)** respectively. Repeating the reactions using an excess of potassium hydride produced the complexes $KOPh^{F1}$ (prepared from THF) **(4.7)** and $KOPh^{F1}$ (prepared in ether) **(4.8).** Crystals of all of the products were isolated from the reaction mixtures, however only the preparation of $KOPh^{F1}$ in ether **(4.8)** afforded crystals suitable for x-ray analysis.

Complexes of the sodium and potassium di-flurophenol were prepared in THF $NaOPh^{F2}$ **(4.9)** and $KOPh^{F2}$ **(4.10).** The reactions performed in ether afforded products that were completely insoluble in ether and precipitated put of solution immediately. It was therefore not possible to separate these compounds from the excess NaH and KH for further analysis. This suggests that nature of the solvent influences the structures of the 2,6 difluorophenoxides in solution. Complexes **4.9** and **4.10** were both crystalline but not suitable for x-ray analysis.

The elemental analysis for these complexes were variable. Results for the di-fluoro substituted phenoxides prepared in THF were consistent the formulation $MOPh^{F1}$ (M = Na, K). The penta-fluorophenoxide of sodium and potassium prepared in ether had experimental values for carbon consistent with those calculated, whilst no hydrogen was found, there was curiously some nitrogen in both complexes.

When prepared in THF, $NaOPh^{F5}$ and $KOPh^{F5}$ both showed a trace of hydrogen in their analysis, this is possibly due to exposure to moisture during the analysis. The carbon value for the sodium complex is high. The elemental analysis for the complex $NaOPh^{F2}$ **(4.9)** prepared in THF was consisted with its expected formulation whereas the corresponding potassium complex showed low carbon values and high hydrogen values. Complexes from ether solutions displayed high carbon values. In order to examine whether there was a problem with the combustion of the complexes during the analysis, we took an elemental analysis of the parent alcohol ($HOPh^{F5}$) (purchased from Aldrich). The values calculated for this complex are C: 39.13 %, H: 0.54 % and N: 0%. The experimental values were recorded as C: 30.07 %, H: 0.72 %, and N: 0%. These values confirm that the presence of fluorine groups on the aromatic ring makes these complexes harder to burn and this incomplete combustion prevents the recording of reliable elemental analyses.

NMR analysis

^1H NMR spectra of the sodium and potassium 2,6-difluorophenoxide complexes **(4.9)** and **(4.10)** were recorded in acetonitrile. The spectra are virtually super-imposable with very little difference in chemical shifts of the protons for the respective complexes. The meta protons of the phenoxide ring give rise to a multiplet of peaks between 6.6 and 6.7 ppm. A second multiplet, integrating for a single proton, appears further up-field at 5.9 to 6.1 ppm, this is the para-hydrogen of the phenoxide ring. The splitting patterns are complex (Figure 4.7) and cannot be assigned fully based on the rules for assigning first order spectra. The frequency differences between the proton environments and the coupling constants are of a similar size, resulting in very strong coupling and thus second order patterns. This causes an overlap of the peaks in the spectrum thus making it essentially uninterpretable. [196]

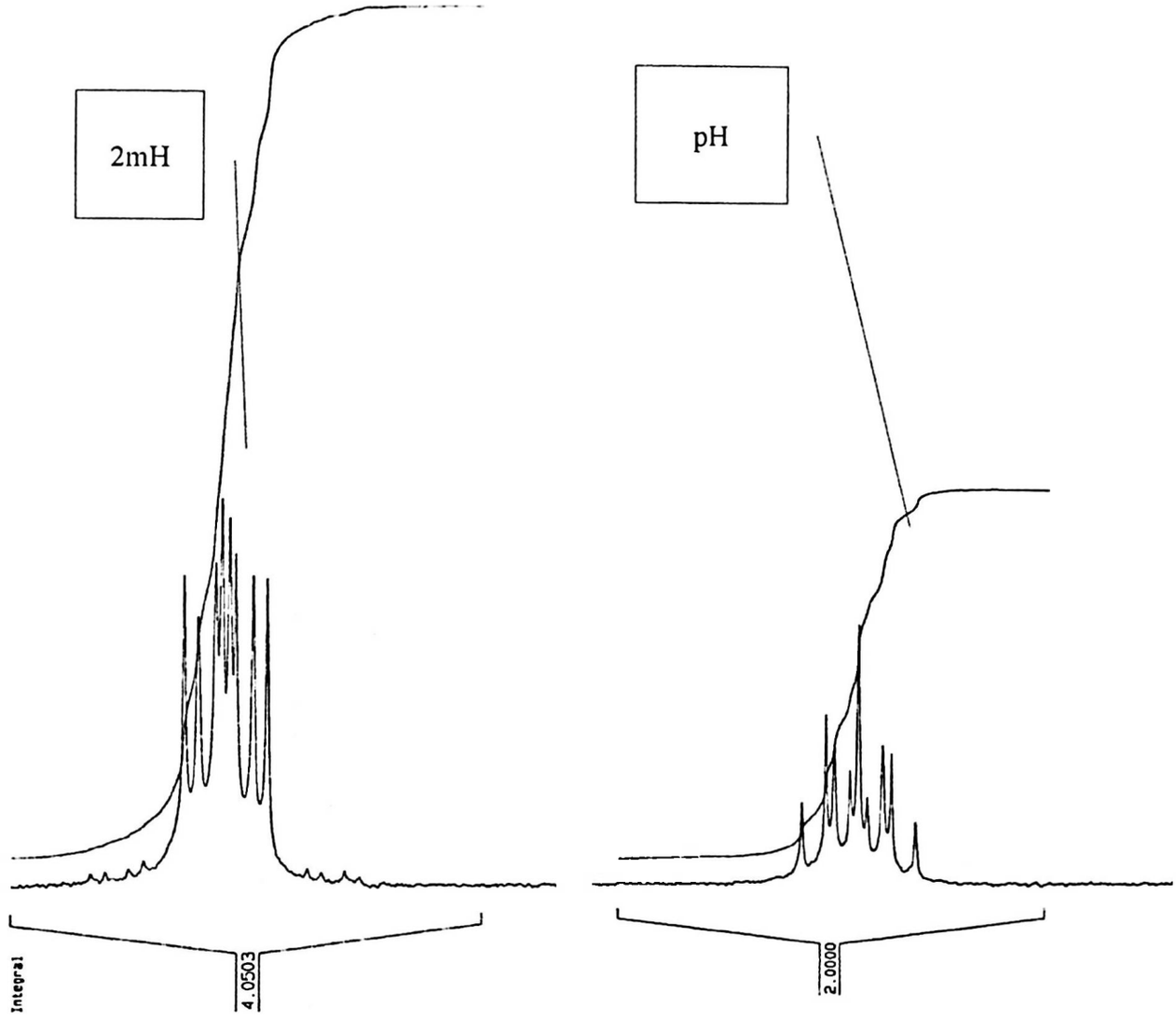

Figure 4.7: splitting patterns in the spectrum of $NaOPh^{F2}$

The para substituted phenoxides **(4.5-4.8)** demonstrate similarly complicated splitting patterns of the ortho and meta protons. **(Figure 4.8).** Two multiplets integrating to two protons each were evident for the ortho and meta protons. It is tempting to assign the meta protons as being shifted down-field relative to the ortho protons due to their closer proximity to the electronegative fluorine. However, whilst σ bonding of the fluorine atoms will reduce electron density, fluorophenoxides are also π donors thus 'returning' electron density making it difficult to assign the protons accurately. In addition to the strong coupling in the system, the ortho protons are chemically equivalent but magnetically inequivalent, resulting in a more complicated spin system. This is also the case with the meta

protons.

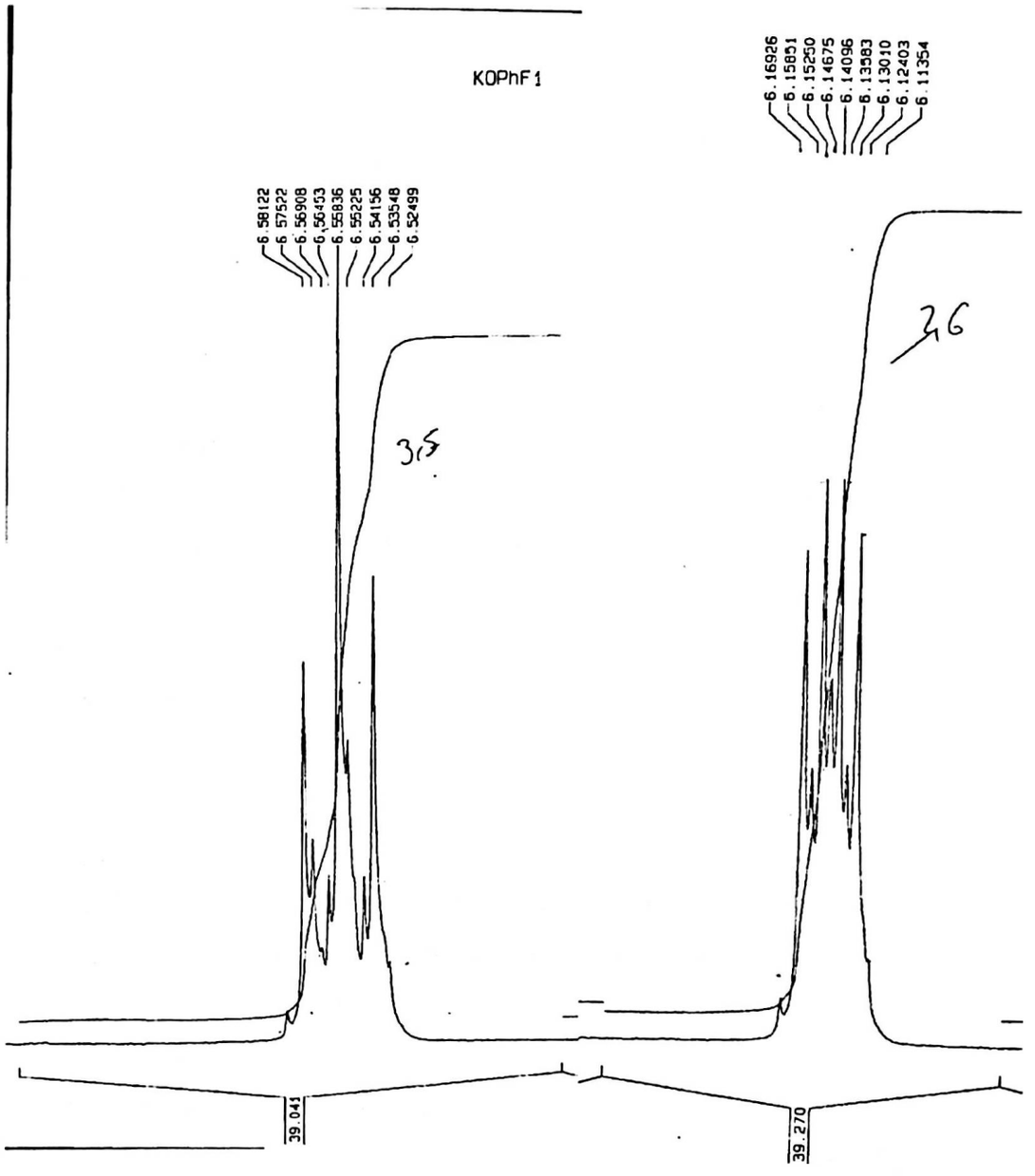

Figure 4.8: Splitting patterns in KOPh^{F1}

Signer Osmometry experiments

In order to obtain information on the speciation of the complexes in solution and to compare the behaviour of the complexes in THF and Et_2O respectively, we carried out vapour phase osmometry in ether and THF, using the signer method.[197]-[198] The molecular weight values obtained are given in the table below. **Table 4.1**

Complex (x)	Solvent	Mwx	Suggested structure in solution.
$NaOPh^{F5}$	THF	436.78	Dimeric
$KOPh^{F5}$	Et_2O	747.48	Tetrameric
$KOPh^{F1}$	Et_2O	442.31	Tetrameric
$NaOPh^{F1}$	THF	190.69	Dimeric

Table 4.1: Table of Vapour Phase Osmometry results.

The results indicate that the extent of aggregation of these complexes in solution is greatly influenced by the nature of the solvent. If one takes into account an experimental error of +/- 10-20% then in THF, the species are essentially dimers, $[M(OPh^{Fn})]_2$.

Edelmann *et al* have reported similar dimeric species for the 2,4,6-tris(trifluoromethyl)phenoxide complexes with sodium and potassium prepared in THF: $[Na(OR)(thf)_2]_2$ and $K(OR)(thf)_2(\mu\text{-}thf)]_2$.[195]

In diethyl ether however, the osmomeric date suggests that tetramers are formed, $[M(OPh^{fn})]_4$. These results show that the better donor solvent, THF has the ability to compete with the phenoxide ligands for binding to the metal centre producing dimeric structures. This difference in aggregation was not reported by Chisholm *et al* for the tetrameric complexes $[MO^tBu]_4$ (M = Na, K), which retains its tetrameric structure in both hydrocarbon and ethereal solvents.[199]

Crystal structures

The simplest of the crystals grown was that of the potassium salt of the 4-fluorophenol. (**4.8**) These were grown by adding a layer of toluene to a concentrated solution of the complex in ether and cooling in the freezer for

approximately 24 hours after which time large colourless blocks had formed. These blocks crystallised in the monoclinic space group $P2_1/c$. The structure consists of isolated tetrameric cubes of KOC_6H_4F with an ether molecule capping each four coordinate potassium ion. There are no intermolecular contacts between the cubes. **Figure 4.9**

Each cube is fairly regular with internal angles of approximately 90°. The distances between potassium ions and the phenoxide oxygens are between 2.280(2) – 2.293(2) Å, which is considerably shorter than in the corresponding bond length observed by Chisholm in the related cuboidal structure, $[KOBu^t]_4$; 2.623(13) Å.[199] The distances between the potassium ions are very similar with values between 3.242(16) and 3.201(11) Å.

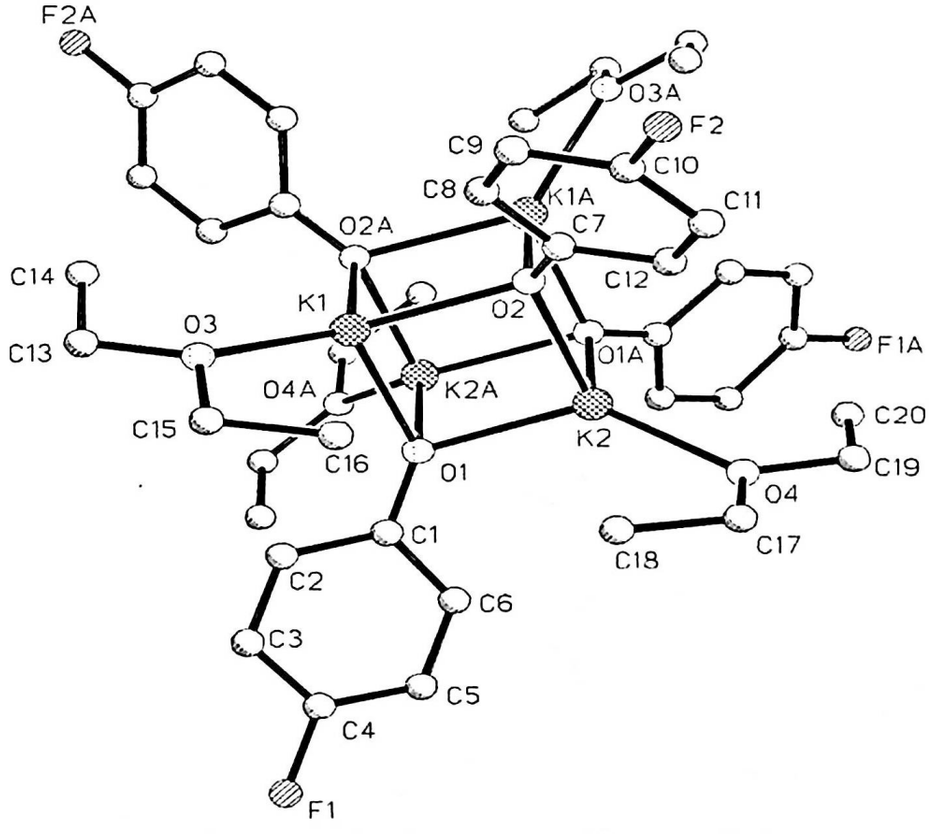

Figure 4.9: The crystal structure of $KOPh^F.Et_2O$. Hydrogens omitted for clarity.

Crystals of $NaOPhF^5$ from THF (4.1) and $KOPhF^5$ from THF (4.3) were grown by placing Schlenk flasks containing very concentrated THF solutions of the complexes inside dewar flasks in a freezer at approximately -20°C. Overnight large clear crystals had formed.

Crystals of the pentafluorophenoxide salt of potassium (4.3) crystallised in the monoclinic space group C2/c and were found to have the formula $[KOC_6F_5(THF)_2]_4$. The structure consists of isolated tetrameric cubes that lie on a C2 axis with THF molecules capping the potassium centres. In this complex the ortho-fluorines on each of the phenoxides interact with the nearest potassium ion making the potassium ions seven coordinate. These bridging and chelating fluorophenoxide ligands makes the overall symmetry of each of these cubes approximately D2d. **Figure 4.10**

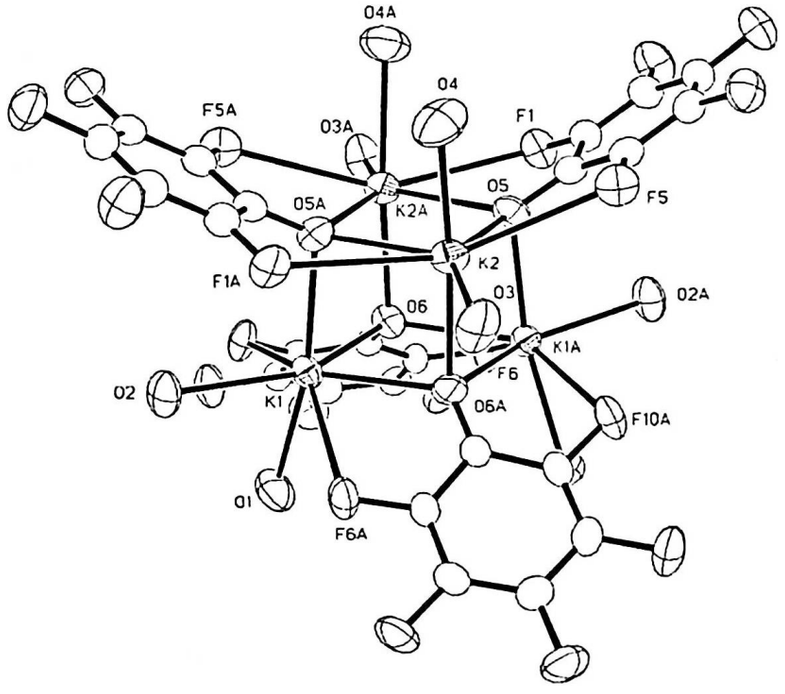

Figure 4.10: Crystal structure of $[KOPh^{F5}(THF)_2]_4$. hydrogens omitted for clarity

The bridging of the phenoxides between the potassium ions appears to force them

apart, with K..K bond distances of 3.907 – 4.084 Å compared with those in the $KOPh^F.Et_2O$ complex (3.201-3.424 Å). The K..O distances are also considerably longer, 2.665(3) – 2.708(3) Å compared with 2.280(2) – 2.293(2) Å for the non-chelated complex. They are however similar to that of the $[KO^tBu]_4$ teteramer reported by Chisholm.[199] The K_4O_4 cube is more distorted than in the $KOPh^F$ complex with tighter internal angles at potassium of between 80.5(1)° and 85.6(1)°. The angles at the triply bridging oxygen atoms are much more open at 93.4(1)° - 99.4(1)°. The K-F contacts throughout the structure are relatively long at *ca* 3 Å representing weak interactions.

Crystals of the sodium complex, $NaOPh^{F5}$(**4.1**), like those of $KOPh^{F5}$, crystallised in the monoclinic space group C_2/c. The difference in the unit cell parameter of the two crystals are significant enough to conclude that the crystals are not isomorphous. The crystals of $NaOPh^{F5}.THF$ also exist as isolated tetramers, $[NaOPh^{F5}(THF)_2]_4$, however on close observation it is apparent that two very distinct phenoxide ligands are present. Two of the phenoxides within the crystal bind to sodium metal centres through both of their ortho fluorine atoms, however the remaining two ligands demonstrate single fluorine bonding through one of the ortho fluorine groups. **Figure 4.11**

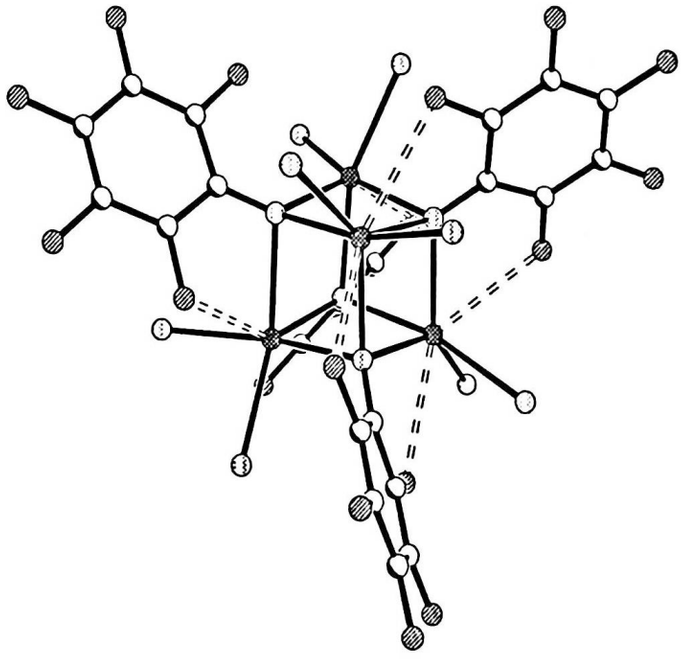

Figure 4.11: Crystal structure of $[NaOPh^{F5}(THF)_2]_4$ hydrogens omitted for clarity.

Thus two of the sodium metal centres are seven coordinate whilst the singly bridged sodium atoms are six coordinate. The difference in structure between the sodium and potassium complexes can be explained by considering the the difference in atomic radii between the two ions, (Na^+= 1.12 Å and K^+ = 1.46 Å).[200] The smaller sodium ion can not accommodate addition fluorine groups and thus the phenoxide ligand twists slightly to move one of the ortho fluorines away from adjacent sodium ions. This twisting does however give rise to weak Na^+···F interactions between two of the phenoxides and sodium ions on opposite faces of the cube. This is in contrast to the $[KOPH^{F5}(THF)_2]_4$ structure where the potassium atoms on the same face of the cube are bridged by the same phenoxide ligand. Edelman *et al* observed differences between the crystal structures of the dimeric complexes $[Na(OR)(THF)_2]_2$ and $[K(OR)(THF)_2(\mu\text{-}THF)_2]_2$ (R = 2,4,6-tris(trifluoromethyl)phenol. The larger potassium cation binds two more, bridging , THF molecules and forms more interactions with the fluorine then the smaller sodium cation which contains only terminally bound THF molecules.[195] The polymeric thiolate complexes , also observed by Edelman, [Na(SR)

$(THF)_2.0.25thf]_x$ and $[K(SR)(THF)]_x$ (SR = 2,4,6-tris(trifluoromethyl)benzenethiol), demonstrate significant differences in their crystal structures. The sodium complex is an asymmetric zigzag chain polymer, the backbone of which is formed by alternating six coordinate sodium atoms and doubly bridged sulphur atoms. **Figure 4.12** .The larger potassium cation, coordinates a third 2,4,6-tris(trifluoromethyl)benzenethiol ligand, giving rise to a 'ladder' polymer. **Figure 4.13**

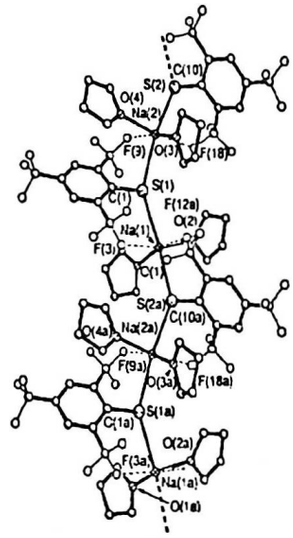

Figure 4.12: Polymeric chain structure of $[Na(SR)(THF)_2 0.25THF]_x$ [177]

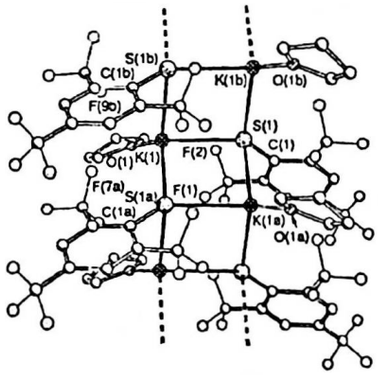

Figure 4.13: Polymeric 'ladder' structure of [K(SR) (THF)]$_x$ [177]

The Na...F bond lengths in (**4.1**) are in the range 2.839(2) to 2,865(2) Å which are comparable to the weaker interactions observed by Caulton *et al* in $[NaOCH(CF_3)_2]_n$ (2.64(2) – 2.86(2) Å)

and by Whitmire *et al* for the complex $[Na[Bi(OC_6F_5)_4(THF)]$ (2.47(2) – 2.99(2) Å).[28] M...F bond interactions for the 2,4,6=tris(trifluoromethyl)phenol complexes of sodium and potassium reported by Edelman and described above are also reasonably weak, the shortest of the bond length being 2.664 Å and 2.867 Å for the sodium and potassium complexes respectively.

Crystals of the sodium salt of pentafluorophenol (**4.2**) prepared in ether were grown by layering a concentrated solution of the complex in ether with toluene and placing in the freezer for slow cooling. The clear colourless crystals formed in the triclinic space group P_1 and have the formula $[(NaOC_6F_5)_4(Et_2O)_3](C_7H_8)_{0.5}$. The crystal structure is far more complex than the previous systems discussed. **Figure 4.14**

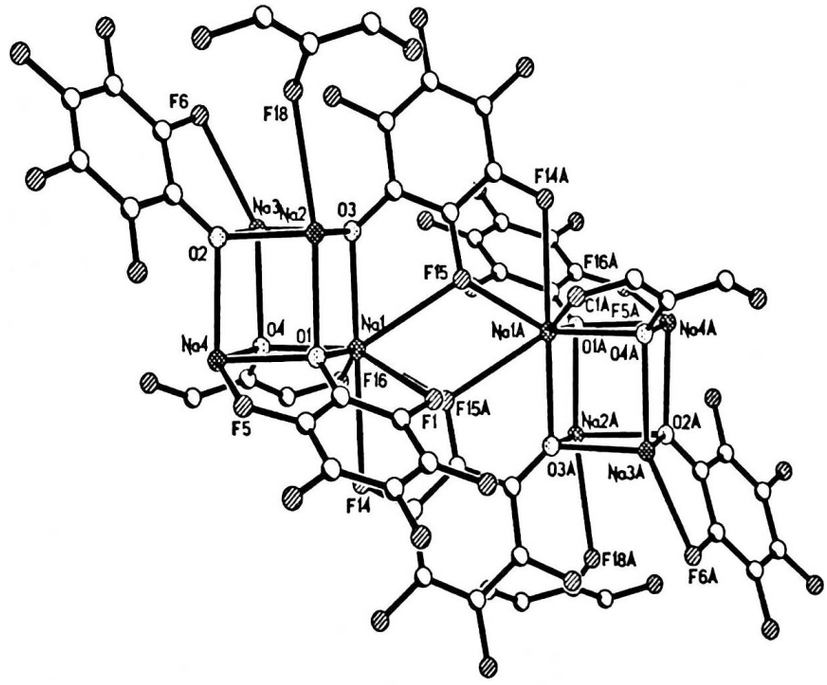

Figure 4.14: Crystal structure of $(NaOPh^{F5})4(Et2O)_3$. Solvent molecules and hydrogens omitted for clarity.

The structure consists of cubic Na_4O_4 units similar to those observed in the previous structures. This time they are arranged in pairs related by a C_2 axis and a variety interconnections between the ligands. Only three ether molecules are present in each cube, capping three of the sodium atoms. This is in contrastt o **4.1** and **4.3** where each metal atom is capped by a solvent molecule.

Each cube contains three, crystallographically distinct bidentate coordinated OPh^{F5} groups with one of the ortho fluorine atoms being coordinated and the other being free. The remaining fluorophenoxide ligand adopts a very different binding mode. The oxygen atom is positioned on the corner of the cube as expected but one of the ortho-fluorine atom (F15) bridges one sodium on one cube (Na1) and a second sodium on a second cube (Na1A). This bridging arrangement brings the meta fluorine atom (F14A) of the bridging OPh^{F5} ligands in to the coordination sphere of the sodium on the second cube (Na1A) . The OPh^{F5} ligand can therefore be regarded as a corner of one cube, the bridge to the second cube and a cap for the sodium atom (Na1A) of the second cube.

There are other interactions between the pair of cubes. The para fluorine atom (F18) of one of the bidentate OPh^{F5} ligands interacts with a sodium atom of the second cube. Through these interactions, the pairs of cubes are linked into infinite columns parallel to the a-axis of the structure. **Figure 4.15** Caulton has observed this type of interconnection between cubes for the sodium fluoroalkoxide complex $[NaOCH(CF_3)_2]_n$ [188]

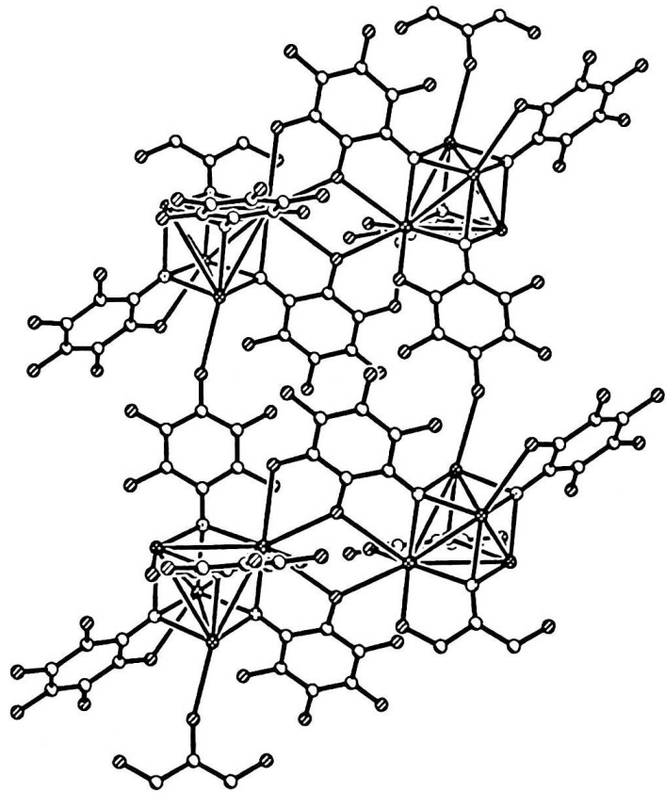

Figure 4.15: Para Fluorine atoms link together pairs of tetramers to form an extended structure.

The sodium atoms on each of the cubes are significantly different and can thus be considered as unique. Na1 is eight coordinate, bound to three oxygens and three fluorines from the 'internal' bidentate OPh^{F5} ligands, it is also bound to the ortho and meta fluorines from the bridging aryloxide of the adjacent cube. The internal Na1-F16 bond distance is 2.660(1) Å which may be considered average when comparing with other complexes displaying F – M interactions. The two fluorine atoms, F15 and F15A that bridge Na and Na1, do so unsymmetrically with the Na – F15 distance being 2.569(1) Å and an Na – F15A distance of 2.809(1) Å. The internal angles of the cubes, i.e, O – Na – O are reasonably tight, ranging from 83.55(6) – 87.70(6)°.

Na2 has a very different coordination geometry to that of Na1. It is five coordinate, bound to three aryloxide oxygens, one ether molecule and also the para

fluorine atom (F18) form the neighbouring cube. F18 'approaches' Na2 at an angle of 125°. The interaction can be considered to be reasonably strong, with a bond length of 2.683(1) Å which is well within the range typically observed for these type of systems. Na3 is also five coordinate, bound to three oxygens from the fluorinated aryloxide ligands, an ether and the chelating fluorine (F6). The Na3 – F6 distance is 2.672(2) Å, again an average bond length for these systems. Na4 is bound to three aryloxide oxygens and a chelating fluorine (F5) and the third solvent molecule and is thus also five coordinate. Despite the difference in coordination numbers of the odium atoms, the sodium – oxygen bond distances remain fairly constant, for example the distance between eight coordinate Na1 and O1 is 2.307 Å compared with 2.320 Å for the five coordinate Na4 and O1. This suggests that the bond distances within the core of the cubes are insensitive to coordination number.

Attempts to break up the lattices using crown ethers.

First synthesised by Pedersen in 1967,[201] Crown ethers are heterocyclic chemical compounds that consist of a ring containing ether groups. The most common crown ethers are oligomers of ethylene oxide, the repeating unit being ethyleneoxy, i.e., $-CH_2CH_2O-$. Important members of the series are the tetramer, the pentamer and the hexamer. Figure 4.16. Crown ethers strongly bind certain cations. The oxygen atoms are well situated to coordinate with a cation located at the interior of the ring, whereas the exterior of the ring is hydrophobic. The resulting cations often form salts that are soluble in non-polar solvents and for this reason crown ethers are useful in phase transfer catalysis. The density of the polyether influences the affinity of the crown ether for various cations. For example, 18-crown-6 has a high affinity for potassium cation and 15-crown-5 for the sodium cation.

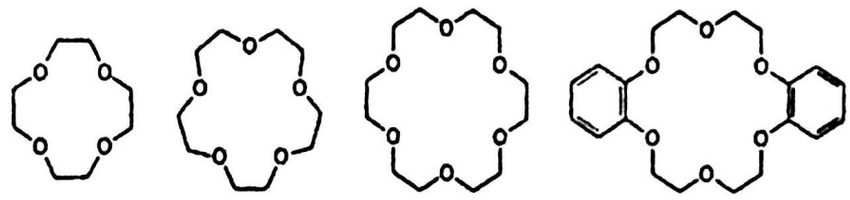

(a) (b) (c) (d)

Figure 4.16: Structures of common crown ethers. (a) 12-crown-4 (b) 15-crown-5 (c) 18-crown-6 (d) dibenz and diaza-18-crown-6.

In attempts to break up the extended lattices observed in the structures of Na and K penta-fluorophenoxides, crown ethers were combined with solutions of $NaOPh^{F5}$ and $KOPh^{F5}$ in ether. An equivalent of 15-crown5 was added to $NaOPh^{F5}$ and likewise an equivalent of 18-crown-6 was combined with $KOPh^{F5}$ due to its greater affinity for the potassium cation. The resulting products were insoluble in ether and precipitated immediately from solution, suggesting that the structure in solution has altered. The products were extracted into THF and concentrated solutions were placed in the freezer for crystallisation. Both products precipitated as crystalline products however only crystals of $NaOPh^{F5}$ (**4.11**) were suitable for x-ray analysis. **Figure 4.17**

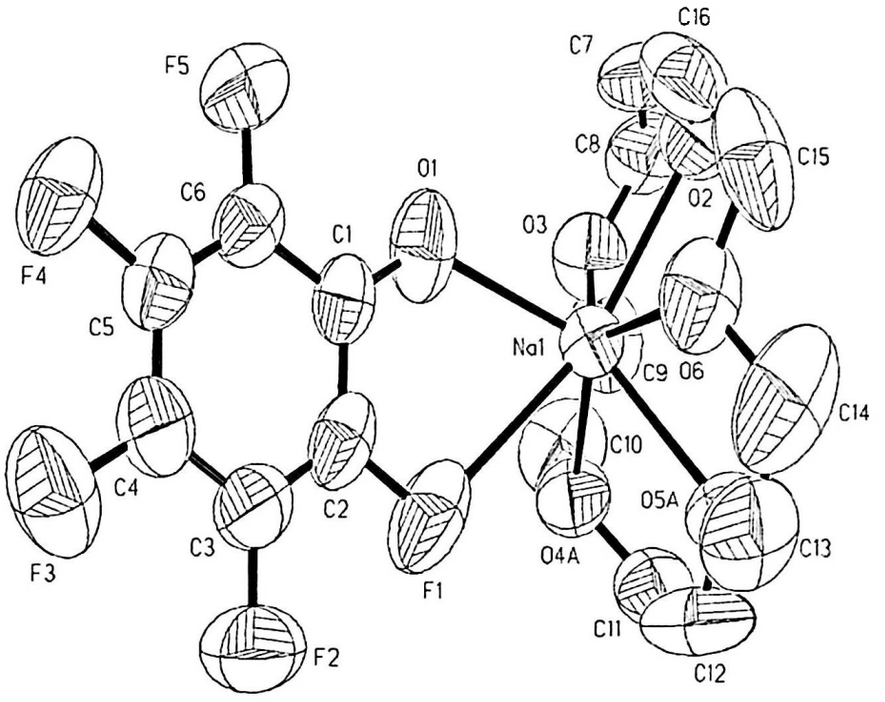

Figure 4.17: NaOPh^{F5}15-crown-5

The clear colourless crystals formed in the monoclinic space group p_1/n and have the formula $C_{16}H_{20}F_5NaO_6$. The sodium is isolated and capped by the crown ether which prevents the formation of dimeric or tetrameric structures. The phenoxide group binds to the metal centre via its oxygen and an otho fluoro group (F_1), demonstrating another example of a complex with M—F interactions. The Na—F_1 bond is fairly long at 2.799 (4) Å. The Na—O_1 bond distance in line for that observed in chelating ligand at 2.774 (3) Å.

Combining the complexes of MOPh^{Fn} with TPm*

Having successfully synthesised and structurally characterised several sodium and potassium complexes with the fluorinated aryloxide ligands the next step was to complex these with the tris(3,5-dimethylpyrazolyl) methane ligand (TPm*), to synthesise complexes with the generic formula MTPm*(OPh^{Fn}). (M = Na, K. n = 1, 2, 5)

Dias *et al* have crystallised two sodium complexes with the related polyfluorinated tris(pyrazolyl)borate ligand, $[HB\text{-}\{3,5\text{-}(C_2F_5)_2Pz\}_3Na(THF)]_2$[41] and $HB\{3,5\text{-}(CF_3)_2Pz\}_3Na\text{-}(H_2O)$[202] **Figure 4.18**. Also described are the crystal structures of the dimers $[\{H_2B(3,5\text{-}(CF_3)_2Pz)_2\}K]_2$ and $[\{HB(3,5\text{-}(CF_3)_2Pz)_3\}K\{\mu_2\text{-}(MeCONMe_2)\}]_2$ which are closely related to the sodium complexes.

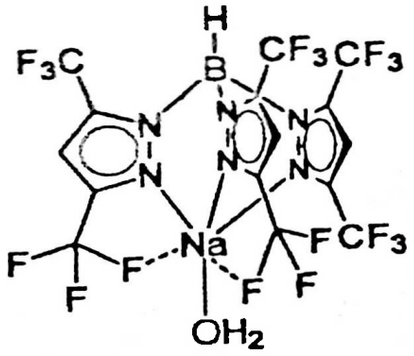

Figure 4.18: $HB\{3,5\text{-}(CF_3)_2Pz\}_3Na\text{-}(H_2O)$[201]

Combining a solution of $NaOPh^{F5}$ in ether to a molar equivalent of TPm* dissolved in ether, resulted in the immediate precipitation of a white solid. Clearly the product resulting from this combination is completely insoluble in ether, therefore after drying the powder was dissolved in a minimum amount of THF in attempts to extract crystals suitable for X-ray analysis. The analogous $KOPh^{F5}$TPm* (4.14) was prepared in THF by the combination of solutions of $KOPh^{F5}$ and TPm*. The product precipitated from a concentrated solution after slow cooling in the freezer, whilst the product appeared crystalline on observation, there were no crystals suitable for x-ray analysis.

The elemental microanalysis of these products were not entirely consistent with the formulation MTPm*(OPh^{F5}), particularly for the sodium complex which gave values that are low for carbon and hydrogen and especially low for nitrogen. The potassium complex fared better with both the carbon and hydrogen values being

correct. The nitrogen value was however still low (expected 16.15 %, Found 14.94). It is unclear as to why the nitrogen values are so low, however thus far elemental analysis has not been a particularly reliable analytical tool

^{1}HNMR of KOPh^{F5}TPm* **(4.14)** recorded in acetonitrile displays the expected resonances for the TPm* ligand, there is a small amount of THF present. On comparing the chemical shifts of the TPm* in this complex with those of the free ligand the resonances of the complexed ligand are shifted down field slightly, suggesting that the TPm* has complexed to the fluorinated phenoxide and experiences slight de-shielding effects from the fluorine groups. According to the spectra, the complex is pure and displays no minor products on the baseline. The ^{1}HNMR spectra for the sodium complex [Na(TPm*)(OPh^{F5})] **(4.13)** also shows resonances for the CH and the three PzCH protons, in addition to this, a quarter of a molecule of THF is present. The two peaks for the methyl groups in the 3 and 5 positions of the pyrazolyl rings are much broader and overlaped compared with the sharp resonances in the potassium complex **(4.14).**

The broadness of resonance in an ^{1}H NMR spectrum is determined by chemical exchange, relaxation time effects and dipolar couplings.[196] Since we would not expect the 3 and 5 methyl groups of the TPm* ligand to mutually exchange, the effects must be due to relaxation times, driven by a combination of the motions of the molecules. One can hypothesise, for the complex [NaTPm*(OPh^{F5})], the ortho fluoro groups of the phenoxide ring, swing towards the 5 methyl groups of the ligand pyrazolyl ring and then relax back away from the ring. The mechanism of nuclear spin relaxation lies in magnetic interaction, the most important being dipolar coupling. The dipolar coupling between two nuclei depends on their separation r, and on θ, the angle between the internuclear vector and the static field. This anisotropic coupling does not lead to splitting patterns in the NMR spectra of molecules in liquids however it is by no means negligible in the appearance of the spectra. The translation, rotation and vibrations of the molecules in solution alter r and θ in a complicated way causing the interaction between protons to fluctuate rapidly. The dipolar coupling, modulated by molecular

motions, in this case the periodic interaction with the fluoro groups, causes nuclear spins to experience time dependant local magnetic fields which, if they contain a component of the NMR frequency, can induce the radiationless transitions which return the spins to equilibrium. Its possible that the presence of fluorides in a complex produces strong dipolar coupling and the presence of broad peaks, It is not clear however why this coupling should be present in sodium systems but not in those of potassium.

Our attentions turned to the 2,6 difluorinated sodium and potassium phenoxides and their reactions with the TPm* ligand. The reactions, using THF as the solvent, resulted in the formation of semi-crystalline solids. We were unsuccessful in extracting crystals suitable for X-ray analysis by slow cooling of concentrated THF solutions of the products. The elemental analyses of the products were consistent with the formulation $MOPh^{F2}TPm^*$ (M = Na, K). The ^1H NMR spectrum for the potassium complex, recorded in acetonitrile displays the expected TPm* resonances for a coordinated ligand. The chemical shifts are virtually identical to those recorded for the pentafluorinated complex: $[KOPh^{F5}TPm^*]$ **(4.14)**, thus the degree of fluorination of the phenoxide ligand has little or no effect on the degree of shielding of the TPm* protons. The 3,5 dimethyl resonances are sharp, appearing at 2.09081 and 1.97001 ppm. The resonances for the *para* and the *meta* protons of the pyrazolyl ring appear as multiplets at 5.874 and 6.607 ppm, (centre peaks) integrating for 2 and 1 protons respectively. The splitting patterns are complicated, consisting of eight peaks for the *meta* protons and nine for the *para* proton. The pattern is, as anticipated, identical to that observed in the ^1H NMR of the $KOPh^{F2}$ (4.10) complex, demonstrating the second order coupling patterns in the system. **Figure 4.7**

The sodium complex , $NaOPH^{F2}TPm^*$, also displays clear sharp resonances for the CH and the 3 PzCH protons. The two 3,5 dimethyl resonances are present at δ 2.07 and 2.00 ppm with each peak integrating for 9 protons. The resonances are broad, such as observed for the sodium pentafluoro substituted complex $[NaTPm^*(OPh^{F5})]$ **(4.13).**

Finally, the potassium TPm* complex of the para fluoro substituted phenoxide was synthesised (**4.15**). As with previous preparations a white semi crystalline solid was isolated from the reaction mixture. The elemental analysis for carbon was correct for a product of formulation [$KOPh^{F1}TPm^*$] the hydrogen value was slightly high. The pyrazoyl-1-yl ring protons appear as sharp resonances in the ^1H NMR spectrum. As with many of the other preparations, there is THF present in the complex. TPm* resonances appear at the same frequencies as those observed in the 2,6 difluoro-substituted phenoxide complex and in the pentafluoro substituted complex. The ortho and meta protons are present at 6.57 and 6.15 ppm. The resoltuion of the spectra does not allow for the splitting of the ortho and meta protons to be observed accurately. However one would expect the same pattern as observed in the $KOPh^{F1}$ complex. **Figure 4.8**

Synthesising Lanthanide Fluorinated Phenoxide complexes $Ln(OPh^{Fn})_3$

Having demonstrated crystallographically that sodium and potassium ions can be complexed successfully with a number of fluorinated aryloxide ligands and for cohesion with work from chapter 2 and 3, our attentions turned to substituting the sodium and potassium metals for lanthanides. Plenio reports very few examples of lanthanide complexes containing fluorinated alkoxo or aryloxo ligands. San Filipo and co-workers may have been the first to suggest a special CF-M interaction.[203] Whilst monitoring the ^1H NMR spectra of fluorinated hydrocarbons such as *n*-octylfluoride, in the presence of the shift reagents $Eu(fod)_3$ and $Yb(fod)_3$, they observed that the metal induced shifts of the proton resonances decreased as the distance from the fluorine nucleus increased. To account for this, the formation of a CF coordinated lanthanide - fluoroalkane complex was postulated.

Bradley *et al* has observed CF...Pr contacts of between 2.75 (1) and 3.00 (1) Å in the complex $Pr(O(CH_3)_2CF_3)_3$.[204][189] More recently Brennan *et* al have described the preparation of trivalent lanthanide compounds with fluorinated thiolate ligands ($Ln(SC_6F_5)_3$.[205] Transmetalation reactions of the lanthanide with $Hg(SC_6F_5)_2$ in THF gives the corresponding trivalent thiolates.

$$2\,Ln + 3\mathrm{Hg}(SC_6F_5)_2 \xrightarrow{THF} 2(THF)_n Ln(SC_6F_5)_3 + 3\mathrm{Hg}$$

The Cerium complex crystallised as a dimer with a pair of bridging thiolates connecting two eight coordinate Ce(III) ions, with four sulphur atoms, three oxygen atoms and one fluorine atom comprising the primary coordination sphere. Figure 4.19 The shortest Ce-F interaction was recorded at 2.749 (2) Å. The smaller holmium complex forms a monometallic structure, structural analysis reveals a pentagonal bipyramidal product with two axial thiolates and one equatorial thiolate. Figure 4.20 The dative interaction between holmium and fluorine is 2.579 (2) Å.

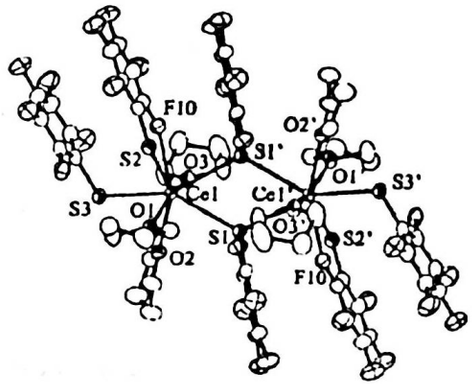

Figure 4.19:Molecular structure of 2(THF)$_n$Ce(SC$_6$F$_5$)$_3$[205]

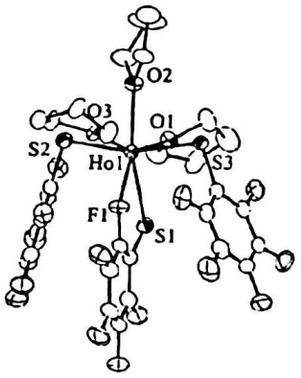

Figure 4.20: Molecular structure of Ho(SC$_6$F$_5$)$_3$[205]

The metathesis reaction between the appropriate lanthanide trichloride and three equivalents of sodium or potassium fluorinated aryloxide in THF is expected to produce a complex of the type M(OPh^{Fn})$_3$ (n = 1,2,4,5).

$$LnCl_3 + 3\mathrm{MOPh}^{Fn} \xrightarrow{THF} Ln(OPh^{Fn})_3 + 3\mathrm{MCl}$$

Samarium and yttrium complexes of the pentaflurophenoxides **(4.19, 4.18),** were prepared by warming the respective lanthanide trichloride/THF solutions in a water bath to aid dissolution after which three equivalents of a solution of KOPh^{F5}

in THF was added resulting in the formation of turbid solutions. $KOPh^{F5}$ was chosen in preference to the sodium complex as the reactant because KCl is a more effective 'leaving group' than NaCl and thus the risk of salt incorporation within the products is reduced.

The resulting turbid solutions were filtered to remove potassium chloride and leave a clear solution of the yttrium complex **(4.18)** and a yellow solution of the samarium complex **(4.19)**. Attempts at growing crystals by placing concentrated THF solutions of the complexes in the freezer for slow cooling were unsuccessful and thus the excess solvent was removed under reduced pressure.

Analysis for the complexes are reasonable if one takes into account that solvent molecules are present in the coordination sphere of the metal. The analyses suggest samarium has an additional THF within its coordination sphere whereas inextricably the smaller yttrium appears to accommodate two solvent molecules.

Attempts were made to synthesise the yttrium and samarium complexes of the para-flurophenoxide ligand **(4.20, 4.21).** The reactions proceeded in much the same manner as for the penta-fluorophenoxide complexes. Combining THF solutions of the reactants resulted in the precipitation of KCl which was removed by filtration. This was a particularly laborious process for the yttrium complex as the precipitate appeared unusually 'oily'. Efforts to crystallise the products by slow cooling from concentrated solutions were unsuccessful and thus THF was removed under reduced pressure to afford a white yttrium product and a pale yellow samarium product.

Elemental analysis results for both products were not consistent for complexes with the formula $Ln(OPh^{F1})_3$, being low in carbon and high in hydrogen, markedly so for the yttrium complex. This may again be due to incomplete combustion of the complexes.

The complexes of 2,6 difluoro-phenoxide **(4.22, 4.23)** were prepared in analogous reactions to those described above. Again, elemental analysis show values lower

than expected for carbon and higher for hydrogen. It is clear from the discrepancies in the calculated and found values for elemental analysis through the series of complexes studied that the problems with incomplete combustion persist.

^{1}H NMR spectra of $Y(OPh^{F1})_3$ **(4.20)**, $Sm(OPh^{F1})_3$ **(4.21)**, $Y(OPh^{F2})_3$ **(4.22)** and $Sm(OPh^{F2})_3$ **(4.23)** were recorded in acetonitrile. **4.20** has a single very broad resonance for the ortho and meta protons with a single integration for 12 protons. The corresponding yttrium complex **(4.20)** displays a similar spectrum, the ortho and meta protons are broadly split into three peaks, again with a single integration for 12 protons. Presumably the broadness of this resonance in the samarium product is exacerbated by the paramagnetic nature of the samarium metal centre. In addition to the phenoxide peaks, the samarium complex displays 2/3 of a THF group present and the yttrium complex ½ of a THF.

We would expect two multiplets of peaks for the ortho and meta protons with equal integrals and complex splitting patterns such as observed in the potassium and sodium complexes of this ligand. **(Figure 4.8).** Whilst we cannot be sure of the nuclearity of yttrium and samarium complexes in solution, a possibility is that they might be dimeric structures with a combination of one bridging and two terminal phenoxide ligands. **Figure 4.21**

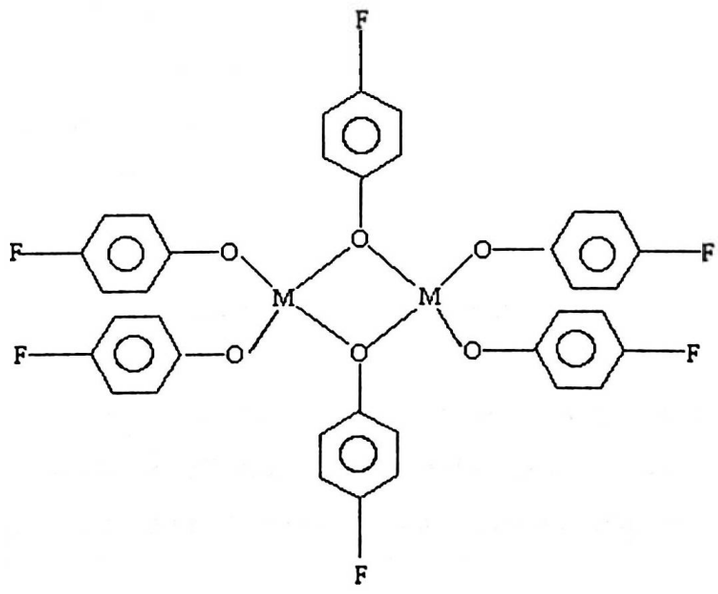

Figure 4.21: Possible bridging and terminal ligands in $M(OPh^{F1})_3$

A rapid exchange between the bridging and terminal ligands would show the protons in a 2:1 ratio, presumably on the NMR time-scale, the exchange is not fast enough to produce sharp resonances and and very broad peaks are observed.

The situation is further complicated in the 2,6 difluorophenoxide complexes. **(4.22, 4.23).** ^{1}H NMR spectra similarly show broad resonances for the meta and para phenoxide protons integrating for nine protons. There is also THF present in both complexes. Assuming again that the complexes exist as dimers with exchanging terminal and bridging phenoxide ligands, this rapid exchange would give the meta and para hydrogens in a 2:1 ratio. The exchange at room temperature is not fast enough for the resonances to fully sharpen. When the exchange between the bridging and terminal ligands is slow, or 'frozen', the two meta and the para protons are all inequivalent, giving rise to mass of overlapping peaks. Possible chelation between the ortho-fluorine groups and the metal centres would alter coupling in the system further, adding to the complex splitting patterns expected for the protons.

A variable temperature proton spectrum recorded for $Y(OPh^{F2})_3$ **(4.22)**in acetonitrile, revealed that on warming to 348 K, the broad peaks resolved into essentially a 2:1 ratio of environments. Whilst the splitting is not fully resolved, this observation supports the hypothesis that the complex exists as dimers, with two terminal ligand proton environments and one bridging environment. Corresponding dynamics were observed in the fluorine NMR, however it was not possible to assign the peaks.

Preparation of complexes of the type $LnTPm^*(OPh^{Fn})_3$

NMR investigations have shown that the TPm* ligand is able to bind to sodium and potassium complexes of the fluorine substituted phenoxides. Having successfully synthesised the trivalent yttrium and samarium TPm* complexes with

chlorides as the ancillary ligands. (chapter 2), we attempted to substitute these chloride ions for the fluorinated phenoxide ligands, by metathesis reactions between sodium or potassium fluorophenoxides and YTPm*Cl_3 or SmTPm*Cl_3.

$$MTPm^{*}Cl_3 + 3M'OPh^{Fn} \xrightarrow{THF} MTPm^{*}(OPh^{Fn})_3 + 3M'Cl$$

$$(M = Y,\ Sm),\ (M' = K,\ Na)$$

Solutions of YTPm*Cl_3 and SmTPm*Cl_3 were prepared in situ and three equivalents of $KOPh^{F5}$ dissolved in THF was added gradually. KCl precipitated from solution after approximately 30 minutes and was removed by filtration. Attempts made to crystallise the product from THF were unsuccessful and the solvent was removed under reduced pressure to leave white powders which were dried under dynamic vacuum. Elemental analysis of SmTPm*$(OPh^{F5})_3$ (**4.24**) was slightly high for carbon and hydrogen suggesting there may be a small amount of solvent present. The nitrogen value is inextricably high,

The analysis for the yttrium (**4.25**) complex is less accurate for carbon and hydrogen, the recorded values are considerably higher than calculated, this may be due to a large excess of solvent present which seems unlikely for the much smaller yttrium metal centre. Again the value for nitrogen is very high. The ^1H NMR spectrum of the yttrium complex in acetonotrile conveys a different picture to that of the elemental analysis. There is less than ¼ mole of THF present in the sample and a very small amount of minor product on the base line. The four peaks associated with the TPm* ligand are present at chemical shifts identical to those observed in the potassium complex, $KOPh^{F5}$TPm*(**4.14**). Conversely the spectrum of the samarium complex is more complicated. There are many minor products present on the baseline and some THF present. One of the methyl peaks form the TPm* ligand is visible at 1.81 ppm, whilst the other one is masked by the acetonitrile solvent peak. On closer observation it is apparent that the resonances of the TPm* peaks are shifted up-field relative to those observed in similar complexes, the values are similar to those observed in the free TPm* ligand. Considering this and the minor products on the base line, it is possible that this

product has been exposed to air or moisture and has degraded to the free ligand and other minor products.

The preparations of the complexes $SmTPm^*(OPh^{F2})_3$ **(4.26)**, $YTPm^*(OPh^{F2})_3$ **(4.27)** and the para-fluorophenoxide complexes, $SmTPm^*(OPh^{F1})_3$ **(4.28)** and $YTPm^*(OPh^{F1})_3$ **(4.29)**,were carried out using the same procedures as previous preparations. Attempts to grow crystals were not successful and analysis was carried on the complexes as isolated white powders.

The elemental analysis of the complexes were not consistent with compound of the formulation $MTPm^*(OPh^{Fn})_3$ (M = Y, Sm, n = 1,2). With nitrogen values varying to extremes of high to very low, in the later case indicating that the TPm* ligand is not present at all. The carbons and hydrogens also vary from high to low throughout the series of complexes. Again the problems encountered with recording elemental analyses of the products renders this method of analysis unreliable for complexes containing fluorine groups.

The ^1H NMR spectrum of the yttrium complex $[YTPm^*(OPh^{F1})_3]$ **(4.29)**, clearly displays the sharp resonances expected for the TPm* protons. In addition to these, the ortho and meta protons of the phenoxide ligand are present as multiplets at *ca* 6.16 and 6.56 ppm, however these resonances integrate to only two protons each, suggesting that the yttrium metal binds only one fluorinated phenoxide ligand and not the expected three ligands. In contrast to this, the samarium complex $[SmTPm^*(OPh^{F1})_3]$ **(4.28)** displays the TPm* ligand resonances and has a very broad resonance at 6.92 ppm. The integral for this peak is correct for eight protons. This indicates that the larger samarium binds two fluorinated phenoxide ligands. There are evidently dynamics occurring within this samarium complex in solution that cause the very broad peak for the ortho and meta protons. One would expect the protons to be separated into two broad peaks however presumably the peaks overlap, suggesting the protons may be in very similar environments. Without crystal data for these complexes it is difficult to comment on the possible structures.

The di-fluoro substituted complex [SmTPm*(OPh^{F2})$_3$] (**4.26**), has a complicated ^{1}H NMR spectrum. The TPm* protons are present, however one of the 3, 5-dimethyl protons peaks is masked by the acetonitrile peak. Two broad peaks in the aromatic region in a ratio of 2:1 are the meta and para protons of the phenoxide ligand. The integrals are correct for the presence of three phenoxide ligands, in comparison with two suggested by the NMR spectrum of (**4.28**). There is another minor product present which is thought to be free ligand. The broad resonances of the phenoxide protons suggests dynamics occurring in solution, it is possible that the fluorine atoms interacts with the metal centre causing a change in the dipolar coupling between the protons and a broadening of their line width.

Summary

In this chapter we have reported the preparation and characterisation of four new sodium and potassium alkoxides containing fluorine substituents on the aromatic ring. $NaOPh^{F5}$ prepared in THF(**4.1**), $KOPh^{F5}$ prepared in THF (**4.3**) $KOPh^{F1}$ prepared in Et_2O (4.8) and $NaOPh^{F5}$ prepared in Et_2O (**4.2**) . X-ray analysis shows the key structural motif for these complexes in the solid state are cubane-type structures. $KOPh^{f5}$ and $NaOPh^{F5}$ prepared in THF, demonstrate M-F interactions between the metal centres and the ortho substituents of the aryloxide ligand. The M-F interactions are considered weak at *ca* 3 Å.

$NaOPh^{f5}$ and $KOPh^{f5}$ are not isomorphous. In (**4.3**) each potassium is seven coordinate, whereas for the sodium complex, two different types of phenoxide ligands are present. Two ligands are bound to the metal centres through bonds involving both the ortho fluorine, whereas the other two ligands exhibit binding to the sodium centre through only one ortho fluorine. Thus two sodium atoms are six coordinate whilst the other two are seven coordinate. This difference in bonding is accounted for by the difference in size between the sodium and potassium ions.

$NaOPh^{F5}$ (**4.2**) prepared in Et_2O has a particularly complex structure. Three sodium ions are 5 coordinate whereas the remaining ion is eight coordinate. The

parafluorine atoms interact with sodium ions on neighbouring cubes causing the cubic structures to be connected into infinite parallel columns.

15 crown 5 was combined with $NaOPh^{F5}$ in solution and successfully broke up the extended crystal lattice formed in ether by isolating a sodium ion and capping it with a 15 crown 5 group.

Speciation of the complexes in solution is dependent on the nature of the solvent with the complexes in THF exhibiting essentially dimeric structures whereas those in Et_2O were terameric.

Complexing the flourinated phenoxides with TPm* did not produce complexes suitable for analysis by X-ray crystallography and recording of reliable elemental analysis was not possible due to the incomplete combustion of the products on account of the fluorine groups. proton NMR spectra were reasonable for complexes of the type $MTPm^*(OPh^{Fn})$. However the sodium complexes demonstrated broad peaks for the dimethyl groups of the TPm* ligand pointing to strong dipolar couplings within the system, possibly due to the presence of the fluorine ions.

Complexes of the type $Ln(OPh^{Fn})_3$ were prepared by metathesis reactions between the appropriate sodium or potassium fluorophenoxide and $LnCl_3$ (Ln = Y, Sm). Whilst the difficulties obtaining reliable elemental analysis remained, ^1H NMR studies of para and 2,6 difluorophenoxide complexes display broad proton resonances due to alternating terminal and bridging modes of the phenoxide ligands. A low temperature proton NMR of $Y(OPh^{F2})_3$ confirms this.

Finally analysis for the complexation of $Ln(OPh^{Fn})_3$ with TPm* have been somewhat uninterpretable. It would seem that the metal centres are not able to coordinate the TPm* ligand and three fluorinated phenoxide groups. The ^1H NMR spectrum of $[Y(Tpm^*)(OPh^{fl})_3]$ **(4.29)** indicates that only one OPh^{F1} group is bound to the metal centre as opposed to the expected three. Likewise the larger samarium metal centre in $[Sm(Tpm^*)(OPh^{F1})_3]$ **(4.28)** binds only two OPh^{F1}

groups.

Chapter 5 Experimental details

General procedures

Unless otherwise stated, all preparations and manipulations were carried out under an atmosphere of dry nitrogen using standard Schlenk line techniques or in a vacuum Atmospheres HE-493 glove box. All air sensitive compounds and the reagents required for their synthesis were stored in a glove box after preparation. Sublimations were either carried out in horizontal tubes of diameter *ca* 30mm with a tube furnace as the heat source or by using a water condenser cold finger with an oil bath as the heat source. Molecular sieves were pre-dried in an oven at 150 °C for several days and activated prior to use by heating to *ca* 200 °C under vacuum.

Purification of Reagents

Nitrogen used for the glove box was not pre-purified but was circulated continuously through R311 catalyst and 5 Å molecular sieves to ensure an atmosphere free from oxygen and moisture. The atmosphere was monitored regularly by the use of a toluene solution of $(Cp_2TiCl_2)_2Zn$ (which remains green in the absence of oxygen and moisture).

Reaction solvents were pre-dried over sodium wire with the exception of dichloromethane which was dried over molecular sieves and acetonitrile which was not pre-dried. Prior to use, solvents were distilled under a flow of nitrogen gas from the appropriate drying agent as follows: Na (toluene) Na and K (tetrahydrofuran) Na/K alloy (petroleum ether bp 40-60 °C, diethyl ether) CaH_2 (dichloromethane, acetonitrile). Tetrahydrofuran, toluene, diethyl ether and petrol 40-60 °C were stored in ampoules over sodium mirrors, dichloromethane and acetonitrile were stored over molecular sieves. Solvents used for the preparation of pyrazolylmethane ligands were not dried or otherwise pre-purified.

NH_4I was heated overnight in an oven at *ca* 120 °C. NH_3 gas was not pre-dried. KH (80 % suspension in mineral oil, Aldrich) and NaH (60 % suspension in mineral oil, Aldrich) were washed with several portions of 40/60 petrol, dried under dynamic vacuum and stored in a glove box. Sodium tris(3,5-dimethyl-1-pyrazolyl)borane (NaTp*), Sodium Cyclopentadiene (NaCp), $Y[N(SiMe_3)_2]_3$ (Y(TMS amide)) and $Yb[N(SiMe_3)_2]_2$ were prepared by Dr. M. Russo and stored in a glove box. YCl_3, $SmCl_3$ and the trifluoromethanesulphonates (triflates) of Ce, Ho Nd, Dy and Y were prepared by Dr. G. Maunder and stored in a glove box. Yb metal was purchased from Aldrich as ingots (99.9 %) 3,5-di'butylycatechol was donated by Professor A. Deeming.

The following reagents were purchased from various suppliers: Phenol, 2,6-dimethylyphenol, 2,6-di'butylphenol, 2,6-diphenylphenol, 2,6-diisopropylphenol, pentafluorophenol, 2,6-difluorophenol, 4-fluorophenol 2,3,5,6-tetraflurophenol, acetylacetone, di'butylacetoacetone, diphenylacetoacetone, 3,5-dimethylypyrazole, tetra-*n*-butylammonium bromide and $Na(So_4)_2$ (anhydrous).

All NMR solvents were purchased from Aldrich. d_6-Benzene was died over a 1:3 alloy of sodium and potassium and then filtered through glass wool into a clean dry ampoule and stored in a glove box. D-Chloroform was stored over activated 3 Å molecular sieves in a glove box, Cd_3CN was stored in a dry ampoule in a glove box.

Instrumentation

^1H and ^{13}C – $\{^1H\}$ NMR spectra were recorded on Bruker Avance 500, VXR – 400, and AMX – 300 spectrometers in Wilmad NMR tubes equipped with Youngs valves. Spectra were referenced internally to residual protio solvent (^1H) or solvent (^{13}C) resonances and are reported relative to tetramethylsilane. ^{11}B spectra were referenced externally to $BF_3.Et_2O$. IR spectra were recorded as KBr pellets on a Shimadzu FTIR-8700 spectrometer. UV/vis spectra were run on a Shimadzu UV-160-A spectrometer using a specialised UV/vis cell sealed with a Youngs tap.

All elemental micro-analyses were performed by Mr. Alan Stones or Mrs. Jill Maxwell of the Christopher Ingold laboratories Analytical Services, UCL. The analysis of more reactive compounds was achieved by sealing the sample inside a pre-weighed aluminium analysis boat in a glove box, then reweighing to determine the mass of the sample, and analysing in the normal way.

X-ray Crystallographic analysis

Single crystals of **2.1**, **2.2**, **2.12**. and **2.13** were mounted on a glass fibre and all geometric and intensity data were taken from this sample on a Bruker SMART APEX CCD diffractometer using graphite – monochromated Mo Kα radiation (λ = 0.71073 Å) at 150 ± 2 K. Data reduction and integration were carried out with SAINT+[206] and absorption corrections applied using the program SADABS.[207] Structures were solved by direct methods and developed using alternating cycles of least-squares refinement and difference Fourier synthesis. All non-hydrogen atoms were refined anisotropically. Hydrogen atoms were placed in geometrically reasonable positions and allowed to ride on the atoms to which they were attached. Structure solution and refinement used the SHELXTL PLUS V6.12 program package.[208]

Single crystals of **2.6** and **2.7**. were mounted on a thin glass fiber using silicon grease and were cooled on the diffractometer to 120 K using an Oxford Cryostream low-temperature attachment. Approximate unit cell dimensions were determined by the Nonius Collect programme[209] from five index frames of width 2 ° in ϕ using a Nonius Kappa CCD diffractometer with a detector to crystal distance of 30 mm. The Collect program was then used to calculate a data collection strategy to 99.5 % completeness for $\theta = 27.5^{\circ}$ using a combination of 2 ϕ and θ scans of 10-120 s deg^{-1} exposure times (depending on crystal quality). Crystals were indexed using the DENZO-SMN package,[210] and positional data were refined along with diffractometer constants to give the final unit cell parameters. Integration and scaling (DENZO-SMN, scalepack[2]) resulted in unique data sets corrected for Lorentz and polarization effects and for effects of crystal

decay and absorption by a combination of averaging of equivalent reflections and an overall volume and scaling correction. Structures were solved using SHELXS-97 and developed via alternating least squares cycles and difference Fourier synthesis (SHELXS-97) with the aid of the program Xseed.[211] All non-hydrogen atoms were modelled anisotropically, except one disordered THF molecule in the case of **2.7** while hydrogen atoms were assigned an isotropic thermal parameter 1.2 times that of the parent atom (1.5 for terminal atoms) and allowed to ride.

Single crystals of **4.1, 4.2, 4.3** and **4.7b** were mounted on a glass fibre and all geometric and intensity data were taken from this sample on a Bruker SMART APEX CCD diffractometer using graphite-monochromated Mo-Kα radiation (λ = 0.71073 Å) at 150 ± 2 K. Data reduction and integration was carried out with SAINT+ and absorption corrections applied using the programme SADABS. Structures were solved by direct methods and developed using alternating cycles of least-squares refinement and difference-Fourier synthesis. All non-hydrogen atoms were refined anisotropically. Hydrogen atoms were placed in geometrically reasonable positions and allowed to ride on the atoms to which they were attached. Structure solution and refinement used the SHELXTL PLUS V6.12 program package.[212]

Molecular weight determinations were carried out the Signer isothermal distillation method, which relies on the diffusion of a solvent from one solution to another until the mole fraction of solute in each solution is the same. The Signer Osmometer apparatus (fig 5.1) was prepared by the glass blowing department of university College London and consists of two glass bulbs fitted with capillary tubes and joints for connection to a vacuum line.

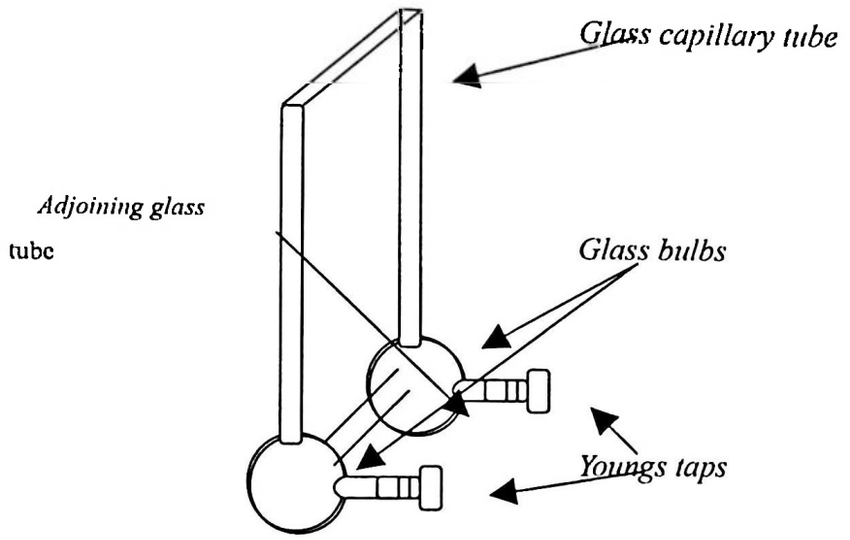

Figure 5.1: Sketch of a Signer Osmometer showing all relevant parts

An accurately weighed amount of ferrocene standard is placed in one bulb and the same amount of sample placed in the other. A similar amount of inert solvent is then placed in each bulb, the apparatus is sealed, removed from the box and partially evacuated. Its is then set aside for a few days to allow for equilibration. Volume changes are monitored by tipping the solutions into the capillary tubes until no further change occurs, the final volumes are then recorded. The molecular weight of the sample is determined from the expression below:-

$$MW_x = \frac{wt_x vol_s MW_s}{Wt_s vol_x}$$

Where MW_x is the molecular weight of the compound, MW_s is the molecular weight of ferrocene, wt_x is the weight of the compound, wt_s the weight of ferrocene and vol_x and vol_s are the volumes of the solutions of the compound and ferrocene respectively.

Starting materials

Preparation of Tris(3,5-dimethyl-1-pyrazoyl)methane (TPm*).

Distilled water (350 ml) was added to a 2 L round bottomed flask containing a mixture of 3,5-dimethyl pyrazole (34.05 g, 353.5 mmol) and tetra-*n*-butylammonium bromide (5.7 g, 17.5 mmol). With vigorous mechanical stirring, sodium carbonate (293 g, 2.1 mol) was added gradually to the reaction mixture resulting in an exothermic reaction. After allowing to cool to near room temperature, chloroform (175 ml) was added and the flask was equipped with a reflux condenser. The mixture was heated at gentle reflux for three days over which time it became a red emulsion. The mixture was left to cool to room temperature and filtered through a Büchner funnel to remove the excess base. The organic layer was separated from the aqueous layer and and washed with distilled water (3 x 40 ml), it was then dried over sodium sulphate. The drying agent was removed by filtration through a Büchner funnel. The solvent was removed by rotary evaporation, a thick dark red oil remained. The oil was triturated several times using 40/60 petrol and the solvent was removed by filtration to leave a yellow solid. Excess 3,5-dimethyl pyrazole was removed by overnight sublimation using a water condensing cold finger and tris(3,5-dimethyl-1-pyrazoyl)methane was left as a free flowing white/yellow powder. Yield: 7.31 g (0.024 mol, 48 %).

^{1}H NMR ($CDCl_3$): δ 8.05 (s, 1H, C-H); 5.85 (s, 3H, 4-H (pz)); 2.16, 1.99 (s, s, 9H, 9H, 3,5-Me). Analysis (%) calculated for $C_{16}H_{22}N_6$: C, 64.43; H, 28.19; N, 7.38. Found: C, 64.05; H, 28.05; N, 7.52.

Preparation of Ytterbium Diiodide (YbI_2)

A piece of ytterbium metal (6.4 g, 0.037 mol) was placed in a three-necked round bottomed flask containing a glass stir bar and fitted with a take of adaptor and a cardice condenser. The flask was evacuated, cooled to –78 °C and liquid ammonia (200 ml) was condensed onto the metal. Immediately a blue solution was formed and the contents of the flask were stirred for *ca.* 30 minutes to allow the ytterbium metal to dissolve. Ammonium iodide (10.18 g, 0.07 mol) was added in several

portions under a counterflow of nitrogen resulting in the formation of a yellow/orange precipitate of $YbI_2(NH_3)_n$. Once the addition was complete, the contents of the flask was stirred at –78 °C for approximately 2 hours before the ammonia was allowed to warm to reflux and boil off. The resulting yellow solid was heated under dynamic vacuum overnight (200 °C) to remove any solvated ammonia. YbI_2 was left as a fine free flowing yellow powder. Yield: 14.2 g, (0.033 mol, 90 %).

Analysis (%) Calculated for YbI_2: C, 0.00; H, 0.00; N, 0.00. Found: C, 0.00; H, 0.00; N, 0.70.

Preparation of Neodymium trichloride ($NdCl_3$)

Nd_2O_3 (5 g, 0.015 mol) was dissolved, with gentle heating in conc. HCl and ammonium chloride (11.16 g, 0.0209 mol) added. The mixture was heated with stirring until all the HCl had boiled off to leave a dry blue/grey solid. The solid was ground up using a pestle and mortar and placed in a sublimation tube. Excess ammonium chloride was removed by sublimation under dynamic vacuum for two hours at 100 °C. The temperature then was increased in increments of 30 °C over a 6 hour period until a temperature of 250 °C was reached. The solid was sublimed at 250 °C for 20 hours and then at 350 °C for a further 16 hours to afford $NdCl_3$ as a free flowing pale blue powder. Yield: 5.90 g, (0.023 mol, 79 %).

Preparation of Sodium phenoxide (NaOPh)

Phenol (5 g, 0.053 mol) was placed in a Schlenk flask and dissolved in THF. In a separate flask a slight excess of sodium hydride (≈1.5 g) was stirred in THF. The phenol solution was then added drop-wise to the sodium hydride. An exothermic reaction occurred with the evolution of hydrogen gas. The flask was fitted with a subaseal and exit needle and the solution stirred until the evolution of hydrogen gas had ceased, *ca.* 3 hours. The solution was filtered to remove excess sodium

hydride and THF was removed under reduced pressure to afford a pale yellow/white powder. Yield: 5.9 g, (0.051 mol, 96 %).

The following sodium phenoxide salts were prepared using the same procedure: $NaOPh^{(Me)2}$, $NaOPh^{(tBu)2}$, $NaOPh^{(iPr)2}$, $NaOPh^{(Ph)2}$.

Preparation of Sodium acetylacetonate (Na acac)

Acetylacetone (2 g, 0.019 mol) was dissolved in THF, this solution was then added drop-wise to an excess of sodium hydride (≈ 1 g) in THF. Immediately an exothermic reaction occurred with the evolution of hydrogen gas. The resulting solution was stirred for a further 2 hours until the evolution of hydrogen gas had ceased. Sodium hydride was removed by filtration and THF was removed under reduced pressure to leave Na acac as a white powder. Yield: 2.15 g, (0.017 mol, 90 %).

The following salts were also prepared using the procedure described above:
Na $acac^{tBu2}$ and Na $acac^{Ph2}$.

Experimental of Chapter 2

Preparation of [YTPm*Cl_3] (2.1)

TPm* (0.5 g, 0.0016 mol) was dissolved in MeCN in a Schlenk flask to produce a pale yellow solution. This was then added gradually to a separate flask containing a clear colourless solution of YCl_3 (0.33 g, 0.0016 mol) in MeCN. A white precipitate formed immediately. Stirring was continued for a further 1 hour before the solvent was removed by filtration and the solid dried under dynamic vacuum overnight to give YTPm*Cl_3 as a white insoluble powder. Yield: 0.66 g, (0.0013 mol, 80 %). Large colourless crystals were obtained by dissolving a minimum amount of YCl_3 in MeCN and transferring this to a narrow sealable tube, followed by a layer of MeCN and then a layer of one equivalent of TPm* dissolved in MeCN. The tube was sealed using a Youngs tap and the solutions left to diffuse over a period of two weeks.

Analysis (%) calculated for $C_{16}H_{22}N_6Cl_3Y$: C, 38.90; H, 4.46; N, 17.02. Found: C, 38.03; H, 4.37; N, 17.44.

IR (KBR pellet, cm^{-1}) 3129 m, 3095 w, 2924 m, 1560 s, 1458 s, 1414 s, 1379 s, 1304 s, 1261 s, 1155 w, 1109 m, 1040 s, 981 m, 905 m, 861 s, 795 m, 705, 633 m, 482 m.

^{1}HNMR (CD_3CN, 400MHz, 293 K) δ 7.90 (s, 1H, C-H) 6.08 (s, 3H, Tpm 4-CH), 2.64 (s, 9H, 5-Me), 2.52 (3-Me).

Preparation of [SmTPm*Cl_3] (2.2).

$SmCl_3$ (0.86 g, 0.0033 mol) was placed in a Schlenk flask and stirred in THF produce a slightly turbid solution, this was stirred for 2 hours. To this a pale yellow solution of TPm* (1 g, 0.0033 mol) in THF was added drop-wise to immediately

afford a clear solution. Stirring was continued overnight after which a white precipitate had formed. The solvent was removed by filtration and the white solid dried under dynamic vacuum to afford SmTPm*Cl_3 as a white powder. Yield: 0.96 g, (0.0017 mol, 52 %)

Analysis (%) calculated for $C_{16}H_{22}N_6Cl_3Sm$: C, 34.60; H, 3.96; N, 15.14. Found: C, 34.41; H, 3.96; N, 14.91.

IR (Kbr Pellet cm^{-1}) 3138 w, 3084 w, 2970 m, 2890 m, 1562 sh, 1558 sh, 1460 s, 1416 m, 1380 m, 1304 s, 1262 s, 1038 s, 980 w, 860 s, 821 m, 721 m, 708 sh, 636 m, 482 w.

^{1}HNMR (CD_3CN, 400 MHz, 293 K): δ 1.67 (s, 9H, 3-Me), 1.80 (m, 4H, THF), 3.62 (m, 4H, THF) 2.76 (s, 9H, 5-Me), 6.00 (s, 3H, Tpm 4-CH), 8.59 (s, 1H, Tpm C-H).

Preparation of [NdTPm*Cl_3] (2.3).

$NdCl_3$ (0.4 g, 0.0016 mol) was placed in a Schlenk flask and THF added to give a pale blue cloudy suspension, this was stirred for 2 hours. To this a solution of TPm* (0.48 g, 0.0016 mol) in THF was added drop-wise, the blue colour of the $NdCl_3$ suspension immediately disappeared and a clear dark yellow solution was formed. Stirring was continued overnight. The volume of THF was reduced under reduced pressure and a pale blue crystalline solid precipitated out of solution. The flask was placed in the freezer overnight after which time more product had precipitated out of solution. The solvent was removed by filtration and the solid dried under dynamic vacuum to give NdTPm*Cl_3 as a light blue semi-crystalline powder. Yield: 0.48 g, (0.0009 mol, 54.5 %).

Analysis (%) calculated for $C_{16}H_{22}N_6Cl_3Nd$: C, 34.99; H, 4.01; N, 15.31. Found: C, 34.00; H, 3.61; N, 14.53.

IR (KBR pellet cm^{-1}) 3140 w, 3086 w, 2970 m, 2890 m, 1564 sh, 1558 sh, 1458 s, 1415 m, 1380 m, 1307 s, 1262 s, 1031 s, 904 m, 858 s, 823 m, 710 sh, 701 sh, 481

w.

^{1}HNMR (CD_3CN, 400 MHz, 293 K): δ 1.94 (s, 9H, 3-Me), 2.34 (s, 1H, Tpm C-H), 3.09 (s, 9H, 5-Me), 7.36 (s, 3H, Tpm 4-CH).

Preparation of [Yb(TPm*)Cl_3], (2.4)

The reaction was carried out in THF analogous to the procedure described for 2.1 using $YbCl_3$ (0.94 g, 0.0034 mol) and TPm* (0.1 g, 0.0034 mol) to afford Yb(TPm*)Cl_3 as a cream coloured insoluble powder. Yield: 0.124 g (0.00217 mol, 64%).

Analysis (%) calculated for $C_{16}H_{22}N_6Cl_3Yb$: C, 33.3; H, 3.8; N, 14.5. Found: C, 33.6; H, 3.7; N, 14.2.
IR (KBr pellet, cm^{-1}): ,3132 m, 3090 w, 2970 w, 2920 m, 1561 s, 1456 s, 1411 s, 1380 s, 1301 s, 1259 s, 1155 w, 1109 m, 1041 s, 980 m, 905 m, 859 s, 795 m, 704 m, 635 w, 483 m.

Preparation of [Ce(TPm*)Cl_3] (2.5)

$CeCl_3$ (0.125 g, 0.0051 mol) was stirred in THF to produce a dark cream suspension. Upon addition of Tpm* (0.15 g, 0.0051 mol) the solid dissolved to afford a slightly turbid dark cream solution. Stirring was continued for 2 hours after which the solution was filtered. The volume of the filtrate was reduced to *ca* 5 ml and hexane was added drop-wise, the flask was cooled to -20°C in the freezer. After 24 hours an off white semi-crystalline solid had precipitated. The product was dried under vacuum at 50°C to afford [Ce(TPm*)Cl_3]. Yield: 0.12 g, (34%).

Analysis (%) calculated for $C_{16}H_{22}N_6Cl_3Ce$: C, 35.3; H, 4.1; N, 15.4. Found: C, 35.7; H, 4.3; N, 15.0. IR (KBr pellet, cm^{-1}): 3141 w, 3086 w, 2970 m, 2890 m, 1564 s, 1456 s, 1415 m, 1379 m, 1306 s, 1268 s, 1037 s, 976 w, 904 m, 858 s, 823 m, 709 sh, 702 sh, 481 w.

^{1}HNMR (CD_2Cl_2, 400 MHz, 293 K): δ 1.93 (s, 9H, 5-Me), 2.3 (v br s, 9H, 3-Me), 4.21 (s, 3H, Tpm 4-CH), 6.40 (s, 1H, C-H).

Preparation of [YTPm*(OTf)$_3$.THF] (2.6).

TPm* (0.3 g, 0.001 mol) in THF was added drop-wise to a slightly turbid solution of Y(Otf)$_3$ (0.54 g, 0.001 mol) in THF. A clear pale yellow solution was produced and Stirring was continued overnight. The solution was filtered and the volume of THF was decreased under reduced pressure until the solution was saturated. The precipitated product was re-dissolved by warming the flask. The flask was then placed inside a dewar and put into the freezer overnight for slow cooling. YTPm*(OTf)$_3$ was formed as clear flat crystals. Yield: 0.37 g, (0.0004 mol, 40.67 %).

Analysis (%) calculated for $C_{23}H_{30}N_6O_{10}S_3F_9Y$: C, 30.46; H, 3.31; N, 9.27. Found: C, 29.92; H, 3.23, N, 9.54.

IR (KBr, Cm^{-1}): 3150 w, 2998 m, 2938 m, 1570 m, 1460 m, 1424 m, 1328 s, 1208 s , br, 1018 s, 911 w, 860 m, 804 w, 707 m, 633 s, 586 w, 512 m..

1HNMR (CD_3CN, 400 MHz, 293 K) δ 1.84 (m, 4H, THF), 2.43 (s, 9H, 3,5-Me), 2.59 (s, 9H, 3,5-Me), 3.67 (m, 4H, THF), 6.16 (s, 3H, 4-H, Tpm), 7.96 (s, 1H, Tpm C-H).

Preparation of [HoTPm*(OTf)$_3$.THF] (2.7).

A solution of TPm* (0.2 g, 0.00067 mol) in THF was added drop-wise to a turbid solution of Ho(OTf)$_3$ (0.41 g, 0.00067 mol) in THF. A clear pale yellow solution formed immediately and stirring was continued overnight. The solution was filtered and the volume of solvent reduced under reduced pressure until the

solution was saturated. The flask was placed in a dewar and then into the freezer for slow cooling. After 48 hours HoTPm*$(OTf)_3$ had formed as clear crystals. Yield: 0.29 g, (0.0003 mol, 44.6 %).

Analysis (%) calculated for $C_{23}H_{30}N_6O_{10}S_3F_9Ho$: C, 28.22; H, 3.07; N, 8.56. Found: C, 27.61; H, 3.03; N, 8.35.

IR (KBr Cm^{-1}): 3152 w, 2994 m, 2923 m, 1570 m, 1462 m, 1422 m, 1390 w, 1337 s, 1208 s br, 1021 s, 909 w, 861 m, 802 w, 707 m, 636 s, 586 w, 512 m.

1207.4 (S-O).

The compound was NMR silent

Preparation of [DyTPm*$(OTf)_3$.THF] (2.8).

The preparation of 2.8 was carried out analogously to that of 2.4 and 2.5 using TPm* (0.13 g, 0.00044mol) and $Dy(OTf)_3$ (0.27 g, 0.00044 mol). DyTPm*$(OTf)_3$ was formed as flat colourless crystals. Yield: 0.18 g, (0.00044 mol, 41.86 %).

Analysis (%) calculated for $C_{23}H_{30}N_6O_{10}S_3F_9Dy$: C, 28.2; H, 3.1; N, 8.6. Found: C, 27.8; H, 3.0; N, 8.5.

IR (KBr Cm^{-1}) 3145 w, 2996 m, 2930 m, 1569 m, 1465 m, 1419 m, 1391 m, 1337 s, 1206 s br, 1187 s, 1019 s, 909 w, 861 m, 802 w, 767 w, 705 m, 636 s, 586 w, 511 m.

The compound was NMR silent.

Preparation of [YTPm*$(OPh)_3$NaCl] (2.9).

YTPm*Cl_3 (0.07 g, 0.0014 mol) was stirred in THF as a white, slightly turbid suspension. NaOPh (0.05 g, 0.0043 mol) was dissolved in THF to form a clear solution this was added drop-wise to the YTPm*Cl_3/THF suspension. The resulting cloudy white mixture was stirred overnight. On leaving to settle a clear solution and white precipitate had formed. The mixture was filtered. The white solid was identified as NaCl. The volume of the supernatant was reduced under reduced pressure and the flask was placed in the freezer. Crystallisation was unsuccessful and the solvent was removed and the resulting white solid pumped to dryness. Subsequent attempts at recrystallisation form THF and a THF/toluene mixture were also unsuccessful. Yield: 0.06 g, (0.00009 mol, 66 %).

Analysis (%) calculated for $C_{34}H_{37}H_6O_3YNa_{1.6}Cl_{1.6}$: C, 53.75; H, 4.87; N, 11.06. Found: C, 53.56; H, 5.76; N, 10.57.

IR (KBR pellet, cm^{-1}) 2962, 2917, 2871, 2344, 1593, 1568, 1480, 1447, 1414, 1386, 1368, 1295, 1261, 1159, 1148, 1099, 1064, 1028, 993, 974, 907, 861, 801, 758, 693, 705, 693, 592.

^{1}H NMR (CD_3CN 400 MHz, 293 K): δ 2.01 (s, 9H, 3,5-Me), 2.09 (s, 9H, 3,5-Me), 5.92 (s, 3H, Pz), 6.59 (s, br, 8H, Ph), 7.03 (s, br, 8H, Ph), 8.03 (s, 1H, C-H).

Preparation of [SmTPm*$(OPh)_3$NaCl] (2.10).

The preparation of 2.10 was carried out analogously to that of 2.9, using SmTPm*Cl_3 (0.1 g, 0.00018 mol) and NaOPh (0.063 g, 0.00054 mol). Crystallisation from THF and a THF/Toluene mixture was unsuccessful, hence the solvent was removed under reduced pressure and the resulting white powder was pumped to dryness. Yield: 0.09 g, (0.0011 mol, 64.3 %).

Analysis (%) calculated for $C_{34}H_{37}N_6O_3SmNaCl$: C, 51.92; H, 4.71; N, 10.69. Found: C, 52.11; H, 4.92; N, 10.71.

IR (Kbr pellet cm^{-1}): 3411 w br, 2960 w, 2922 w, 2856 (sh), 1589 s, 1566 (sh) 1481 s br, 1448 (sh), 1413 m, 1288 s, 1261 s, 1159 w, 1105 w, 1028 m br, 858 s, 802 (sh), 758 m, 694 m, 705 m, 584 w.

Preparation of [YTPm*$(OPh^{Me2})_3$](2.11).

A turbid white solution of YCl_3 (0.15 g, 0.00077 mol) in THF was stirred in a Schlenk flask. To this a pale yellow solution of TPm* (0.23 g, 0.00077 mol) was added drop-wise to afford a yellow solution and a white precipitate. Stirring was continued overnight after which time a yellow solution and heavy white solid remained. $NaOPh^{Me2}$ (0.33 g, 0.0023 mol) was dissolved in THF and then added drop-wise to YTPm*Cl_3 in THF. Gradually (*ca* 3 hrs) the white YTPm*Cl_3 precipitate disappeared and a clear orange solution remained. On stirring for a further 2-3 hrs, a white precipitate of NaCl had formed. NaCl was removed by filtration and the volume of THF reduced under reduced pressure. The flask was placed in a dewar and put in the freezer for slow cooling. After *ca* 48 hrs, YTPm*$(OPh^{Me2})_3$ had formed as large insoluble colourless crystals. Yield: 0.47 g (0.00058 mol, 75.8 %).

Analysis (%) calculated for $C_{40}H_{49}N_6O_3Y$: C, 64.0; H, 6.6; N, 11.2. Found: C, 63.8; H, 6.7; N, 11.0.

IR (Kbr pellet cm^{-1}) 3137 w, 3100 w, 3008 m, 2915 s, 2849 m, 1590 s, 1566 m, 1463 s, 1427 s, 1379 m, 1306 s, 1285 s, 1241 m, 1090 m, 1038 m, 979 w, 906 w, 859 m, 800 w, 759 m, 746 m, 705 s, 531.

^{1}HNMR (CD_2Cl_2, 300 MHz, 293 K): δ 1.95 (s, 18H, Me-OAr), 2.06 (s, 9H, 3,5-Me), 2.58 (s, 9H, 3,5-Me), 5.94 (s, 3H, Tpm 4-CH), 6.31 (t, *J*= 7.2 Hz, 3H, OAr *p*-H), 6.78 (d, *J* = 7.2 Hz, 6H, OAr *m*-H), 8.05 (s, 1H, Tpm C-H),

$^{113}C\{^1H\}$ NMR (CD_2Cl_2, 75.44 MHz, 293 K): δ 11.48 (OAr*Me*), 13.28 (3,5 Me), 17.59 (3,5-Me), 68.75 (Tpm CH), 107.94 (Tpm 4-CH), 114.54 (*p*-OAr), 126.60 (2-C-OAr), 127.76 (*m*-OAr), 140.00 (5-C Tpm*), 155.12b(3-C Tpm*), 162.89 (d, J_{YC} = 5.4 Hz, ipso-OAr)

Preparation of [SmTPm*(OPh^{Me2})$_3$] (2.12).

The preparation of 2.12 was carried out analogously to that of 2.11 using $SmCl_3$ (0.15 g, 0.00058 mol), TPm* (0.17 g, 0.00058 mol) and $NaOPh^{Me2}$ (0.25 g, 0.0018 mol). The dark orange solution of SmTPm*(OPh^{Me2})$_3$ in THF was filtered to remove the NaCl and the volume of THF was reduced under vacuum. The flask was placed in a dewar and put in the freezer for crystallisation. After two days, large pale orange crystals of SmTPm*(OPh^{Me2})$_3$ had formed. Yield: 0.31 g, (0.00036 mol, 62 %).

Analysis (%) calculated for $C_{40}H_{49}N_6O_3Sm$: C, 59.0; H, 6.1; N, 10.3. Found: C, 59.5; H, 6.5; N, 10.00.
IR (KBr pellet, cm^{-1}) 3140 w, 3105 w, 2923 s, 2852 s, 1606 w, 1568 m, 1475 s br, 1423 s, 1380 m, 1309 s, 1260 s, 1159 m, 1109 w, 1036 m, 956 w, 860 m, 818 s, 796 m sh, 707 m, 509 s.
^{1}HNMR (CD_2Cl_2, 300 MHz, 293 K): δ 1.22 (s, 18H, Me-OAr), 1.62 (s, 9H, 3-Me), 2.18 (s, 9H, 5-Me), 4.91 (s, 1H, Tpm C-H), 5.23 (s, 3H, *p*-H), 5.80 (s, 3H, Tpm 4-CH), 6.81 (s, 6H, *m*-H).

Preparation of [NdTPm*(OPh^{Me2})$_3$] (2.13).

NdTPm*Cl_3 (0.1 g, 0.00018 mol) was dissolved in THF to form a light blue solution. A clear solution of $NaOPh^{Me2}$ (0.08 g, 0.00054 mol) was then added drop-wise and a dull brown/green solution formed immediately. Stirring was continued for a further 2 hours after which a white precipitate of NaCl had formed. The NaCl was removed by filtration to give a light green solution. The volume of THF was reduced under vacuum and the flask was placed in the freezer for crystallisation. After *ca* 48 hours, light blue crystals of NdTPm*(OPh^{Me2})$_3$ had formed which desolvated upon removal of the solvent under reduced pressure. Yield: 0.11 g (0.00013 mol, 68.75 %).

Analysis (%) calculated for $C_{40}H_{49}N_6O_3Nd$: C, 59.6; H, 6.1; N, 10.4. Found: C, 59.6; H, 6.2; N, 10.3.

IR (KBr pellet cm^{-1}) 3135 w, 3108 w, 2920 s, 2855 s, 1600 w, 1563 m, 1475 s br, 1429 s, 1380 m, 1300 s, 1275 s, 1236 m, 1159 m, 1088 w, 1033 m, 978 w, 857 m, 820 s, 794 m sh, 721 m, 512 s.

^{1}HNMR (CD_2Cl_2, 400 MHz, 204 K): δ 0.34 (br s, 18H, Me-OAr), 0.49 (s, 9H, 5-Me), 2.62 (s, 1H, Tpm C-H), 4.65 (br s, 9H, 3-Me), 6.72 (s, 3H, Tpm 4-CH), 6.91 (br t, J = 5.1 Hz, 3H, *p*-H), 8.50 (br, 6H, *m*-H).

^{13}CNMR (CD_2Cl_2, 100.58b MHz, 293 K): δ 8.03 (3,5 Me), 11.76 (3,5 -Me), 15.55 (OArMe), 64.55 (Tpm C-H), 119.27 (Tpm 4-CH), 122.05 (*p*-OAr), 128.17 (*m*-OAr), 141.38 (br, 2-OAr), 146.08 (Tpm* qt), 210.95 (br, ipso-OAr).

Preparation of [Yb(TPm*)OAr^{Me2})$_3$] (2.14)

The preparation was carried out analogous to that of 2.13 using $YbCl_3$ (0.187 g, 0.00067 mo), Tpm* (0.20 g, 0.00067 mol) and $NaOAr^{Me2}$ (0.245 g, 0.002 mol). The resulting pale yellow solution was cooled to -20°C and small shiny crystals were produced. These desolvated upon removal of the solvent and drying under reduced pressure to afford a cream coloured powder. Yield: 0.017g, (30 %).

Analysis (%) calculated for $C_{40}H_{49}N_6O_3Yb$: C, 57.5; H, 5.9; N, 10.1. Found: C, 57.7; H, 5.9; N, 10.1.

IR (KBr pellet cm^{-1}): 3140 w, 3106 w, 2907 s, 2851 m, 1606 m, 1570 m, 1470 s, 1423 s, 1375 m, 1306 s, 1253 s, 1160 sh, 1035 m, 1010 m, 1007 w, 955 w, 855 s, 820 s, 745 m, 707 m, 508 s. ^{1}HNMR (CD_2Cl_2, 100.58 MHz, 204 K): δ -52.1 (s, 9H, 3-Me), -32.1 (br s, 9H, Me-OAr), -6.3 (br s, 3H, *m*-H), 1.5 (t, J = 5.1 Hz, 3H, *p*-H), 10.4 (br s, 3H, *m*-H), 22.1 (s, 9H, 5-Me), 78.9 (br s, 9H, Me-OAr), 74.1 (s, 1H, Tpm C-H).

Attempted Preparation of [YTPm*(OPh-4-Bu^t)$_3$NaCl] (2.15).

YTPm*Cl$_3$ (0.1 g, 0.0002 mol) was placed in a Schlenk flask and THF was added to form a cloudy white suspension. NaOPh^{tBu} (0.11 g, 0.00061 mol) was dissolved in THF and the solution was added drop-wise to the YTPm*Cl$_3$/THF suspension. The resulting solution became immediately clear and was stirred for a further two hours after which time a white precipitate of NaCl had formed. The solution was filtered and the solvent removed under reduced pressure to afford a white solid. The solid was extracted into a minimum amount of toluene and the solution was filtered again to remove excess NaCl. The flask was placed into the freezer for crystallisation. Crystallisation from toluene was unsuccessful and hence the solvent was removed under reduced pressure and the resulting white powder was pumped to dryness.
Yield: 0.1 g, (0.00011 mol, 55.6 %).

Analysis (%) calculated for $C_{46}H_{61}N_6O_3YNaCl$: C, 61.8; H, 6.83; N, 9.41. Found: C, 58.98; H, 7.51; N, 9.62.
IR (Kbr pellet cm^{-1}): 2960 m, 2927 (sh), 2862 (sh), 1602 m, 1568 m, 1506 s, 1461 m br, 1415 m, 1390 w, 1359 w, 1299 s, 1263 s, 1174 m, 1105 w br, 1037 m br, 977 w, 867 w, 833 m, 798 (sh), 705 m, 686 m, 553 w, 480 w.

Attempted Preparation of [SmTPm*(OPh-4-Bu^t)$_3$NaCl] (2.16).

The preparation of 2.16 was carried out analogously to that of 2.15, using SmTPm*Cl$_3$ (0.1 g, 0.00018 mol) and NaOPh^{tBu} (0.093 g, 0.00054 mol). Crystallisations from THF and toluene were unsuccessful and solvents were removed under reduced pressure to afford a white free flowing powder. Yield: 0.11 g, (0.00012 mol, 64.7 %).

Analysis (%) calculated for $C_{46}H_{61}N_6O_3SmNaCl$: C, 57.8; H, 6.39; N, 8.80. Found: C, 50.47; H, 5.94; N, 7.88.

IR(KBr pellet cm^{-1}): 3022 w (sh), 2960 s, 2904 (sh), 2864 (sh), 1602 m, 1566 m, 1506 s, 1463 w br, 1415 w, 1296 m br, 1261 s, 1174 m, 105 m br, 974 w, 862 m, 833 s, 800 (sh), 705 m, 682 w, 553 w, 478 w.

Attempted preparation of [YTPm*$CpCl_2$] (2.17)

YTPm*Cl_3 (0.12 g, 0.00024 mol) was placed in a Schlenk flask and stirred in THF. In a separate flask NaCp.THF (0.039 g, 0.00024 mol) was dissolved in THF to form a clear light pink solution which was then added drop-wise to the YTPm*Cl_3/THF suspension resulting in a yellow, slightly cloudy solution. Stirring was continued overnight and a yellow solution and white precipitate had formed. The precipitate was removed by filtration and the volume of the supernatant was reduced under vacuum. The flask was placed in the freezer for slow cooling. Crystallization from THF was unsuccessful thus the THF was removed completely under reduced pressure and the resulting pale yellow solid pumped to dryness. Yield: 0.07 g (0.00013 mol, 56%).

Analysis (%) calculated for $C_{21}H_{27}N_6Cl_2Y$: C, 48.19; H, 5.16; N, 16.66 . Found: C, 48.44; H, 6.03; N, 16.56.
IR (KBr, cm^{-1}) 3419, 3095, 2962, 2925, 2871, 2744, 1737, 1560, 1460, 1415, 1380, 1340, 1307, 1261, 1099, 1024, 895, 904, 869, 790, 711, 661, 482.

Attempted preparation of [SmTPm*($CpCl_2$)] (2.18)

SmTPm*Cl_3 (0.034 g, 0.000061 mol) was placed in a Schlenk flask and THF added resulting in a white turbid suspension. NaCp.THF (0.01 g, 0.000061 mol) was dissolved in THF to form a pale pink solution. This solution was added drop-wise to the SmTPm*Cl_3/THF suspension. After approximately one hour a turbid yellow solution had formed and stirring was continued overnight On stopping the stirring, the contents of the flask settled to form a white precipitate and a pale

yellow supernatant. The precipitate was removed by filtration, the volume of the solution was reduced and the flask placed in the freezer for slow cooling. Crystallisation was unsuccessful, the THF was removed under reduced pressure resulting in a pale yellow powder. Yield: 0.023 g (0.00039 mol, 63 %).

Analysis (%) calculated for $C_{21}H_{27}N_6Cl_2Sm$: C, 43.12; H, 4.62; N, 14.37. Found: C, 55.26; H, 6.72; N, 18.74.
^1H NMR (CD_3CN, 400 MHz, 300 K): δ 8.11 (s, 1H, TPm* C-H), 5.97 (s, 3H, TPm* 4-H), 2.13 (s, 9H, 3,5 Me), 2.03 (s. 9H, 3,5 Me).

Attempted reparation of YTPm*Tp*Cl_2 (2.19)

YCl_3 (0.4 g, 0.002 mol) was stirred in THF. In a separate flask TPm* (0.54 g, 0.002 mol) was dissolved in THF, the resulting solution was added drop-wise to the YCl_3 suspension. The resulting solution was initially pale yellow and became turbid after approximately 30 minutes of stirring. NaTp*.THF (0.65 g, 0.002 mol was dissolved in THF to produce a clear solution which was then added drop-wise to the YCl_3/TPm* mixture in THF. Stirring was continued overnight resulting in a pale yellow supernatant and white precipitate. The precipitate was removed by filtration, the volume of the supernatant as reduced and the flask was placed in the freezer inside a dewar for slow cooling. Crystallisation was unsuccessful. Attempts at crystallisation from toluene were also unsuccessful hence the solvent was removed completely under vacuum and the resulting white solid dried. Yield: 0.2 g (0.00026 mol, 15 %).

Analysis (%) calculated for $C_{31}H_{44}N_{12}Cl_2BY$: C, 49.28; H, 5.83; N, 22.26. Found: C, 48.93; H, 6.11; N, 21.27.
IR (Kbr, pellet cm^{-1}): 3396 w br, 3136 w br, 2962 m, 2925 m, 2868 (sh), 2551 w br, 2362 w, 1566 m, 1541 s, 1444 s, 1417 s, 1383 m, 1367 m, 1317 m, 1261 s, 1197 s, 1072 s, 1041 s br, 981 w, 860 m, 804 s br, 693 m, 650 m, 459 w.

Preparation of SmTpm*Tp*Cl_2. (2.20)

$SmCl_3$ (0.2 g, 0.0013 mol) was stirred in THF. Meanwhile Tpm* (0.4 g, 0.00133 mol) was dissolved in THF and subsequently added drop-wise to the $SmCl_3$/THF solution. On addition a cream/white precipitate started to form. In a separate flask NaTp* (0.44 g, 0.00133 mol) was dissolved in THF, this solution was then added drop-wise to the $SmCl_3$/Tpm* mixture in THF. No obvious change occurred on addition and the contents of the flask were stirred overnight. The resulting white precipitate was removed by filtration and THF was removed under reduced pressure and to give a white powder, which was pumped dry. The white powder was extracted into toluene, the solution filtered and the flask placed in the freezer for slow cooling. Crystallisation was unsuccessful thus the toluene was removed under reduced pressure and the resulting white solid dried. Yield: 0.39 g (28%).

Analysis (%) calculated 4 $C_{31}H_{44}H_{12}Cl_2B_1Sm$ C, 51.68; H, 5.40;L N, 21.63. Found: C, 51.96, H, 6.42; N, 21.34.
IR (KBr cm^{-1}): 3390 m br, 2925 m, 2871 (sh), 2549 w br, 2343 w, 1566 s, 1541 m, 1446 s, 1417 s, 1380 m, 1367 m, 1319 m, 1263 s, 1197 m, 1070 m, 1039 s, 977 w, 860 s, 806 m, 788 (sh), 705 m, 650 w, 457 w.

Preparation of [Nd(Tpm*)$(BH_4)_3$(THF)] (2.21)

A solution of Tpm* (0.298 g, 0.001 mol) in THF was added slowly to as solution of $Nd(BH_4)_3(THF)_3$ (0.40 g, 0.001 mol) also in THF. The resulting yellow/green solution was stirred overnight. The volume was was reduced under reduced pressure to a point where solid was starting to precipitate (*ca* 10 ml). The flask was placed in a freezer at -20°C overnight after which the supernatant was decanted off and the pale blue solid dried under reduced pressure. Yield: 0.21 g, (38 %).

Analysis (%) calculated for $C_{20}H_{42}N_6B_3ONd$: C, 43.0; H, 7.6; N, 15.0. Found: C, 42.5; H, 7.3; N, 14.6.

IR(KBr pellet cm^{-1}): 2962 m, 2895 m, 2461 s, 2452 s br, 2227 s br, 2160 (sh), 1566 m, 1457 s, 1414 m, 1371 m, 1306 m, 1262 s, 1171 s, 1096 s, 1036 m, 1007 m, 897, 860 s, 804 m, 721, 702 s, 482 w. ^{11}BNMR (THF, 160.46 MHz, 293 K): δ 168.

Attempted preparation of Y[N(SiMe$_3$)$_2$]$_3$TPm* (2.22)

$Y[N(SiMe_3)_2]_3$ (0.15 g, 0.0026 mol) was dissolved in THF, to this a solution of TPm* (0.08 g, 0.00026 mol) was added drop wise resulting in a pale orange solution. This solution was stirred overnight. The THF was removed under reduced pressure and the resulting white solid was pumped until dry. Recrystallisation by dissolving in THF and layering with a few drops of 40/60 petrol was unsuccessful. Yield: 0.14 g (0.00016 mol, 62 %).

Analysis (%) calculated for $C_{34}H_{76}N_9Si_6Y$: C, 47.06; H, 8.77; N, 14.53. Found: C, 45.03; H, 6.73; N, 15.87.

IR(KBr cm^{-1}) 3419, 2960, 2925, 2869, 1560, 1448, 1415, 1382, 1363, 1340, 1321, 1271, 1099, 1024, 974, 869, 790, 775, 713, 628, 588.

^{1}H NMR (C_6D_6, 400 MHz, 300 K) δ 8.24 (s, 1H, TPm* C-H), 5.63 (s, 3H, TPm* 4-H), 2.08 (s, 9H 3,5-Me), 1.90 (s, 9H, 3,5 Me), 0.36 (s, br, 54H, NR2 H).

Experimental of Chapter 3

Preparation of YbI$_2$TPm*.THF (3.1)

TPm* (0.7 g, 0.00234 mol) was dissolved and stirred in THF. In a separate

Schlenk, YbI_2 (1 g, 0.00234 mol) was dissolved in THF to afford a clear light yellow solution. To this, the solution of TPm* was added drop-wise, immediately a colour change from pale yellow to deep red occurred and after *ca* 1 minute an orange/red precipitate formed. The mixture was stirred for a further hour after which time the THF was removed by filtration. Once isolated the product was only sparingly soluble in THF, thus attempts at recrystallisation from THF by slow cooling were unsuccessful as were attempts by layering THF solutions of the reactants either side of a layer of THF in a sealed youngs tube. Yield: 0.87 g (0.00166 mol, 70.73 %).

Analysis (%) calculated for $C_{20}H_{30}N_6OI_2Yb$: C, 30.12; H, 3.77; N, 10.56. Found: C, 30.54; H, 3.90; N, 9.44

UV-Vis (THF) 357.6 nm; 475.8 nm.

IR (KBR, cm^{-1}) 2924, 2854, 2746, 2424, 1566, 1458, 1413, 1384, 1301, 1261, 1105, 1040, 978, 902, 860, 798 704.

Deprotontion of $YbTPm^*I_2$ using $NaNPh_2$ (3.2)

'$YbTPm^*I_2$' was prepared *in situ* by loading YbI2 (0.4 g, 0.00094 mol) into a Schlenk flask inside the glove box. THF was added to form a yellow solution and some grey precipitate. The precipitate was removed by filtration leaving a yellow solution. TPm* (0.56 g, 0.00188 mol) was dissolved and stirred in THF and then added drop-wise to the solution of YbI_2 in THF. The resulting solution immediately turned deep red and an orange/red precipitate formed. $NaNPh_2$ (0.36 g, 0.00189 mol) was measured into a Schlenk in the glove box and THF was added resulting in a yellow/green solution. This solution was added drop-wise to the orange YbI_2TPm^* emulsion. A burgundy solution and precipitate formed immediately on addition. Stirring was continued for 20 minutes after which the solvent was removed by filtration and the red solid dried under dynamic vacuum. Extraction of the solid into toluene resulted in a bright purple solution. The solid is only partially soluble in toluene thus the solution was filtered to remove the

undissolved product. The solvent was removed under dynamic vacuum to leave a slightly oily purple solid. Yield: 0.47 g (0.00061 mol, 65.3 %).

Analysis calculated for C, 50.06; H, 5.48; N, 21.90. Found: C, 49.12, H, 4.27; N, 8.52.
IR (KBr cm^{-1}) 3383, 2963, 2924, 2853, 2359, 2341, 2274, 1593, 1508, 1495, 1458, 1418, 1387, 1313, 1261, 1173, 1084, 1026, 862, 802, 748, 691, 667.
UV vis (toluene) 350.2 nm, 523.6 nm.

Preparation of YbTPm*ITp*.THF (3.3)

YbTPm*I_2 (0.25 g, 0.000345 mol) was stirred in THF to form a turbid orange solution which became clear after approximately 30 minutes. In a separate Schlenk, NaTp* (0.11 g, 0.000345 mol) was dissolved in THF and gradually added to the YbTPm*I_2/THF solution. The orange solution immediately became pale yellow. After stirring for *ca* 30 minutes a white precipitate formed, this was removed by filtration. The THF was removed under dynamic vacuum and the resulting pale yellow solid was extracted into toluene. Crystallisation by slow cooling in the freezer was not successful, thus the toluene was also removed under dynamic vacuum and the pale yellow solid dried. Yield: 0.272 g (0.000284 mol, 82.4 %).

Analysis (%) calculated for $C_{35}H_{52}N_{12}OBIYb$: C, 43.4; H, 5.4; N, 17.39. Found: C, 44.92; H, 6.17; N, 17.59.

Preparation of YbTPm*(OPhMe2)$_2$.THF (3.4)

YbTPm*I_2 (0.25 g, 0.000345 mol) was stirred in THF. After *ca* 30 minutes the solution turned from turbid orange to clear orange. A pale brown solution of

$NaOPh^{Me2}$ (0.1 g, 0.00069 mol) in THF was added drop-wise, the orange solution became a much darker orange/red. After approximately 5 minutes the red/orange solution turned pale yellow. The volume of THF was reduced under vacuum and the flask placed in the freezer for slow cooling. Crystallisation was not successful thus the solvent was removed completely under dynamic vacuum leaving a free flowing pale yellow powder. Yield: 0.19 g (0.000262 mol, 76 %).

Analysis (%) calculated for $C_{36}H_{48}N_6O_2Yb$: C, 55.03; H, 6.11; N, 10.70. Found: C: 35.85; H, 4.32; N, 7.86.

^{1}HNMR: (CD_3CN, 400 MHz, 293 K) δ 7.90 (s, 1H, CH) 6.90 (d, 4H, 3,5H OPh) 6.66 (t, 2H, *p*H OPh) 5.93, (3H, Pz) 3.63 (s, 3H THF) 2.31 (s, 9H, pzMe) 2.25 (9H PzMe) 2.103 (s, b, 12H, OPhMe) 1.76 (s 3H THF)

Attempted preparation of YbTPm*(OPh)$_2$ (3.5)

YbI_2 (0.14 g, 0.00035 mol) was loaded into a Schlenk inside the glove box and THF added. To this a solution of one equivalent of TPm* (0.1 g, 0.000345 mol) in THF was added drop-wise, resulting in an orange/red emulsion. Two equivalents of NaOPh (0.08 g, 0.00068 mol) was placed in a separate schlenk. The sodium phenoxide dissolved readily in THF to give a clear solution. This solution was added drop-wise to the YbTPm*I_2 suspension in THF. There was no obvious immediate colour change. After stirring overnight the emulsion had become more orange/brown in colour. Filtering resulted in a bright orange solution and a brown solid. The volume of the solution was reduced under reduced pressure and the flask was placed inside the freezer for crystallisation. After *ca* 12 hours orange crystals had formed.

Yield: 0.152 g (0.00023 mol, 66.1 %)

Analysis (%) calculated for $C_{28}H_{32}N_6O_2Yb$: C, 51.14; H, 4.87; N, 12.78. Found: C, 14.95; H, 2.52; N, 0.17.

Experimental of Chapter 4

Preparation of $NaOPh^{F5}$ from THF. (4.1)

$KOPh^{F5}$ (5g 0.0272 mols) was dissolved in THF. The resulting solution was added drop-wise via a cannula to an excess of NaH in THF. Effervescence occurred immediately and hydrogen gas was produced. Once the production of hydrogen gas had ceased, the excess NaH was removed by filtration. The volume of solvent was reduced under vacuum resulting in the solution becoming cloudy and a crystalline solid beginning to precipitate. The flask was placed in warm water until the solid had redissolved. It was then placed inside a dewar in the freezer for slow cooling. After *ca* 15 hours clear crystals had formed. Yield: 3.69 g (0.018 mols, 66 %)

Analysis (%) calculated for C_6F_5NaO: C, 34.95; H, 0; N, 0. Found: C, 37.82; H, 0.89, N, 0.45.

Preparation of $NaOPh^{F5}$ from Et_2O (4.2)

The preparation of $Na(OPh^{F5})$ from ether was carried out analogously to its preparation in THF. The combination of pentafluorophenol, (2g 0.01087 mols), in Et_2O with an excess of NaH in Et_2O led to the isolation of $Na(OPh^{F5})$. Yield: 1.72 g (0.0083 moles 76.4 %).
Crystals suitable for crystallographic analysis were grown from slow cooling of a concentrated solution of the product in ether layered with toluene.

Analysis (%) calculated for C_6F_5NaO: C, 34.95; H, 0, N, 0. Found: C, 34.86; H, 0; N, 1.62.

Preparation of $KOPh^{f5}$ in THF (4.3)

Preparation of $KOPh^{f5}$ was carried out in an identical manner to the preparation of $NaOPh^{f5}$ in THF. After slow cooling of the Schlenk flask, opaque crystals of $KOPh^{f5}$ had formed. The THF was decanted off and the crystals dried. Yield:- 1.57g (0.0071 moles 65 %)

Analysis (%) calculated for C_6F_5KO: C, 32.43; H, 0; N, 0. Found: C, 32.63; H, 0.39; N, 0.

Crystal structure obtained.

Preparation of $KOPh^{f5}$ in Et_2O (4.4)

As for the preparation of $KOPh^{f5}$ in THF, substituting Et_2O for THF as the solvent. The reaction and subsequent crystallisation afforded small clear crystals. The solvent was decanted off and the crystals dried under reduced pressure. Yield: 0.73 g (0.0033 moles 61.3 %).

Analysis (%) calculated for C_6F_5KO: C, 32.43; H, 0; N, 0. Found C, 32.46; H, 0; N, 2.15.

Preparation of $NaOPh^{f1}$ from Et_2O. (4.5)

4-Fluorophenol, (1 g, 0.0089 mols) was dissolved in ether in a Schlenk. The resulting solution was added drop-wise to an excess of potassium hydride in a minimal volume of ether. Vigorous effervescence occurred immediately on contact and hydrogen gas was produced. The solution was stirred until the reaction had ceased. The excess KH was removed by filtration and the volume of ether reduced under vacuum. Toluene was layered on top of the ether and the flask was placed in

the freezer for slow cooling overnight after which clear needle like crystals had formed. Yield: 0.62 g (0.0046 mol, 52 %).

Analysis (%) calculated for C_6H_4OFNa: C, 53.73; H, 2.98; N, O. Found C, 42.93; H, 2.81; N, 0.

Preparation of $NaOPh^{Fl}$ From THF (4.6)

The preparation of $NaOPh^{Fl}$ from THF was carried out using the same method as its production from ether. Adding 4-flurophenol in THF to an excess of NaH in THF resulted in the isolation of a crystalline product of $NaOPh^{Fl}$. Yield: 3.70 g, (0.0276 mols, 62 %).

Analysis (%) calculated for C_6H_4OFNa: C, 53.73; H, 2.98; N, 0. Found: C, 56.50; H, 4.94; N, 0.

^1H NMR (CD_3 CN, 400 MHz, 293K); δ 6.92 (M,2H,OPh,3,5-H) 6.28 (M,2H,OPh,2,6-H)

Preparation of $KOPh^{Fl}$ from THF (4.7)

The reaction was carried out in an identical manner to the previous reactions. Crystallisation afforded needle like crystals of $KOPh^{fl}$. Yield: 2.68g (0.018 mol, 69.6 %)

Analysis (%) calculated for $C_{12}H_4OKF$: C, 48.0; H, 2.67; N, 0. Found: C, 46.14; H, 3.21; N, 0.

^1H NMR (CD_3CN, 400 MHz, 293 K): δ 6.53 (m, 2H, OPh 3.5-H), 6.16 (m, 2H, OPh 2,6-H).

Preparation of $KOPh^{F1}$ from ether (4.8)

The preparation of (**4.8**) was carried out in an identical manner to the previous reactions.

Yield: 2.98g (0.019 mol 65%)

Analysis(%) calculated for C_{12} H_4 OKF: C;48.0 H;2.67 N;0. Found; C;46.14 H;3.21 N;0

Preparation of $NaOPh^{F2}$ from THF (4.9)

3,5 difluorophenol (1 g, 0.0077mol) was dissolved in THF. The solution was added drop-wise to an excess of NaH in THF. The reaction was immediate and vigorous with the production of hydrogen gas. The excess NaH was removed by filtration. The volume of THF was reduced under vacuum and the reaction flask was placed in the freezer for crystallisation. After approximately 24 hours of cooling, a crystalline solid had precipitated. The solvent was removed by filtration and the white solid dried under reduced pressure. Yield: 0.86 g (0.0056 mol 0.73 %).

Analysis (%) calculated for $C_6H_3F_2ONa$: C, 47.37; H, 1.97; N, 0. Found: C, 47.49; H, 1.99; N, 0.

^1H NMR (CD_3CN, 400 MHz, 293 K): δ 6.68 (m, 2H, OPh 3,5-H), 6.09 (m, 1H, OPh 4-H).

NB: The attempted preparation of $NaOPh^{F2}$ using diethylether as the solvent was unsuccessful on account of the fact the product is completely insoluble in Et_2O and crashes straight out thus making it impossible to separate from the NaH.

Preparation of $KOPh^{F2}$ from THF. (4.10)

Synthesis of 4.10 was carried out in an identical manner to that of 4.9. Slow cooling afforded a white crystalline solid. Yield: 0.91 g (0.0054 mol 70.5 %).

Analysis (%) expected for $C_6H_3OF_2K$: C, 42.86; H, 1.79; N, 0. Found: C, 42.80; H, 1.79; N, 0.

^1H NMR (CD_3CN, 400 MHz, 293 K): δ 6.16 (m, 2H, OPh 3,5-H), 5.88 (m, 1H, OPh 4-H)

NB: The attempted preparation of $KOPh^{F2}$ from diethylether was unsuccessful. The product was completely insoluble in the solvent and thus could not be separated from the KH.

Reaction between $NaOPh^{F5}$ and 15 crown 5 (4.11)

$NaOPh^{F5}$ (0.15 g, 0.00073 mol) was dissolved in ether and stirred. A solution of dibenzo15crown5 (0.16 g, 0.00073 mol) in ether was added drop-wise A white solid immediately precipitated. The ether was removed and the white solid was extracted into THF. The volume of the THF was reduced to a minimum under vacuum and the flask was placed into the freezer for cooling. After approximately 24 hours small clear crystals had formed. The solvent was removed by filtration and the crystals dried under reduced pressure. Yield: 0.24 g (0.00058 mol 80 %).

Analysis (%) calculated for $C_{16}H_{10}F_5O_6Na$: C, 46.15; H, 2.4; N, 0. Found: C, 44.29; H, 4.60, N, 0.56

Reaction between $KOPh^{F5}$ and dibenzo 18 crown 6. (4.12)

$KOPh^{F5}$ (0.2 g 0.0009 mol) was dissolved and stirred in THF . An equivalent of dibenzo18crown6 (0.32 g 0.0009 mol) was stirred in THF and heated to aid dissolution. This solution was added drop-wise to the $KOPh^{F5}$/THF solution and stirring was continued for approximately 4 hours. The volume of THF was reduced under vacuum and the flask placed in the freezer. After approximately 24 hours very small crystals had formed. Attempts to grow crystals suitable for crystal structure analysis were unsuccessful. Yield: 0.38 g (0.00067 mol, 76 %).

Analysis (%) calculated for $C_{26}H_{16}O_7F_5K$: C, 54.35; H, 2.79; N, 0. Found: C, 46.06; H, 3.83; N, 0.

Reactions between the basic starting materials and Tpm*

Preparation of $NaOPh^{F5}TPm^*$ (4.13)

A solution of Tpm* (0.58 g, 0.0019 mol) in ether was added drop-wise to a solution of $NaOPh^{F5}$ (0.4 g, 0.0019 mol) in ether. A white solid precipitated immediately. Attempts to redissolve the products by gentle heating and stirring were unsuccessful. Thus the ether was removed by filtration and the white powder was dried by heating the flask in an oil bath. The product was then dissolved in THF and filtered. The flask was placed in the freezer to cool. Overnight a crystalline solid had formed. The solid was isolated by filtration and dried under reduced pressure. Yield: 0.62 g, (0.0012 mol, 64.4%).

Analysis (%) calculated for $C_{22}H_{22}N_6F_5ONa$: C, 52.38; H, 4.27; N, 16.67. Found:

C, 49.61; H, 4.06; N, 13.0.

^{1}H NMR (CD_3CN, 400 MHz, 293 K): δ 7.99 (s, 1H, TPm* C-H), 5.93 (s, 3H, TPm* 4-H), 2.07 (d, br, 19H, 3,5-Me).

Preparation of $KOPh^{F5}TPm^*$ (4.14)

$KOPh^{F5}$ (0.2 g, 0.0009 mol) was dissolved in THF. A solution of Tpm* (0.27 g, 0.0009 mol) in THF was added drop-wise Stirring was continued for two hours after which the volume of THF was reduced under reduced pressure. The reaction flask was placed in the freezer to cool. Overnight a white solid had precipitated. The THF was removed by filtration and the solid dried under vacuum. Several attempts at growing crystals suitable for analysis were unsuccessful. Yield: 0.31 g, (0.0006 mol, 66 %.

Analysis (%) calculated for $C_{22}H_{22}N_6F_5OK$: C, 50.77; H, 4.23; N, 16.15. Found: C, 50.57; H, 4.57; N, 14.94.

^{1}H NMR (CD_3CN, 400 MHz, 293 K): δ 8.06 (s, 1H, TPm* C-H), 5.92 (s, 3H, TPm* 4-H), 3.62 (m, 2H, THF), 2.09 (s, 9H, 3,5-Me), 1.96 (s, 9H, 3,5-Me).

Preparation of $KOPh^{F1}TPm^*$ (4.15)

$KOPh^F$ (0.3 g, 0.002 mol) was dissolved in THF. A solution of Tpm* (0.6 g, 0.002 mol) in THF was added drop-wise After stirring for *ca* 2 hours, the volume of THF was reduced and the flask was cooled in the freezer. The resulting white solid was isolated by filtration and dried under reduced pressure. Yield: 0.53 g, (0.001 mol, 57.8 %).

Analysis (%) calculated for $C_{22}H_{22}N_6OKF$: C, 58.96; H, 5.8; N, 18.75. Found: C,

58.48; H, 6.15; N, 18.16.

^{1}H NMR (CD_3CN, 400 MHz, 293 K): δ 8.06 (s, 1H, TPm* C-H), 6.57 (m, 2H, OPh 2,6-H), 6.15 (m, 2H, OPh 3,5-H), 5.92 (s, 3H, TPm* 4-H), 5.63 (m, 1H, THF), 2.89 (s, 9H, 3,5-Me), 1.97 (s, 9H, 3,5-Me), 1.79 (m, 1H, THF).

Preparation of $NaOPh^{F2}TPm^*$ (4.16)

$NaOPh^{F2}$ (0.1 g, 0.00067 mol) was dissolved in THF as with previous preparations and solution of Tpm* (0.19 g 0.00067 mol) in THF was added. Cooling overnight afforded a white semi-crystalline solid. The solid was dried under reduced pressure. Yield: 0.21 g (0.00042 mol 63.3 %).

Analysis (%) Calculated for $C_{22}H_{22}ONaF_2$:

^{1} H NMR (CD_3CN, 400 MHz, 293 K): δ 8.05 (s, 1H, TPm* C-H), 6.66 (m, 2H, OPh 3,5-H), 6.04 (m, 1H, OPh 4-H), 2.07 (s, br, 9H, 3,5 Me), 2.00 (s, Br, 9H, 3,5 Me).

Preparation of $KOPh^{F2}TPm^*$ (4.17)

$KOPh^{F2}$ (0.1 g, 0.0006 mol) was dissolved and stirred in THF. A solution of Tpm* (0.18 g 0.0006 mol) in THF was added gradually. The volume of the solvent was reduced and the flask placed in the freezer. The resulting white solid was isolated by filtration and dried under vacuum. Yield: 0.19 g (0.0004 mol, 67 %).

Analysis (%) calculated for $C_{22}H_{22}N_6OKF_2$: C, 56.65; H, 5.85; N; 18.89. Found: C, 57.04; H, 5.85; N, 18.89.

1 H NMR (CD3CN, 400 MHz, 293 K) δ 8.07 (s, 1H, TPm* C-H), 6.61 (m, 2H, OPh 3,5 Me), 5.92, (s, 3H, TPm* 4-H), 5.87 (m, 1H, Oph 4-H), 3.63 (m, 1H, THF), 2.09 (s, 9H, TPm* 3,5 Me), 1.97 (s, 9H, 3,5 Me), 1.79 (m, 1H, THF)

Preparation of $Y(OPh^{F5})_3.2THF$. (4.18)

YCl_3 (0.2 g, 0.001 mol) was stirred in THF with gentle heating to aid dissolution, the solution remained turbid. Three equivalents of $KOPh^{F5}$ (0.68 g, 0.0031 mol) in THF was added drop-wise The resulting cloudy mixture was stirred for *ca* 3 hours. A white powder settled out of solution and was removed by filtration. The remaining THF was removed under vacuum and the resulting white solid dried. Yield: 0.53 g (0.0007 mol, 67.9 %).

Analysis (%) calculated for $C_{26}H_{16}O_5F_{15}Y$: C, 39.9; H, 2.05. Found: C, 39.12; H, 2.25.

Preparation of $Sm(OPh^{F5})_3.THF$ (4.19)

$SmCl_3$ (0.2 g, 0.00078 mol) was stirred in THF and heated gently with a water bath. Once dissolved, a solution of $KOPh^{F5}$ (0.52 g, 0.0023 mol) in THF was added drop-wise A very pale yellow turbid solution formed immediately. Stirring was continued for *ca* 2 hours. The yellow solution was separated form the pale white solid by filtration and the solvent was removed under reduced pressure to afford a free flowing yellow powder. Yield: 0.42 g, (0.00054 mol, 70 %).

Analysis (%) calculated for $C_{22}H_8F_{15}Sm$: C, 44.23; H, 1.04. Found: C, 43.55; H, 1.23.

Attempted preparation of $Y(OPh^{F1})_3$ (4.20)

YCl_3 (0.2 g, 0.001 mol) was stirred in THF to form a turbid solution. A solution of $KOPh^{F1}$ (0.46 g, 0.0031 mol) in THF was added drop-wise The resulting cloudy solution was stirred for *ca* 3 hours after which time a fine white solid had settled.

The solid was presumed to be KCl. THF was removed by filtration into a separate Schlenk flask. Filtration was slow and laborious due to the oily nature of the residue. The residue was dried under vacuum.

The solvent in the second flask was removed under reduced pressure to leave a fine white powder. Yield: 0.23 g, (0.00057 mol 55.8 %).

Analysis (%) calculated for $C_{18}H_{12}O_3F_3Y$: C, 51.19 ; H, 2.84; N, 0. Found: C, 44.39; H, 4.26; N, 0.75.

^{1} H NMR (CD_3CN, 400 MHz, 293 K): δ 6.61 (m, Br, 12H, OPh 3,4,5-H), 3.64 (m, 2H, THF), 1.81 (m, 2H, THF)

Attempted preparation of $Sm(OPh^{F1})_3$ (4.21)

$SmCl_3$ (0.1 g, 0.0004 mol) was dissolved in THF with the aid of gentle heating. Three equivalents of $KOPh^{F1}$ (0.18 g, 0.0012 mol) in THF was added drop-wise After *ca* 1 hour the solution became slightly turbid and pale yellow. The precipitate was left to settle and then separated from the solvent by filtration. The remaining THF was removed under reduced pressure to leave a pale yellow powder. Attempts at recrystallization were unsuccessful. Yield: 0.12 g, (0.00025 mol, 63.16 %).

Analysis (%) calculated for $C_{18}H_{12}O_3F_3Sm$: C, 44.69; H, 2.48. Found: C, 42.90; H, 3.36.

^{1}H NMR (CD_3CN, 400 MHz, 293 K): δ 6.85 (s, br, 12H, OPh 2,6,3,5-H), 3.62 (M, 3H, THF), 1.80 (m, 3h, THF)

Attempted preparation of $Y(OPh^{F2})_3$ (4.22)

A solution of $NaOPh^{F2}$ (0.23g 0.0015 mol) in THF was added drop-wise to a

solution of YCl_3 (0.1 g, 0.00051 mol) . After *ca* 3 hours stirring was stopped and the volume of THF reduced under vacuum. The flask was placed in the freezer for cooling. Crystallisation was not successful thus the THF was removed under reduced pressure to leave a white powder. Yield: 0.16 g, (0.00034 mol 67 %).

Analysis (%) calculated for $C_{18}H_9O_3F_6Y$: C, 45.39; H, 1.89. Found: C, 37.41; H, 3.32.

^{1}H NMR (CD_3CN, 400 MHz, 293 K): δ 6.61 (br, 9H, Oph 3,4,5-H), 3.64 (m, 5H, THF), 1.79 (m, 5H, THF)

Attempted preparation of $Sm(OPh^{F2})_3$ (4.23)

$SmCl_3$ (0.1 g 0.00039 mol) was stirred in THF. $NaOPh^{F2}$ (0.18 g, 0.0012 mol) in THF was added drop-wise Attempts at crystallisation by slow cooling were unsuccessful, therefore the THF was removed under reduced pressure to leave a cream powder. Yield: 0.14 g (0.00026 mol, 70 %).

Analysis (%) calculated for $C_{18}H_9O_3F_6Sm$: C, 40.19; H, 1.76. Found: C, 38.14; H, 2.65.

^{1} H NMR (CD_3CN, 400 MHz, 293 K): δ 6.43 (br, 6H, OPh 3,5-H), 6.28 (br, 3H, OPh 4-H), 3.63 (m. 3H, THF), 1.81 (M, 3H, THF)

Attempted preparation of $SmTPm^*(OPh^{F5})_3$ (4.24)

$SmCl_3$ (0.1 g, 0.00039 mol) was stirred in THF. A solution of TPm* (0.12 g, 0.00039 mol) in THF was added drop-wise After *ca* two hours a clear solution of three equivalents of $KOPhF^5$ (0.26 g, 0.00116 mol) was added. KCl precipitated

out of solution and was removed by filtration leaving a clear solution. The volume of solvent was reduced under reduced pressure and the flask placed in the freezer for crystallisation. Attempts at growing crystals were unsuccessful therefore the THF was removed completely and the white solid pumped to dryness. Yield: 0.27 g (0.00027 mol, 69.2 %).

Analysis (%) calculated for $C_{34}H_{22}N_6O_3F_{15}Sm$: C, 42.26; H, 2.28; N, 8.7. Found: C, 43.28; H, 2.62; N, 10.94.

Preparation of YTPm*$(OPh^{F5})_3$ (4.25)

Preparation of YTPm*$(OPh^{F5})_3$ was carried out in the same was as the synthesis of 4.24. The product was isolated as a white powder. Yield: 0.32 g (0.00034 mol, 66.7 %).

Analysis (%) calculated for $C_{34}H_{22}N_6O_3F_{15}Y$: C, 43.59; H, 2.35; N, 8.97. Found: C, 50.07; H, 4.37; N, 14.54.

^{1}H NMR (CD_3CN, 400 MHz, 293 K): δ 8.06 (s, 1H, TPm* C-H), 5.92 (s, 3H, TPm* 4-H), 2.09 (s, 9H, 3,5 Me), 1.98, (s, 9H, 3,5 Me).

Preparation of SmTPm*$(OPh^{F2})_3$ (4.26)

As is the case with similar preparations a solution of SmTPm*Cl_3 was prepared in THF by adding a THF solution of TPm* (0,12 g, 0.00039 mol) drop-wise to and equivalent of $SmCl_3$ in THF resulting in the formation of a slightly turbid solution. Three equivalents of $NaOPh^{F2}$ (0.178 , 0.00117 mol) dissolved in THF were added and the mixture stirred for *ca* 2 hours. KCl was removed by filtration. Crystallisation of the product was unsuccessful, thus the solvent was removed under reduced pressure and taken into the glove box for analysis. Yield: 0.24g (0.00029 mol, 72%).

Analysis (%) calculated for $C_{34}H_{31}N_6O_3F_6Sm$: C, 48.84; H, 3.71; N, 10.06. Found:

C, 47.51; H, 4.01; N, 10.85.

^{1} H NMR (CD_3CN, 400 MHz, 293 K): δ 8.06 (s, 1H, TPm* C-H), 6.85 (br, 6H, OPh 3,5-H), 6.71 (br, 3H, OPh 4-H), 5.92 (s, 3H, TPm* 4-H), 2.089 (s, 9H, 3,5 Me), 1.97 (s, 9H, 3,5 Me).

Preparation of $YTPm^*(OPh^{F2})_3$ (4.27)

The preparation was carried out in an identical fashion to that of $SmTPm^*(OPh^{F2})_3$. Yield: 0.28 g (0.00037 mol, 71.2 %).

Analysis (%) calculated for $C_{34}H_{31}N_6O_3F_6Y$: C, 52.72; H, 4.00; N, 10.85. Found: C, 37.23; H, 3.21, N, 0.10.

Preparation of $SmTPm^*(OPh^{F1})_3$ (4.28)

$SmCl_3$ (0.1 g, 0.00039 mol) was stirred in THF. An equivalent of TPm* (0.12 g, 0.00039 mol) dissolved in THF was added drop-wise to afford a clear solution. Stirring was continued for a further two hours resulting in a slightly more turbid solution. Three equivalents of $KOPh^{F1}$ (0.175 g, 0.00116 mol) in THF was added gradually and the mixture stirred for *ca* 2 hours. The white precipitate of KCl was left to settle and then removed by filtration. The volume of the remaining clear solution was reduced under vacuum and the flask placed inside the freezer for crystallisation. After *ca* 48 hours no crystals had formed, therefore the solvent was removed under vacuum to afford a pale cream solid. Yield: 0.19 g (0.0026 mol, 65.1 %).

Analysis (%) calculated for $C_{34}H_{34}N_6O_3F_3Sm$: C, 52.22; H, 4.35; N, 10.75. Found: C, 43.31; H, 3.35; N, 0.13.

^{1} H NMR (CD_3CN, 400 MHz, 293 K): 8.06 (s, 1H, TPm* C-H), 6.925 (s, br, 8H, OPh 2,6,3,5-H), 2.08 (s, 9H, 3,5 Me), 1.98 (s, 9H, 3,5 Me)

Preparation of YTPm*$(OPh^{F1})_3$ (4.29)

The procedure was identical to that of 4.28. Attempts at crystallisation by slow cooling in the freezer were unsuccessful, thus the THF was removed by reduced pressure to afford a white free flowing powder. Yield: 0.27 g (0.00039 mol, 77.6 %).

Analysis (%) calculated for $C_{34}H_{34}N_6O_3F_3Sm$: C, 56.67; H, 4.72; N, 11.67. Found: C, 58.56; H, 6.12; N, 18.23.

^{1} H NMR (CD_3CN, 400 MHz, 293 K): 8.06 (s, 1H, TPm* C-H), 6.57 (m, 2H, OPh 3,5-H), 6.16 (m, 2H, OPh 2,6-H), 5.92 (s, 3H, TPm* 4-H), 2.09 (s, 9H, 3,5 Me), 1.97 (s, 9H, 3,5 Me).

Chapter 6 References

[1]... The Rare Earths,, F. H. Spedding, A.H. Daane,, , *Wiley, London*, **1961**
[2]... The f elements,, N. Kaltsoyannis, P. Scott,, , *Oxford University Press, Oxford*, **1999**
[*3*]... J.A. Marinsky, L.E. Glendenin, C.D. Coryell, *J. Am. Chem. Soc.*, **69**, 2781, **1947**
[4]... A Comprehensive Treatise on Inorganic and Theoretical Chemistry first ed. vol 7,, J.W. Mellor,44, pp 174, *Longmans Green and Co., London*, **1924**
[*5*]... E.R. Tomkins J.X., Khym W.E. Cohn, *J. Am. Chem. Soc.*, **69**, 2769, **1947**
[*6*]... F.H. Spedding, A.F. Voigt, E. M. Gladrow ,N.R. Sleight, *J. Am. Chem. Soc.*, **69**, 2777, **1947**
[*7*]... D.F. Peppard, J.P. Faris, P.R. Gray, G.W. Mason, *J. Phys. Chem.*, **57**, 294, **1953**
[*8*]... A.J. Freeman, R.E. Watson, *Phys. Rev.*, **127**, 2058, **1962**
[*9*]... R.D. Shannon, *Acta Cryst*, **A32**, 751, **1976**
[*10*]... R.E. Connick, *J. Chem. Soc.*, **235**, Suppl, **1949**
[*11*]... D. S. McCure, Z. Kliss, *J. Chem. Phys.*, **39**, 3251, **1963**
[*12*]... N.B. Mikheev, A.N. Kamenskaya, *Coord. Chem. Rev.*, **109**, 1, **1991**
[*13*]... G. A. Molander, *Chem. Rev.*, **92**, 29, **1992**
[14]... Some Thermodynamic Aspects of Inorganic Chemistry second ed.,, D. A. Johnson,6.8, pp 158., *Cambridge University press, Cambridge*, **1982**
[*15*]... A. Greco, S. Cesca, G. Bertolini, *J. Organomet. Chem.*, **113**, 321, **1976**
[*16*]... M. Wedler, A. Recknagel, F. T. Edelmann, *J. Oragonomet. Chem.*, **395**, C26, **1990**
[*17*]... M. N. Bochkarev, I. L. Fedushkin, A. A. Fagin, T. V. Petrovskaya, J. W. Zillier, R. N. R. Broomhall Dillard, W. Evans, *J. Angew. Chem. (Intl. Ed.) Ehgl.*, **36**, 133, **1997**
[*18*]... M. C. Cassani, M. F. Lappert, F. Laschi., *J. Chem. Soc. Chem. Commun.*, , 1563, **1997**
[*19*]... F. Cloke, *Chem. Soc. Revs*, **22**, 17, **1993**
[*20*]... J. G. Brennan, F. G. N. Cloke, A. A. Sameh, A. Zalkin, *J. Chem. Soc Chem. Commun.*, , 1668, **1987**
[*21*]... D. M. Anderson, F. G. N. Cloke, P. A. Cox, N. Edelstein, J.C. Green, T. Pang, A. A. Sameh, G. Shalimoff, *J. Chem. Soc. Chem. Commun.*, , 53, **1989**
[*22*]... K.N. Raymond, C.W. Eigenbrot. Jr. , *Acc. Chem. Res.* , **13**, 276, **1980**
[*23*]... T. K. Hollis, J. K. Burdett, B. Bosnich, *Organometallics.*, **12**, 3385, **1993**
[*24*]... B. Bosnich, *Chem. Soc. Rev.*, **23**, 387, **1994**
[25]... Chemistry of the elements first ed.,, N.N Greenwood, A. Earnshaw,30, pp 1423, *Pergamon Press, Oxford*, **1986**
[26]... Physical methods for Chemists; 2nd ed,,R. S. Drago,, , *Saunders: Philadelphia*, **1992**
[*27*]... P.L. Watson, G.W. Parshall, *Acc. Chem. Res.*, **18**, 51, **1985**
[*28*]... G. Wilkinson, J. M. Birmingham, *J. Am. Chem. Soc.*, **76**, 6210, **1954**
[*29*]... J. M. Birmingham G. Wilkinson, *J. Am. Chem. Soc*, **78**, 42, **1956**
[*30*]... F.O. Fischer, H. Fischer , *J Organometallic Chem.*, **3**, 181, **1965**

[*31*]... R.E. Maginn, S. Manastyrskyj, M. J. Dubeck, *Am. Chem. Soc.*, **85**, 672, **1963**
[*32*]... T.J. Marks, *Prog. Inorg. Chem.*, **24**, 51, **1978**
[*33*]... D.L. Clark, A.P. Sattelberger, S.G. Bott,R.N. Vrtis, *Inorg. Chem.*, **28**, 1771, **1989**
[*34*]... D.L. Clark, J.G. Watkin, *Inorg. Chem.*, **32**, 1766, **1993**
[*35*]... D.L. Clark, T.M. Frankcom, M.M. Miller, J.G. Watkin, *Inorg. Chem.*, **31**, 1628, **1992**
[*36*]... P.L. Watson, J.F. Whitney, R.L. Harrow, *Inorg. Chem.* , **20**, 3271, **1981**
[*37*]... H. Gornitzka,A. Steiner,D. Stalke,U. Kilimann, F.T. Edelmasnn, K. Jacob, K.H. Thiele, *Organomet. Chem.*, **439**, C6, **1992**
[*38*]... P. Girard, J.L. Namy, H.B. Kagan, *J. Am. Chem. Soc.*, **102**, 2693, **1980**
[*39*]... S. Trofimenko, *J. Am. Chem. Soc.*, **88**, 1842, **1996**
[*40*]... S. Trofimenko, *Chem. Rev*, **93**, 943, **1993**
[*41*]... K. W. Bagnall, A. C. Tempest, J. Takats, A. P. Masino. , *Inorg. Nucl. Chem. Letts.*, **12**, 555, **1976**
[*42*]... I. Santos, N, Marques. , *New J. Chem.* , **19**, 551, **1995**
[*43*]... N. Marques, A. Sella, J. Takats., *Chem. Rev.*, **102**, 2137, **2002**
[*44*]... W. D. Moffat, M. V. R. Stainer, J. Takats. , *Inorg. Chem. Acta*, **139**, 75, **1987**
[*45*]... D. L Reger, J. A. Lindeman, L. Lebioda. , *Inorg, Chim. Acta*, **139**, 71, **1987**
[*46*]... D. L. Reger, J. A. Lindeman, L. Lebioda. , *Inorg. Chem*, **27**, 3923, **1988**
[*47*]... C. D. Sun, W. T. Wong. , *Inorg. Chim. Acta*, **255**, 355, **1997**
[*48*]... M. Onishi, N. Nagaoka, K. Hirald, K. Itch. , *J. Alloys Cmpds.* , **236**, 6, **1996**
[*49*]... W. D. Moffat, M. V. R. Stainer, J. Takats. , *Inorg. Chim. Acta.* , **139**, 75, **1897**
[*50*]... D. L. Reger, S. J. Knox, J. A. Lindeman, L. Lebioda., *Inorg. Chem.* , **29**, 416, **1990**
[*51*]... A. C. Hillier, S. Y. Liu, A. Sella. M. R. J. Elsegood., *Inorg. Chem.*, **39**, 2635, **2000**
[*52*]... D. P. Long, A. Chandrasekaran, R. O. Day, P. A. Bianconi, A. L. Rheingold., *Inorg. Chem.*, **39**, 4475, **2000**
[*53*]... J. A. Blackwell, C. Lehr, Y. Sun, W. E. Piers, S. D. Pearce-Batchilder, M. J. Zaworotko, V. G. J. Young. Can., *J. Chem.*, **75**, 702, **1997**
[*54*]... D. P. Long, P. A. Bianconi., *J. Am. Chem. Soc*, **118**, 12453, **1996**
[*55*]... C. Apostolidis, A. Carvalho, A. Domingos, B. Kanellakopulos, R. Maier, N. Marques, A. F. de Matos, J. Rebizant., *Polyhedron*, **18**, 263, **1998**
[*56*]... J. Takats, X. W. Zhang, V. W. Day, T. A. Eberspacher. , *Organometallics*, **12**, 4286, **1993**
[*57*]... G. H. Maunder, A. Sella, D. A. Tocher , *J. Chem. Soc. Chem Commun.*, , 2689, **1994**
[*58*]... L. Hasinoff, J. Takats, X. W. Xang, P. H. Bond, R. D. Rogers. , *J. Am. Chem. Soc.*, **116**, 8833, **1994**
[59]... G. H. Maunder. ,Ph.D. Thesis, University of London, London, **1996**
[*60*]... J. Takats, *J. Alloys. Cmpds.* , **249**, 52, **1997**
[*61*]... G. M. Ferrence, R. McDonald, J. Takats. Angew. , *Chem. Int. Ed. Eng.*, **38**, 2233, **1999**
[*62*]... S. C. Lawrence, B. D. Ward. S. R. Dubberley, C. M. Kozak, P. Mountford. , *Chem. Commun.*, , 2880, **2003**

[63]... R. D. Kohn, Z. Pan, G. Kociok-Kohn, M. F. Mahon. , *Dalton*, , 2344, **2002**
[64]... W. J. Evans, *Polyhedron*, **6**, 803, **1987**
[65]... S. Hajela, W. P. Schaefer, J. E. Bercaw, *J. Organomet. Chem.*, **532**, 45, **1997**
[66]... C. G. J. Tazelaar, S. Bambirra, D. van Leusen, A. Meetsma, B. Hessen, J. H. Teuben, *Organometallics.* , **23**, 937, **2004**
[67]... S. Bambirra, D. van Leusen, A. Meetsma, B. Hesen, J. H. Teuben, *Chem. Commun.*, , 637, **2001**
[68]... S. C. Lawrence, B. D. Ward, S. R. Dubberley, K. M. Kozack, P. Mountford, *Chem. Commun.*, , 2880, **2003**
[69]... W. Huckel, H. Bretschneider. , *Chem. Ber.*, **9**, 2024, **1937**
[70]... D. L. Reger, T. C. Grattan, *Synthesis*, , 350, **2003**
[71]... W. Klaui, M. Berghahn, G. Rheinwald, H. Lang. Angew., *Chem. Int. Ed*, **39**, 2464, **2000**
[72]... W. Klaui, M. Berghahn, W. Frank. G. J. Reib, T. Sconherr, G. Rheinwald, H. Lang. Eur., *J. Inorg. Chem.*, , 2059, **2003**
[73]... S. Trofimenko, *J. Am. Chem. Soc.*, **92**, 5118, **1970**
[74]... A. Macchioni, G. Bellachioma, G. Cardaci, V. Gramlich, H. Ruegger, S. Terenzi, L. M. Venanzi., *Organometallcs*, , **16**, 2139, **1997**
[75]... D. L. Reger, J. E. Collins, D. L. Jameson, R. K. Castellano, A. J. Canty, H. Jin, *Inorg. Syn.* , **32**, 63, **1998**
[76]... D. L. Reger, J. E. Collins, M. A. Mathews, A. L. Rheingold, L. M. Laible-Sands, L. A. Guzei., *Inorganic Chem*, **36**, 6266, **1997**
[77]... D. L. Reger, J. E. Collins, W. A. Flomer, A. L. Rhiengold, C. Incarvito, L. A. Guzei., *Polyhedron*, **20**, 2491, **2001**
[78]... D. L. Reger, C. A. Little, M. D. Smith. , *Inorg. Chem.*, **41**, 19, **2002**
[79]... S. C. Lawrence, M. E. G. Skinner, J. C. Green, P. Mountford, *Chem. Commun.*, , 705, **2001**
[80]... A. Sanchez-Mendez, G. F. Silvestri, E. de Jesus, F. J. de la Mata, J. C. Flores, R. Gomez, P. Gomez-Sal. , *Eur. J. Inorg. Chem*, , 3287, **2004**
[81]... F. Mani, *Inorg. Chim. Acta.*, **38**, 97, **1980**
[82]... D. V. Fomitchev, C. C. McLauchlan, R. H. Holm, *Inorg. Chem*, **41**, 958, **2002**
[83]... J. Fernandez-Baeza, F. A. Jalon, A. Otera, M. E. Rodrigo-Blanco, *J. Chem. Soc. Dalton. Trans.* , , 1015, **1995**
[84]... S. Trofimenko, *J. Am. Chem. Soc*, **92**, 5118, **1970**
[85]... P. K. Byers, N. Carr, F. G. A. Stone, *J. Chem. Soc. Dalton. Trans.*, , 3701, **1990**
[86]... P. K. Byers, F. G. A. Stone , *J. Chem. Soc. Dalton. Trans.*, , 93, **1991**
[87]... I. K. Dhawan, M. A. Bruck, B. Schilling, C. Grittini, J. H. Enemark, *Inorg. Chem*, **34**, 3801, **1995**
[88]... D. H. Gibson, M. S. Mashuta, H. He, *Acta. Crysatllogr, sect c*, **57**, 1135, **2001**
[89]... S. B. Seymore, S. N. Brown., *Inorg. Chem*, **39**, 325, **2000**
[90]... L. D. Field, B. A. Messerle, L. P. Soler, T. W. Hambley, P. Turner, *J. Organomet. Chem*, **655**, 146, **2002**
[91]... L. D. Field, B. A. Messerle, L. Soler, I. E. Buys, T. W. Hambley, *J. Chem. Soc. Dalton Trans.*, , 1959, **2001**
[92]... A. Llobet, M. E. Curry, H. T. Evans, T. J. Meyer, *Inorg. Chem*, **28**, 3131,

1989
[*93*]... B. Moubaraki, K. S. Murray, E. R. T. Tiekink, Z. Kristallogr., *NCS*, **218**, 349, **2003**
[*94*]... M. Fajardo, A. de la Hoz, E. Diez-Barra, F. A. Jalon, A. Otero, A. Rodriguez, J. Tejeda, D. Belletti, M. Lanfranchi, M. A. Pellinghelli, *J. Chem. Soc. Dalton Trans.*, , 1935, **1993**
[*95*]... S. Bhambri, D. A. Tocher, *Polyhedron*, **15**, 2763, **1996**
[*96*]... S. Bhambri, D. A. Tocher, *J. Chem. Soc, Dalton Trans.*, , 3367, **1997**
[*97*]... S. Bhambri, A. Bishop, N. Kalysoyannis, D. A. Tocher, *J. Chem. Soc. Dalton Trans.*, , 3379, **1998**
[*98*]... D. J. O'Sullivan, F. J. Lalor , *J. Organomet. Chem*, **57**, c58, **1973**
[*99*]... C. K. Ghosh, W. A. G. Graham, *J. Am. Chem. Soc.*, **109**, 4726, **1987**
[*100*]... D.M. Heinekey, W. J. J. Oldham, J. S. Wiley, *J. Am. Chem. Soc.*, **118**, 12842, **1996**
[*101*]... M. A. Esteruelas, L. A. Oro, M. C. Apreda, C. Foces-Foces, F. H. Cano, R. M. Claramunt, C. Lopez, J. Elguero, M. Begtrup, *J. Organomet. Chem.*, **344**, 93, **1988**
[*102*]... C. J. Adams, N. G. Connelly, D. J. H. Emslie, O. D. Hayward, T. Manson, A. GuyOrpen, P. H. Rieger., *J. Chem. Soc. Dalton. Trans.*, , 2835, **2003**
[*103*]... W. Klaui, D. Schramm, W. Peters, *Eur. J. Inorg. Chem.*, , 3113, **2001**
[*104*]... A. J. Canty, N. J. Minchin, L. M. Englehardt, . W. Skelton, A. H. White, *J. Chem. Soc. Dalton Trans.*, , 645, **1986**
[*105*]... T. W. Green, J. A. Krause Bauer, N. L. Coker, W. B. Connick, *Acta. Crystallogr. Sect E*, **59**, m1035, **2003**
[*106*]... P. K. Byers, A. J. Canty, B. W. Skelton, A. H. White., *Organmetallics*, **9**, 826, **1990**
[*107*]... A. J. Canty, N. J. Minchin, J. M. Patrick, A. H. White. , *J. Chem. Soc. Dalton Trans.*, , 1253, **1983**
[*108*]... B. Binotti, G. Bellachioma, G. Cardaci, A. Macchioni, C. Zuccaccia. , *Oragnometallics*, **21**, 346, **2002**
[*109*]... D. L. Reger, J. E. Collins, A. L. Rheingold, L. M. Liable-Sands. , *Organometallics*, **15**, 2029, **1996**
[*110*]... M. CvetKovic, S. R. Batten, B. Moubaraki, K. S. Murray, L. Spiccia, *Inorg. Cim. Acta*, **324**, 131, **2001**
[*111*]... M. A. Mesubi, F. O. Anumba, *Transition Met. Chem.*, **10**, 5, **1985**
[*112*]... A. Cingolani Effendy, D. Martini, M. Pellei, C. Pettinari, B. W. Skelton, A. H. White, *Inorg. Chin. Acta*, **328**, 87, **2002**
[*113*]... D.L Reger, J. E. Collins, A. L. Rheingold, L. M. Liable-Sands, G. P. A. Yap, *Organometallics*, **16**, 349, **1997**
[*114*]... A. J. Canty, N. J. Minchin, P. C. Healey, A. H. White., *J. Chem. Soc. Dalton Trans.*, , 1795, **1982**
[*115*]... A. Looney, G. Parkin, *Polyhedron*, **9**, 265, **1990**
[*116*]... D. L. Reger, J. E. Collins, R. Layland, R. D. Adams, *Inorg. Chem*, **35**, 1372, **1996**
[*117*]... C. Pettinari, M. Pellei, A. Cingolani, D. Martini, A. Drozdov, S. Troyanov, W. Panzeri, A. Mele., *Inorg. Chem.*, **38**, 5777, **1999**
[*118*]... C. S. Tredget, S. C. Lawrence, B. D. Ward, R. G. Howe, A. R. Cowley, P. Mountford , *Organometallics* , **24**, 3136, **2005**
[*119*]... W. Huckel, H. Bretshneider. , *Chem. Ber.* , **9**, 2024, **1937**

[*120*]... E. R. Humphrey, K. L. V. Mann, Z. R. Reeves, A. Behrendt, J. C. Jeffrey, J. P. Maher, J. A. McCleverty, M. D. Ward. , *New J. Chem.*, **23**, 417, **1999**
[*121*]... C. Titze, J. Hermann, H. Vahrenkamp. , *Chem. Ber.*, **128**, 1095, **1995**
[*122*]... F. de Angelis, A. Gambarcorta,m R. Nicoletti. , *Org. Synth.*, , 798, **1976**
[*123*]... S. Julia, J. M. Del Mazo, L. Avila, J. Elguero, *Org. Prep. Proced. Int.*, **16**, 299, **1984**
[*124*]... D. L. Reger, T. C. Grattan, K. J. Brown, C. A. Little, J. J. S. Lamba, A. L. Rheingold, R. D. Sommer, *J. Organomet Chem.* , **607**, 120, **2000**
[*125*]... H. R. Bigmore, S. C. Lawrence, P. Mountford, C. S. Tredget, *Dalton Trans.*, , 635, **2005**
[*126*]... S. J. Chen, Y. Z. Li, X. T. Chen, Y. J. Shi, X. Z. You. , *Acta Crystallogr., sect. E* , **E58**, m753, **2002**
[127]...G. H Maunder,Ph.D. Thesis, University Of London, London, **1996**
[*128*]... D. P. Long, A. Chandrasekaran, R. O. Day, P. A. Bianconi, A. L. Rheingold, *Inorg. Chem.*, **39**, 4476, **2000**
[*129*]... J. Cheng, R. McDonald, J. Takats, *Unpublished results*, , ,
[*130*]... A. C. Hillier, X. W. Zhang, G. H. Maunder, S. Y. Liu, T. A. Eberspacher, M. V. Metz, R. McDonald, A. Domingos, N. Marques, V. W. Day, A. Sella, J. Takats. , *J. Inorg. Chem.*, **40**, 5106, **2001**
[*131*]... G. Y. Lin, G. C. Wei, Z. S. Zin, W. Q. Chen. , *Jiegou Huaxue.*, **11**, 200, **1992**
[*132*]... A. C. Hilliar, A. Sella, M. R. J. Elsegood. , *J. Chem. Soc., Dalton. Trans.*, , 3871, **1998**
[*133*]... M. E. M. Hamidi, J. L. Pascal. , *Polyhedron* , **13**, 1787, **1994**
[*134*]... G. A. Lawrence. , *Chem. Rev.*, **86**, 17, **1986**
[*135*]... H. Schumann, J. A. Meese-Marktscheffel, A. Dietrich, *J. Organomet. Chem*, **377**, C5, **1989**
[*136*]... J. Stehr, R. D. Fischer, *J. Organomet. Chem.*, **430**, C1-C4, **1992**
[*137*]... S. Y. Liu, G. H. Maunder, A. Sella, M. Stevenson, D. A. Tocher, *Inorg. Chem.*, **35**, 76, **1996**
[*138*]... S. Amin, C. Marks, L. M. Toomey, M. R. Churchill, J. R. Morrow., *Inorg. Chim. Acta.* , **246**, 99, **1996**
[139]...A.C. Hiller,Ph.D. Thesis, University College London, London, **1998**
[140]...Basic One and Two dimensional NMR spectroscopy. 2nd ed.,, Horst Friebolin. ,, , *VCH Verlagsgesellschaft, Weinheim (Federal Republic of Germany)*, **1993**
[*141*]... L. F. Zhang, Z. Q. Shen, C. P. Yu, L. Fan, *Polym. Int.*, **53**, 1013, **2004**
[*142*]... L. F. Zhang, Z. Q. Shen, C. P. Yu, L. Fan., *J. Macromol. Sci. Chem.*, **A41**, 927, **2004**
[*143*]... W. J. Evans, J. M. Olofson, J. W. Ziller. , *Inorg. Chem.*, **28**, 4308, **1989**
[*144*]... D. M. Barnhart, D. L. Clark, J. C. Huffman, R. L. Vincent, J. G. Watkin, B. D. Zwick. , *Inorg. Chem.*, **33**, 4387, **1994**
[*145*]... D. L. Clark, J. C. Gordon, J. G. Watkin, J. G. Huffman, B. D. Zwick. , *Polyhedron.*, **15**, 2279, **1996**
[*146*]... G. B. Deacon, T. Feng, C. M. Forsyth, A. Gitlits, D. C. R. Hockless, Q. Shen, B. W. Skelton, A. H. White, *J. Chem. Soc. Dalton Trans.*, , 961, **2000**
[*147*]... A. C. Hillier, S. Y. Liu, A. Sella, M. R. Elsegood. , *J. Inorg. Chem.* , **39**, 2635, **2000**
[*148*]... W. J. Evans, R. E. Golden, J. W. Ziller. , *Inorg. Chem.*, **32**, 3041, **1993**

[*149*]... K. G. Caulton, L. G. Hubert-Pfalgraf, *Chem. Rev.*, **90**, 969, **1990**
[*150*]... M. Ephritikhine. , *Chem. Rev.* , **97**, 2193, **1997**
[*151*]... T. J. Marks, J. R. Kolb. , *Chem . Rev.* , **77**, 263, **1977**
[*152*]... E. B. Lobkovsky, Y. K. Gun'ko, B. M. Bulychev, G. L. Soloveichik, M. Y. Antipin. , *J. Organomet. Chem.* , **406**, 343, **1991**
[*153*]... Y. K. Gun'Ko, B. M. Bulychev, G. L. Soloveichik, V. K. Belsky. , *J. Organomet. Chem.* , **424**, 289, **1992**
[*154*]... T. J. Marks, G. W. GrynKewich, *Inorg. Chem.* , **15**, 1302, **1976**
[*155*]... U. Mirsaidov, T. G. Rotenberg, T. N. Dymova. , *Chem. Abstr.*, **85**, 136374, **1976**
[*156*]... I. Albrecht,E. Hahn, J. Pickardt, H. Schumann, *Inorg. Chim. Acta.*, **110**, 145, **1985**
[*157*]... D. L. Reger. , *Comments. Inorg. Chem.* , **21**, 1-28, **1999**
[*158*]... M. C. Kuchta, H. V. R. Dias, S. G. Bott, G. Parkin. , *Inorg. Chem.*, **35**, 943, **1996**
[*159*]... C. M. Dowling, D. Leslie, M. H. Chisholm, G. Parkin , *Main Group Met. Chem.* , **1**, 29, **1995**
[*160*]... R. G. Hayes, J. L. Thomas., *Inorg. Chem.*, **8**, 2521, **1969**
[*161*]... R. A. Williams, T. P. Hanusa, J. C. Huffman, *Chem . Commun.*, , 1045, **1988**
[*162*]... W. J. Evans, L. A. Hughes, T. P. Hanusa. , *J. Am. Chem. Soc.* , **106**, 4720, **1984**
[*163*]... G. B. Deacon, A. J. Koplick, T. D. Tuong. Aust. , *J. Chem.*, **35**, 941, **1982**
[*164*]... G. B. Deacon, A. J. Koplick, *J. Organomet. Chem.* , **146**, C3, **1976**
[*165*]... W. J. Evans, S. C. Engerer, K. M. Coleson, *J. Am. Chem. Soc.*, **103**, 6672, **1981**
[*166*]... W. J. Evans, *Polyhedron.*, **6**, 803, **1987**
[*167*]... W. J. Evans, D. K. Drummond, *J. Am . Chem. Soc.*, **111**, 3329, **1989**
[*168*]... W. B. Evans, J. W. Grate, K. R. Levan, I. Bloom, T. T.Peterson, R. J. Doedens, J. L. Atwood, *Inorg. Chem.*, **25**, 3614, **1986**
[*169*]... G. B. Deacon, G. D. Fallon, P. I. MacKinnon, R. H. Newnham, G. N. Pain, T. D. Tuong, D. L. Wilkinson, *J. Organomet. Chem.*, **277**, C21, **1984**
[*170*]... W. B. Evans, I. Bloom, J. W. Grate, W. E. Hunter, J. L. Atwood, *J. Am. Chem. Soc.*, **107**, 405, **1985**
[*171*]... D. J. Berg, C. J. Burns, R. A. Anderson, A. Zalkin, *Organometallics*, **8**, 1865, **1989**
[*172*]... G. H. Maunder, A. Sella, D. A. Tocher, *J. Chem. Soc. Chem. Commun.*, , 2689, **1994**
[173]...A.C. Hiller,*Ph.D. Thesis*, University College London, London, **1998**
[174]...G. H Maunder,*Ph.D. Thesis*, University of London, London, **1996**
[*175*]... D.C. Bradley, R.C. Mehrotra, I.P. Rothwell, A. Singh, *Alkoxo and Aryloxo Derivatives of Metals*, , , **2001**
[*176*]... D.C. Bradley, *Chem Rev.*, **1317**, , **1989**
[*177*]... D.C. Bradley, R.C. Mehrotra, D.P. Gaur, *Metal Alkoxides*, , , **1978**
[*178*]... P.J. Wheatley, *J. Chem. Soc.*, **4270**, , **1960**
[*179*]... H.D. Lutz, *Z. Anorg. Allg. Chem.* , **353**, 207, **1967**
[*180*]... K.M. Fromm, E.D. Gueneau, *Polyhedron*, **23**, 1479, **2004**
[*181*]... T.Greiser, E. Weiss, *Chem Ber*, **110**, 3388, **1997**
[*182*]... E. Weiss, H. Alsdorf, H. Kuhr, H.F Grutzmacher, *Chem. Ber.* , **101**, 3777,

1968
[*183*]... D.E. Pearson, C.A. Buehler, *Chem Rev.*, **74**, 45, **1974**
[*184*]... W.J. Evans, R.E. Golden, J.W. Zillier, *Inorg chem*, **32**, 3041, **1993**
[*185*]... J.I. Amor, N.C.Burton, T. Cuenca, P. Gomez-al, P. Royo, *J. Organometalli Chem.*, **485**, 153, **1995**
[*186*]... P. Murray-Rust, W .C. Stallings, C. T. Monti, R. K. Preston, J. Glusker. , *J Am Chem Soc.* , **105**, 3206, **1983**
[*187*]... Plenio, H., *Chem rev*, **97**, 3363, **1997**
[*188*]... J.A. Samuels, E.B. Lobkovsky, W.E. Streib, K. Folting, J.C. Huffman, J.W. Zwanziger, K.G. Caulton, *J. Am. Chem. Soc.* , **115**, 5093, **1993**
[*189*]... D.C. Bradley, H. Chudzynska, M.B. Hursthouse, M. Motevalli, R. Wu., *Polyhedron*, **13**, 1, **1994**
[*190*]... F. Labrize, L.G. Hubert-Pfalzgraf, *Polyhedron*, **14,7**, 881, **1995**
[*191*]... S. Daniele, L.G. Hubert-Pfalzgraf, M. Perrin, *Polyhdron*, **21**, 1985, **2002**
[*192*]... J.L. Jolas, S. Hoppe, K.H. Whitmere. , *Inorg Chem.* , **36**, 3335, **1997**
[*193*]... Y. Sun, M.V. Metz, C. L. Stern, T.J. Marks., *Organometallics*, **19**, 1625, **2000**
[*194*]... J. A.Samuels, E. B. Lobkovsky, W. E. Strieb, K. Folting, J. C. Huffman, J. W. Zwanziger, K. G. Caulton, *J. Am. Chem. Soc.*, **115**, 5093, **1993**
[*195*]... S. Brooker, F. T. Edelmann, T. Kottke, H. W. Roesky, G. M. Sheldrick, D. Stalke, K. H. Whitmere., *J. Chem. Soc, Chem Commun.* , , 144, **1991**
[*196*]... H Friebolin., *Basic one and two dimensional NMR spectroscopy. 2nd ed.*, , pp 109,
[*197*]... R. Signer., *Annalen*, **478**, 246, **1930**
[*198*]... A. L. Wayda, M. Y. Darensbourg Eds., *Experimental Organometallic Chemistry: A practicum in Synthesis and Characterisation.*, **vol 357**, , **1987**
[*199*]... M. H. Chisholm, S. R. Drake, A. A. Naiini, W. E. Streib., *Polyhedron*, **10**, 337, **1991**
[*200*]... R. D. Shannon , *Acta. Cryst, sect. B*, **26**, 1046, **1976**
[*201*]... C. J. Pederson. , *J. Am. Chem. Soc.* , **89**, 7017, **1967**
[*202*]... H. V. R. Dias, W. Jin, H. J. Kim, H. L. Lu, *Inorg. Chem.*, **35**, 2317, **1996**
[*203*]... J. Filippo, R. G. Nuzzo, L. J. Romano. , *J. Am. Chem. Soc.*, **97**, 2546, **1975**
[*204*]... D. C. Bradley, H. Chuzynska, M. E. Hammond, M. B. Hursthouse, M. Montevalli, W. Ruowen, *Polyhedron*, **11**, 375, **1992**
[*205*]... J. H. Melman, C. Rohde, T. J. Emge, J. C. Brennan, *Inorg. Chem.*, **41**, 28, **2002**
[206]...Area detector control and data integration and reduction software,,,, , *Brüker AXS Inc. Madison WI, USA*, **2001**
[*207*]...G. M. Sheldrick, University of Gottingen, Gottingen, Germany,**1997**
[208]...SHELXTL PLUS,,,, , *Brüker AXS Inc. Madison WI, USA*, **2001**
[209]...Collect,,Nonius B. V.,, , *Delft, The Netherlands*, **1998**
[210]...,vol. 276,Z. Otwinowski, W. Minor. (C. W. Carter, R. M. Sweet, Eds.),, 307, *Academic Press: New York*, **1997**
[*211*]...L. J. Barbour., *J. Supramol. Chem.*, **1**, 189, **2001**
[212]...In Methods in Enzymology,,Sheldrick, G. M.,, , *Brüker AXS Inc. Madison WI, USA*, **2001**

Chapter 7 Appendix

Chapter 8 Crystal data Chapter 2

Selected structural parameters for Complexes (2.1),(2.2)(2.6)(2.7)(2.13)(2.12)

	(2.1)	(2.2)	(2.6)	(2.7)	(2.13)	(2.12)
Formula	$C_{36}H_{52}Cl_3N_4Y$	$C_{31}H_{48}Cl_3N_4O_2Sm$	$C_{53}H_{68}F_8N_4O_{10}S_2Y$	$C_{57}H_{68}FeHoN_4O_{12}S_2$	$C_{32}H_{54}N_4NdO_6$	$C_{32}H_{54}N_4O_6Sm$
Formula wieglu (g mol^{-1})	575.76	699.30	1122.93	1126.85	1022.40	1028.51
a=(Å)	9.5040(6)	10.5541(16)	28.698(3)	29.2750(2)	12.5317(11)	12.4975(8)
b=(Å)	16.3094(10)	13.335(2)	19.426(2)	19.6570(10)	16.2143(14)	16.2324(10)
c= (Å)	17.1537(6)	21.004(3)	19.807(2)	19.8299(15)	16.3503(14)	16.3598(10)
α	90	90	90	90	60.7790(10)	60.6900(10)
β	94.378(3)	90	97.185(2)	95.481(3)	77.2050(10)	77.2960(10)
γ	90	90	90	90	82.5080(10)	82.4930(10)
Volume (Å^3)	2651.1(3)	2956.0(8)	10955(2)	11359.1(10)	2826.5(4)	2822.1(3)
Z	4	4	8	8	2	2
Crystal system	monoclinic	orthorhombic	monoclinic	monoclinic	triclinic	triclinic
Space group	$P2_1ln$	$P2_12_12_1$	$C2/c$	$C2/c$	$P\bar{1}$	$P\bar{1}$
Temperature (K)	100(2)	150(2)	293(2)	120(2)	150(2)	150(2)
Wavelength (Å)	0.71073	0.71073	0.71073	0.71073	0.71073	0.71073
ρ_{calcd} (g cm^{-3})	1.443	1.571	1.362	1.318	1.201	1.210
μ (mm^{-1})	2.525	2.289	1.266	1.581	0.966	1.088
Independent reflns	6006 (R_{int}=0.1140)	7102(R_{int}=0.0252)	12804(R_{int}=0.0608)	7478(R_{int}=0.0793)	12977(R_{int}=0.0224)	12821(R_{int}=0.0175)
no.of parameters	298	325	605	616	587	587
R1[a]	0.0614	0.0308	0.0881	0.0733	0.0502	0.0414
wR_2[b]	0.1442	0.0760	0.2502	0.1798	0.1447	0.1266

Selected Average Bond Distances (Ang) and Angles(o) for Complexes (2.1),(2.2) (2.6)(2.7)(2.13)(2.12)

Complex	(2.1)	(2.2)	(2.6)	(2.7)	(2.13)	(2.12)
Ln-N_{av}/Å	2.459(5)	2.572(5)	2.4498	2.4616	2.5995	2.5655
Ln-X_{av}/Å	2.555(2)	2.621(2)	2.2437	2.258(12)	2.2075	2.1803
Ln-O_{ax}/Å		2.486(3)	2.3914	2.3916		
∠(X-Ln-X)$_{av}$	100.35(5)	115.296	114.93	114.85	107.32	107.32
∠(N-Ln-N)$_{av}$	73.8(2)	70.42	73.43	73.13	68.22	69.21
∠(X-Ln-O_ax)$_{av}$		77.33	77.03	76.93		
∠(C_{Tpm}-Ln-X)$_{av}$	117.5(2)	102.73	103.43	103.524	111.62	111.82

Chapter 9 Crystal Data Chapter 4

KOPh5.THF (4.3)

Table 1. Crystal data and structure refinement for STR0046.

Identification code	str0046
Chemical formula	C56H64F20K4O12
Formula weight	1465.47
Temperature	150(2) K
Radiation, wavelength	MoKα, 0.71073 Å
Crystal system, space group	monoclinic, C2/c
Unit cell parameters	a = 23.884(3) Å α = 90°
	b = 12.4599(16) Å β = 97.188(2)°
	c = 22.472(3) Å γ = 90°
Cell volume	6634.8(15) Å3
Z	4
Calculated density	1.467 g/cm3
Absorption coefficient μ	0.380 mm-1
F(000)	3008
Crystal colour and size	colourless, 0.48 × 0.45 × 0.12 mm3
Data collection method	Bruker SMART APEX diffractometer
	ω rotation with narrow frames
θ range for data collection	1.72 to 28.28°
Index ranges	h -30 to 29, k -16 to 16, l -28 to 29
Completeness to θ = 26.00°	99.8 %
Reflections collected	28356
Independent reflections	7879 (Rint = 0.0377)
Reflections with F2>2σ	4692
Absorption correction	semi-empirical from equivalents
Min. and max. transmission	0.8386 and 0.9558
Structure solution	direct methods
Refinement method	Full-matrix least-squares on F2
Weighting parameters a, b	0.1769, 18.9036
Data / restraints / parameters	7879 / 0 / 415
Final R indices [F2>2σ]	R1 = 0.0785, wR2 = 0.2187
R indices (all data)	R1 = 0.1277, wR2 = 0.2724
Goodness-of-fit on F2	0.837
Largest and mean shift/su	0.000 and 0.000
Largest diff. peak and hole	0.591 and -0.249 e Å3

Table 2. Atomic coordinates and equivalent isotropic displacement parameters (Å2) for STR0046. Ueq is defined as one third of the trace of the orthogonalized Uij tensor.

	x	y	z	Ueq
K(1)	0.04156(4)	0.27341(8)	0.17757(4)	0.0584(3)
K(2)	0.07639(4)	0.05636(8)	0.30219(5)	0.0607(3)
O(1)	0.0330(2)	0.4815(3)	0.1436(2)	0.1020(14)
O(2)	0.11827(14)	0.2537(4)	0.09969(16)	0.0869(11)
O(3)	0.18340(15)	0.0764(4)	0.35662(18)	0.1012(14)
O(4)	0.1050(2)	0.1566(4)	0.3066(2)	0.1191(17)
O(5)	-0.03323(12)	0.0593(3)	0.31414(14)	0.0631(8)
O(6)	-0.06621(12)	0.2699(3)	0.20326(14)	0.0632(8)
F(1)	-0.14764(10)	0.0297(2)	0.30236(12)	0.0750(8)
F(2)	-0.19516(12)	-0.0885(3)	0.38372(15)	0.0950(10)
F(3)	-0.13091(15)	-0.1793(3)	0.47829(15)	0.0952(10)
F(4)	-0.01715(14)	-0.1451(3)	0.49281(12)	0.0855(9)
F(5)	0.03160(10)	-0.0294(2)	0.41212(13)	0.0777(8)
F(6)	-0.14737(11)	0.3775(3)	0.25664(11)	0.0798(8)
F(7)	-0.21674(12)	0.5182(3)	0.19392(14)	0.0862(9)
F(8)	-0.20881(15)	0.5553(3)	0.07564(15)	0.0960(10)
F(9)	-0.12966(14)	0.4494(3)	0.02208(12)	0.0967(10)
F(10)	-0.05955(11)	0.3076(3)	0.08394(11)	0.0796(8)
C(1)	-0.0001(3)	0.5662(4)	0.1615(2)	0.0779(14)
C(2)	-0.0097(4)	0.6403(6)	0.1079(3)	0.110(2)
C(3)	0.0363(5)	0.6155(7)	0.0756(4)	0.159(4)
C(4)	0.0565(4)	0.5126(7)	0.0912(4)	0.135(3)
C(5)	0.1765(2)	0.2667(6)	0.1132(2)	0.0874(17)

C(6)	0.2000(3)	0.2753(7)	0.0575(3)	0.103(2)
C(7)	0.1628(3)	0.2070(8)	0.0174(3)	0.124(3)
C(8)	0.1074(3)	0.2145(6)	0.0395(3)	0.0969(19)
C(9)	0.2311(3)	0.1169(7)	0.3323(4)	0.116(2)
C(10)	0.2741(4)	0.1284(10)	0.3877(6)	0.179(5)
C(11)	0.2387(5)	0.1443(12)	0.4351(5)	0.194(6)
C(12)	0.1899(4)	0.0882(9)	0.4172(3)	0.145(3)
C(13)	0.0854(3)	0.2243(5)	0.2592(3)	0.0948(18)
C(14)	0.1360(3)	0.2704(6)	0.2362(3)	0.111(2)
C(15)	0.1847(3)	0.2241(7)	0.2748(4)	0.128(3)
C(16)	0.1615(4)	0.1930(7)	0.3287(4)	0.153(4)
C(17)	0.05581(16)		0.0048(3)	0.35375(18) 0.0510(9)
C(18)	0.11450(16)		0.0135(4)	0.34950(19) 0.0556(10)
C(19)	0.13871(18)		0.0723(4)	0.3904(2) 0.0630(11)
C(20)	0.1068(2)	0.1174(4)	0.4385(2)	0.0653(11)
C(21)	0.0497(2)	0.1016(4)	0.44513(19)	0.0592(10)
C(22)	0.02522(16)		0.0425(3)	0.40422(19) 0.0536(9)
C(23)	0.10054(15)		0.3358(3)	0.17304(17) 0.0475(8)
C(24)	0.14259(16)		0.3937(3)	0.19765(17) 0.0519(9)
C(25)	0.17795(17)		0.4657(4)	0.1665(2) 0.0576(10)
C(26)	0.17417(19)		0.4840(4)	0.1070(2) 0.0623(11)
C(27)	0.13411(19)		0.4297(4)	0.08037(18) 0.0612(11)
C(28)	0.09908(16)		0.3588(3)	0.11196(17) 0.0521(9)

Table 3. Bond lengths [Å] and angles [°] for STR0046.

K(1)-O(6A)	2.669(3)	K(1)-O(5A)	2.683(3)
K(1)-O(2)	2.698(3)	K(1)-O(1)	2.703(4)
K(1)-O(6)	2.708(3)	K(1)-F(10)	3.028(3)
K(1)-F(6A)	3.053(3)	K(1)-C(17A)	3.446(4)
K(1)-C(23)	3.471(4)	K(1)-K(2)	3.9071(14)
K(1)-K(2A)	3.9723(14)	K(1)-K(1A)	4.0196(17)
K(2)-O(5)	2.665(3)	K(2)-O(6A)	2.673(3)
K(2)-O(5A)	2.688(3)	K(2)-O(3)	2.703(4)
K(2)-O(4)	2.738(5)	K(2)-F(5)	3.009(3)
K(2)-F(1A)	3.086(3)	K(2)-C(12)	3.526(8)
K(2)-C(17A)	3.536(4)	K(2)-K(1A)	3.9722(13)
K(2)-K(2A)	4.0835(18)	O(1)-C(1)	1.408(7)
O(1)-C(4)	1.419(7)	O(2)-C(5)	1.396(6)
O(2)-C(8)	1.431(7)	O(3)-C(12)	1.359(8)
O(3)-C(9)	1.417(8)	O(4)-C(13)	1.393(8)
O(4)-C(16)	1.452(10)	O(5)-C(17)	1.290(5)
O(5)-K(1A)	2.683(3)	O(5)-K(2A)	2.688(3)
O(6)-C(23)	1.292(5)	O(6)-K(1A)	2.669(3)
O(6)-K(2A)	2.673(3)	F(1)-C(18)	1.352(5)
F(1)-K(2A)	3.086(3)	F(2)-C(19)	1.353(5)
F(3)-C(20)	1.362(5)	F(4)-C(21)	1.356(5)
F(5)-C(22)	1.356(5)	F(6)-C(24)	1.360(4)
F(6)-K(1A)	3.053(3)	F(7)-C(25)	1.346(5)
F(8)-C(26)	1.351(5)	F(9)-C(27)	1.350(5)
F(10)-C(28)	1.358(5)	C(1)-C(2)	1.511(8)
C(2)-C(3)	1.423(10)	C(3)-C(4)	1.399(10)
C(5)-C(6)	1.438(8)	C(6)-C(7)	1.458(10)
C(7)-C(8)	1.472(9)	C(9)-C(10)	1.518(12)
C(10)-C(11)	1.454(14)	C(11)-C(12)	1.375(13)
C(13)-C(14)	1.488(10)	C(14)-C(15)	1.478(10)
C(15)-C(16)	1.447(12)	C(17)-C(22)	1.400(6)
C(17)-C(18)	1.412(5)	C(17)-K(1A)	3.446(4)
C(17)-K(2A)	3.536(4)	C(18)-C(19)	1.360(6)
C(19)-C(20)	1.363(7)	C(20)-C(21)	1.367(7)
C(21)-C(22)	1.365(6)	C(23)-C(28)	1.407(5)
C(23)-C(24)	1.405(5)	C(24)-C(25)	1.364(6)
C(25)-C(26)	1.369(6)	C(26)-C(27)	1.369(7)
C(27)-C(28)	1.355(6)		

O(6A)-K(1)-O(5A)	85.59(10)	O(6A)-K(1)-O(2)	124.52(11)
O(5A)-K(1)-O(2)	90.97(12)	O(6A)-K(1)-O(1)	107.37(13)
O(5A)-K(1)-O(1)	165.81(13)	O(2)-K(1)-O(1)	86.40(13)
O(6A)-K(1)-O(6)	83.22(10)	O(5A)-K(1)-O(6)	83.59(9)
O(2)-K(1)-O(6)	151.33(11)	O(1)-K(1)-O(6)	92.05(12)
O(6A)-K(1)-F(10)	139.11(8)	O(5A)-K(1)-F(10)	97.38(9)
O(2)-K(1)-F(10)	96.28(10)	O(1)-K(1)-F(10)	69.11(13)
O(6)-K(1)-F(10)	56.88(8)	O(6A)-K(1)-F(6A)	57.03(8)
O(5A)-K(1)-F(6A)	116.93(10)	O(2)-K(1)-F(6A)	76.39(9)
O(1)-K(1)-F(6A)	75.99(13)	O(6)-K(1)-F(6A)	130.92(9)

F(10)-K(1)-F(6A)	144.75(10)	O(6A)-K(1)-C(17A)	100.02(10)
O(5A)-K(1)-C(17A)	19.71(9)	O(2)-K(1)-C(17A)	71.75(12)
O(1)-K(1)-C(17A)	151.61(12)	O(6)-K(1)-C(17A)	98.55(10)
F(10)-K(1)-C(17A)	94.89(9)	F(6A)-K(1)-C(17A)	114.50(10)
O(6A)-K(1)-C(23)	97.19(9)	O(5A)-K(1)-C(23)	98.27(9)
O(2)-K(1)-C(23)	137.91(11)	O(1)-K(1)-C(23)	74.82(12)
O(6)-K(1)-C(23)	19.57(9)	F(10)-K(1)-C(23)	41.94(8)
F(6A)-K(1)-C(23)	131.78(9)	C(17A)-K(1)-C(23)	109.43(9)
O(6A)-K(1)-K(2)	43.04(7)	O(5A)-K(1)-K(2)	43.37(7)
O(2)-K(1)-K(2)	107.51(10)	O(1)-K(1)-K(2)	150.24(11)
O(6)-K(1)-K(2)	87.64(7)	F(10)-K(1)-K(2)	132.47(7)
F(6A)-K(1)-K(2)	81.83(6)	C(17A)-K(1)-K(2)	57.07(7)
C(23)-K(1)-K(2)	107.20(7)	O(6A)-K(1)-K(2A)	86.82(7)
O(5A)-K(1)-K(2A)	41.87(6)	O(2)-K(1)-K(2A)	124.13(10)
O(1)-K(1)-K(2A)	130.99(11)	O(6)-K(1)-K(2A)	42.09(7)
F(10)-K(1)-K(2A)	70.12(7)	F(6A)-K(1)-K(2A)	142.17(6)
C(17A)-K(1)-K(2A)	56.75(7)	C(23)-K(1)-K(2A)	56.69(7)
K(2)-K(1)-K(2A)	62.42(3)	O(6A)-K(1)-K(1A)	41.99(7)
O(5A)-K(1)-K(1A)	83.99(7)	O(2)-K(1)-K(1A)	165.80(9)
O(1)-K(1)-K(1A)	101.62(9)	O(6)-K(1)-K(1A)	41.26(7)
F(10)-K(1)-K(1A)	97.52(6)	F(6A)-K(1)-K(1A)	94.05(5)
C(17A)-K(1)-K(1A)	103.70(7)	C(23)-K(1)-K(1A)	56.18(6)
K(2)-K(1)-K(1A)	60.13(2)	K(2A)-K(1)-K(1A)	58.53(2)
O(5)-K(2)-O(6A)	84.60(9)	O(5)-K(2)-O(5A)	80.55(10)
O(6A)-K(2)-O(5A)	85.41(10)	O(5)-K(2)-O(3)	146.94(12)
O(6A)-K(2)-O(3)	90.24(13)	O(5A)-K(2)-O(3)	131.66(11)
O(5)-K(2)-O(4)	104.68(15)	O(6A)-K(2)-O(4)	170.71(15)
O(5A)-K(2)-O(4)	96.43(12)	O(3)-K(2)-O(4)	81.72(16)
O(5)-K(2)-F(5)	57.83(8)	O(6A)-K(2)-F(5)	110.59(9)
O(5A)-K(2)-F(5)	132.15(9)	O(3)-K(2)-F(5)	94.27(11)
O(4)-K(2)-F(5)	74.86(13)	O(5)-K(2)-F(1A)	136.08(9)
O(6A)-K(2)-F(1A)	97.35(9)	O(5A)-K(2)-F(1A)	56.09(8)
O(3)-K(2)-F(1A)	76.95(10)	O(4)-K(2)-F(1A)	76.38(14)
F(5)-K(2)-F(1A)	150.85(9)	O(5)-K(2)-C(12)	126.82(16)
O(6A)-K(2)-C(12)	88.8(2)	O(5A)-K(2)-C(12)	151.35(16)
O(3)-K(2)-C(12)	20.17(16)	O(4)-K(2)-C(12)	85.3(2)
F(5)-K(2)-C(12)	75.99(16)	F(1A)-K(2)-C(12)	97.09(15)
O(5)-K(2)-C(17A)	94.93(9)	O(6A)-K(2)-C(17A)	97.75(10)
O(5A)-K(2)-C(17A)	18.15(8)	O(3)-K(2)-C(17A)	118.13(11)
O(4)-K(2)-C(17A)	82.11(12)	F(5)-K(2)-C(17A)	136.85(9)
F(1A)-K(2)-C(17A)	41.20(8)	C(12)-K(2)-C(17A)	138.22(15)
O(5)-K(2)-K(1)	86.49(7)	O(6A)-K(2)-K(1)	42.96(7)
O(5A)-K(2)-K(1)	43.27(7)	O(3)-K(2)-K(1)	111.39(11)
O(4)-K(2)-K(1)	136.57(11)	F(5)-K(2)-K(1)	140.25(6)
F(1A)-K(2)-K(1)	67.49(6)	C(12)-K(2)-K(1)	121.51(19)
C(17A)-K(2)-K(1)	54.88(7)	O(5)-K(2)-K(1A)	42.20(7)
O(6A)-K(2)-K(1A)	42.76(6)	O(5A)-K(2)-K(1A)	84.88(7)
O(3)-K(2)-K(1A)	121.95(10)	O(4)-K(2)-K(1A)	146.38(13)
F(5)-K(2)-K(1A)	79.50(6)	F(1A)-K(2)-K(1A)	128.82(7)
C(12)-K(2)-K(1A)	109.31(17)	C(17A)-K(2)-K(1A)	102.98(7)
K(1)-K(2)-K(1A)	61.34(3)	O(5)-K(2)-K(2A)	40.49(7)
O(6A)-K(2)-K(2A)	84.50(7)	O(5A)-K(2)-K(2A)	40.08(6)
O(3)-K(2)-K(2A)	170.46(11)	O(4)-K(2)-K(2A)	102.79(11)
F(5)-K(2)-K(2A)	95.03(6)	F(1A)-K(2)-K(2A)	95.80(6)
C(12)-K(2)-K(2A)	166.12(15)	C(17A)-K(2)-K(2A)	55.06(6)
K(1)-K(2)-K(2A)	59.57(2)	K(1A)-K(2)-K(2A)	58.01(2)
C(1)-O(1)-C(4)	109.0(5)	C(1)-O(1)-K(1)	131.6(3)
C(4)-O(1)-K(1)	118.2(4)	C(5)-O(2)-C(8)	107.6(4)
C(5)-O(2)-K(1)	126.0(3)	C(8)-O(2)-K(1)	125.9(3)
C(12)-O(3)-C(9)	110.6(6)	C(12)-O(3)-K(2)	116.5(4)
C(9)-O(3)-K(2)	128.2(4)	C(13)-O(4)-C(16)	106.3(5)
C(13)-O(4)-K(2)	120.1(4)	C(16)-O(4)-K(2)	122.2(5)
C(17)-O(5)-K(2)	124.2(2)	C(17)-O(5)-K(1A)	115.8(3)
K(2)-O(5)-K(1A)	95.93(9)	C(17)-O(5)-K(2A)	121.4(2)
K(2)-O(5)-K(2A)	99.43(10)	K(1A)-O(5)-K(2A)	93.36(10)
C(23)-O(6)-K(1A)	124.3(2)	C(23)-O(6)-K(2A)	124.1(3)
K(1A)-O(6)-K(2A)	93.99(10)	C(23)-O(6)-K(1)	115.8(2)
K(1A)-O(6)-K(1)	96.75(10)	K(2A)-O(6)-K(1)	95.15(10)
C(18)-F(1)-K(2A)	108.3(2)	C(22)-F(5)-K(2)	112.8(2)
C(24)-F(6)-K(1A)	111.7(2)	C(28)-F(10)-K(1)	106.5(2)
O(1)-C(1)-C(2)	105.4(5)	C(3)-C(2)-C(1)	102.9(6)
C(4)-C(3)-C(2)	109.6(6)	C(3)-C(4)-O(1)	107.4(6)
O(2)-C(5)-C(6)	107.8(5)	C(5)-C(6)-C(7)	102.7(5)
C(6)-C(7)-C(8)	105.0(5)	O(2)-C(8)-C(7)	106.1(5)

O(3)-C(9)-C(10)	102.2(7)	C(11)-C(10)-C(9)	102.6(7)
C(12)-C(11)-C(10)	105.4(8)	O(3)-C(12)-C(11)	109.5(8)
O(3)-C(12)-K(2)	43.3(3)	C(11)-C(12)-K(2)	144.8(8)
O(4)-C(13)-C(14)	106.8(6)	C(15)-C(14)-C(13)	105.1(6)
C(16)-C(15)-C(14)	103.8(8)	O(4)-C(16)-C(15)	103.6(6)
O(5)-C(17)-C(22)	124.0(3)	O(5)-C(17)-C(18)	122.4(4)
C(22)-C(17)-C(18)	113.6(4)	O(5)-C(17)-K(1A)	44.5(2)
C(22)-C(17)-K(1A)	121.3(3)	C(18)-C(17)-K(1A)	105.4(3)
O(5)-C(17)-K(2A)	40.45(19)	C(22)-C(17)-K(2A)	150.8(3)
C(18)-C(17)-K(2A)	87.1(2)	K(1A)-C(17)-K(2A)	68.04(8)
F(1)-C(18)-C(19)	119.2(4)	F(1)-C(18)-C(17)	117.9(4)
C(19)-C(18)-C(17)	122.9(4)	F(2)-C(19)-C(20)	118.5(4)
F(2)-C(19)-C(18)	120.4(4)	C(20)-C(19)-C(18)	121.0(4)
F(3)-C(20)-C(19)	120.9(4)	F(3)-C(20)-C(21)	120.5(4)
C(19)-C(20)-C(21)	118.6(4)	F(4)-C(21)-C(22)	119.7(4)
F(4)-C(21)-C(20)	119.6(4)	C(22)-C(21)-C(20)	120.6(4)
F(5)-C(22)-C(21)	118.8(4)	F(5)-C(22)-C(17)	117.9(4)
C(21)-C(22)-C(17)	123.3(4)	O(6)-C(23)-C(28)	123.4(4)
O(6)-C(23)-C(24)	123.9(3)	C(28)-C(23)-C(24)	112.7(4)
O(6)-C(23)-K(1)	44.61(18)	C(28)-C(23)-K(1)	86.0(2)
C(24)-C(23)-K(1)	148.0(3)	F(6)-C(24)-C(25)	118.5(4)
F(6)-C(24)-C(23)	117.3(4)	C(25)-C(24)-C(23)	124.2(4)
F(7)-C(25)-C(24)	120.1(4)	F(7)-C(25)-C(26)	120.0(4)
C(24)-C(25)-C(26)	119.9(4)	F(8)-C(26)-C(25)	120.5(4)
F(8)-C(26)-C(27)	120.8(4)	C(25)-C(26)-C(27)	118.7(4)
F(9)-C(27)-C(28)	120.6(4)	F(9)-C(27)-C(26)	118.6(4)
C(28)-C(27)-C(26)	120.8(4)	C(27)-C(28)-F(10)	118.9(4)
C(27)-C(28)-C(23)	123.7(4)	F(10)-C(28)-C(23)	117.4(4)

KOPh-4-F.Et2O (4.8)

Table 1. Crystal data and structure refinement for str0053a.

Identification code	str0053a
Chemical formula	C40H56F4Na4O8
Formula weight	832.81
Temperature	150(2) K
Radiation, wavelength	MoKα, 0.71073 Å
Crystal system, space group	monoclinic, C2/c
Unit cell parameters	a = 26.924(5) Å α = 90°
	b = 9.8114(17) Å β = 127.845(2)°
	c = 21.685(4) Å γ = 90°
Cell volume	4523.5(14) Å3
Z	4
Calculated density	1.223 g/cm3
Absorption coefficient μ	0.126 mm-1
F(000)	1760
Crystal colour and size	colourless, 0.28 ' 0.24 ' 0.22 mm3
Data collection method	Bruker SMART APEX diffractometer
	ω rotation with narrow frames
θ range for data collection	1.92 to 28.32°
Index ranges	h -33 to 34, k -13 to 13, l -28 to 27
Completeness to θ = 26.00°	99.9 %
Reflections collected	19404
Independent reflections	5364 (Rint = 0.0382)
Reflections with F2>2σ	3961
Absorption correction	semi-empirical from equivalents
Min. and max. transmission	0.9656 and 0.9728
Structure solution	direct methods
Refinement method	Full-matrix least-squares on F2
Weighting parameters a, b	0.0770, 1.6448
Data / restraints / parameters	5364 / 0 / 253
Final R indices [F2>2σ]	R1 = 0.0578, wR2 = 0.1338
R indices (all data)	R1 = 0.0823, wR2 = 0.1469
Goodness-of-fit on F2	1.044
Largest and mean shift/su	0.000 and 0.000
Largest diff. peak and hole	0.352 and -0.224 e Å-3

Table 2. Atomic coordinates and equivalent isotropic displacement parameters (Å2) for str0053a. Ueq is defined as one third of the trace of the orthogonalized Uij tensor.

	x	y	z	Ueq
K(1)	0.06110(3)	0.29206(7)	0.25303(4)	0.0273(2)
K(2)	0.04397(3)	0.52253(8)	0.34457(4)	0.0279(2)
O(1)	0.06193(6)	0.52580(14)	0.25390(8)	0.0296(3)
O(2)	0.04458(6)	0.28907(13)	0.34511(8)	0.0294(3)
O(3)	0.14259(6)	0.19036(14)	0.26062(8)	0.0286(3)
O(4)	0.10089(7)	0.61664(15)	0.46968(8)	0.0372(4)
F(1)	0.23866(6)	0.85687(13)	0.28144(8)	0.0441(3)
F(2)	0.17947(7)	-0.05564(15)	0.59614(8)	0.0545(4)
C(1)	0.10423(8)	0.60613(19)	0.26028(11)	0.0242(4)
C(2)	0.14184(9)	0.5614(2)	0.23959(12)	0.0279(4)
C(3)	0.18647(9)	0.6447(2)	0.24651(12)	0.0308(4)
C(4)	0.19407(9)	0.7738(2)	0.27429(12)	0.0306(4)
C(5)	0.15855(10)	0.8242(2)	0.29484(12)	0.0334(5)
C(6)	0.11415(9)	0.7399(2)	0.28795(12)	0.0296(4)
C(7)	0.07660(8)	0.20585(19)	0.40561(11)	0.0245(4)
C(8)	0.09339(10)	0.0742(2)	0.39915(12)	0.0327(5)
C(9)	0.12734(11)	-0.0131(2)	0.46222(13)	0.0380(5)
C(10)	0.14480(9)	0.0305(2)	0.53308(12)	0.0350(5)
C(11)	0.12945(10)	0.1561(2)	0.54298(12)	0.0333(5)
C(12)	0.09555(9)	0.2437(2)	0.47954(11)	0.0287(4)
C(13)	0.13560(9)	0.1383(2)	0.19393(12)	0.0308(4)
C(14)	0.06820(11)	0.0987(3)	0.13270(14)	0.0456(6)
C(15)	0.20691(9)	0.2204(2)	0.32391(12)	0.0317(4)
C(16)	0.20945(11)	0.2818(3)	0.38912(13)	0.0403(5)
C(17)	0.16735(11)	0.6007(2)	0.52768(13)	0.0437(6)
C(18)	0.19371(13)	0.5475(3)	0.48927(16)	0.0611(7)
C(19)	0.07211(12)	0.6657(3)	0.50270(13)	0.0472(6)
C(20)	0.00306(14)	0.6809(4)	0.43933(17)	0.0802(11)

Table 3. Bond lengths [Å] and angles [°] for str0053a.

K(1)-O(2A)	2.2795(16)	K(1)-O(1)	2.2933(16)		
K(1)-O(2)	2.2970(15)	K(1)-O(3)	2.3221(15)		
K(1)-K(2A)	3.2014(11)	K(1)-K(1A)	3.2114(15)		
K(1)-K(2)	3.2233(11)	K(2)-O(1A)	2.2845(16)		
K(2)-O(2)	2.2906(16)	K(2)-O(1)	2.2951(15)		
K(2)-O(4)	2.3366(16)	K(2)-K(1A)	3.2014(11)		
K(2)-K(2A)	3.2421(16)	O(1)-C(1)	1.321(2)		
O(1)-K(2A)	2.2845(16)	O(2)-C(7)	1.320(2)		
O(2)-K(1A)	2.2795(16)	O(3)-C(15)	1.433(2)		
O(3)-C(13)	1.433(2)	O(4)-C(19)	1.424(3)		
O(4)-C(17)	1.431(3)	F(1)-C(4)	1.379(2)		
F(2)-C(10)	1.374(2)	C(1)-C(6)	1.399(3)		
C(1)-C(2)	1.406(3)	C(2)-C(3)	1.383(3)		
C(3)-C(4)	1.363(3)	C(4)-C(5)	1.371(3)		
C(5)-C(6)	1.384(3)	C(7)-C(8)	1.404(3)		
C(7)-C(12)	1.402(3)	C(8)-C(9)	1.380(3)		
C(9)-C(10)	1.371(3)	C(10)-C(11)	1.358(3)		
C(11)-C(12)	1.387(3)	C(13)-C(14)	1.500(3)		
C(15)-C(16)	1.499(3)	C(17)-C(18)	1.482(4)		
C(19)-C(20)	1.494(4)				

O(2A)-K(1)-O(1)	91.19(5)	O(2A)-K(1)-O(2)	90.85(5)		
O(1)-K(1)-O(2)	90.67(5)	O(2A)-K(1)-O(3)	130.13(6)		
O(1)-K(1)-O(3)	115.16(6)	O(2)-K(1)-O(3)	127.68(6)		
O(2A)-K(1)-K(2A)	45.67(4)	O(1)-K(1)-K(2A)	45.52(4)		
O(2)-K(1)-K(2A)	91.13(4)	O(3)-K(1)-K(2A)	139.78(5)		
O(2A)-K(1)-K(1A)	45.66(4)	O(1)-K(1)-K(1A)	90.28(4)		
O(2)-K(1)-K(1A)	45.21(4)	O(3)-K(1)-K(1A)	154.50(4)		
K(2A)-K(1)-K(1A)	60.35(2)	O(2A)-K(1)-K(2)	90.90(4)		
O(1)-K(1)-K(2)	45.39(4)	O(2)-K(1)-K(2)	45.28(4)		
O(3)-K(1)-K(2)	138.05(5)	K(2A)-K(1)-K(2)	60.61(3)		
K(1A)-K(1)-K(2)	59.67(2)	O(1A)-K(2)-O(2)	91.13(5)		
O(1A)-K(2)-O(1)	89.84(5)	O(2)-K(2)-O(1)	90.79(5)		
O(1A)-K(2)-O(4)	129.28(6)	O(2)-K(2)-O(4)	113.06(6)		
O(1)-K(2)-O(4)	131.02(6)	O(1A)-K(2)-K(1A)	45.74(4)		
O(2)-K(2)-K(1A)	45.39(4)	O(1)-K(2)-K(1A)	90.50(4)		
O(4)-K(2)-K(1A)	136.95(5)	O(1A)-K(2)-K(1)	90.14(4)		
O(2)-K(2)-K(1)	45.44(4)	O(1)-K(2)-K(1)	45.35(4)		
O(4)-K(2)-K(1)	138.81(5)	K(1A)-K(2)-K(1)	59.98(3)		
O(1A)-K(2)-K(2A)	45.06(4)	O(2)-K(2)-K(2A)	90.22(4)		
O(1)-K(2)-K(2A)	44.80(4)	O(4)-K(2)-K(2A)	156.71(4)		

K(1A)-K(2)-K(2A)	60.03(2)	K(1)-K(2)-K(2A)	59.36(2)
C(1)-O(1)-K(2A)	127.43(12)	C(1)-O(1)-K(1)	126.94(12)
K(2A)-O(1)-K(1)	88.74(5)	C(1)-O(1)-K(2)	122.68(12)
K(2A)-O(1)-K(2)	90.14(5)	K(1)-O(1)-K(2)	89.26(5)
C(7)-O(2)-K(1A)	128.01(11)	C(7)-O(2)-K(2)	128.45(12)
K(1A)-O(2)-K(2)	88.93(5)	C(7)-O(2)-K(1)	120.99(11)
K(1A)-O(2)-K(1)	89.13(5)	K(2)-O(2)-K(1)	89.27(5)
C(15)-O(3)-C(13)	111.91(14)	C(15)-O(3)-K(1)	120.90(11)
C(13)-O(3)-K(1)	123.24(11)	C(19)-O(4)-C(17)	111.59(16)
C(19)-O(4)-K(2)	123.10(13)	C(17)-O(4)-K(2)	123.59(13)
O(1)-C(1)-C(6)	122.02(17)	O(1)-C(1)-C(2)	121.60(17)
C(6)-C(1)-C(2)	116.38(17)	C(3)-C(2)-C(1)	121.92(18)
C(4)-C(3)-C(2)	118.81(19)	C(3)-C(4)-C(5)	122.19(18)
C(3)-C(4)-F(1)	118.88(18)	C(5)-C(4)-F(1)	118.93(18)
C(4)-C(5)-C(6)	118.59(19)	C(5)-C(6)-C(1)	122.10(18)
O(2)-C(7)-C(8)	121.60(17)	O(2)-C(7)-C(12)	122.02(17)
C(8)-C(7)-C(12)	116.38(17)	C(9)-C(8)-C(7)	122.01(19)
C(10)-C(9)-C(8)	118.7(2)	C(11)-C(10)-F(2)	119.17(19)
C(11)-C(10)-C(9)	122.13(19)	F(2)-C(10)-C(9)	118.7(2)
C(10)-C(11)-C(12)	118.97(19)	C(11)-C(12)-C(7)	121.79(19)
O(3)-C(13)-C(14)	108.90(16)	O(3)-C(15)-C(16)	108.36(16)
O(4)-C(17)-C(18)	108.44(19)	O(4)-C(19)-C(20)	108.98(19)

NaOPhF5.EtherToluene (4.2)

Table 1. Crystal data and structure refinement for STR0048.

Identification code	str0048
Chemical formula	C39.50H34F20Na4O7
Formula weight	1092.63
Temperature	150(2) K
Radiation, wavelength	MoKα, 0.71073 Å
Crystal system, space group	triclinic, P-1
Unit cell parameters	a = 11.1363(13) Å α = 81.115(2)°
	b = 11.7882(14) Å β = 87.435(2)°
	c = 19.441(2) Å γ = 65.071(2)°
Cell volume	2286.1(5) Å3
Z	2
Calculated density	1.587 g/cm3
Absorption coefficient μ	0.192 mm-1
F(000)	1102
Crystal colour and size	colourless, 0.46 ´ 0.44 ´ 0.20 mm3
Data collection method	Bruker SMART APEX diffractometer
	ω rotation with narrow frames
θ range for data collection	1.93 to 28.34°
Index ranges	h -14 to 14, k -15 to 15, l -25 to 25
Completeness to θ = 26.00°	99.2 %
Reflections collected	20132
Independent reflections	10501 (Rint = 0.0146)
Reflections with F2>2σ	8168
Absorption correction	semi-empirical from equivalents
Min. and max. transmission	0.9168 and 0.9626
Structure solution	direct methods
Refinement method	Full-matrix least-squares on F2
Weighting parameters a, b	0.1066, 1.8765
Data / restraints / parameters	10501 / 0 / 640
Final R indices [F2>2σ]	R1 = 0.0494, wR2 = 0.1377
R indices (all data)	R1 = 0.0650, wR2 = 0.1543
Goodness-of-fit on F2	0.829
Largest and mean shift/su	0.001 and 0.000
Largest diff. peak and hole	0.432 and -0.355 e Å-3

Table 2. Atomic coordinates and equivalent isotropic displacement parameters (Å2) for STR0048. Ueq is defined as one third of the trace of the orthogonalized Uij tensor.

	x	y	z	Ueq
Na(1)	1.00023(8)	1.01983(7)	0.11899(4)	0.02921(18)

Na(2)	0.73490(7)	1.00646(7)	0.20161(4)	0.02736(17)
Na(3)	1.02359(7)	0.79306(7)	0.25324(4)	0.02918(18)
Na(4)	0.93060(8)	1.09082(8)	0.28734(4)	0.03353(19)
O(1)	0.82675(14)	1.15236(13)	0.17844(8)	0.0330(3)
C(1)	0.75068(19)	1.26894(18)	0.15230(11)	0.0290(4)
C(2)	0.7382(2)	1.31278(19)	0.08108(11)	0.0311(4)
C(3)	0.6577(2)	1.4357(2)	0.05304(12)	0.0385(5)
C(4)	0.5870(2)	1.5215(2)	0.09578(15)	0.0450(6)
C(5)	0.5981(2)	1.4847(2)	0.16613(15)	0.0428(6)
C(6)	0.6773(2)	1.3611(2)	0.19350(12)	0.0359(5)
F(1)	0.81102(14)	1.23064(13)	0.03791(7)	0.0433(3)
F(2)	0.65172(18)	1.47247(16)	-0.01584(8)	0.0595(4)
F(3)	0.51040(18)	1.64259(13)	0.06882(11)	0.0692(5)
F(4)	0.53347(18)	1.56924(15)	0.20921(11)	0.0673(5)
F(5)	0.68764(17)	1.32738(14)	0.26354(8)	0.0537(4)
O(2)	0.84866(14)	0.93670(14)	0.30646(7)	0.0306(3)
C(7)	0.80487(19)	0.8980(2)	0.36460(10)	0.0306(4)
C(8)	0.7319(2)	0.9786(3)	0.41140(12)	0.0426(5)
C(9)	0.6885(3)	0.9353(4)	0.47403(14)	0.0626(9)
C(10)	0.7169(3)	0.8093(4)	0.49206(14)	0.0668(10)
C(11)	0.7867(3)	0.7280(3)	0.44781(14)	0.0572(8)
C(12)	0.8280(2)	0.7715(2)	0.38556(12)	0.0391(5)
F(6)	0.89732(15)	0.68753(14)	0.34272(8)	0.0505(4)
F(7)	0.8172(2)	0.6040(2)	0.46526(11)	0.0918(7)
F(8)	0.6765(2)	0.7689(3)	0.55329(9)	0.1080(9)
F(9)	0.6209(2)	1.0185(3)	0.51659(10)	0.0990(8)
F(10)	0.70510(17)	1.10233(17)	0.39503(9)	0.0636(5)
O(3)	0.91415(13)	0.87017(13)	0.14562(7)	0.0279(3)
C(13)	0.90069(17)	0.80475(17)	0.10073(10)	0.0247(4)
C(14)	0.8852(2)	0.69216(19)	0.11973(11)	0.0314(4)
C(15)	0.8716(2)	0.6235(2)	0.07157(13)	0.0377(5)
C(16)	0.8716(2)	0.6638(2)	0.00149(13)	0.0364(5)
C(17)	0.8881(2)	0.77297(19)	-0.01971(11)	0.0297(4)
C(18)	0.90163(18)	0.83997(17)	0.02885(10)	0.0254(4)
F(11)	0.88733(15)	0.64798(13)	0.18800(7)	0.0483(4)
F(12)	0.86215(16)	0.51397(14)	0.09355(10)	0.0582(4)
F(13)	0.85762(15)	0.59743(14)	-0.04562(9)	0.0531(4)
F(14)	1.10794(15)	1.18541(13)	0.08800(7)	0.0442(3)
F(15)	0.91900(13)	0.94663(11)	0.00512(6)	0.0330(3)
O(4)	1.10409(13)	0.94889(13)	0.22855(8)	0.0305(3)
C(19)	1.22971(18)	0.92150(18)	0.23429(10)	0.0263(4)
C(20)	1.31505(19)	0.89631(18)	0.17779(10)	0.0258(4)
C(21)	0.44795(19)	0.86815(18)	0.18275(10)	0.0268(4)
C(22)	0.50272(18)	0.86427(19)	0.24521(11)	0.0292(4)
C(23)	0.4241(2)	0.8879(2)	0.30251(11)	0.0325(4)
C(24)	1.2913(2)	0.9161(2)	0.29678(11)	0.0313(4)
F(16)	1.26278(12)	0.90040(13)	0.11548(6)	0.0372(3)
F(17)	0.52444(12)	0.84580(13)	0.12686(7)	0.0389(3)
F(18)	0.63253(11)	0.84102(13)	0.24987(7)	0.0403(3)
F(19)	0.47746(14)	0.88507(16)	0.36356(7)	0.0497(4)
F(20)	1.21617(14)	0.94026(16)	0.35386(7)	0.0478(4)
O(5)	0.51905(13)	1.12826(14)	0.16146(8)	0.0321(3)
C(25)	0.4135(2)	1.1875(2)	0.20624(13)	0.0452(6)
C(26)	0.4696(3)	1.1713(2)	0.27759(13)	0.0479(6)
C(27)	0.4752(2)	1.1543(2)	0.09068(12)	0.0402(5)
C(28)	0.5896(2)	1.0850(2)	0.04734(12)	0.0406(5)
O(6)	1.20306(16)	0.60729(15)	0.29127(9)	0.0431(4)
C(29)	1.2281(3)	0.5502(3)	0.36247(16)	0.0652(8)
C(30)	1.1872(3)	0.6485(3)	0.40791(16)	0.0658(8)
C(31)	1.2631(3)	0.5173(3)	0.24521(17)	0.0568(7)
C(32)	1.2384(3)	0.5837(3)	0.17197(17)	0.0654(8)
O(7)	0.9778(2)	1.24026(19)	0.33756(9)	0.0523(5)
C(33)	0.9698(5)	1.2563(4)	0.40720(18)	0.0847(12)
C(34)	0.9672(4)	1.1463(4)	0.45170(16)	0.0735(9)
C(35)	0.9957(6)	1.3402(4)	0.2940(2)	0.0960(15)
C(36)	1.0392(4)	1.3069(3)	0.22661(18)	0.0664(8)
C(40)	0.4996(5)	0.6151(4)	0.4829(4)	0.111(2)
C(41)	0.5506(5)	0.5282(6)	0.4373(4)	0.1124(18)
C(42)	0.5526(5)	0.4094(5)	0.4541(4)	0.121(2)
C(43)	0.5931(11)	0.5542(10)	0.3786(5)	0.107(3)

Table 3. Bond lengths [Å] and angles [°] for STR0048.

Na(1)–O(1)	2.3070(17)	Na(1)–O(3)	2.3234(16)
Na(1)–O(4)	2.3299(16)	Na(1)–F(15A)	2.5687(14)

Na(1)–F(16)	2.6603(15)	Na(1)–F(14)	2.6753(17)
Na(1)–F(1)	2.7881(17)	Na(1)–F(15)	2.8092(15)
Na(1)–Na(2)	3.3504(11)	Na(1)–Na(3)	3.3682(11)
Na(1)–Na(4)	3.4764(12)	Na(2)–O(2)	2.2961(16)
Na(2)–O(5)	2.3154(15)	Na(2)–O(3)	2.3222(15)
Na(2)–O(1)	2.3259(16)	Na(2)–F(18)	2.6826(16)
Na(2)–Na(3)	3.2192(11)	Na(2)–Na(4)	3.3438(11)
Na(3)–O(6)	2.2976(17)	Na(3)–O(2)	2.3049(16)
Na(3)–O(3)	2.3230(16)	Na(3)–O(4)	2.3421(16)
Na(3)–F(6)	2.6718(17)	Na(3)–Na(4)	3.3801(12)
Na(4)–O(1)	2.3204(17)	Na(4)–O(2)	2.3302(16)
Na(4)–O(4)	2.3466(16)	Na(4)–O(7)	2.3853(19)
Na(4)–F(5)	2.9436(19)	O(1)–C(1)	1.306(2)
C(1)–C(2)	1.393(3)	C(1)–C(6)	1.397(3)
C(2)–F(1)	1.352(2)	C(2)–C(3)	1.381(3)
C(3)–F(2)	1.338(3)	C(3)–C(4)	1.364(4)
C(4)–F(3)	1.350(3)	C(4)–C(5)	1.364(4)
C(5)–F(4)	1.346(3)	C(5)–C(6)	1.380(3)
C(6)–F(5)	1.354(3)	O(2)–C(7)	1.305(2)
C(7)–C(8)	1.393(3)	C(7)–C(12)	1.398(3)
C(8)–F(10)	1.348(3)	C(8)–C(9)	1.393(4)
C(9)–F(9)	1.336(4)	C(9)–C(10)	1.372(5)
C(10)–F(8)	1.343(3)	C(10)–C(11)	1.352(5)
C(11)–F(7)	1.343(4)	C(11)–C(12)	1.377(3)
C(12)–F(6)	1.350(3)	O(3)–C(13)	1.302(2)
C(13)–C(18)	1.396(3)	C(13)–C(14)	1.401(3)
C(14)–F(11)	1.346(2)	C(14)–C(15)	1.380(3)
C(15)–F(12)	1.342(2)	C(15)–C(16)	1.372(3)
C(16)–F(13)	1.346(2)	C(16)–C(17)	1.374(3)
C(17)–F(14A)	1.348(2)	C(17)–C(18)	1.371(3)
C(18)–F(15)	1.360(2)	F(14)–C(17A)	1.348(2)
F(15)–Na(1A)	2.5687(14)	O(4)–C(19)	1.302(2)
C(19)–C(24)	1.401(3)	C(19)–C(20)	1.403(3)
C(20)–F(16)	1.353(2)	C(20)–C(21B)	1.378(3)
C(21)–F(17)	1.339(2)	C(21)–C(22)	1.369(3)
C(21)–C(20C)	1.378(3)	C(22)–F(18)	1.358(2)
C(22)–C(23)	1.374(3)	C(23)–F(19)	1.341(2)
C(23)–C(24C)	1.378(3)	C(24)–F(20)	1.351(2)
C(24)–C(23B)	1.378(3)	O(5)–C(27)	1.425(3)
O(5)–C(25)	1.425(3)	C(25)–C(26)	1.499(4)
C(27)–C(28)	1.497(3)	O(6)–C(31)	1.420(3)
O(6)–C(29)	1.427(3)	C(29)–C(30)	1.472(5)
C(31)–C(32)	1.492(4)	O(7)–C(33)	1.390(4)
O(7)–C(35)	1.422(4)	C(33)–C(34)	1.454(5)
C(35)–C(36)	1.430(5)	C(40)–C(42D)	1.374(8)
C(40)–C(41)	1.380(8)	C(41)–C(43)	1.260(11)
C(41)–C(42)	1.380(7)	C(42)–C(40D)	1.374(8)

O(1)–Na(1)–O(3)	87.70(6)	O(1)–Na(1)–O(4)	83.55(6)
O(3)–Na(1)–O(4)	87.51(5)	O(1)–Na(1)–F(15A)	131.09(6)
O(3)–Na(1)–F(15A)	118.25(5)	O(4)–Na(1)–F(15A)	133.92(6)
O(1)–Na(1)–F(16)	144.01(6)	O(3)–Na(1)–F(16)	108.71(5)
O(4)–Na(1)–F(16)	66.03(5)	F(15A)–Na(1)–F(16)	69.50(4)
O(1)–Na(1)–F(14)	94.15(5)	O(3)–Na(1)–F(14)	177.95(6)
O(4)–Na(1)–F(14)	91.81(5)	F(15A)–Na(1)–F(14)	61.05(4)
F(16)–Na(1)–F(14)	69.25(5)	O(1)–Na(1)–F(1)	64.09(5)
O(3)–Na(1)–F(1)	107.71(5)	O(4)–Na(1)–F(1)	142.88(6)
F(15A)–Na(1)–F(1)	68.51(4)	F(16)–Na(1)–F(1)	133.67(5)
F(14)–Na(1)–F(1)	73.95(5)	O(1)–Na(1)–F(15)	113.61(5)
O(3)–Na(1)–F(15)	63.89(4)	O(4)–Na(1)–F(15)	144.68(5)
F(15A)–Na(1)–F(15)	57.25(5)	F(16)–Na(1)–F(15)	102.38(4)
F(14)–Na(1)–F(15)	116.02(4)	F(1)–Na(1)–F(15)	69.81(4)
O(1)–Na(1)–Na(2)	43.91(4)	O(3)–Na(1)–Na(2)	43.83(4)
O(4)–Na(1)–Na(2)	85.28(4)	F(15A)–Na(1)–Na(2)	140.15(4)
F(16)–Na(1)–Na(2)	142.77(4)	F(14)–Na(1)–Na(2)	138.04(4)
F(1)–Na(1)–Na(2)	83.49(4)	F(15)–Na(1)–Na(2)	87.23(3)
O(1)–Na(1)–Na(3)	85.38(4)	O(3)–Na(1)–Na(3)	43.53(4)
O(4)–Na(1)–Na(3)	44.01(4)	F(15A)–Na(1)–Na(3)	142.44(4)
F(16)–Na(1)–Na(3)	85.53(4)	F(14)–Na(1)–Na(3)	135.68(4)
F(1)–Na(1)–Na(3)	140.74(4)	F(15)–Na(1)–Na(3)	104.37(4)
Na(2)–Na(1)–Na(3)	57.26(2)	O(1)–Na(1)–Na(4)	41.44(4)
O(3)–Na(1)–Na(4)	88.46(4)	O(4)–Na(1)–Na(4)	42.16(4)
F(15A)–Na(1)–Na(4)	153.22(4)	F(16)–Na(1)–Na(4)	105.47(4)
F(14)–Na(1)–Na(4)	92.33(4)	F(1)–Na(1)–Na(4)	103.14(4)

F(15)–Na(1)–Na(4)	145.85(4)	Na(2)–Na(1)–Na(4)	58.62(2)
Na(3)–Na(1)–Na(4)	59.16(2)	O(2)–Na(2)–O(5)	137.66(6)
O(2)–Na(2)–O(3)	91.78(6)	O(5)–Na(2)–O(3)	129.50(6)
O(2)–Na(2)–O(1)	87.92(6)	O(5)–Na(2)–O(1)	101.30(6)
O(3)–Na(2)–O(1)	87.28(6)	O(2)–Na(2)–F(18)	84.02(5)
O(5)–Na(2)–F(18)	81.89(5)	O(3)–Na(2)–F(18)	97.36(5)
O(1)–Na(2)–F(18)	170.80(6)	O(2)–Na(2)–Na(3)	45.71(4)
O(5)–Na(2)–Na(3)	169.28(5)	O(3)–Na(2)–Na(3)	46.14(4)
O(1)–Na(2)–Na(3)	88.63(4)	F(18)–Na(2)–Na(3)	88.90(4)
O(2)–Na(2)–Na(4)	44.12(4)	O(5)–Na(2)–Na(4)	128.37(5)
O(3)–Na(2)–Na(4)	91.76(4)	O(1)–Na(2)–Na(4)	43.91(4)
F(18)–Na(2)–Na(4)	127.66(4)	Na(3)–Na(2)–Na(4)	61.96(3)
O(2)–Na(2)–Na(1)	91.25(4)	O(5)–Na(2)–Na(1)	123.66(5)
O(3)–Na(2)–Na(1)	43.86(4)	O(1)–Na(2)–Na(1)	43.46(4)
F(18)–Na(2)–Na(1)	140.90(4)	Na(3)–Na(2)–Na(1)	61.65(2)
Na(4)–Na(2)–Na(1)	62.57(2)	O(6)–Na(3)–O(2)	134.94(7)
O(6)–Na(3)–O(3)	130.96(6)	O(2)–Na(3)–O(3)	91.53(5)
O(6)–Na(3)–O(4)	106.27(6)	O(2)–Na(3)–O(4)	87.35(6)
O(3)–Na(3)–O(4)	87.23(5)	O(6)–Na(3)–F(6)	82.24(6)
O(2)–Na(3)–F(6)	66.15(5)	O(3)–Na(3)–F(6)	111.49(6)
O(4)–Na(3)–F(6)	147.10(6)	O(6)–Na(3)–Na(2)	165.44(6)
O(2)–Na(3)–Na(2)	45.49(4)	O(3)–Na(3)–Na(2)	46.12(4)
O(4)–Na(3)–Na(2)	88.18(4)	F(6)–Na(3)–Na(2)	86.52(4)
O(6)–Na(3)–Na(1)	128.96(6)	O(2)–Na(3)–Na(1)	90.65(4)
O(3)–Na(3)–Na(1)	43.54(4)	O(4)–Na(3)–Na(1)	43.73(4)
F(6)–Na(3)–Na(1)	147.43(4)	Na(2)–Na(3)–Na(1)	61.09(2)
O(6)–Na(3)–Na(4)	131.56(6)	O(2)–Na(3)–Na(4)	43.47(4)
O(3)–Na(3)–Na(4)	90.84(4)	O(4)–Na(3)–Na(4)	43.92(4)
F(6)–Na(3)–Na(4)	106.74(4)	Na(2)–Na(3)–Na(4)	60.83(2)
Na(1)–Na(3)–Na(4)	62.02(2)	O(1)–Na(4)–O(2)	87.25(6)
O(1)–Na(4)–O(4)	82.90(6)	O(2)–Na(4)–O(4)	86.65(6)
O(1)–Na(4)–O(7)	118.74(7)	O(2)–Na(4)–O(7)	145.86(7)
O(4)–Na(4)–O(7)	116.42(7)	O(1)–Na(4)–F(5)	61.47(5)
O(2)–Na(4)–F(5)	102.68(6)	O(4)–Na(4)–F(5)	142.22(6)
O(7)–Na(4)–F(5)	75.03(6)	O(1)–Na(4)–Na(2)	44.04(4)
O(2)–Na(4)–Na(2)	43.31(4)	O(4)–Na(4)–Na(2)	85.18(4)
O(7)–Na(4)–Na(2)	152.90(6)	F(5)–Na(4)–Na(2)	77.87(4)
O(1)–Na(4)–Na(3)	84.90(4)	O(2)–Na(4)–Na(3)	42.89(4)
O(4)–Na(4)–Na(3)	43.82(4)	O(7)–Na(4)–Na(3)	149.89(6)
F(5)–Na(4)–Na(3)	135.03(4)	Na(2)–Na(4)–Na(3)	57.21(2)
O(1)–Na(4)–Na(1)	41.15(4)	O(2)–Na(4)–Na(1)	87.59(4)
O(4)–Na(4)–Na(1)	41.80(4)	O(7)–Na(4)–Na(1)	126.49(6)
F(5)–Na(4)–Na(1)	101.39(4)	Na(2)–Na(4)–Na(1)	58.81(2)
Na(3)–Na(4)–Na(1)	58.82(2)	C(1)–O(1)–Na(1)	123.03(13)
C(1)–O(1)–Na(4)	124.67(13)	Na(1)–O(1)–Na(4)	97.40(6)
C(1)–O(1)–Na(2)	118.89(12)	Na(1)–O(1)–Na(2)	92.63(6)
Na(4)–O(1)–Na(2)	92.06(6)	O(1)–C(1)–C(2)	122.89(19)
O(1)–C(1)–C(6)	122.9(2)	C(2)–C(1)–C(6)	114.24(18)
F(1)–C(2)–C(3)	119.0(2)	F(1)–C(2)–C(1)	117.78(18)
C(3)–C(2)–C(1)	123.2(2)	F(2)–C(3)–C(4)	119.7(2)
F(2)–C(3)–C(2)	120.3(2)	C(4)–C(3)–C(2)	120.0(2)
F(3)–C(4)–C(5)	120.3(2)	F(3)–C(4)–C(3)	120.3(2)
C(5)–C(4)–C(3)	119.3(2)	F(4)–C(5)–C(4)	120.2(2)
F(4)–C(5)–C(6)	119.7(2)	C(4)–C(5)–C(6)	120.1(2)
F(5)–C(6)–C(5)	118.9(2)	F(5)–C(6)–C(1)	118.01(19)
C(5)–C(6)–C(1)	123.0(2)	C(2)–F(1)–Na(1)	107.72(12)
C(6)–F(5)–Na(4)	104.73(12)	C(7)–O(2)–Na(2)	125.02(12)
C(7)–O(2)–Na(3)	119.38(13)	Na(2)–O(2)–Na(3)	88.80(6)
C(7)–O(2)–Na(4)	127.36(13)	Na(2)–O(2)–Na(4)	92.57(6)
Na(3)–O(2)–Na(4)	93.64(6)	O(2)–C(7)–C(8)	123.1(2)
O(2)–C(7)–C(12)	122.8(2)	C(8)–C(7)–C(12)	114.1(2)
F(10)–C(8)–C(9)	119.7(2)	F(10)–C(8)–C(7)	117.8(2)
C(9)–C(8)–C(7)	122.4(3)	F(9)–C(9)–C(10)	120.8(3)
F(9)–C(9)–C(8)	118.7(3)	C(10)–C(9)–C(8)	120.5(3)
F(8)–C(10)–C(11)	121.4(4)	F(8)–C(10)–C(9)	119.6(3)
C(11)–C(10)–C(9)	119.0(2)	F(7)–C(11)–C(10)	119.7(3)
F(7)–C(11)–C(12)	120.0(3)	C(10)–C(11)–C(12)	120.3(3)
F(6)–C(12)–C(11)	118.6(2)	F(6)–C(12)–C(7)	117.70(19)
C(11)–C(12)–C(7)	123.7(3)	C(12)–F(6)–Na(3)	108.00(12)
C(13)–O(3)–Na(2)	122.34(11)	C(13)–O(3)–Na(3)	127.34(12)
Na(2)–O(3)–Na(3)	87.74(5)	C(13)–O(3)–Na(1)	123.85(12)
Na(2)–O(3)–Na(1)	92.31(5)	Na(3)–O(3)–Na(1)	92.92(6)
O(3)–C(13)–C(18)	122.91(17)	O(3)–C(13)–C(14)	123.46(18)
C(18)–C(13)–C(14)	113.62(17)	F(11)–C(14)–C(15)	118.97(19)

F(11)-C(14)-C(13)	118.16(19)	C(15)-C(14)-C(13)	122.8(2)
F(12)-C(15)-C(16)	119.5(2)	F(12)-C(15)-C(14)	119.6(2)
C(16)-C(15)-C(14)	120.86(19)	F(13)-C(16)-C(15)	121.0(2)
F(13)-C(16)-C(17)	120.6(2)	C(15)-C(16)-C(17)	118.44(19)
F(14A)-C(17)-C(18)	119.51(18)	F(14A)-C(17)-C(16)	120.56(18)
C(18)-C(17)-C(16)	119.9(2)	F(15)-C(18)-C(17)	117.57(17)
F(15)-C(18)-C(13)	118.13(16)	C(17)-C(18)-C(13)	124.30(18)
C(17A)-F(14)-Na(1)	115.93(11)	C(18)-F(15)-Na(1A)	120.20(11)
C(18)-F(15)-Na(1)	107.63(10)	Na(1A)-F(15)-Na(1)	122.75(5)
C(19)-O(4)-Na(1)	119.50(12)	C(19)-O(4)-Na(3)	121.61(12)
Na(1)-O(4)-Na(3)	92.26(6)	C(19)-O(4)-Na(4)	126.84(13)
Na(1)-O(4)-Na(4)	96.04(6)	Na(3)-O(4)-Na(4)	92.26(5)
O(4)-C(19)-C(24)	123.32(18)	O(4)-C(19)-C(20)	122.59(18)
C(24)-C(19)-C(20)	114.09(17)	F(16)-C(20)-C(21B)	118.97(17)
F(16)-C(20)-C(19)	117.63(16)	C(21B)-C(20)-C(19)	123.40(18)
F(17)-C(21)-C(22)	119.31(17)	F(17)-C(21)-C(20C)	120.75(18)
C(22)-C(21)-C(20C)	119.93(18)	F(18)-C(22)-C(21)	120.19(18)
F(18)-C(22)-C(23)	120.44(18)	C(21)-C(22)-C(23)	119.33(18)
F(19)-C(23)-C(22)	119.35(18)	F(19)-C(23)-C(24C)	120.52(19)
C(22)-C(23)-C(24C)	120.12(18)	F(20)-C(24)-C(23B)	118.77(18)
F(20)-C(24)-C(19)	118.11(17)	C(23B)-C(24)-C(19)	123.12(18)
C(20)-F(16)-Na(1)	109.08(11)	C(22)-F(18)-Na(2)	125.14(12)
C(27)-O(5)-C(25)	111.94(17)	C(27)-O(5)-Na(2)	125.29(13)
C(25)-O(5)-Na(2)	122.77(13)	O(5)-C(25)-C(26)	108.93(19)
O(5)-C(27)-C(28)	108.96(18)	C(31)-O(6)-C(29)	111.9(2)
C(31)-O(6)-Na(3)	119.58(16)	C(29)-O(6)-Na(3)	123.70(16)
O(6)-C(29)-C(30)	110.0(2)	O(6)-C(31)-C(32)	109.2(2)
C(33)-O(7)-C(35)	111.8(3)	C(33)-O(7)-Na(4)	127.3(2)
C(35)-O(7)-Na(4)	120.05(19)	O(7)-C(33)-C(34)	111.0(3)
O(7)-C(35)-C(36)	111.2(3)	C(42D)-C(40)-C(41)	123.2(5)
C(43)-C(41)-C(42)	117.4(9)	C(43)-C(41)-C(40)	122.2(8)
C(42)-C(41)-C(40)	120.3(7)	C(40D)-C(42)-C(41)	116.5(7)

NaOPhF5.THF (4.1)

Table 1. Crystal data and structure refinement for str0044.

Identification code	str0044
Chemical formula	C56H64F20Na4O12
Formula weight	1401.03
Temperature	150(2) K
Radiation, wavelength	MoKα, 0.71073 Å
Crystal system, space group	monoclinic, C2/c
Unit cell parameters	a = 22.2875(16) Å α = 90°
	b = 12.5736(9) Å β = 94.0630(10)°
	c = 22.5693(16) Å γ = 90°
Cell volume	6308.8(8) Å3
Z	4
Calculated density	1.475 g/cm3
Absorption coefficient μ	0.163 mm-1
F(000)	2880
Crystal colour and size	colourless, 0.38 ˙ 0.34 ˙ 0.28 mm3
Data collection method	Bruker SMART APEX diffractometer
	ω rotation with narrow frames
θ range for data collection	1.81 to 28.33°
Index ranges	h -28 to 29, k -16 to 16, l -30 to 30
Completeness to θ = 26.00°	99.8 %
Reflections collected	27286
Independent reflections	7498 (Rint = 0.0278)
Reflections with F2>2σ	5715
Absorption correction	semi-empirical from equivalents
Min. and max. transmission	0.9407 and 0.9558
Structure solution	direct methods
Refinement method	Full-matrix least-squares on F2
Weighting parameters a, b	0.1074, 16.4831
Data / restraints / parameters	7498 / 0 / 442
Final R indices [F2>2σ]	R1 = 0.0781, wR2 = 0.2011
R indices (all data)	R1 = 0.0982, wR2 = 0.2174
Goodness-of-fit on F2	1.010
Largest and mean shift/su	0.008 and 0.000
Largest diff. peak and hole	0.663 and -0.492 e Å-3

Table 2. Atomic coordinates and equivalent isotropic displacement parameters (Å2)

for str0044. Ueq is defined as one third of the trace of the orthogonalized Uij tensor.

	x	y	z	Ueq
Na(1)	0.03804(5)	0.30413(9)	0.18354(5)	0.0311(3)
Na(2)	0.07181(5)	0.11966(9)	0.29066(5)	0.0351(3)
O(1)	0.03179(11)	0.48113(19)	0.14199(10)	0.0463(5)
O(2)	0.10785(9)	0.27831(19)	0.10846(9)	0.0424(5)
O(3)	0.16666(10)	0.1445(2)	0.34810(10)	0.0526(6)
O(5)	-0.03015(9)	0.11869(16)	0.30935(9)	0.0355(4)
O(6)	-0.06279(8)	0.30796(16)	0.21507(9)	0.0346(4)
F(1)	-0.15057(8)	0.07444(18)	0.30110(9)	0.0532(5)
F(2)	-0.19743(9)	-0.06824(19)	0.37496(11)	0.0623(6)
F(3)	-0.12616(11)	-0.16498(18)	0.46131(10)	0.0637(6)
F(4)	-0.00632(11)	-0.11643(18)	0.47293(10)	0.0645(6)
F(5)	0.04072(8)	0.02477(18)	0.39910(10)	0.0566(5)
F(6)	-0.14480(9)	0.43800(19)	0.26541(8)	0.0539(5)
F(7)	-0.21581(9)	0.56899(17)	0.19814(11)	0.0589(6)
F(8)	-0.20891(10)	0.5758(2)	0.07809(11)	0.0718(7)
F(9)	-0.12984(11)	0.4448(2)	0.02678(9)	0.0714(7)
F(10)	-0.05798(8)	0.31211(16)	0.09400(8)	0.0475(5)
C(1)	0.0199(2)	0.5741(3)	0.17325(17)	0.0652(11)
C(2)	0.0346(4)	0.6657(4)	0.1330(3)	0.130(3)
C(3)	0.0294(3)	0.6224(4)	0.0754(2)	0.0912(18)
C(4)	0.0429(2)	0.5086(3)	0.08210(17)	0.0663(12)
C(5)	0.17102(15)	0.2986(4)	0.11573(16)	0.0572(10)
C(6)	0.19423(18)	0.2961(4)	0.05574(18)	0.0696(12)
C(7)	0.1502(3)	0.2346(8)	0.0209(3)	0.144(4)
C(8)	0.09410(17)	0.2383(3)	0.04948(14)	0.0517(8)
C(9)	0.22077(17)	0.1829(5)	0.3247(2)	0.0725(12)
C(10)	0.27080(19)	0.1488(5)	0.3680(3)	0.0864(16)
C(11)	0.2414(3)	0.1410(10)	0.4235(3)	0.168(4)
C(12)	0.17696(18)	0.1350(4)	0.41067(17)	0.0636(11)
C(17)	-0.05283(12)	0.0532(2)	0.34599(11)	0.0297(5)
C(18)	-0.11426(12)	0.0269(2)	0.34346(12)	0.0330(6)
C(19)	-0.13828(13)	-0.0442(2)	0.38100(14)	0.0383(6)
C(20)	-0.10253(15)	-0.0932(2)	0.42511(13)	0.0403(7)
C(21)	-0.04228(15)	-0.0690(2)	0.43047(13)	0.0400(7)
C(22)	-0.01843(13)	0.0018(2)	0.39229(13)	0.0347(6)
C(23)	-0.09786(11)	0.3701(2)	0.18278(12)	0.0293(5)
C(24)	-0.14004(12)	0.4389(2)	0.20594(12)	0.0344(6)
C(25)	-0.17637(13)	0.5063(2)	0.17209(15)	0.0388(7)
C(26)	-0.17326(14)	0.5094(3)	0.11171(15)	0.0451(8)
C(27)	-0.13319(14)	0.4432(3)	0.08616(13)	0.0433(7)
C(28)	-0.09688(12)	0.3758(2)	0.12050(12)	0.0346(6)
O(4)	0.1045(2)	-0.0647(3)	0.2884(2)	0.1000(13)
C(13A)	0.0714(4)	-0.1381(14)	0.3008(5)	0.090(5)
C(13B)	0.0785(3)	-0.1613(7)	0.2643(5)	0.058(2)
C(14A)	0.1108(7)	-0.177(2)	0.3513(6)	0.204(12)
C(14B)	0.1311(8)	-0.2255(10)	0.2635(10)	0.165(9)
C(15A)	0.1692(4)	-0.1761(10)	0.3358(6)	0.080(3)
C(15B)	0.1777(7)	-0.1866(11)	0.2840(14)	0.155(9)
C(16)	0.1706(3)	-0.0951(7)	0.2957(5)	0.154(4)

Table 3. Bond lengths [Å] and angles [°] for str0044.

Na(1)–O(6A)	2.316(2)	Na(1)–O(5A)	2.345(2)
Na(1)–O(2)	2.402(2)	Na(1)–O(6)	2.405(2)
Na(1)–O(1)	2.415(3)	Na(1)–F(10)	2.839(2)
Na(1)–Na(2)	3.3960(15)	Na(1)–Na(2A)	3.4519(15)
Na(1)–Na(1A)	3.549(2)	Na(2)–O(5)	2.340(2)
Na(2)–O(5A)	2.379(2)	Na(2)–O(6A)	2.379(2)
Na(2)–O(3)	2.421(2)	Na(2)–O(4)	2.431(4)
Na(2)–F(5)	2.852(3)	Na(2)–F(1A)	2.865(2)
Na(2)–Na(1A)	3.4519(15)	Na(2)–Na(2A)	3.575(2)
O(1)–C(1)	1.401(5)	O(1)–C(4)	1.434(4)
O(2)–C(5)	1.429(4)	O(2)–C(8)	1.436(4)
O(3)–C(12)	1.419(4)	O(3)–C(9)	1.434(5)
O(5)–C(17)	1.295(3)	O(5)–Na(1A)	2.345(2)
O(5)–Na(2A)	2.379(2)	O(6)–C(23)	1.293(3)
O(6)–Na(1A)	2.316(2)	O(6)–Na(2A)	2.379(2)
F(1)–C(18)	1.348(3)	F(1)–Na(2A)	2.865(2)
F(2)–C(19)	1.350(3)	F(3)–C(20)	1.349(3)
F(4)–C(21)	1.344(3)	F(5)–C(22)	1.348(3)
F(6)–C(24)	1.354(3)	F(7)–C(25)	1.346(3)

F(8)-C(26)	1.349(3)	F(9)-C(27)	1.348(3)
F(10)-C(28)	1.351(3)	C(1)-C(2)	1.516(7)
C(2)-C(3)	1.407(8)	C(3)-C(4)	1.468(6)
C(5)-C(6)	1.483(5)	C(6)-C(7)	1.439(7)
C(7)-C(8)	1.446(7)	C(9)-C(10)	1.493(6)
C(10)-C(11)	1.458(9)	C(11)-C(12)	1.447(7)
C(17)-C(18)	1.406(4)	C(17)-C(22)	1.409(4)
C(18)-C(19)	1.367(4)	C(19)-C(20)	1.376(4)
C(20)-C(21)	1.374(5)	C(21)-C(22)	1.372(4)
C(23)-C(24)	1.405(4)	C(23)-C(28)	1.409(4)
C(24)-C(25)	1.368(4)	C(25)-C(26)	1.370(5)
C(26)-C(27)	1.377(5)	C(27)-C(28)	1.373(4)
O(4)-C(13A)	1.226(13)	O(4)-C(13B)	1.437(10)
O(4)-C(16)	1.520(8)	C(13A)-C(13B)	0.899(13)
C(13A)-C(14A)	1.473(13)	C(13A)-C(14B)	1.96(2)
C(13B)-C(14B)	1.425(16)	C(14A)-C(15A)	1.370(19)
C(14B)-C(15B)	1.21(2)	C(14B)-C(15A)	1.89(2)
C(14B)-C(16)	1.975(16)	C(15A)-C(15B)	1.21(3)
C(15A)-C(16)	1.365(14)	C(15B)-C(16)	1.194(15)

O(6A)-Na(1)-O(5A)	88.10(8)	O(6A)-Na(1)-O(2)	125.38(8)		
O(5A)-Na(1)-O(2)	88.25(8)	O(6A)-Na(1)-O(6)	82.49(8)		
O(5A)-Na(1)-O(6)	85.61(8)	O(2)-Na(1)-O(6)	151.25(8)		
O(6A)-Na(1)-O(1)	111.56(9)	O(5A)-Na(1)-O(1)	160.12(9)		
O(2)-Na(1)-O(1)	82.71(9)	O(6)-Na(1)-O(1)	93.84(8)		
O(6A)-Na(1)-F(10)	144.81(7)	O(5A)-Na(1)-F(10)	91.57(7)		
O(2)-Na(1)-F(10)	89.76(7)	O(6)-Na(1)-F(10)	62.42(6)		
O(1)-Na(1)-F(10)	70.81(8)	O(6A)-Na(1)-Na(2)	44.40(6)		
O(5A)-Na(1)-Na(2)	44.44(6)	O(2)-Na(1)-Na(2)	106.74(7)		
O(6)-Na(1)-Na(2)	88.14(6)	O(1)-Na(1)-Na(2)	155.44(7)		
F(10)-Na(1)-Na(2)	130.44(6)	O(6A)-Na(1)-Na(2A)	88.24(6)		
O(5A)-Na(1)-Na(2A)	42.50(5)	O(2)-Na(1)-Na(2A)	122.06(7)		
O(6)-Na(1)-Na(2A)	43.52(6)	O(1)-Na(1)-Na(2A)	131.50(7)		
F(10)-Na(1)-Na(2A)	68.65(5)	Na(2)-Na(1)-Na(2A)	62.94(4)		
O(6A)-Na(1)-Na(1A)	42.22(5)	O(5A)-Na(1)-Na(1A)	84.23(5)		
O(2)-Na(1)-Na(1A)	165.55(7)	O(6)-Na(1)-Na(1A)	40.32(5)		
O(1)-Na(1)-Na(1A)	108.07(6)	F(10)-Na(1)-Na(1A)	102.73(6)		
Na(2)-Na(1)-Na(1A)	59.56(3)	Na(2A)-Na(1)-Na(1A)	58.01(3)		
O(5)-Na(2)-O(5A)	81.51(8)	O(5)-Na(2)-O(6A)	86.31(8)		
O(5A)-Na(2)-O(6A)	85.86(8)	O(5)-Na(2)-O(3)	136.58(9)		
O(5A)-Na(2)-O(3)	140.91(9)	O(6A)-Na(2)-O(3)	88.17(9)		
O(5)-Na(2)-O(4)	107.14(14)	O(5A)-Na(2)-O(4)	94.15(12)		
O(6A)-Na(2)-O(4)	166.42(14)	O(3)-Na(2)-O(4)	83.27(13)		
O(5)-Na(2)-F(5)	62.94(7)	O(5A)-Na(2)-F(5)	135.22(8)		
O(6A)-Na(2)-F(5)	115.99(8)	O(3)-Na(2)-F(5)	81.39(8)		
O(4)-Na(2)-F(5)	73.18(13)	O(5)-Na(2)-F(1A)	141.42(8)		
O(5A)-Na(2)-F(1A)	62.04(7)	O(6A)-Na(2)-F(1A)	102.24(8)		
O(3)-Na(2)-F(1A)	81.73(7)	O(4)-Na(2)-F(1A)	66.16(13)		
F(5)-Na(2)-F(1A)	137.37(8)	O(5)-Na(2)-Na(1)	87.88(6)		
O(5A)-Na(2)-Na(1)	43.63(6)	O(6A)-Na(2)-Na(1)	42.94(5)		
O(3)-Na(2)-Na(1)	115.75(8)	O(4)-Na(2)-Na(1)	133.45(12)		
F(5)-Na(2)-Na(1)	147.31(6)	F(1A)-Na(2)-Na(1)	74.76(5)		
O(5)-Na(2)-Na(1A)	42.59(6)	O(5A)-Na(2)-Na(1A)	85.97(6)		
O(6A)-Na(2)-Na(1A)	44.13(5)	O(3)-Na(2)-Na(1A)	115.22(8)		
O(4)-Na(2)-Na(1A)	149.45(13)	F(5)-Na(2)-Na(1A)	85.29(6)		
F(1A)-Na(2)-Na(1A)	137.18(6)	Na(1)-Na(2)-Na(1A)	62.43(4)		
O(5)-Na(2)-Na(2A)	41.16(5)	O(5A)-Na(2)-Na(2A)	40.35(5)		
O(6A)-Na(2)-Na(2A)	84.43(5)	O(3)-Na(2)-Na(2A)	172.39(7)		
O(4)-Na(2)-Na(2A)	104.33(11)	F(5)-Na(2)-Na(2A)	100.22(6)		
F(1A)-Na(2)-Na(2A)	101.60(6)	Na(1)-Na(2)-Na(2A)	59.30(3)		
Na(1A)-Na(2)-Na(2A)	57.77(3)	C(1)-O(1)-C(4)	109.0(3)		
C(1)-O(1)-Na(1)	125.6(2)	C(4)-O(1)-Na(1)	125.4(2)		
C(5)-O(2)-C(8)	108.2(2)	C(5)-O(2)-Na(1)	125.24(19)		
C(8)-O(2)-Na(1)	126.51(19)	C(12)-O(3)-C(9)	108.3(3)		
C(12)-O(3)-Na(2)	126.6(2)	C(9)-O(3)-Na(2)	124.9(2)		
C(17)-O(5)-Na(2)	123.12(17)	C(17)-O(5)-Na(1A)	123.65(17)		
Na(2)-O(5)-Na(1A)	94.92(8)	C(17)-O(5)-Na(2A)	117.73(17)		
Na(2)-O(5)-Na(2A)	98.48(8)	Na(1A)-O(5)-Na(2A)	91.93(8)		
C(23)-O(6)-Na(1A)	131.43(18)	C(23)-O(6)-Na(2A)	121.69(17)		
Na(1A)-O(6)-Na(2A)	92.65(8)	C(23)-O(6)-Na(1)	112.67(16)		
Na(1A)-O(6)-Na(1)	97.46(7)	Na(2A)-O(6)-Na(1)	92.36(8)		
C(18)-F(1)-Na(2A)	103.46(16)	C(22)-F(5)-Na(2)	106.68(16)		
C(28)-F(10)-Na(1)	100.42(15)	O(1)-C(1)-C(2)	106.0(3)		
C(3)-C(2)-C(1)	104.7(5)	C(2)-C(3)-C(4)	106.1(4)		

O(1)-C(4)-C(3)	106.5(3)	O(2)-C(5)-C(6)	107.2(3)		
C(7)-C(6)-C(5)	103.9(4)	C(8)-C(7)-C(6)	108.5(4)		
O(2)-C(8)-C(7)	106.8(3)	O(3)-C(9)-C(10)	105.7(4)		
C(11)-C(10)-C(9)	102.8(4)	C(12)-C(11)-C(10)	109.3(4)		
O(3)-C(12)-C(11)	106 5(4)	O(5)-C(17)-C(18)	123.2(2)		
O(5)-C(17)-C(22)	123.3(2)	C(18)-C(17)-C(22)	113.5(2)		
F(1)-C(18)-C(19)	119.2(3)	F(1)-C(18)-C(17)	117.3(2)		
C(19)-C(18)-C(17)	123.5(3)	F(2)-C(19)-C(18)	120.4(3)		
F(2)-C(19)-C(20)	119.0(3)	C(18)-C(19)-C(20)	120.6(3)		
F(3)-C(20)-C(21)	121.1(3)	F(3)-C(20)-C(19)	120.4(3)		
C(21)-C(20)-C(19)	118.5(3)	F(4)-C(21)-C(22)	119.8(3)		
F(4)-C(21)-C(20)	119.6(3)	C(22)-C(21)-C(20)	120.5(3)		
F(5)-C(22)-C(21)	119.1(3)	F(5)-C(22)-C(17)	117.6(3)		
C(21)-C(22)-C(17)	123.3(3)	O(6)-C(23)-C(24)	123.8(2)		
O(6)-C(23)-C(28)	122 8(3)	C(24)-C(23)-C(28)	113.4(2)		
F(6)-C(24)-C(25)	118.3(3)	F(6)-C(24)-C(23)	117.7(2)		
C(25)-C(24)-C(23)	124.0(3)	F(7)-C(25)-C(26)	119.9(3)		
F(7)-C(25)-C(24)	119.9(3)	C(26)-C(25)-C(24)	120.2(3)		
F(8)-C(26)-C(25)	120.5(3)	F(8)-C(26)-C(27)	120 8(3)		
C(25)-C(26)-C(27)	118.7(3)	F(9)-C(27)-C(28)	119.9(3)		
F(9)-C(27)-C(26)	119.4(3)	C(28)-C(27)-C(26)	120.7(3)		
F(10)-C(28)-C(27)	119.2(3)	F(10)-C(28)-C(23)	117.9(2)		
C(27)-C(28)-C(23)	123.0(3)	C(13A)-O(4)-C(13B)	38.4(6)		
C(13A)-O(4)-C(16)	112.3(6)	C(13B)-O(4)-C(16)	100.9(5)		
C(13A)-O(4)-Na(2)	121.8(7)	C(13B)-O(4)-Na(2)	134.6(4)		
C(16)-O(4)-Na(2)	121.8(4)	C(13B)-C(13A)-O(4)	83.5(9)		
C(13B)-C(13A)-C(14A)	117.8(14)	O(4)-C(13A)-C(14A)	95.2(13)		
C(13B)-C(13A)-C(14B)	41.8(9)	O(4)-C(13A)-C(14B)	83 5(8)		
C(14A)-C(13A)-C(14B)	76.1(10)	C(13A)-C(13B)-O(4)	58.0(11)		
C(13A)-C(13B)-C(14B)	113.3(13)	O(4)-C(13B)-C(14B)	100.1(7)		
C(15A)-C(14A)-C(13A)	109.0(12)	C(15B)-C(14B)-C(13B)	116.8(11)		
C(15B)-C(14B)-C(15A)	38.4(14)	C(13B)-C(14B)-C(15A)	97.0(11)		
C(15B)-C(14B)-C(16)	34.5(7)	C(13B)-C(14B)-C(16)	82.5(7)		
C(15A)-C(14B)-C(16)	41.3(5)	C(15B)-C(14B)-C(13A)	101.5(13)		
C(13B)-C(14B)-C(13A)	24.9(6)	C(15A)-C(14B)-C(13A)	73.8(8)		
C(16)-C(14B)-C(13A)	71.0(7)	C(15B)-C(15A)-C(16)	54.9(9)		
C(15B)-C(15A)-C(14A)	117.6(13)	C(16)-C(15A)-C(14A)	104.0(11)		
C(15B)-C(15A)-C(14B)	38.5(11)	C(16)-C(15A)-C(14B)	72.7(9)		
C(14A)-C(15A)-C(14B)	80.9(11)	C(16)-C(15B)-C(14B)	110.6(13)		
C(16)-C(15B)-C(15A)	69.3(13)	C(14B)-C(15B)-C(15A)	103(2)		
C(15B)-C(16)-C(15A)	55.8(13)	C(15B)-C(16)-O(4)	111.2(11)		
C(15A)-C(16)-O(4)	101.1(8)	C(15B)-C(16)-C(14B)	35.0(9)		
C(15A)-C(16)-C(14B)	66.1(9)	O(4)-C(16)-C(14B)	76.5(6)		

NaOPHF5-15C5 (4.11)

Table 1. Crystal data and structure refinement for str0060.

Identification code	str0060
Chemical formula	C16H20F5NaO6
Formula weight	426.31
Temperature	293(2) K
Radiation, wavelength	MoKα, 0.71073 Å
Crystal system, space group	monoclinic, P1/n
Unit cell parameters	a = 10.9424(11) Å α = 90°
	b = 7.9356(8) Å β = 97.344(2)°
	c = 21.865(2) Å γ = 90°
Cell volume	1883.1(3) Å3
Z	4
Calculated density	1.504 g/cm3
Absorption coefficient μ	0.162 mm1
F(000)	880
Crystal colour and size	colourless, 0.44 x 0.40 x 0.12 mm3
Data collection method	Bruker SMART APEX diffractometer
	ω rotation with narrow frames
θ range for data collection	1.88 to 28.33°
Index ranges	h 14 to 14, k 10 to 10, l 29 to 28
Completeness to θ = 26.00°	99.7 %
Reflections collected	16166
Independent reflections	4507 (Rint = 0.0184)
Reflections with F2>2σ	3086
Absorption correction	semi-empirical from equivalents

Min. and max. transmission	0.9319 and 0.9808
Structure solution	direct methods
Refinement method	Full-matrix least-squares on F2
Weighting parameters a, b	0.1777, 0.9264
Data / restraints / parameters	4507 / 0 / 271
Final R indices [F2>2σ]	R1 = 0.0995, wR2 = 0.2837
R indices (all data)	R1 = 0.1252, wR2 = 0.3145
Goodness-of-fit on F2	1.053
Largest and mean shift/su	0.002 and 0.000
Largest diff. peak and hole	0.620 and 0.404 e Å3

Table 2. Atomic coordinates and equivalent isotropic displacement parameters (Å2) for str0060. Ueq is defined as one third of the trace of the orthogonalized Uij tensor.

	x	y	z	Ueq
Na(1)	0.47432(11)		0.38756(16)	0.16602(5)0.0576(4)
O(1)	0.3875(3)	0.1919(4)	0.09788(15)	0.0938(10)
O(2)	0.6816(3)	0.3558(4)	0.13614(13)	0.0838(9)
O(3)	0.5986(3)	0.1828(4)	0.23079(15)	0.0912(9)
O(4A)	0.4084(5)	0.3721(6)	0.2669(2)	0.0859(12)
O(4B)	0.4944(7)	0.4305(11)	0.2802(3)	0.0683(18)
O(5A)	0.4562(6)	0.6664(8)	0.2031(3)	0.0780(14)
O(5B)	0.3944(12)	0.663(2)	0.1982(10)	0.104(5)
O(6)	0.5143(4)	0.5926(4)	0.09049(15)	0.0981(10)
F(1)	0.2176(3)	0.4088(4)	0.14045(12)	0.1141(11)
F(2)	-0.0134(3)	0.4329(4)	0.08085(18)	0.1242(11)
F(3)	-0.0796(3)	0.2549(4)	-0.02502(17)	0.1190(11)
F(4)	0.0877(3)	0.0529(4)	-0.06774(11)	0.1005(9)
F(5)	0.3138(3)	0.0160(3)	-0.00802(13)	0.0980(8)
C(1)	0.2762(3)	0.2066(4)	0.06954(15)	0.0623(8)
C(2)	0.1859(4)	0.3147(5)	0.08962(16)	0.0739(11)
C(3)	0.0694(4)	0.3319(5)	0.0594(2)	0.0776(11)
C(4)	0.0354(4)	0.2428(5)	0.0055(2)	0.0768(10)
C(5)	0.1205(4)	0.1390(5)	-0.01484(15)	0.0671(9)
C(6)	0.2340(4)	0.1209(4)	0.01558(16)	0.0640(8)
C(7)	0.7168(5)	0.1871(8)	0.1503(3)	0.1136(19)
C(8)	0.7180(5)	0.1625(6)	0.2173(3)	0.1003(15)
C(9)	0.5878(5)	0.1944(8)	0.2940(2)	0.1057(17)
C(10)	0.4663(7)	0.2488(9)	0.3021(2)	0.118(2)
C(11)	0.4114(5)	0.5317(8)	0.2951(2)	0.1053(17)
C(12)	0.3885(6)	0.6742(10)	0.2536(3)	0.128(2)
C(13)	0.4183(7)	0.7768(7)	0.1547(4)	0.123(2)
C(14)	0.5007(10)	0.7603(8)	0.1067(3)	0.151(3)
C(15)	0.6264(6)	0.5635(11)	0.0647(2)	0.127(3)
C(16)	0.6618(4)	0.3850(9)	0.0729(2)	0.1012(17)

Table 3. Bond lengths [Å] and angles [°] for str0060.

Na(1)–O(1)	2.274(3)	Na(1)–O(5A)	2.373(6)
Na(1)–O(6)	2.398(3)	Na(1)–O(4A)	2.409(4)
Na(1)–O(3)	2.450(3)	Na(1)–O(2)	2.452(3)
Na(1)–O(5B)	2.490(18)	Na(1)–O(4B)	2.502(7)
Na(1)–F(1)	2.799(4)	Na(1)–C(16)	3.070(4)
O(1)–C(1)	1.300(4)	O(2)–C(16)	1.392(6)
O(2)–C(7)	1.416(7)	O(3)–C(8)	1.386(6)
O(3)–C(9)	1.405(6)	O(4A)–O(4B)	1.057(8)
O(4A)–C(10)	1.352(7)	O(4A)–C(11)	1.408(7)
O(4B)–C(11)	1.285(10)	O(4B)–C(10)	1.563(11)
O(5A)–O(5B)	0.671(11)	O(5A)–C(13)	1.396(9)
O(5A)–C(12)	1.407(9)	O(5B)–C(12)	1.22(2)
O(5B)–C(13)	1.36(2)	O(6)–C(14)	1.390(7)
O(6)–C(15)	1.432(8)	F(1)–C(2)	1.347(4)
F(2)–C(3)	1.338(5)	F(3)–C(4)	1.350(5)
F(4)–C(5)	1.352(4)	F(5)–C(6)	1.355(4)
C(1)–C(6)	1.389(5)	C(1)–C(2)	1.419(6)
C(2)–C(3)	1.366(6)	C(3)–C(4)	1.384(6)
C(4)–C(5)	1.360(6)	C(5)–C(6)	1.339(6)
C(7)–C(8)	1.475(9)	C(9)–C(10)	1.429(8)
C(11)–C(12)	1.451(9)	C(13)–C(14)	1.474(10)
C(15)–C(16)	1.473(10)		

O(1)–Na(1)–O(5A)	144.50(17)	O(1)–Na(1)–O(6)	96.30(12)
O(5A)–Na(1)–O(6)	68.49(19)	O(1)–Na(1)–O(4A)	114.58(16)
O(5A)–Na(1)–O(4A)	71.8(2)	O(6)–Na(1)–O(4A)	140.11(16)
O(1)–Na(1)–O(3)	94.61(12)	O(5A)–Na(1)–O(3)	119.03(17)

O(6)-Na(1)-O(3)	135.34(14)	O(4A)-Na(1)-O(3)	69.28(15)
O(1)-Na(1)-O(2)	94.50(12)	O(5A)-Na(1)-O(2)	107.90(18)
O(6)-Na(1)-O(2)	68.27(13)	O(4A)-Na(1)-O(2)	129.35(15)
O(3)-Na(1)-O(2)	67.79(12)	O(1)-Na(1)-O(5B)	130.7(4)
O(5A)-Na(1)-O(5B)	15.6(3)	O(6)-Na(1)-O(5B)	72.6(5)
O(4A)-Na(1)-O(5B)	68.2(5)	O(3)-Na(1)-O(5B)	127.5(5)
O(2)-Na(1)-O(5B)	122.4(4)	O(1)-Na(1)-O(4B)	136.3(2)
O(5A)-Na(1)-O(4B)	62.1(3)	O(6)-Na(1)-O(4B)	126.5(2)
O(4A)-Na(1)-O(4B)	24.76(19)	O(3)-Na(1)-O(4B)	62.7(2)
O(2)-Na(1)-O(4B)	108.3(2)	O(5B)-Na(1)-O(4B)	65.6(5)
O(1)-Na(1)-F(1)	65.53(11)	O(5A)-Na(1)-F(1)	83.47(16)
O(6)-Na(1)-F(1)	95.08(12)	O(4A)-Na(1)-F(1)	77.02(14)
O(3)-Na(1)-F(1)	128.63(11)	O(2)-Na(1)-F(1)	153.13(10)
O(5B)-Na(1)-F(1)	67.9(3)	O(4B)-Na(1)-F(1)	98.6(2)
O(1)-Na(1)-C(16)	79.59(15)	O(5A)-Na(1)-C(16)	109.0(2)
O(6)-Na(1)-C(16)	49.56(16)	O(4A)-Na(1)-C(16)	155.58(16)
O(3)-Na(1)-C(16)	90.60(15)	O(2)-Na(1)-C(16)	26.28(12)
O(5B)-Na(1)-C(16)	118.8(5)	O(4B)-Na(1)-C(16)	133.0(2)
F(1)-Na(1)-C(16)	127.35(12)	C(1)-O(1)-Na(1)	122.6(3)
C(16)-O(2)-C(7)	112.2(4)	C(16)-O(2)-Na(1)	102.5(2)
C(7)-O(2)-Na(1)	105.9(3)	C(8)-O(3)-C(9)	114.7(4)
C(8)-O(3)-Na(1)	115.0(3)	C(9)-O(3)-Na(1)	114.5(3)
O(4B)-O(4A)-C(10)	79.9(6)	O(4B)-O(4A)-C(11)	60.9(6)
C(10)-O(4A)-C(11)	114.7(5)	O(4B)-O(4A)-Na(1)	82.5(5)
C(10)-O(4A)-Na(1)	112.6(4)	C(11)-O(4A)-Na(1)	111.3(4)
O(4A)-O(4B)-C(11)	73.2(6)	O(4A)-O(4B)-C(10)	58.4(5)
C(11)-O(4B)-C(10)	109.0(6)	O(4A)-O(4B)-Na(1)	72.7(5)
C(11)-O(4B)-Na(1)	111.3(5)	C(10)-O(4B)-Na(1)	100.6(4)
O(5B)-O(5A)-C(13)	73(2)	O(5B)-O(5A)-C(12)	60(2)
C(13)-O(5A)-C(12)	115.6(6)	O(5B)-O(5A)-Na(1)	92.1(19)
C(13)-O(5A)-Na(1)	110.8(5)	C(12)-O(5A)-Na(1)	112.6(5)
O(5A)-O(5B)-C(12)	91(2)	O(5A)-O(5B)-C(13)	79(2)
C(12)-O(5B)-C(13)	133.2(15)	O(5A)-O(5B)-Na(1)	72.3(18)
C(12)-O(5B)-Na(1)	114.0(12)	C(13)-O(5B)-Na(1)	106.2(11)
C(14)-O(6)-C(15)	112.3(6)	C(14)-O(6)-Na(1)	116.0(3)
C(15)-O(6)-Na(1)	113.7(3)	C(2)-F(1)-Na(1)	106.1(3)
O(1)-C(1)-C(6)	123.4(4)	O(1)-C(1)-C(2)	123.6(3)
C(6)-C(1)-C(2)	113.0(3)	F(1)-C(2)-C(3)	118.0(4)
F(1)-C(2)-C(1)	118.3(4)	C(3)-C(2)-C(1)	123.7(3)
F(2)-C(3)-C(2)	121.5(4)	F(2)-C(3)-C(4)	119.0(4)
C(2)-C(3)-C(4)	119.6(4)	F(3)-C(4)-C(5)	121.1(4)
F(3)-C(4)-C(3)	121.1(4)	C(5)-C(4)-C(3)	117.8(4)
C(6)-C(5)-F(4)	119.9(4)	C(6)-C(5)-C(4)	122.2(3)
F(4)-C(5)-C(4)	117.9(4)	C(5)-C(6)-F(5)	118.6(3)
C(5)-C(6)-C(1)	123.8(4)	F(5)-C(6)-C(1)	117.6(3)
O(2)-C(7)-C(8)	108.0(4)	O(3)-C(8)-C(7)	107.9(4)
O(3)-C(9)-C(10)	109.8(4)	O(4A)-C(10)-C(9)	121.6(5)
O(4A)-C(10)-O(4B)	41.7(4)	C(9)-C(10)-O(4B)	91.0(5)
O(4B)-C(11)-O(4A)	45.9(4)	O(4B)-C(11)-C(12)	113.5(5)
O(4A)-C(11)-C(12)	115.7(5)	O(5B)-C(12)-O(5A)	28.5(6)
O(5B)-C(12)-C(11)	122.4(10)	O(5A)-C(12)-C(11)	113.0(5)
O(5B)-C(13)-O(5A)	28.2(5)	O(5B)-C(13)-C(14)	129.0(8)
O(5A)-C(13)-C(14)	109.6(6)	O(6)-C(14)-C(13)	111.2(5)
O(6)-C(15)-C(16)	109.5(4)	O(2)-C(16)-C(15)	106.5(4)
O(2)-C(16)-Na(1)	51.24(19)	C(15)-C(16)-Na(1)	83.4(3)